Investigating the Role of T-cells in Chronic Lymphocytic Leukemia

Reiss A. Reid

Institute of Cancer & Genetics
School of Medicine,
Cardiff University

Supervisors: Dr. Stephen Man
Prof. Chris Pepper

A dissertation submitted to Cardiff University in candidature for the degree of Doctor of Philosophy

April 2015

DECLARATION

This work has not previously been accepted in substance for any degree and is not concurrently submitted in candidature for any degree.

Signed ..... (candidate) Date.....

STATEMENT 1

This thesis is being submitted in partial fulfillment of the requirements for the degree of.....(insert MCh, MD, MPhil, PhD etc, as appropriate)

Signed .....(candidate) Date.....

STATEMENT 2

This thesis is the result of my own independent work/investigation, except where otherwise stated.

Other sources are acknowledged by explicit references.

Signed .....(candidate) Date.....

STATEMENT 3

I hereby give consent for my thesis, if accepted, to be available for photocopying and for interlibrary loan, and for the title and summary to be made available to outside organisations.

Signed .....(candidate) Date.....

STATEMENT 4: PREVIOUSLY APPROVED BAR ON ACCESS

I hereby give consent for my thesis, if accepted, to be available for photocopying and for interlibrary loans **after expiry of a bar on access previously approved by the Graduate Development Committee**.

Signed .....(candidate) Date.....

Acknowledgment

First and foremost I would like to thank both my supervisors, Dr. Steve Man and Prof. Chris Pepper for their guidance, support and encouragement throughout the course of this project. I could not have asked for a better pair of supervisors.

I would also like to acknowledge Prof. Chris Fegan, Dr Ceri Jones and Dr Guy Pratt for supplying patient samples that were invaluable for all the work. In addition, to everyone who ever donated blood, without your donations I never would have been able to get my T-cell clones to grow!

I want to extend my gratitude to everyone in the lab, past and present, for providing advice, support and who helped me through my many "conniptions". – Dr Rosaria Alexandre, Dr Sophie Betteridge, Melanie Boyd, Dr Paul Brennan, Lauren Elston, Laura Escudero, Dr Shimaz Hashimdeen, Sam Hyatt, Tom Lewis, Dr Thet Thet Lin, Dr Liam Morgan, Dr Victoria Proctor, Dr Elisabeth Walsby and Dr Ryan Wong.

I am also extremely grateful to mum for her never-ending support and belief in me.

I would also like to thank all my friends for helping me with through the highs and lows of the past 3 and half years and for always being there with support and advice. Specifically my partner in crime Kirien Sangha, but also Sinead Balgobin, Jon Carruthers, Francesca Iadicicco, Dr Marcus Keatinge, Liam Lawlor, Gareth Logsdon, Ayomi Rupasinghe, and David Simpson.

The Medical Research Council and Cancer Research Wales supported this research.

Abstract

T-cells appear to have multiple conflicting roles in CLL. On the one hand tumour-specific T-cells could be used to deliver effective immunotherapy; on the other hand, certain T-cell populations may enhance CLL survival and disease progression. The aim of this thesis was to address these contradictory aspects and to provide a deeper understanding of the role of T-cells in CLL.

Firstly, candidate peptides from the pro-apoptotic protein Bax were used to activate potential CLL specific T-cells from HLA-A2$^+$ patients. A CD8$^+$ T-cell clone (6C5) was isolated and it's specificity was initially mapped to ($Bax_{161-170}$; LLSYFGTPT) and ($Bax_{160–170}$; GLLSYFGTPT). However, 6C5 failed to recognise HLA-A2$^+$ CLL cells *in vitro*, and failed to recognise highly purified forms of the peptides. Further characterisation, involving mass spectrometry and HPLC, mapped T-cell specificity to a modified peptide (LLSY(3-*t*Bu)FGTPT).

A second strand of this project involved detailed phenotypic analysis of T-cells from CLL patients (n=97) in order to investigate the basis for immune dysfunction. This analysis indicated that patients with an inverted CD4:CD8 ratio (CLL^{IR}), displayed a skewing towards a highly differentiated T-cell phenotype, as well as expression of markers associated with replicative senescence (CD57$^+$, CD27$^-$) within CD4$^+$ and CD8$^+$ T-cell compartments. In addition, CD4$^+$ T-cells expressing markers associated with immunosuppression (PD-1$^+$, TIM-3$^+$) were also increased in CLL^{IR}. Importantly, the inversion of the CD4:CD8 ratio was associated with shorter progression-free survival. Furthermore, the frequencies of distinct T-cell populations were also shown to have prognostic impact in both univariate analysis (CD4$^+$PD-1$^+$, CD4$^+$CD57$^+$, CD8$^+$CD57$^+$ and CD8$^+$CD27$^-$) and multivariate analysis (CD4$^+$CD27$^-$PD-1$^+$LAG-3$^+$ and CD8$^+$CD27$^-$ CD57$^+$PD-1$^+$).

To further evaluate the differences between CLL^{IR} and CLL^{NR} patients, preliminary transcriptional analysis was performed, focusing on genes associated with T-cell function.

By contrast, transcriptional analysis suggested that genes associated with activation rather than suppression were enriched in CLL^{IR}.

Abbreviations

aa	amino acid
ACT	Adoptive T-cell transfer
ADCC	Antibody-Dependent Cell-mediated Cytotoxicity
AHR	Aryl Hydrocarbon Receptor
AID	Activation-induced cytidine deaminase
ALL	Acute Lymphoblastic Leukaemia
Apaf1	Apoptotic Protease Activating Factor 1
APCs	Antigen Presenting Cells
β2m	β2-microglobulin
BAT-3	HLA-B-associated Transcript 3
Bax	Bcl-2-associated X protein
Bcl6	B-cell lymphoma 6 protein
BCR	B-cell receptor
BiTE	Bi-specific T-cell Engaging Antibodies
BoC20	di-*tert*-butyl dicarbonate
BSA	Bovine Serum Albumin
BTK	Bruton's Tyrosine Kinase
C	constant domains
CAR-T	Chimeric Antigen Receptors Therapy
CARs	Chimeric Antigen Receptors
CCR4	Chemokine (C-C motif) Receptor 4
CD	Cluster of Differentiation
CD40L	CD40 ligand
CDC	Complement-dependent Cytotoxicity
CFSE	Carboxyfluorescein Succinimidyl Ester
CLIP	Class II–associated Invariant Chain Peptide
CLL	Chronic lymphocytic leukaemia
CLL^{IR}	CLL inverted ratio patient
CLL^{NR}	CLL normal ratio patient
CLP	Common leukocyte progenitor
CM	Central Memory T-cells
COOT	Crystallographic Object-Oriented Toolkit
CP	Core Particle
cSMAC	Central Supramolecular Activation Cluster
CSR	Class switch recombination
CT	Cycle Threshold
CTL	Cytotoxic T-Lymphocyte
CTLA-4	Cytotoxic T-lymphocyte–associated antigen 4
D	Diversity Gene Segment
DCs	Dendritic Cells
DISC	Death-inducing Signalling Complex
DMEM	Dulbecco's Modified Eagle's Media
DMSO	Dimethyl Sulfoxide
dSMAC	Distal Supramolecular Activation Cluster
E1s	Ubiquitin-activating Enzymes
E2s	Ubiquitin-conjugating Enzymes
E3s	Ubiquitin-ligating Enzymes
EBV	Epstein-Barr Virus
EC_{50}	Half maximal effective concentration
EDTA	Ethylenediaminetetraacetic Acid
EFF	Effector T-cells

ELISA	Enzyme-linked Immunosorbent Assay
EM	Effector Memory T-cells
EMRA	Effector Memory RA+ T-cells
ER	Endoplasmic Reticulum
Fab	Fragment antigen-binding Region
FACS	Fluorescence-activated Cell Sorting
FADD	Fas-Associated protein with Death Domain
FasL	FAS Ligand
FasR	Fas Receptor
Fc	Fragment Crystallisable Region
FCR	Fludarabine, Cyclophosphamide and Rituximab
FCS	Foetal Calf Serum
FDA	Food and Drug Administration
FISH	Fluorescent *In Situ* Hybridisation
FITC	Fluorescein Isothiocyanate
Foxp3	Forkhead Box P3
GAL-9	Galectin-9
GO	Gene Ontology
GSEA	Gene Set Enrichment Analysis
Gzm	Granzyme
GVL	Graft versus leukaemia
GVHD	Graft versus host disease
H	Heavy chain
HD	Healthy Donor
HEPES	4-(2-hydroxyethyl)-1-piperazineethanesulfonic Acid
HEV	High Endothelial Venules
HLA-DM	Human Leukocyte Antigen DM
HPV	Human Papillomavirus
HSC	Haematopoietic Stem Cells
HSCT	Haematopoietic Stem Cell Transplantation
hTERT	Telomerase Reverse Transcriptase
HTLV-I	Human T-cell Lymphotropic Virus-I
IFN-γ	Interferon Gamma
Ig	Immunoglobulin
IGHV	Immunoglobulin Heavy Chain Variable region
IgV	Immunoglobulin Variable Domain
Ii	Invariant Chain
IL	Interleukin
IS	Immunological Synapse
ITAM	Immunoreceptor Tyrosine-based Activation Motif
ITIM	Immunoreceptor Tyrosine-based Inhibitor Motif
ITK	Inducible T-cell Kinase
iTregs	Induced Regulatory T-cells
J	Joining Gene Segments
KLRG1	Killer cell Lectin-like Receptor subfamily G member 1
L	Light chain
LAG-3	Lymphocyte-activation Gene 3
LAT	Linker for Activation of T cells
LC	Liquid Culture
Lck	Lymphocyte-specific Protein Tyrosine Kinase
LCMS	Liquid Chromatography-mass Spectrometry
LFA-1	Lymphocyte Function-associated Antigen 1
MACS	Magnetic-activated Cell Sorting

MDSC	Myeloid Derived Suppressor Cells
MFI	Mean Fluorescence Intensity
MHC-I	Major Histocompatibility Complex Class I
MHC-II	Major Histocompatibility Complex Class II
MIP-1β	Macrophage inflammatory protein 1 beta
MIICs	MHC class II Containing Compartments
NF-κB	Nuclear Factor-κB
NK cells	Natural Killer Cells
NTL	Non-transfected Murine Fibroblasts
nTregs	Natural Regulatory T-cells
OS	Overall Survival
PAMPs	Pathogen-associated Molecular Patterns
PBMCs	Peripheral Blood Mononuclear Cells
PBS	Phosphate Buffered Saline
PD-1	Programmed Cell Death 1 receptor
PDB	Protein Data Bank
PDK1	Phosphoinositide-dependent Protein Kinase 1
PDL	Programmed Cell Death 1 Ligand
PE	Phycoerythrin
PerCP	Peridinin Chlorophyll Protein
PFA	Paraformaldehyde
PFS	Progression-free Survival
PHA	Phytohaemagglutinin
PI3K	Phosphatidylinositol 3-kinase
PIP2	Phosphatidylinositol 4,5-bisphosphate
PIP3	Phosphatidylinositol (3,4,5)-trisphosphate
PKB	Protein Kinase B
PKC	Protein Kinase C
PLC	Peptide Loading Complex
POT1	Protection of Telomeres Protein 1
PRRs	Pattern Recognition Receptors
pSMAC	Peripheral Supramolecular Activation Cluster
RIN	RNA Integrity Number
ROR1	Receptor Tyrosine Kinase-like Orphan Receptor 1
RORγt	RAR-related Orphan Receptor Gamma
ROS	Reactive Oxygen Species
RPLP0	Ribosomal Protein Large P0
RPMI	Roswell Park Memorial Institute
SA-HRP	Streptavidin-horseradish Peroxidase
SCCHN	Squamous Cell Carcinomas of the Head and Neck
SHM	Somatic hyper mutation
SNP	Single Nucleotide Polymorphisms
SPT	Serine Palmitoyltransferase
TAAs	Tumour-associated Antigens
TAP	Transporter associated with Antigen Processing
tBu	Tertiary Butyl
TCR	T-cell Receptor
TFA	Trifluoroacetic Acid
Tfh	Follicular T helper cells
TGF-β	Transforming Growth Factor Beta
Th1	T helper1 cells
Th2	T helper2 cells
TIM-3	T-cell Immunoglobulin and Mucin Domain 3

TLR	Toll Like Receptors
TMB	3,3,5,5-tetramethylbenzidine
TNF	Tumour Necrosis Factor
Tregs	Regulatory T-cells
TTFT	Time to First Treatment
Tyr	Tyrosine
V	Variable Gene Segment / Variable Domain
VCAM-1	Vascular Cell Adhesion Molecule-1
ZAP70	Zeta Associated Protein 70
NO	Nitric Oxide
7AAD	7-amino-actinomycin D

List of suppliers

AbD Serotec	AbD Serotec , Kidlington, OX5 1GE, UK
Agilent Technologies	Agilent Technologies Ltd, Cheshire, UK
BD	Becton Dickinson UK Ltd., Oxford, UK
Beckmen Coulter	Beckman Coulter (UK) Ltd, High Wycombe, UK
Bio-Rad	Bio-Rad, Watford, UK
Biolegend	BioLegend, London, UK
ebioscience	ebioscience Ltd, Hatfield, UK
Fisher Scientific	Fisher Scientific, Loughborough
Greiner Bio-one	Greiner Bio-one Ltd, Stonehouse, UK
Hycor	Hycor Biomedical INC, California, USA
Invitrogen	Invitrogen Ltd., Paisley, UK
LEO Pharma	LEO Pharma UK, Berkshire,UK
Mabtech	Mabtech, Nacka Strand, Sweden
Merck Laboratory Supplies	Merck Ltd, Dorset, UK
Millipore	Millipore (U.K.) Ltd., Watford, UK
Miltenyi	Milenyi Biotec Ltd., Bisley, Surrey UK
Mimotope	Mimotopes Ltd., Wirral, uk
Peprotech	PeproTech EC Ltd., London, UK
Pepscan	Pepscan, Lelystad, Netherlands
Peptide synthetics	Peptide Protein Research Ltd, Hampshire, UK
ProImmune	Prolmmune Limited,Oxford, UK
Proleukin	Proleukin, Novartis, Frimley, UK
Qiagen	Qiagen Ltd, Manchester, UK
R&D Systems	R&D Systems Europe Ltd, Oxfordshire, UK
SA Biosciences	Qiagen Ltd, Manchester, UK
Sigma	Sigma, Poole, Dorset, UK
Thermo scientific	Thermo Fisher Scientific, Hempstead, UK
Tree star	Tree star inc, Ashland, Oregon, USA
Welsh blood service	WBTS, Pontyclun, Port Talbot, UK

Contents

Chapter 1 Introduction 1

1.1 Immune system 1

1.1.1 Innate immunity 1

1.1.2 Adaptive immunity 3

1.1.2.1 B-cells and Humoral immunity 3

1.1.2.2 Cell mediated immunity 7

1.1.2.2.1 $CD4^+$ T-cells 7

1.1.2.2.2 $CD8^+$ T-cells 11

1.1.2.2.3 Antigen presenting cells 12

1.1.2.2.3.1 MHC-I and the presentation of endogenous peptides 13

1.1.2.2.3.2 MHC-II and the presentation of exogenous peptides 15

1.1.2.2.3.3 Cross presentation 16

1.1.2.2.4 T-cell activation 19

1.1.2.2.5 Formation of the immunological memory 20

1.2 Cancer immunology 25

1.2.1 Immunosurveillance and immunoediting 25

1.2.2 Immune response to cancer 26

1.2.3 Mechanism of immune evasion 28

1.2.3.1 T-cell suppression through immunosuppressive receptors 29

1.2.3.1.1 Programmed cell death 1 receptor (PD-1) 29

1.2.3.1.2 T-cell Immunoglobulin and Mucin Domain 3 (TIM-3) 31

1.2.3.1.3 Lymphocyte-activation gene 3 (LAG-3) 32

1.2.3.2 Regulatory cells 33

1.2.3.3 Soluble factors 33

1.2.3.4 Reduction in antigen presentation capacity 34

1.3 Cancer immunotherapy 34

1.3.1 Monoclonal Antibodies 34

1.3.1.1 Mono-specific 34

1.3.1.2 Bi-specific T-cell engaging antibodies (BiTEs) 36

1.3.2 Therapeutic vaccines 37

1.3.2.1 Peptide vaccines 37

1.3.2.2 Dendritic cell vaccines 38

1.3.3 Adoptive T-cell transfer (ACT) 39

1.3.3.1 Genetic modification of T-cells 40

1.3.3.1.1 TCR gene transfer 41

1.3.3.1.2 Chimeric Antigen Receptors Therapy (CAR-T) 41

1.4 Chronic lymphocytic leukaemia 42

1.4.1 Aetiology and epidemiology 42

1.4.2 Symptoms and diagnosis 43

1.4.3 Staging 43

1.4.4 Prognostic markers 44

1.4.4.1 ZAP-70 44

1.4.4.2 CD38 45

1.4.4.3 CD49d 46

1.4.4.4 Immunoglobulin heavy chain variable (*IGHV*) mutation 46

1.4.4.5 Genetic aberrations 47

1.4.4.6 CD4:CD8 ratio 48

1.4.5 The lymph node microenvironment 48

1.4.6 Immunological defects within CLL 49

1.4.7 Treatments 52

1.4.7.1 Chemotherapy 52

1.4.7.1.1 Alkylating agents 52

1.4.7.1.2 Purine analogues 53

1.4.7.2 Emerging pharmaceutical agents 53

1.4.7.3 Haematopoietic stem cell transplantation (HSCT) 54

1.4.7.4 Immunotherapy 55

1.4.7.4.1 CLL specific monoclonal antibody therapy 55

1.4.7.4.2 T-cell based therapies 56

1.4.7.4.2.1 CLL associated tumor antigens 56

1.4.7.4.3 CLL specific CAR-T 57

1.4.7.5 Combination therapy 59

1.5 Hypothesis and Aims 59

Chapter 2 Materials and Methods 61

2.1 Tissue culture basics 61

2.1.1 Media and buffers 61

2.1.2 Tissue culture plastics 62

2.1.3 Cell counts and viability 62

2.1.4 Routine maintenance of cell lines 63

2.2 Peptide Libraries 63

2.2.1 Bax peptide pool P601 – P623 63

2.2.2 Nonamer combinatorial peptide library (CPL) 64

2.2.3 Peptides identified from the CPL screen 65

2.3 Peptide binding assay 65

2.4 Blood origin and preparation 66

2.4.1 Blood donors 66

2.4.2 Isolation of PBMCs 66

2.5 Primary cell cultures 67

2.5.1 CLL cell co-culture 67

2.5.2 *In vitro* culture of T-cells and CLL cells 67

2.5.3 Nonamer CPL screen 67

2.5.4 Expansion of T-cells using allogeneic feeder cells 68

2.6 Cell enrichment 68

2.6.1 Enrichment of T-cells and CLL cells using magnetic microbeads 68

2.6.2 Enrichment of IFN-γ secreting T-cells 69

2.7 Generating peptide-specific T-cell clones 70

2.7.1 Generation of T-cell lines from peptide-specific T-cells under limited dilution 70

2.7.2 Screening of peptide-specific lines 71

2.8 Detection of peptide-specific responses 71

2.8.1 IFN-γ ELISpot 71

2.8.2 IFN-γ Intracellular staining 72
2.8.3 IFN-γ enzyme-linked immunosorbent assay (ELISA) 73
2.8.4 MIP-1β ELISA 74
2.8.5 CD107α surface staining 75
2.9 Flow cytometry and Monoclonal Antibodies 75
2.9.1 Single and multi-colour immunophenotyping 75
2.9.2 Antibody panels 75
2.10 RT^2 *polymerase chain reaction array* 77
2.10.1 RNA extraction 77
2.10.2 RNA quantification and quality control 78
2.10.3 Reverse transcription 79
2.10.4 Real-time PCR 79
2.11 Statistical analysis 84
2.12 Pathway enrichment analysis 84

Chapter 3 Generation and Characterisation of Bax-Specific CD8$^+$ T-cell Clones from CLL patients 85

3.1 Activation of CLL cells 87
3.2 Donor response 89
3.3 Cloning by limiting dilution 89
3.4 Epitope mapping of Bax-specific T-cells 91
3.5 Avidity of 6C5 and 8C9 for Bax P603 and P605 94
3.6 Analysis of the TCR Vβ chain used by 6C5 94
3.7 Recongition of primary CLL cells by 6C5 95
3.8 Recognition of crude P603 (77% pure) but not pure P603 (>95%) by 6C5 100
3.9 Identification of active component within crude P603 (77% pure) 102
3.10 Recognition of P603 *t*Bu by 6C5 107
3.11 Peptide binding to HLA-A2 on the T2 cell line 113
3.12 Peptide:MHC computer modelling 116
3.13 Nonamer Combinatorial Peptide Library (CPL) screen 116

3.14 Identification and screening of cross-reactive peptides 121

3.15 Discussion 124

Chapter 4 Immunophenotyping of CLL patients 131

4.1 CD4+ T-cells 135

4.1.1 Memory subsets 135

4.1.2 Expression of CD57 and CD27 137

4.1.3 Immunosuppressive receptors 141

4.1.3.1 PD-1 141

4.1.3.2 TIM-3 142

4.1.3.3 LAG-3 142

4.1.4 Combined expression of immunosuppressive receptors 146

4.2 CD8+ T-cells 150

4.2.1 Memory subset 150

4.2.2 Expression of CD57 and CD27 152

4.2.3 Immunosuppressive receptors 155

4.2.4 Combined expression of immunosuppressive receptors 159

4.3 Prognostic relevance of T-cells in CLL 163

4.3.1 Univariate analysis 163

4.3.2 Multivariate analysis 167

4.4 Expression of complementary ligands by CLL cells 169

4.5 Summary of phenotypic analysis 173

4.6 Discussion 174

Chapter 5 Gene expression analysis of T-cells in CLL 187

5.1 CD4+ T-cell analysis 189

5.2 CD8+ T-cell analysis 193

5.3 Discussion 196

5.4 Suggested further work 204

Chapter 6 Final Discussion 205

Appendix **217**

Bibliography **239**

List of figures

Figure 1.1 Struture of Immunoglobulin 6

Figure 1.2 Development of $CD4^+$ T-cells subsets 10

Figure 1.3 Structure of MHC-I and MHC-II molecules. 17

Figure 1.4 MHC-I and MHC-II peptide processing and presentation 18

Figure 1.5 Antigen experienced T-cell development 24

Figure 1.6 The CLL tumour microenvironment 51

Figure 3.1 Experimental design for the cloning and characterisation of Bax-specific T-cells from CLL patients. 86

Figure 3.2 Analysis of the expression of the activation maker HLA-DR and co-stimulatory ligand CD86. 88

Figure 3.3 Bax T-cell response in CLL Patient samples after 5 weeks of stimulation 90

Figure 3.4 T-cell cultures generated under limiting dilution conditions were tested for Bax immunogenicity by IFN-γ ELISpot. 92

Figure 3.5 Epitope mapping of T-cell clones 6C5 and 8C9.. 93

Figure 3.6 Peptide dose-response for 8C9 and 6C5 recognition for P603 and P605 pulsed target cells. 97

Figure 3.7 Analysis of the TCR Vβ chain used by Bax specific T-cell line. 98

Figure 3.8 6C5 recognition of HLA-$A2^-$ and HLA-$A2^+$ activated CLL cells. 99

Figure 3.9 6C5 recognition of crude P603 but not pure P603 101

Figure 3.10 Mapping 6C5 response to peptide preparation representing potentially active contaminates identified from crude P603. 104

Figure 3.11 Mapping 6C5 response to the fractions generated from peptide preparation 1 105

Figure 3.12 LCMS analysis of purified and crude P603 peptide samples. 106

Figure 3.13 Recognition of butylated P603 by 6C5 T-cells 109

Figure 3.14 Production of IFN-γ by 6C5 T-cells in response to P603 *t*Bu 110

Figure 3.15 Expression of CD107α in 6C5 T-cells in response to P603 *t*Bu. 111

Figure 3.16 Peptide dose-response for 6C5 recognition of crude P603 and P603 *t*Bu pulsed target cells. 112

Figure 3.17 Binding of candidate peptides to HLA-A2. 115

Figure 3.18 Peptide/MHC modelling of unmodified and Tyr(3-*t*Bu) modified peptide bound to HLA-A*0201. 118

Figure 3.19 Nonamer CPL screen 119

Figure 3.20 Peptide dose-response for 6C5 recognition of candidate peptide identified from CPL 123

Figure 4.1 Immunophenotyping strategy. 132

Figure 4.2 Representative results of T-cell analysis. 133

Figure 4.3 $CD4^+$ T-cell memory subsets in total CLL cohort (n=97) and age-matched healthy donor (HD) controls (n=21). 136

Figure 4.4 $CD4^+$ T-cell memory subsets in the stratified CLL cohort (CLL^{IR}, n=32 and CLL^{NR}, n=65) and age-matched healthy donor (HD) controls (n=21). 136

Figure 4.5 CD57 expression within $CD4^+$ T-cells of the total CLL cohort (n=97) and age-matched healthy donor (HD) controls (n=21) 139

Figure 4.6 CD57 expression within $CD4^+$ T-cells of the stratified CLL cohort (CLL^{IR}, n=32 and CLL^{NR}, n=65) and age-matched healthy donor (HD) controls (n=21). 139

Figure 4.7 CD27 expression within $CD4^+$ T-cells of the total CLL cohort (n=97) and age-matched healthy donor (HD) controls (n=21) 140

Figure 4.8 CD27 expression within $CD4^+$ T-cells of the stratified CLL cohort (CLL^{IR}, n=32 and CLL^{NR}, n=65) and age-matched healthy donor (HD) controls (n=21) 140

Figure 4.9 PD-1 expression within $CD4^+$ T-cells of the total CLL cohort (n=97) and age-matched healthy donor (HD) controls (n=21) 143

Figure 4.10 PD-1 expression within $CD4^+$ T-cells of the stratified CLL cohort (CLL^{IR}, n=32 and CLL^{NR}, n=65) and age-matched healthy donor (HD) controls (n=21) 143

Figure 4.11 TIM-3 expression within $CD4^+$ T-cells of the total CLL cohort (n=97) and age-matched healthy donor (HD) controls (n=21).. 144

Figure 4.12 TIM-3 expression within $CD4^+$ T-cells of the stratified CLL cohort (CLL^{IR}, n=32 and CLL^{NR}, n=65) and age-matched healthy donor (HD) controls (n=21) 144

Figure 4.13 LAG-3 expression within $CD4^+$ T-cells of the total CLL cohort (n=97) and age-matched healthy donor (HD) controls (n=21) 145

Figure 4.14 LAG-3 expression within $CD4^+$ T-cells of the stratified CLL cohort (CLL^{IR}, n=32 and CLL^{NR}, n=65) and age-matched healthy donor (HD) controls (n=21) 145

Figure 4.15 Combined expression of immunosuppressive receptors within $CD4^+$ T-cells of the total CLL cohort (n=97) age-matched healthy donor (HD) controls (n=21) 147

Figure 4.16 Combined expression of immunosuppressive receptors within $CD4^+$ T-cells of the stratified CLL cohort (CLL^{IR}, n=32 and CLL^{NR}, n=65) and age-matched healthy donor (HD) controls (n=21).....148

Figure 4.17 $CD8^+$ T-cell memory subsets in the total CLL cohort (n=97) and age-matched healthy donor (HD) controls (n=21) 151

Figure 4.18 $CD8^+$ T-cell memory subsets in the stratified CLL cohort (CLL^{IR}, n=32 and CLL^{NR}, n=65) and age-matched healthy donor (HD) controls (n=21).....151

Figure 4.19 CD57 expression within the $CD8^+$ T-cells of the total CLL cohort (n=97) and age-matched healthy donor (HD) controls (n=21). 153

Figure 4.20 CD57 expression within the $CD8^+$ T-cells of the stratified CLL cohort (CLL^{IR}, n=32 and CLL^{NR}, n=65) and age-matched healthy donor (HD) controls (n=21) 153

Figure 4.21 CD27 expression within the $CD8^+$ T-cells of the total CLL cohort (n=97) and age-matched healthy donor (HD) controls (n=21) 154

Figure 4.22 CD27 expression within the $CD8^+$ T-cells of the stratified CLL cohort (CLL^{IR}, n=32 and CLL^{NR}, n=65) and age-matched healthy donor (HD) controls (n=21). 154

Figure 4.23 PD-1 expression within the $CD8^+$ T-cells of the total CLL cohort (n=97) and age-matched healthy donor (HD) controls (n=21) 156

Figure 4.24 PD-1 expression within the $CD8^+$ T-cells of the stratified CLL cohort (CLL^{IR}, n=32 and CLL^{NR}, n=65) and age-matched healthy donor (HD) controls (n=21) 156

Figure 4.25 TIM-3 expression within the $CD8^+$ T-cells of the total CLL cohort (n=97) and age-matched healthy donor (HD) controls (n=21) 157

Figure 4.26 TIM-3 expression within the $CD8^+$ T-cells of the stratified CLL cohort (CLL^{IR}, n=32 and CLL^{NR}, n=65) and age-matched healthy donor (HD) controls (n=21). 157

Figure 4.27 LAG-3 expression within the $CD8^+$ T-cells of the total CLL cohort (n=97) and age-matched healthy donor (HD) controls (n=21). 158

Figure 4.28 LAG-3 expression within the $CD8^+$ T-cells of the stratified CLL cohort (CLL^{IR}, n=32 and CLL^{NR}, n=65) and age-matched healthy donor (HD) controls (n=21) 158

Figure 4.29 Combined expression of immunosuppressive receptors within the $CD8^+$ T-cells of the total CLL cohort (n=97) and age-matched healthy donor (HD) controls (n=21) 160

Figure 4.30 Combined expression of immunosuppressive receptors within the $CD8^+$ T-cells of the stratified CLL cohort (CLL^{IR}, n=32 and CLL^{NR}, n=65) and age-matched healthy donor (HD) controls (n=21) 161

Figure 4.31 Kaplan–Meier curves for progression-free survival for CLL^{NR} and CLL^{IR} patients.....164

Figure 4.32 Kaplan-Meier curves for the progression-free survival for CD57, CD27, PD-1, TIM-3 and LAG-3 expression in $CD4^+$ T-cells.....165

Figure 4.33 Kaplan-Meier curves for the progression-free survival for CD57, CD27, PD-1, TIM-3 and LAG-3 expression in $CD8^+$ T-cells.....166

Figure 4.34 Kaplan–Meier curves for progression-free survival for the T-cell phenotype $CD4^+CD27^-PD\text{-}1^+LAG\text{-}3^+$ 168

Figure 4.35 Kaplan–Meier curves for progression-free survival for the T-cell phenotype $CD8^+CD27^-CD57^+PD\text{-}1^+$ 168

Figure 4.36 Representative results of B-cell immunosuppressive ligand expression analysis 170

Figure 4.37 PDL-1, GAL-9 and HLA-DR expression within B-cells of CLL patients (n=52) and healthy age-matched healthy donor (HD) controls (n=21) 171

Figure 4.38 PDL-1, GAL-9 and HLA-DR expression within B-cells of stratified CLL patients (CLL^{IR}, n=18 and CLL^{NR}, n=34) and age-matched healthy donor (HD) controls (n=21) 172

Figure 5.1 Schematic of experimental design 188

Figure 5.2 Differentially expressed genes (T-cell activation array) in $CD4^+$ T-cells between CLL^{NR} patients and CLL^{IR} patients. 191

Figure 5.3 Differentially expressed genes (T-cell anergy array) in $CD4^+$ T-cells between CLL^{NR} patients and CLL^{IR} patients 192

Figure 5.4 Differentially expressed genes (T-cell activation array) in $CD8^+$ T-cells between CLL^{IR} patients and CLL^{IR} patients 194

Figure 5.5 Differentially expressed genes (T-cell anergy array) in $CD8^+$ T-cells between CLL^{NR} patients and CLL^{IR} patients 195

List of Tables

Table 2.1 Bax peptide pool P601-623 64

Table 2.2: Candidate peptides identified from nonamer CPL 65

Table 2.3 TCR Vβ chain antibodies 75

Table 2.4 T-cell subsets and immunosuppressive receptors panel 76

Table 2.5 CLL and immunosuppressive ligands panel 76

Table 2.6 General antibodies 77

Table 2.7 Reverse transcription mixture 79

Table 2.8 Real-time PCR mixture 80

Table 2.9 Real-time PCR programme 80

Table 2.10 T-cell & B-cell activation PCR array gene list 80

Table 2.11 Human T-cell Anergy and Immune Tolerance PCR Array gene list 82

Table 3.1 Comparison of purified and crude P603 peptide samples by LCMS. 103

Table 3.2 Summary of data from the nonamer CPL screen performed on 6C5. 120

Table 3.3 Degenerate peptide seqeunces produced from the nonamer CPL 122

Table 3.4 Candidate peptides identified from the nonamer CPL 122

Table 3.5 Candidate peptides that produced MIP-1β responses above background. 123

Table 4.1 Overall $CD4^+$ T-cell pie chart analysis (CLL vs HD) 149

Table 4.2 Detailed $CD4^+$ T-cell pie chart analysis (CLL vs HD) 149

Table 4.3 Overall $CD4^+$ T-cell pie chart analysis (CLL^{NR} vs CLL^{IR} vs HD) 149

Table 4.4 Detailed $CD4^+$ T-cell pie chart analysis (CLL^{NR} vs CLL^{IR} vs HD) 149

Table 4.5 Overall $CD8^+$ T-cell pie chart analysis (CLL vs HD) 162

Table 4.6 Detailed $CD8^+$ T-cell pie chart analysis (CLL vs HD) 162

Table 4.7 Overall $CD8^+$ T-cell pie chart analysis (CLL^{NR} vs CLL^{IR} vs HD) 162

Table 4.8 Detailed $CD8^+$ T-cell pie chart analysis (CLL^{IR} vs CLL^{NR} vs HD) 162

Table 4.9 Multivariate analysis was performed using Cox proportional hazards regression with forward selection 167

Table 4.10 Summary of phenotypic analysis of $CD4^+$ T-cells 173

Table 4.11 Summary of phenotypic analysis of $CD4^+$ T-cells 173

Table 4.12 Summary of phenotypic analysis of $CD19^+$ / $CD19^+CD5^+$ B-cells.....173

Chapter 1

Introduction

1.1 Immune system

The immune system represents a highly developed and integrated system designed to protect the body against pathogens. The cellular components of this remarkable system originate from haematopoietic stem cells (HSC), which through the process of differentiation become committed to specific cellular lineages. The immune system can be divided into the innate immune system, which acts as the front line of defense and protects the host in a non-specific manner, and the adaptive immune system which is specific and develops in response to specific pathogens (Janeway 2012).

1.1.1 Innate immunity

The detection of pathogens occurs through the recognition of pathogen-associated molecular patterns (PAMPs), by pattern recognition receptors (PRRs), such as the toll like receptors (TLR). This process of recognition results in the activation of anti-microbial processes and enhancement of antigen presentation. This in turn allows for the presentation of antigens to the adaptive immune system (Medzhitov and Janeway 2002). The specific cells that contribute to the innate immune system include phagocytes (macrophages, neutrophils and dendritic cells (DCs)), mast cells, basophils, eosinophils and natural killer cells (NK cells) (Janeway and Medzhitov 2002).

Phagocytic cells are principally characterised by their ability to phagocytose and demolish infected and diseased cells. Within the innate immune system neutrophils, macrophages and DCs undertake this task (Savina and Amigorena 2007). Neutrophils detect pathogens and damaged tissue through a range of PRRs, including members of the TLR family. Ligation of these receptors mediates neutrophil activation, phagocytosis, the

release of lytic enzymes and the production of reactive oxygen species (Mantovani et al. 2011).

Macrophages and DCs are derived from precursor monocytes. Their divergent development occurs in response to differing environmental stimuli and they are often distinguished by the expression of distinct surface markers. Macrophages can be divided into numerous subsets that are localised to specific anatomical locations and have distinct functions. "Classically" activated macrophages mediate anti-microbial and anti-tumour responses through the secretion of pro-inflammatory factors such as tumour necrosis factor alpha (TNF-α), nitric oxide (NO) and Interlukin-1 (IL-1). However, "alternatively" activated macrophages have been shown to mediate anti-inflammatory immune responses and regulate wound healing (Murray and Wynn 2011).

DCs are specialised antigen presenting cells (APCs) that facilitate antigen specific activation within the adaptive immune system. DCs present peptides derived from both intracellular and extracellular proteins on major histocompatibility complexes; class I (MHC-I) and class II (MHC-II), respectively. Additionally, lipid antigens are presented on complexes formed through the heterodimerisation of the cluster of differentiation 1 (CD1) and β2-microglobulin (β2m). Furthermore, DCs also express essential co-stimulatory and adhesion molecules required for the formation of the immunological synapse (IS) and subsequent T-cell activation (Adams et al. 2005; Banchereau and Steinman 1998).

Mast cells and basophils are functionally similar cells that contain histamine and heparin stored within intracellular granules. Cross-linking of the high affinity immunoglobulin E (IgE) fragment crystallisable (Fc) receptors initiates the process of cellular activation and degranulation. The *in vivo* functions of these cells are not yet fully understood, nevertheless reports have suggested that mast cells contribute to protecting the host against parasitic and bacterial infections, as well as supporting tumour rejection. While basophils have been indicated to mediate protection against helminths and ticks, moreover

both cell types have been suggested to have a modulatory effect on the adaptive immune system (Voehringer 2013).

Eosinophils are granulocytes implicated in the pathology of allergies and protection against helminths. They express a wide array of receptors that modulate cell survival, proliferation, migration in response to chemoattractants and the release of intracellular granules. This is a process that can occur through three distinct routes, compound exocytosis, piecemeal degranulation and degranulation associated with cytolysis (Rosenberg et al. 2012; Muniz et al. 2012).

NK cells are cytotoxic lymphocytes that possess the capacity to generate cytolytic responses against infected and diseased cells, similar to those observed with $CD8^+$ T-cells. The activation of NK cells occurs through the synergy of multiple activating and inhibitory receptors. The effects of these receptors are mediated through the phosphorylation of immunoreceptor tyrosine-based activation motifs (ITAM) and immunoreceptor tyrosine-based inhibitor motifs (ITIM), respectively (Long et al. 2013).

1.1.2 Adaptive immunity

The adaptive immune system represents a highly specific and specialised branch of the immune system that is characterised by lymphocytes that express antigen specific receptors, T-cell receptors (TCR) and B-cell receptors (BCR). The recognition of a seemingly countless number of antigens occurs through the expression of an array of receptors produced through the somatic rearrangement of the variable (V), diversity (D) and joining (J) gene segments (Boehm 2011). Furthermore, the antigen specific nature of cellular activation allows for the formation of immunological memory which functions to orchestrate rapid immune responses upon re-exposure to pathogens (Gourley et al. 2004).

1.1.2.1 B-cells and humoral immunity

The development of B-cells occurs within the bone marrow, through the commitment of the common leukocyte progenitor (CLP) to the B-cell linage. The process

of differentiation occurs in multiple stages firstly with the emergence of the pro-B-cell, followed by pre-B-cell and finally the immature B-cell. At this stage the B-cell expresses a mature BCR, which allows for the process of negative selection, to eliminate self reactive B-cells. The immature B-cells can then emerge from the bone marrow, as transitional B-cells and migrate to secondary lymphoid organs such as the spleen and lymph nodes to undergo maturation (Cambier et al. 2007).

Upon antigenic challenge, the interaction between the BCR (or surface Ig) (Fig 1.1) and antigen initiates an intracellular signaling cascade which results in antigen internalisation, processing and presentation on MHC-II (as described in section 1.1.2.2.3.2) (Janeway 2012). The resulting MHC-peptide complex can then be recognized by specific helper T-cells, which in turn expression B-cell co-stimulatory ligands such as CD40L (Noelle et al. 1992) and produce IL-4 (Zamorano et al. 2001), which supports B-cell proliferation and survival. Moreover, synergistic IL-4 and CD40L signaling has been shown to induce the expression of activation-induced cytidine deaminase (AID) (Dedeoglu et al. 2004), which plays an integral role in the processes of class switch recombination (CSR) and somatic hyper mutation (SHM) (Stavnezer et al. 2008).

CSR involves the rearrangement of the constant domain genes of the Ig heavy chain locus, which results in the switching of ones isotype to another. The process has no effect upon the antigen specificity of the antibody, but can alter its overall properties and interactions with effector molecules and cells. After several rounds of cell division the B-cells undergo SHM, which induces the diversification of the BCR and the producetion of variants with enhanced binding affinity. The process involves the mutation (commonly single base pair substitutions) of V domain of the BCR at a rate of 10^{-5} to 10^{-3} mutations per base pair per generation, through this phenomenon can occur throughout the entire V domain, it has been shown to be more prevalent within certain motifs (Li 2004).

Following activation within the germinal centres B-cells can differentiate into plasma cells and memory B-cells. Plasma cells produce high levels of soluble Ig and play an

integral role in the humeral immune response. The Ig is then able to bind to specific pathogens through interactions between the Ig fragment antigen-binding region (Fab) and antigens on the pathogen surface. This process can either inhibit the pathogen's ability to enter the host's cell or "tag" the pathogen of destruction by phagocytic cells (Janeway 2012).

Memory B-cells serve to provide protection against secondary pathogen exposure. The mechanism by which B-cells differentiate in memory B-cells is still not fully understood. While it has been suggested that the induction of a master transcription factor may mediate commitment to the memory B-cell linage, none have yet to be defined. An alternative hypothesis is that within the germinal centres, it is the B-cells that exhibit a survival advantage, which have the capacity to go on to form memory B-cells (Kurosaki et al. 2015).

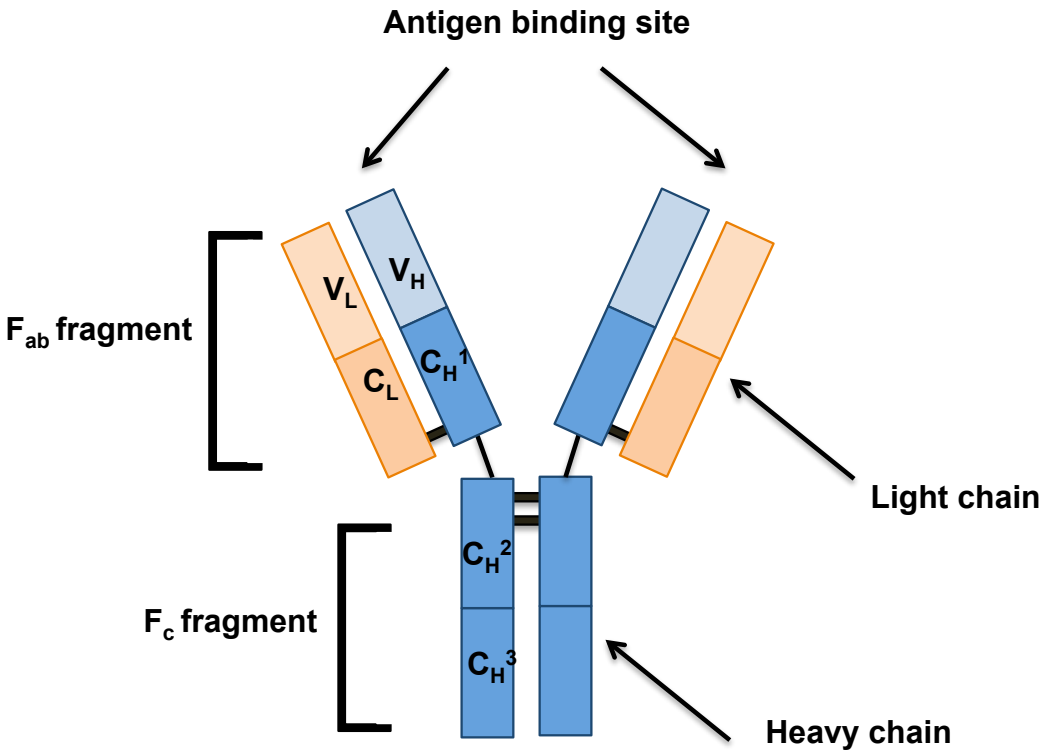

Figure 1.1 Struture of Immunoglobulin. Immunoglobulins consist of two heavy chains (H) and two light chains (L), however it should be noted that the light chain could either a κ or a λ chain. Both chains consist of variable (V) and constant (C) domains, however the heavy chain is made up of three C domains C_H^1, C_H^2 and C_H^3. The structure is maintained through multiple disulfide bonds, located between each heavy and light chain, as well as the two heavy chains. Immunoglobulins can be divided into functionally distinct fragments. The F_{ab} fragments contain the antigen binding sites and are responsible for the specificity associated with the antibody. While the F_c fragment consists of the paired C_H^2 and C_H^3 domains and is able to interact which effector molecules and cells to induce antibody-dependent cell-mediated cytotoxicity (ADCC) and complement-dependent cytotoxicity (CDC) (Schroeder and Cavacini 2010; Janeway 2012).

1.1.2.2 Cell mediated immunity

T-cells are lymphocytes also derived from the bone marrow but which undergo maturation within the thymus. They can be divided into $CD4^+$ T-cells and $CD8^+$ T-cells and then further subdivided into specific subsets with differing functions. Broadly speaking, $CD4^+$ T-cells are involved in assisting and regulating immune responses while $CD8^+$ T-cells are responsible for inducing targeted killing of infected and malignant cells (Janeway 2012).

1.1.2.2.1 $CD4^+$ T-cells

$CD4^+$ T-cells represent a heterogeneous population of lymphocytes that possess effector and regulatory functions (Fig 1.2) (Zhu and Paul 2008). Type 1 helper T-cells (Th1) preferentially express the transcription factor T-bet and produce interferon gamma (IFN-γ), while Type 2 helper T-cells (Th2) express GATA-3 and produce IL-4 (Szabo et al. 2000). Th1 cells provide protection against viruses and intracellular pathogens and support cell mediated immune responses while Th2 cells provide protection against extracellular parasites and support humoral responses (Janeway 2012).

Th9 cells are closely related to Th2 cells, as their development requires many of the same factors, such as IL-4. However, Th9 cells express the master transcription factor PU.1, which induces the expression of IL-9 and inhibit the expression of cytokines associated with a Th2 phenotype such as IL-4, IL-5, IL-10, and IL-13 (Chang et al. 2005; Chang et al. 2010).

Th17 cells produce IL-17 along with other inflammatory cytokines and contribute towards autoimmune diseases. The differentiation of Th17 cells is governed by the expression of the transcription factor RAR-related orphan receptor gamma (RORγt), which is up-regulated in response to TCR ligation in the presence of IL-6 and transforming growth factor beta (TGF-β) (Ivanov et al. 2006).

Th22 cells are a T-cell helper cell subset that is closely related to Th17 cells. Th22 cells are characterised by the expression of chemokine (C-C motif) receptor 4 (CCR4), CCR6, CCR10 and production of IL-22, but not IFN-γ, IL-4 or IL-17 (Trifari et al. 2009). IL-22 producing T-cells have been shown to contribute to the population of localised T-cells in inflammatory human skin disorders such as psoriasis (Boniface et al. 2007). It has been suggested that aryl hydrocarbon receptor (AHR), in combination with other molecules such as RORγt influences the differentiation and development of Th22 cells (Trifari et al. 2009).

Follicular helper cells (Tfh) provide critical support for B-cells, specifically in germinal centres where B-cells undergo activation, proliferation and antibody affinity maturation. The development of Tfh is dependent upon the expression of the transcription factor B-cell lymphoma 6 protein (Bcl6), which is induced by IL-21 and IL-6. Bcl6 orchestrates Tfh differentiation and induces the expression of IL-21R, IL-6R, and CXCR5. Moreover, Bcl6 inhibits the expression and function of transcription factors responsible for the development of other T helper cell lineages (Nurieva et al. 2009).

Regulatory T-cells (Tregs) form a T-cell subset characterised by the expression of CD25 and the transcription factor forkhead box P3 (Foxp3) (Hori et al. 2003), and play an important role in the prevention of autoimmune responses and immunopathology (Sakaguchi et al. 2008).

Tregs can be sub-divided into natural regulatory T-cells (nTregs) and induced regulatory T-cells (iTregs). nTregs are produced in the thymus via signalling through high affinity TCR and the induction of Foxp3 (Relland et al. 2009). iTregs on the other hand are produced in the periphery through the activation of naïve $CD4^+$ T-cells in the presence of anti-inflammatory cytokines such as TGF-β (Chen et al. 2003). Both types exhibit the capacity to suppress immune responses and inhibit T-cell proliferation (Qiao et al. 2007), but the requirement for both cell types in maintaining peripheral tolerance is not yet fully understood. Haribhai *et al* observed there was a vast difference in the TCR repertoires of

nTreg and iTreg, suggesting that the need for both cell types stems from differing antigen specificity (Haribhai et al. 2011).

The exact mechanism by which Tregs act to suppress immune function is not yet fully understood, however research from *in vitro* and *in vivo* systems has provided several concepts for their mode of action (Toda and Piccirillo 2006). Activated Tregs have been shown to produce the immunosuppressive cytokines TGF-β, IL-10, and IL-35, which may play a role in the contact-independent immune regulation by Tregs (Zhu and Paul 2008). Additionally, Tregs have been shown to inhibit the antigen presentation capacity of DCs in a contact-dependent manner, through the down-regulation of the co-stimulatory ligands CD80 and CD86, in a lymphocyte function-associated antigen 1 (LFA-1) and cytotoxic T-lymphocyte antigen 4 (CTLA-4) dependent manner (Onishi et al. 2008). Interestingly, it has been suggested that CTLA-4 has the capacity to sequester CD80 and CD86 from the cell surface (Qureshi et al. 2011). Therefore it could be hypothesised that CTLA-4 present on Tregs acts to physically remove CD80 and CD86 from the cell surface of DCs, rather than inducing their down-regulation.

Whether or not the T-cell subsets described above represent discrete T-cell lineages or are part of a ever changing network on $CD4^+$ T-cells is still the subject of much debate (Nakayamada et al. 2012). For example the down-regulation of Foxp3 and subsequent expression of IL-17 can be induced *in vitro* via treatment with IL-6 and IL-1, indicating plasticity between Tregs and Th17 cells (Yang et al. 2008). This phenomenon has also been reported between Th1 and Th2 (Hegazy et al. 2010) and other $CD4^+$ T-cells (Nakayamada et al. 2012).

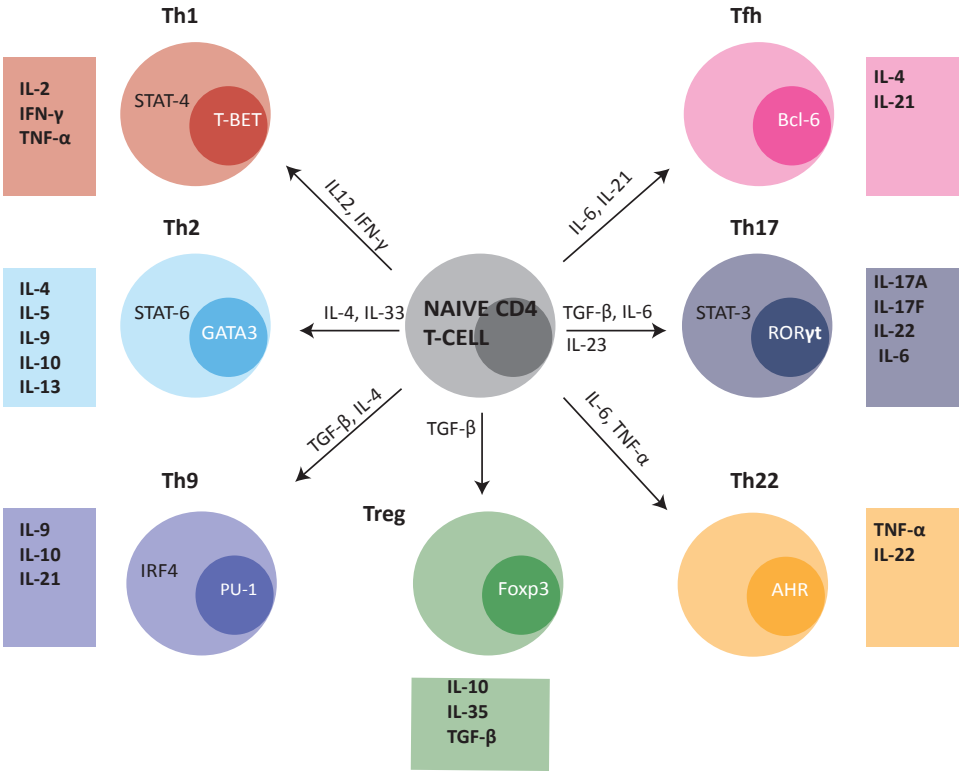

Figure 1.2 Development of CD4⁺ T-cells subsets. CD4⁺ T-cells represent a heterogeneous population of lymphocytes that function to modulate immune responses (Zhu and Paul 2008). CD4⁺ T-cells recognise antigens derived from extracellular proteins presented on MHC-II (Neefjes et al. 2011) and were originally classified as two major subsets (Szabo et al. 2000), Th1 and Th2. However, extensive research has alluded to the potential for CD4⁺ T-cells to differentiate into a wide array of cell types, including, but not limited to, Th9, Th17, Th22, Tfh and Tregs (Jiang and Dong 2013). The differentiation of these subsets is governed by the ligation of the TCR under polarising cytokine conditions and the induction of specific transcription factors (Liu et al. 2013).

1.1.2.2.2 $CD8^+$ T-cells

$CD8^+$ T-cells represent a population of cytotoxic lymphocytes (CTLs) that demonstrate the capacity to induce targeted killing of infected (Koelle et al. 2001) and malignant cells (Nunes et al. 2011; Wang et al. 2006; Kawakami et al. 1995). Activation of $CD8^+$ T-cells is orchestrated through interactions between the TCR and MHC-I peptide complexes expressed on the surface of APCs (Janeway 2012). Furthermore, the strength and stability of this interaction is augmented through the interaction between CD8 and the MHC-I peptide complex (Artyomov et al. 2010).

$CD8^+$ T-cells employ multiple methods of inducing cell death. The principal mechanism utilised involves the delivery of cytotoxic granules into the cytoplasm of the target cell. This process is mediated through the secretion of perforin, granzymes (Gzms) and granulysin (Lieberman 2010).

Perforin is a pore forming molecule that has been shown to be essential for granule mediated cell death (Voskoboinik et al. 2010). It was originally hypothesised that perforin generated pores within the target cell membrane providing a gateway to the cytosol for the Gzms**.** However, Thiery *et al* showed that perforin first acts to create small unstable pores within the plasma membrane, which result in a Ca^{2+} influx and the activation of membrane repair mechanisms. Gzms and perforin are then endocytosed and held within intracellular vesicles. The Gzms can then "escape" from these vesicles and form larger stable pores through the polymerisation of perforin within the vesicle membranes (Thiery et al. 2011).

Gzms are serine proteases that are characterised by the catalytic triad His-Asp-Ser. Humans possess five separate Gzms (A, B, H, K, and M). With the exception of GzmB, the mechanism of action of the Gzms is yet to be elucidated (Ewen et al. 2012).

GzmB has been shown to trigger the activation of the caspase cascade, primarily through the cleavage and activation of caspase-3, which initiates a second tier of caspase activation through processing of caspase-2, caspase-6 and caspase-9 (Adrain et al. 2005). However GzmB can also indirectly activate the caspase cascade by regulating the release of

cytochrome C from the mitochondria (Heibein et al. 2000), which can complex with apoptotic protease activating factor 1 (Apaf1) and other factors, to produce the apoptosome (Riedl and Salvesen 2007).

Granulysin is a cytolytic molecule present in two forms, a 15-kDa form and a truncated 9-kDa form. It is the truncated form that has been shown to be responsible for the cytolytic activity associated with granulysin (Hanson et al. 1999). Granulysin directly interacts with lipids in the plasma membrane and triggers an influx of Ca^{2+} ions, thus alters the balance between intracellular Ca^{2+} and K^{+}. This results in damage to the mitochondrial membrane and the release of cytochrome C (Kaspar et al. 2001) the formation of the apoptosome and activation of the caspase cascade (Riedl and Salvesen 2007).

Another mechanism utilised by $CD8^{+}$ T-cells to induce apoptosis involves the ligation of the Fas receptor (FasR). Activation of T-cells triggers an up-regulation in expression of the Fas ligand (FasL), which enhances the capacity for Fas-mediated cell death (Ju et al. 1995; Dhein et al. 1995). Upon ligation FasRs undergo conformational changes that allow for the recruitment of the adaptor protein Fas-Associated protein with Death Domain (FADD) (Chinnaiyan et al. 1995). This mediates the recruitment of caspase-8 and the formation of the Death-inducing signalling complex (DISC) (Scott et al. 2009). Caspase-8 then undergoes conformational changes that initiate its activation and autoproteolytic cleavage. Consequently the activated caspase-8 is released and is able to target its intracellular substrates (Boatright et al. 2003).

1.1.2.2.3 Antigen presenting cells

The processing and presentation of antigens is essential in enabling the immune system to distinguish between self and non-self. The presentation of antigen occurs through MHC molecules, which can be divided into two classes (Fig 1.3) (Neefjes et al. 2011).

The presentation of antigens can occur by a range of cell types, including but not limited to myeloid and plasmacytoid DCs (Steinman and Idoyaga 2010), macrophages

(Ziegler and Unanue 1981) and B-cells (Rodríguez-Pinto 2005). These cells are commonly referred to as professional APCs because they constitutively express MHC-II and are highly efficient at capturing, processing and presenting antigens (Vyas et al. 2008). Non-professional antigen presenting cells, which include fibroblasts and epithelial cells do not express MHC-II under normal conditions, but it's expression can be induced under inflammatory conditions and exposure to IFN-γ (Steimle et al. 1994).

1.1.2.2.3.1 MHC-I and the presentation of endogenous peptides

MHC-I molecules present antigens of cytosolic origin, produced through the proteolytic processing of intracellular proteins by the proteasome (Fig 1.4a) (Raghavan et al. 2008). The delivery of substrates to the proteasome is mediated through the process of ubiquitination (Hershko et al. 1980). This multi-step reaction is orchestrated by ubiquitin-activating enzymes (E1s), ubiquitin-conjugating enzymes (E2s) and ubiquitin-ligating enzymes (E3s). The E1s bind to ubiquitin molecules in an ATP-dependent manner and induce their activation. The activated ubiquitin is then transferred to E2s and attached to the target protein through the activity of E3s (Glickman and Ciechanover 2002).

Five receptors have been indicated to facilitate ubiquitin recognition. Rpn10 and Rpn13 are proteasomal subunits that mediate the direct recognition at the proteasome. While Rad23, Dsk2, and Ddi1 are shuttle proteins that apprehend substrates within the cytosol and escort them to the proteasome (Finley 2009).

The process of proteolysis is initiated through the activity of ATPases belonging to AAA+ superfamily. Members of this family interact with the 20S core particle (CP) of the proteasome and induce gate opening along with protein unfolding and translocation (Smith et al. 2006). The CP of the proteasome is a cylindrical structure with narrow openings at each end and is comprised of 4 heptameric rings. The inner rings are made up of beta subunits while the outer rings are made up of alpha subunits (Baumeister et al. 1998). Within the beta rings, only 3 out of the 7 subunits are functionally active (β1, β2 and β5) and display differing enzymatic activities (Maupin-Furlow 2011).

The immunoproteasome represents a modified version of constitutionally expressed proteasome and it's specific role is to improve the quality and quantity of MHC-I binding peptides (Schwarz et al. 2000; de Verteuil et al. 2010). Upon exposure to IFN-γ and TNF-α the 3 beta catalytic proteasome subunits are replaced with LMP2 (β1i), MECL-1 (β2i), and LMP7 (β5i) (Nandi et al. 1996). In a study by Basler *et al*, it was suggested that the differential production of peptides by immunoproteasomes *vs.* standard proteasomes was due to differences in proteolytic cleavage specificity, rather than enhanced production of MHC-I binding peptides (Basler et al. 2012).

The loading of the newly formed peptides onto MHC-I then occurs within the endoplasmic reticulum (ER). Transportation of peptide into the ER lumen occurs in an ATP-dependent manner via the assistance of the Transporter associated with Antigen Processing (TAP) (Neefjes et al. 1993; Androlewicz et al. 1993). Within the ER immature MHC-I molecules interact with the TAP complex through the bridging action of tapasin, a molecule that enhances peptide loading and stabilises the TAP1/2 heterodimer (Garbi et al. 2003).

Along with tapasin several other chaperone molecules are required for peptide loading. Calnexin and calreticulin promote the folding of proteins bearing monoglucosylated N-linked glycans (Wearsch and Cresswell 2008), while ERp57 mediates the quality control of newly synthesised protein. Furthermore, when complexed with calnexin, ERp57 facilities the formation of disulphide bonds within the MHC-I heavy chain, thus allowing for an association with β2m (Coe and Michalak 2010).

Collectively these proteins form the peptide-loading complex (PLC) and orchestrate the incorporation of antigenic peptides within MHC-I. The MHC-I/peptide complexes then dissociate from the PLC, exit the ER and are presented on the cell surface for immune surveillance by $CD8^+$ T-cells (Raghavan et al. 2008).

1.1.2.2.3.2 MHC-II and the presentation of exogenous peptides

MHC-II mediates the presentation of peptides of extracellular origin to $CD4^+$ T-cells (Fig 1.4b) (Neefjes et al. 2011). The process of MHC-II formation occurs within the ER and is facilitated by the invariant chain (Ii); which acts as a core allowing the assembly of the α and β subset units of MHC-II (Roche et al. 1991), prevents the inappropriate loading of antigenic peptides (Roche and Cresswell 1990) and mediates the trafficking of MHC-II through the endosomal pathway (Warmerdam et al. 1996).

The proteolytic processing of the Ii chain within the acidic environment of the endosome leaves behind an 20 amino acid (aa) peptide known as the class II–associated invariant chain peptide (CLIP) within the peptide binding groove (Chaturvedi et al. 2000). Human leukocyte antigen DM (HLA-DM) then mediates the translocation of the MHC-II-CLIP complex to the late endosome by virtue of a tyrosine signalling motif located in the cytoplasmic tail of the HLA-DM β chain (Marks et al. 1995). Furthermore, HLA-DM induces conformational changes within the CLIP, which initiates its dissociation from MHC-II and enables the recruitment of antigenic peptides (Denzin and Cresswell 1995; Sloan et al. 1995).

Before the loading of antigenic peptides can occur, proteins from the extracellular space must be sampled and processed. Potential antigens can enter the endocytic pathway through several mechanisms including clathrin and caveolae receptor mediated endocytosis, phagocytosis and macropinocytosis (Landsverk et al. 2009). Upon entry of the endosome/lysosome pathway, proteins encounter environments of increasing acidity and a diverse range of proteolytic enzymes, most notably members of the cathepsin family (Watts 2001). The precise role that each cathepsin plays in the generation of antigenic peptides has yet to be elucidated, however some progress has been made to characterise their activity (Chapman 2006). Cathepsin S is the major proteolytic enzyme involved in Ii chain degradation (Riese et al. 1996). Furthermore, it has been shown to be essential for the *in vitro* generation of antigenic peptides and the maintenance of antigen specific T-cells *in vivo*

in mice (Shen et al. 2004). Additionally, the involvement of cathepsins B, C, H and X in editing the amino- and carboxy-terminal ends of peptides has been suggested (Chapman 2006).

Loading of antigenic peptides occurs within MHC-II containing compartments (MIICs), which are specialised endosomal organelles that contain all the molecules essential for peptide processing, editing and loading (Stern et al. 2006). After antigenic peptides have been successfully loaded on to MHC-II molecules, they are ready to be expressed on the cell surface. This occurs through the shuttling of MIIC vesicles to the plasma membrane. The vesicles then fuse with the plasma membrane, allowing for presentation of MHC-II-peptide complexes to $CD4^+$ T-cells (Chow et al. 2002; Turley et al. 2000).

1.1.2.2.3.3 Cross presentation

Cross presentation is an important yet poorly understood mechanism essential for immunosurveillance by $CD8^+$ T-cells. The process involves the presentation of antigen of extracellular origin on MHC-I and predominantly occurs in professional APCs via two distinct pathways (Rock and Shen 2005). Proteins can be taken up into the cell and are held in early endosomes, before being exported into the cytoplasm for proteasomal processing and subsequently reimported to the endosomal compartment by TAP for loading on MHC-I (Burgdorf et al. 2008). Alternatively proteins can undergo proteolytic processing within endosomal compartments before loading on to pre-formed MHC-I (Di Pucchio et al. 2008). Examples of this phenomenon have been reported *in vitro* and *in vivo* in human and murine systems (Bozzacco et al. 2007; Pham et al. 2012).

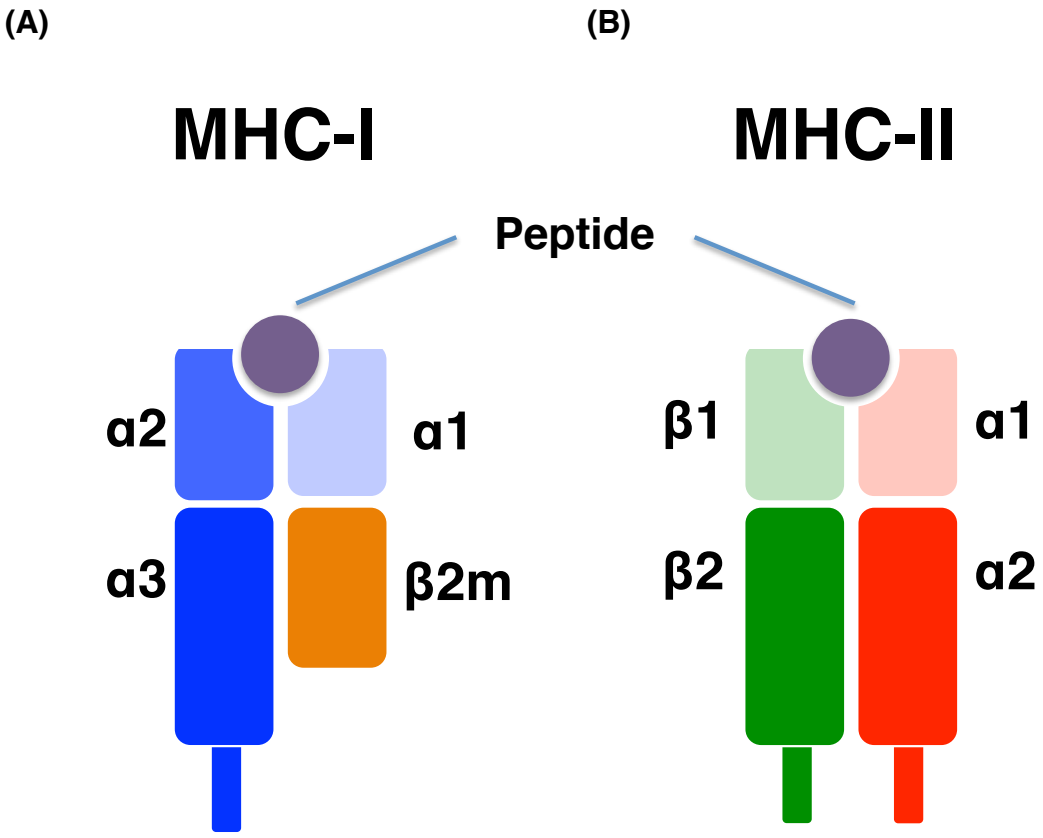

Figure 1.3 Structure of MHC-I and MHC-II molecules. **(A)** MHC-I molecules are transmembrane glycoproteins formed through the non-covalent association of the α chain and β2m. The α chain is arranged into 3 extracellular domains α1, α2 and α3 as well as a transmembrane domain and short intracellular region. The α1 and α2 are the most distal domains and form the peptide binding groove, which allows for the incorporation of antigenic peptides of 8-10 aa residues (Hewitt 2003). However, through alternation in the peptide confirmation, longer or shorter peptides can be accommodated (Meydan et al. 2013). **(B)** MHC-II molecules are transmembrane glycoproteins that are formed by the association of single α and β chains, which are both arranged into two extracellular domains. The α1 and β1 are the most distal domains and form the peptide binding groove. Unlike MHC-I molecules, MHC-II molecules are open ended which allows for peptide over hang and the incorporation of larger peptides (Janeway 2012).

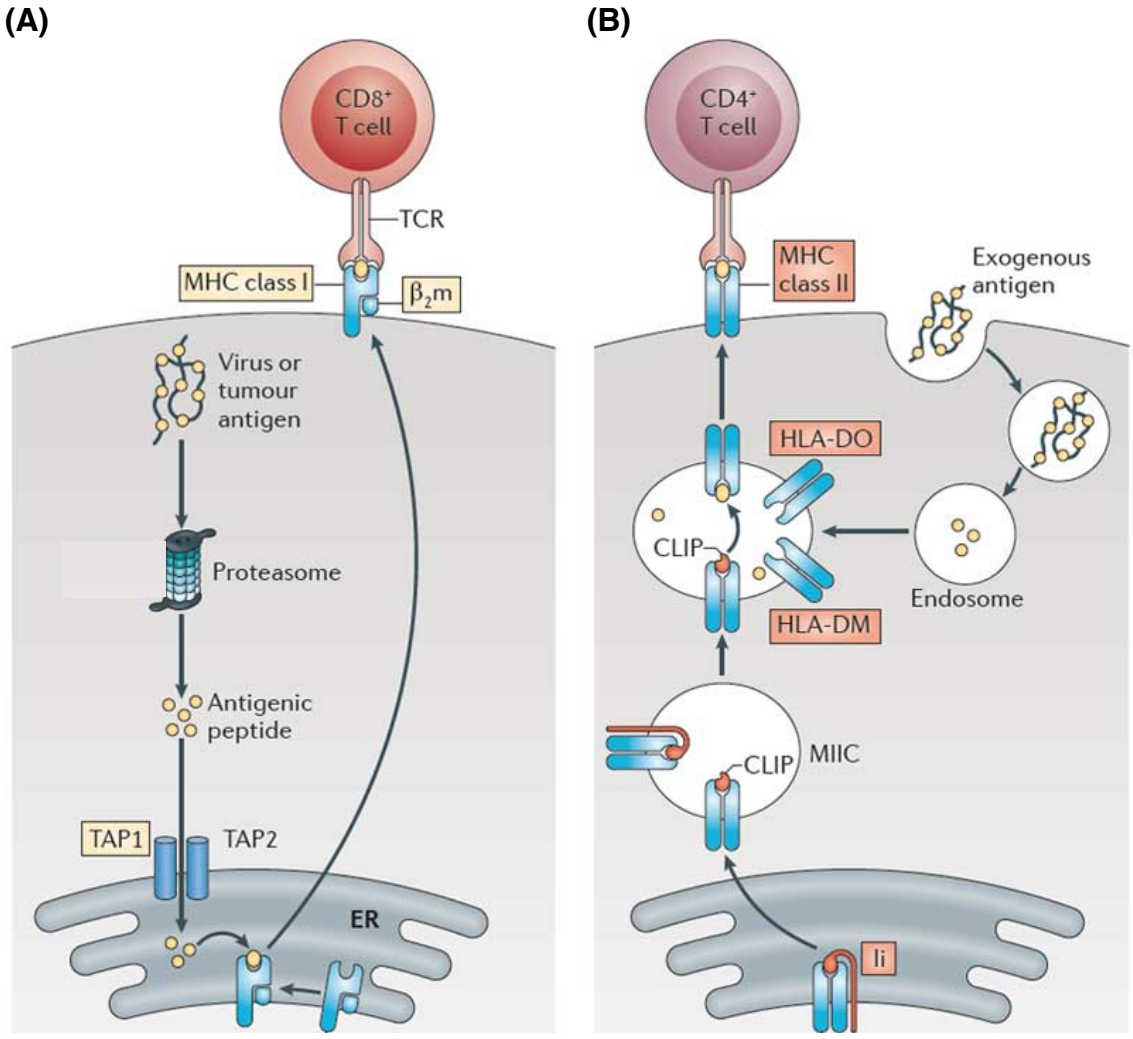

Figure 1.4 MHC-I and MHC-II peptide processing and presentation (Adapted from (Kobayashi and van den Elsen 2012)). (A) The MHC-I presentation route involves the processing of endogenous proteins by the proteasome to generate short antigen peptides to be loaded onto MHC-I molecules. The mature MHC-I-peptide complexes can then be shuttled through the ER/golgi apparatus to be expressed on the cell surface to $CD8^+$ T-cells. **(B)** The MHC-II presentation route involves the "capture" of exogenous proteins which can be passed through multiple endosomal compartments that contain an array of proteolytic enzymes. Before presentation, the peptides must be loaded on the MHC-II, which are first assembled within the ER. Peptide loading can then occur within the MIIC and the mature MHC-II-peptide complexes can then be expressed on the cell surface to $CD4^+$ T-cells (Neefjes et al. 2011).

1.1.2.2.4 T-cell activation

The recognition of antigenic peptides occurs through the presentation of MHC-peptide complexes to TCR-CD3 complexes. For complete cellular activation, this interaction must occur in concert with ligation of the co-stimulatory receptor CD28 by either CD80 or CD86. Furthermore, the process of T-cell activation is modulated through the interaction between CD4 and CD8 with their respective MHC molecules (Sharpe and Freeman 2002).

The interface between the APC and T-cell where TCR signalling occurs is known as the IS. The IS is characterised by three concentric rings of membrane bound receptors and intracellular signalling molecules. The central supramolecular activation cluster (cSMAC) is composed of the TCR-CD3 complex and CD28 as well as intracellular signalling molecules such as protein kinase C (PKC) and lymphocyte-specific protein tyrosine kinase (Lck) (Alarcón et al. 2011). Initially it was thought that the cSMAC served as the site of TCR signalling due to the accumulation of TCR:CD3 complexes and accessory molecules essential for T-cell activation. However, recent evidence has indicated that the cSMAC functions as a site of receptor degradation and thus signal termination. Nevertheless, signalling through the cSMAC has been observed and current models suggest that the cSMAC can be divided into numerous functional domains, one of which being responsible of TCR signalling (Dustin et al. 2010). The cSMAC is surrounded by the peripheral SMAC (pSMAC), which is composed of molecules involved in cell adhesion such as talin and lymphocyte function-associated antigen 1 (LFA-1). Finally, the most external ring is the distal SMAC (dSMAC), which contains molecules such as CD45 (Alarcón et al. 2011), which have been suggested to lower the threshold of T-cell activation (Saunders and Johnson 2010).

Ligation of the TCR-CD3 complex induces the exposure of the ITAM of the CD3 γε, δε and ξξ subunits and allows the recruitment of members of the SRC family of kinases such as Lck. Lck phosphorylates the ITAM allowing for the recruitment and activation of

zeta associated protein 70 (ZAP70), which results in the recruitment and activation of key adaptor molecules such as Linker for Activation of T cells (LAT). In turn LAT recruits numerous adaptors and downstream signalling molecules to orchestrate the activation of multiple signalling pathways responsible for cellular activation, proliferation and survival (Brownlie and Zamoyska 2013).

In conjunction with TCR signalling, signals from the co-stimulatory receptor CD28 are essential for complete activation and the absence of this second stimulatory signal has been shown to induce an unresponsive state known as T-cell anergy (Linsley and Ledbetter 1993). Ligation of CD28 leads to the recruitment of phosphatidylinositol 3-kinase (PI3K). PI3K stimulates the production of the lipids phosphatidylinositol 4,5-bisphosphate (PIP2) and phosphatidylinositol (3,4,5)-trisphosphate (PIP3), which associate with phosphoinositide-dependent protein kinase 1 (PDK1), resulting in the activation protein kinase B (PKB). PDK1 and PKB are then able to phosphorylate downstream signalling molecules and mediate the regulation of multiple signalling pathways necessary for protein synthesis and cell survival (Rudd et al. 2009).

1.1.2.2.5 Formation of the immunological memory

Primary T-cell interactions that occur within the lymph node induce T-cell activation in three phases. Naïve T-cells scan the lymph node forming multiple brief interactions with APCs; stimulatory interactions then induce the expression of activation markers and reduce cell motility. The T-cells then engage in prolonged interactions with APCs and secrete IL-2 and IFN-γ. Finally the cells undergo rapid clonal expansion to generating a population of highly motile effector T-cells (EFFs). The majority of these T-cells undergo apoptosis after antigen clearance, but a small subset remain to give rise to long lived memory T-cells (Fig 1.5) (Mempel et al. 2004; Henrickson et al. 2008; Allam et al. 2009).

Memory T-cells can be broadly divided into two subsets, central memory T-cells (CM) and effector memory T-cells (EM). CM T-cells represent a population of antigen

experienced T-cells that reside within secondary lymphoid organs and have the capacity to generation multiple waves of effector T-cells in response to secondary antigenic challenge. EM T-cells represent a population of antigen experienced T-cells localised to the periphery that allow for rapid responses to be generated upon antigen re-exposure (Sallusto et al. 1999).

CM T-cells are characterised by the expression of CCR7 and CD62L, which are required for migration to secondary lymphoid organs and extravasation via the high endothelial venules (HEV). EM T-cells on the other hand down-regulate CCR7 and exhibit heterogeneous expression of CD62L. Additionally EM T-cells express an assortment of receptors and adhesion molecules that enable them to migrate to sites of inflammation. When compared with CM T-cells, EM T-cells exhibit rapid effector functions and cytokine production. However, they have reduced replicative potential, shorter telomeres and increased sensitivity to apoptosis (Sallusto et al. 2004; Klebanoff et al. 2006). Interestingly EM T-cells can be divided to form 4 distinct subsets based on the expression of the co-stimulatory molecules CD27 and CD28. The progressive loss of CD28 and then CD27 is associated with increased cytotoxicity and cytokine production, but a decrease in replicative potential (Romero et al. 2007; Takata and Takiguchi 2006; Okada et al. 2008).

The specific differentiation pathway taken by naïve T-cells has yet to be fully defined and a single model has yet to be agreed upon (Kaech and Cui 2012). Numerous studies support the theory that antigen experienced naïve T-cells differentiate into EFF T-cells which can then mature into memory T-cells (EM and CM) (Wherry et al. 2003; Champagne et al. 2001). However, the existence of a long live memory T-cell with stem cell-like properties has been hypothesised within the field of immunology for many years. This elusive cell type would theoretically have the capacity to repopulate the pool of fully differentiated effector and memory T-cells following antigenic stimuli.

Polychromatic flow cytometry has identified the existence of a discrete memory stem T-cell population (SCM) that represent ~2–3% of circulating $CD8^+$ and $CD4^+$ T-cells

in humans and non-human primates. These T-cells are characterised by the expression of multiple markers associated with a naïve T-cell phenotype but also express high levels of CD95, IL7Rβ and other differentiation markers (Gattinoni et al. 2011; Lugli et al. 2013). The specific mechanisms that underline the generation of this subset have not yet been defined but *in vitro* activation of naïve T-cells in the presence of IL-2 and IL-7 has been shown to play a critical role (Cieri et al. 2013).

Transcriptional analysis has shown that SCM T-cells exhibit a distinct gene expression profile, which is more closely related to memory T-cells then naïve T-cells. Furthermore, SCM T-cells have been shown to rapidly acquire effector functions following *in vitro* stimulation, exhibit proliferative and survival advantages and have superior anti-tumour activity *in vivo* in mice when compared to other memory subsets (Gattinoni et al. 2011; Cieri et al. 2013).

In chronic viral infection and tumour bearing states, constant antigen exposure drives T-cells further along the differentiation pathway to generate highly differentiated effector memory RA^+ T-cells (EMRA) (Champagne et al. 2001; Valmori et al. 2002) and then "functionally exhausted" T-cells (Klebanoff et al. 2006).

EMRA T-cells are described as "highly" differentiated T-cells that are defined by the re-expression of CD45RA by EM T-cells. The expansion of this population is normally associated with aging, chronic viral infection or tumour burden (Ibegbu et al. 2005; Wills et al. 1999; Nunes et al. 2012). EMRA T-cells also exhibit a reduction in replicative potential which is associated with the expression of CD57 and Killer cell lectin-like receptor subfamily G member 1 (KLRG1) (Ibegbu et al. 2005). Furthermore, EMRA T-cells can be divided into three distinct subsets based on the expression of CD28 and CD27 (Romero et al. 2007).

Functionally exhausted T-cells represent a population that displays significant reductions in cytokine production, effector function, survival and proliferative potential.

Additionally this population is characterised by the expression of immunosuppressive receptors, which upon ligation deliver inhibitory signals to the T-cells (Wherry 2011).

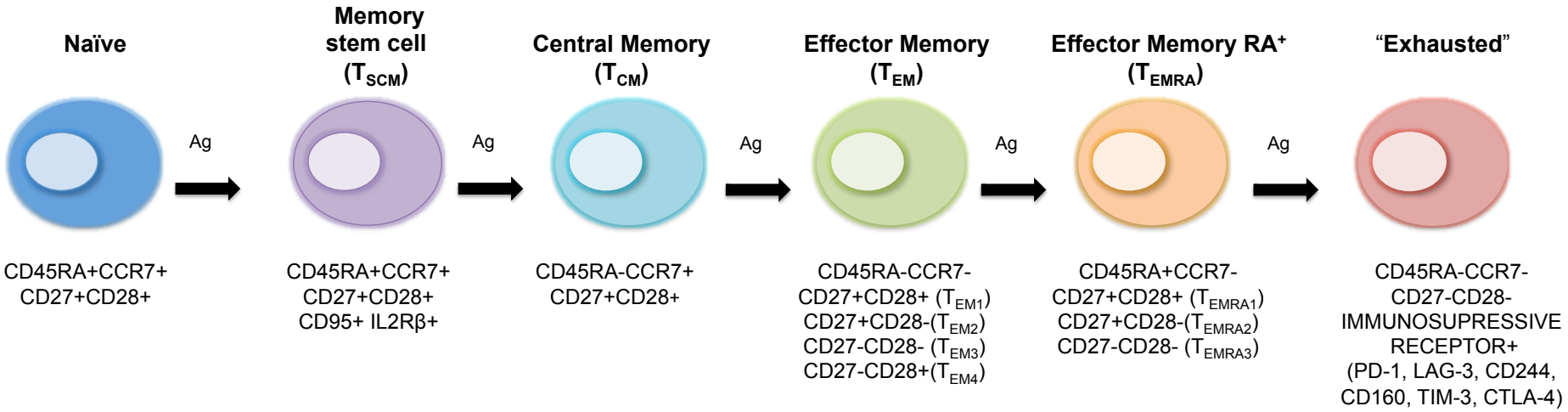

Figure 1.5 Antigen experienced T-cell development. Exposure to cognate antigen induces the clonal expansion of naïve T-cells which undergo the process of functional and phenotypic differentiation to give rise to EFF T-cells. After antigen clearance has occurred remaining EFF T-cells can undergo further differentiation to produce a heterogeneous population of memory T-cells, which includes SCM, CM and EM T-cells. Whether or not these cells types represent discrete subsets or if plasticity occurs between them is still under much debate. However, it is thought that the SCM T-cells may act to maintain and replenish the CM and EM T-cell populations. Under normal conditions, the memory T-cells contribute to host protection from future pathogenic challenge. During chronic viral infections and tumour bearing states, repeated antigen challenge causes T-cells to undergo further differentiation to become EMRA T-cells. Over time the T-cell can become functional exhausted, a state which is characterised by a reduction in proliferative potential and effector function, increased sensitivity to apoptosis and the expression of immunosuppressive receptors (Klebanoff et al. 2006**;** Gattinoni et al. 2011).

1.2 Cancer immunology

The immune system has the capacity to recognise and eliminate tumours but many of these mechanisms become compromised during the process of neoplastic development and progression. Tumours evade the immune system through the activation of inhibitory signalling pathways and creating a hostile microenvironment. Furthermore, given the 'self' nature of tumours, they often exhibit low immunogenicity, which impedes the immune system's ability to "see" the malignant cells (Alderton and Bordon 2012).

Research into the tumour microenvironment and immune systems of cancer patients has provided insights into the evasion mechanisms utilised to prevent the elimination of tumours, many of which are described below. An increasing appreciation of these mechanisms has led to the development of numerous immunotherapeutic strategies (Alderton and Bordon 2012).

1.2.1 Immunosurveillance and immunoediting

The concept of immunosurveillance was hypothesised by Burnet and Thomas (Burnet 1957). Studies involving immunocompromised individuals/animals have shown a greater tendency for the development of malignancies, thus supporting an active role of the immune system in preventing tumour development (Dighe et al. 1994; van den Broek et al. 1996). However, as well as inducing tumour clearance this process can also lead to the selection of "lowly" immunogenic tumour variants. Thus it has been suggested that the immune system can promote tumour growth as well as rejection. Subsequently the concept of immunosurveillance has been revised to include the broad concept of immunoediting (Dunn et al. 2004; DuPage et al. 2012).

Cancer immunoediting can be divided into three processes. The elimination phase represents the process of immunosurveillance. Successful completion of this phase should result in the clearance of the malignant cell population. An alternative process is a period of equilibrium between the host immune system and any remaining malignant cells. While this

process keeps the tumour at bay, it also exerts selective pressure on the remaining heterogeneous population of tumour cells. The final option is tumour escape and is characterised by the rapid proliferation of tumour clones with reduced immunogenicity (Dunn et al. 2002; Kim et al. 2007).

1.2.2 Immune response to cancer

Cellular and humoral responses to cancer are mediated through the recognition of tumour-associated antigens (TAAs), which differentiate malignant cells from their normal counterparts. These TAAs can be divided into numerous categories (Jäger et al. 2001).

Cancer testis antigens are expressed on various malignant tissues, but are absent from all normal tissues except the testis (Jäger et al. 2001). The first example of an cancer testis antigen was reported by Bruggen *et al* who demonstrated the expression of MAGE1 by malignant cells from a single melanoma patient (van der Bruggen et al. 1991). Further analysis of melanoma cancer cell lines led to the identification of the closely related genes MAGE2 (De Smet et al. 1994) and MAGE3 (Gaugler et al. 1994); both also serve as cancer testis antigens.

Melanocyte differentiation antigens are expressed during the process of melanocyte differentiation from epidermal skin cells, and have been associated with CTLs responses to melanoma (Jäger et al. 2001). gp100 is a transmembrane glycoprotein that has been identified as a highly immunogenic TAA for melanoma. Numerous groups have reported the capacity of gp100 specific CTLs to induce killing of $gp100^{+}$ melanoma cells and induce tumour regression (Bakker et al. 1994; Kawakami et al. 1995). Moreover, vaccination with gp100 in combination with IL-2 has been shown to increase clinical responses in a small number of melanoma patients; inducing tumour regression and prolonged progression-free survival (PFS) (Schwartzentruber et al. 2011; Rosenberg et al. 1998).

TAAs can also be generated from normal cellular components that have undergone mutations (Jäger et al. 2001). p53 is an essential tumour suppressor gene that is referred to as the "guardian of the genome" (Menendez et al. 2009). Unsurprisingly mutations of this

gene have been reported in many cancers (Olivier et al. 2010). For example, tumours from squamous cell carcinomas of the head and neck (SCCHN) have been shown to exhibit numerous mutations within p53. Several of these mutations have been shown to yield immunogenic peptides that are recognised by $CD8^+$ CTLs, which can induce the lysis of SCCHN cell lines that possess the specific Y220C mutation (Ito et al. 2007). This phenomenon has also been reported in lung cancer (Ciernik et al. 1996) and in other malignances with mutations of cellular control genes, such as BRAF (V599E) (Andersen et al. 2004).

The overexpression of unmodified self proteins can also serve as a potential source of TAAs (Jäger et al. 2001). The epidermal growth factor receptor HER2 is well-defined example of this. HER2 is normally expressed at low levels on epithelial cells and plays an important role in tissue development. However, its overexpression in breast cancer induces inappropriate cell proliferation and serves as a target for immunotherapy (Vu and Claret 2012). HER2 specific CTLs have been shown to induce the targeted lysis of $HER2^+$ breast, renal and colon cancer cell lines (Brossart et al. 1998). Vaccination with HER2-derived peptides has been shown to induce peptide specific T-cell responses in $HER2^+$ breast cancer patients (Brossart et al. 2000) and has been associated with prolonged PFS (Mittendorf et al. 2011). Furthermore, treatment with monoclonal antibodies against HER2 have been shown to inhibit tumour growth and prevent metastasis in mice (Scheuer et al. 2009) and increase the overall survival (OS) of breast cancer patients (Hudis 2007). However, as only 15-20% of invasive breast cancers are $HER2^+$ there are limitations to the number of patients suitable for HER targeting treatments (Burstein 2005).

The enhanced proteasomal degradation of self-proteins can serve as an additional source of TAAs. The pro-apoptotic protein Bcl-2-associated X (Bax) has been shown to undergo enhanced proteasomal processing in cancer cells (Agrawal et al. 2008; Oh et al. 2010), and subsequently generate peptides that can be presented on MHC-I and allow for T-cell recognition and lysis of tumour cells (Nunes et al. 2011).

Infection with oncogenic viruses has been associated with cell transformation and the development of multiple malignances. Examples include the connection between Epstein Barr virus (EBV) infection and B-cell malignances (Rezk and Weiss 2007), Human T-cell lymphotropic virus-I (HTLV-I) and T-cell malignancies (Taylor 2006) and human papillomavirus (HPV) and cervical cancer. One of the hallmarks of HPV induced cervical cancer is the constitutive expression of the viral proteins E6 and E7, which serve as potential targets for immunotherapy. CTLs specific for peptides derived from HPV E6 and E7 have been shown to induce the targeted lysis of HPV transformed cervical cancer cell lines (Liu et al. 2007; Evans et al. 2001). Therapeutic vaccines against HPV have been tested in patients and have demonstrated that T-cell responses can be induced (Borysiewicz et al. 1996). However the association of a viral infection with the development of cancer, provides an opportunity for cancer prevention through the use of prophylactic vaccine. Encouragingly, in 2006 and 2007 the Food and Drug Administration (FDA) approved the use of prophylactic HPV vaccines Gardasil® and Cervarix®, respectively. Both vaccines have proven to be highly effective in preventing a range of HPV infections and the development of cervical cancerous lesions (Shi et al. 2007; Paavonen et al. 2009). This prophylactic approach can only be applied to cancers caused by infectious agents, and will not work on patients with established disease. For other cancers, targeted immunotherapeutic approaches will be needed.

1.2.3 Mechanism of immune evasion

Tumour evasion of immune responses is one of the confounding factors for the development of effective immunotherapies. Along with reducing tumour immunogenicity there are various other factors involved in the complex process of immune evasion. Immune cells within the tumour microenvironment are usually highly dysfunctional and exhibit an increased expression of immunosuppressive receptors. Furthermore, the tumour microenvironment is characterised by an increased abundance of immunosuppressive cells such as Tregs and myeloid-derived suppressor cells (MDSC) (Kerkar and Restifo 2012;

Wherry 2011). The specific details of the relationship between immunosuppression and tumour progression is still the subject of much research and debate and hence no unified theory on the role of immunosuppression has emerged.

1.2.3.1 T-cell suppression through immunosuppressive receptors

The process of T-cell activation is carefully orchestrated through balancing positive and negative signals received from the environment. While ligation of molecules such as CD28 and CD27 induce an effect that supports T-cell activation, effector function and proliferation, there is a wide array of molecules that have opposing effects. These are generally termed immunosuppressive receptors. Various immunosuppressive receptors have been characterised for human T-cells, however for the purposes of this study three will be discussed in detail: PD-1, TIM-3 and LAG-3.

1.2.3.1.1 Programmed cell death 1 receptor (PD-1)

PD-1 is a transmembrane immunosuppressive receptor belonging to the Ig superfamily. It has two known ligands, programmed cell death ligand 1 and 2 (PDL-1 and PDL-2 respectively), which exhibit differing patterns of distribution. PDL-1 is expressed on a multitude of haematopoietic cells (T-cells, B-cells, DCs, mesenchymal stem cells and mast cells) and non-haematopoietic cells. Furthermore, its expression can be induced in response to type I and II IFNs. PDL-2 however has a much more restricted pattern of expression but it can induced on DCs, macrophages and mast cells (Keir et al. 2008).

The expression of PD-1, like many immunosuppressive receptors is governed by T-cell activation. The intricate link between T-cell activation and the expression of immunosuppressive receptors is thought to act as a "safe guard" to prevent exacerbated T-cell activation and autoimmune responses (Yokosuka et al. 2012). However, in cases of excessive T-cell stimulation, such as chronic viral infections and tumour burden, the increased expression of PD-1 has a detrimental effect upon antigen specific T-cells

essential for viral (Golden-Mason et al. 2007) and tumour clearance (Ahmadzadeh et al. 2009).

Upon expression on the cell surface PD-1 is translocated into the cSMAC and co-localises with the TCR and CD28. Subsequent activation of PD-1 induces the phosphorylation of ITIM and ITSM, and the transient recruitment of the protein-tyrosine phosphatase SHP-2. SHP-2 is then able to dephosphorylate the CD3ζ chain and essential signalling molecules occurring downstream of the TCR (Chemnitz et al. 2004; Yokosuka et al. 2012). It is interesting to note that mutagenesis studies have shown only ITSM is essential for PD-1 functionality (Okazaki et al. 2001; Yokosuka et al. 2012). PD-1 signalling has been shown to inhibit the production pro-inflammatory cytokines and suppress cytotoxic functions, as well as increasing the number of TCR/MHC-peptide interactions required to induce cellular activation (Wei et al. 2013). Engagement of PD-1 also inhibits the phosphorylation and activation signalling molecules downstream of CD28, such as PI3K/AKT (Parry et al. 2005).

Modulating the effects of PD-1 to restore T-cell function and to reverse immune exhaustion has been a focal point of immunotherapeutic research for many years. The use of antagonist PD-1 antibodies both *in vitro* and *in vivo* in murine systems has been shown to increase T-cell survival, proliferative capacity and restore effector functions. This restoration of T-cell function has been shown to have a positive effect on viral and tumour clearance (Blackburn et al. 2008). In light of this encouraging evidence the efficacy of PD-1 antagonistic antibodies has been investigated in numerous early phase clinical trials. One of the key concerns with using antagonistic antibodies against immunosuppressive receptors is the potential loss of immunological control and the generation of autoimmune responses. However, recent reports have indicated that antagonism of PD-1 is well tolerated and has positive clinical outcome in multiple malignances (Brahmer et al. 2012; Topalian et al. 2012; Hamid et al. 2013).

1.2.3.1.2 T-cell Immunoglobulin and Mucin Domain 3 (TIM-3)

TIM-3 is an immunosuppressive receptor expressed upon the surface of IFN-γ producing $CD4^+$ and $CD8^+$ T-cells (Rangachari et al. 2012). Members of the Tim family are characterised by the expression of an extracellular immunoglobulin variable domain (IgV) that possess four non-canonical cysteines, which results in the formation of a unique binding groove not observed in any other members of the Ig superfamily. TIM-3 also possesses a mucin domain, a transmembrane domain and an intracellular domain containing tyrosine based signalling motifs (Sakuishi et al. 2011; Cao et al. 2007). Galectin-9 (GAL-9) has been historically defined as the ligand for TIM-3 and their interactions has been shown to cause cellular aggregation and induce cell death (Zhu et al. 2005). Interactions with other galectin molecules at lower affinities have also been observed (Zhu et al. 2005) as well as galectin-independent interactions (Cao et al. 2007). However, these interactions do not appear to induce the inhibitory effects associated with TIM-3.

The specific molecular events and downstream signalling molecules that mediate TIM-3 activity have not yet been fully defined. However, the ligation of TIM-3 by GAL-9 has been shown to induce the phosphorylation of multi tyrosine residues present within the TIM-3 cytoplasmic tail (van de Weyer et al. 2006; Lee et al. 2011). Rangachari *et al* showed that under "resting" conditions HLA-B-associated transcript 3 (BAT-3) associates with the cytoplasmic tail of TIM-3 through interactions with aa residues 252–270. However, the ligation of TIM-3 induces the phosphorylation of Y256 and Y263 and results in BAT-3 dissociation. This loss of BAT-3 from the cSMAC is of importance due to its association with the catalytically active form of Lck, which plays a key role in T-cell activation. Therefore it has been suggested that the immunosuppressive effects associated with TIM-3 may be mediated by the removal of active Lck from the cSMAC (Rangachari et al. 2012).

The increased expression of TIM-3 on T-cells has been observed in multiple chronic viral infections and tumour bearing states. These T-cells exhibit reductions in their

proliferative potential, effector functions and have been associated with viral persistence and tumour progression. Moreover, the use of antagonist TIM-3 monoclonal antibodies has been shown to rescue exhausted T-cells, restore effector function, promote tumour regression and viral clearance (Zhou et al. 2011; Ngiow et al. 2011; Sakuishi et al. 2011; McMahan et al. 2010). Thus the manipulation of the TIM-3 pathway may represent an attractive avenue for immunotherapy.

1.2.3.1.3 Lymphocyte-activation gene 3 (LAG-3)

LAG-3 is an immunosuppressive receptor closely related to CD4, which associates with MHC-II with greater affinity than CD4 (Huard et al. 1995). The ligation of LAG-3 has been shown to inhibit cytokine production, reduce proliferative potential and cause down-regulation of CD3-TCR complexes in both $CD4^+$ and $CD8^+$ T-cells (Hannier et al. 1998).

The expression of LAG-3 like many immunosuppressive receptors is intrinsically linked to cellular activation. Following antigen recognition and T-cell activation, LAG-3 redistributes and associates with CD3-TCR complexes (Hannier and Triebel 1999). This subsequent recruitment of LAG-3 into the immunological synapse and into close proximity with the TCR may play a role in LAG-3 mediated T-cell suppression.

The exact mechanisms usilised by LAG-3 to inhibit T-cell function are still unknown. Nevertheless it has been shown that the LAG-3 cytoplasmic tail, which contains multiple signalling domains, is essential for function. Specifically the introduction of a mutation within the KIEELE motif has been shown to completely abrogate LAG-3 function (Workman et al. 2002; Workman and Vignali 2003). Thus these findings suggest that the inhibitory effects observed following LAG-3 ligation are due to specific interaction between the KIEELE motif and the recruitment of downstream signalling molecules.

The over expression of LAG-3 has been associated with reduced proliferative potential, effector functions and the exhaustion of antigen specific T-cells in multiple viral infection and malignances. In addition to an inability to induce viral and tumour clearance. However, this can be overcome with the use of antagonistic LAG-3 (Woo et al. 2012; Li et

al. 2013; Matsuzaki et al. 2010), suggesting that manipulation of the LAG-3 pathway has the potential to augment immunotherapy.

1.2.3.2 Regulatory cells

Tregs are a specific subset of $CD4^+$ T-cells that exhibit immunoregulatory properties that has been described in detail in section 1.1.2.2.1.

MDSCs represent a heterogeneous population of partially differentiated myeloid progenitor cells and immature myeloid cells that have been shown to inhibit T-cell function and proliferation. The increased frequency of MDSCs has been reported in numerous human malignances and has been associated with poor prognosis, tumour evasion of host immune system and immune dysfunction. The precise mechanisms responsible for MDSC specific immune dysfunction have not yet been fully defined. However, the high expression of arginase and iNOS by MDSC has been shown to result in the enhanced catabolism of L-arginine, which inhibits T-cell proliferation. Moreover MDSC have also been shown to suppress T-cells through the production of reactive oxygen species (ROS) (Gabrilovich and Nagaraj 2009; Talmadge and Gabrilovich 2013; Khaled et al. 2013).

1.2.3.3 Soluble factors

Various tumour-derived factors have been shown to contribute to the local and systemic immunosuppressive network utilised by cancer cells to evade the immune system. This process has been shown to involve the secretion of immunosuppressive cytokines such as IL-10 and TGF-β, as well as soluble FasL (Kim et al. 2006).

Increased blood serum levels of IL-10 and its production following *in vitro* stimulation have been observed in chronic lymphocytic leukaemia (CLL) patients, when compared with healthy individuals. Moreover high blood serum levels of IL-10 (≥10 pg/mL) has been associated with poor prognosis (Fayad et al. 2001; DiLillo et al. 2012). Similar findings have been observed with regards to soluble FasL; patients classified as ligand "high" (≥6 ng/ml) having shorter median survival (Osorio et al. 2001).

1.2.3.4 Reduction in antigen presentation capacity

Reduced expression of TAAs is a common mechanism utilised by malignant cells to evade immune surveillance. This process can involve various mechanisms, such as gene deletion, point mutations and chromosomal rearrangements to cause the down-regulation or loss of the MHC and/or accessory molecules required for antigen processing and subsequent presentation (Rivoltini et al. 2002).

Loss of TAP (TAP1 and TAP2 subunits) or tapasin expression has been shown to result in a down-regulation of MHC-I molecules, most likely due to the expression of empty and unstable MHC-I molecules, which would be rapidly endocytosed. Furthermore, proteasome defects can lead to impaired peptide processing and reductions in the repertoire of TAAs, thus potentially aiding immune evasion (Hicklin et al. 1999).

Additionally, decreased expression of the co-stimulatory molecules essential for T-cell activation have been observed in numerous malignancies and in some cases have been associated with poor prognosis (Chang et al. 2007).

1.3 Cancer immunotherapy

The principle of cancer immunotherapy is to harness and utilise an individual's immune system to treat their disease and promote tumour clearance. Decades of research have led to the development of numerous strategies and treatments to achieve this goal. Promisingly, cancer immunotherapy was named as the "breakthrough of the year" by the journal Science in 2013, which highlights the immense potential that this field possesses (Couzin-Frankel 2013).

1.3.1 Monoclonal Antibodies

1.3.1.1 Mono-specific

Monoclonal antibodies can exert their effects directly on malignant cells via mechanisms such as ADCC, CDC, blockade of growth factor receptors and the delivery of cytotoxic agents (Scott et al. 2012; King et al. 2008). The use of monoclonal antibodies to

target preferentially expressed antigens has proven to be successful in the treatment of multiple haematological malignancies e.g. CD30 (Brentuximab) in Hodgkin lymphoma (Younes et al. 2012). CD20 (Rituximab) in non-Hodgkin lymphoma (Maloney et al. 1997), Follicular lymphoma (van Oers et al. 2006), Diffuse Large-B-Cell Lymphoma (Feugier et al. 2005) and CLL (Badoux et al. 2011). CD33 (Gemtuzumab ozogamicin) in Acute myeloid leukemia (Larson et al. 2005) and CLL (Robak et al. 2010). CD52 (Alemtuzumab) in CLL (Lundin et al. 2002).

They have also been shown to be useful for the treatment of solid tumours, which includes, ERBB2 (Trastuzumab) in breast cancer (Slamon et al. 2001), VEGF (Bevacizumab) in non–small-cell lung cancer (Sandler et al. 2006), EGFR (Cetuximab) in metastatic colorectal cancer (Jonker et al. 2007).

Additionally monoclonal antibodies can be utilised to modulate T-cell inhibitory co-receptors to enhance anti-tumour immunity. Antagonism of immunosuppressive receptors, including but not limited to, CTLA-4, PD-1, TIM-3 and LAG-3, separately or in combination has been shown to induce anti-tumour immunity and have a significant effect on patient survival in multiple malignances (Sakuishi et al. 2010; Woo et al. 2012; Brahmer et al. 2012; Hodi et al. 2010; Hamid et al. 2013; Wolchok et al. 2013). However, it should be noted that the therapeutic effects observed with single or combined antibody treatment have been shown to be highly variable between patients and between malignancies, therefore strategies will be needed to identify patients that are most likely to respond to treatment.

Alternatively the use of super-agonistic antibodies against stimulatory T-cell co-receptors such CD28 and CD27 could provide an alternative option for the use of monoclonal antibodies in cancer immunotherapy. The use of agonistic anti-CD28 has been shown to induce the proliferation and expansion of T-cells *in vitro*, in a TCR-independent manner (Luhder et al. 2003). However, injection of TGN1412 (an agonistic anti-CD28 antibody) into healthy volunteers caused the massive release of pro-inflammatory cytokines

and induced severe systemic inflammatory reactions. This resulted in the immediate hospitalisation of the volunteers, the termination of the trial and highlighted the potential dangers involved with the modulation of immune checkpoint regulators (Suntharalingam et al. 2006).

The use of agonistic CD27 antibodies has been shown to enhance T-cell proliferation and effector function under sub-optimal TCR activation conditions in murine *ex vivo* experiments. In the absence of TCR signalling no response to CD27 agonistic antibodies was observed. Moreover treatment has been shown to induce tumour regression and increased survival in mice (He et al. 2013). Due to the dependence on TCR signalling to mediate their effects, agonistic anti-CD27 antibodies may be better tolerated clinically, than CD28 agonistic antibodies. The anti-CD27 agnostic antibody CDX-1127 is currently under investigation for safety and efficacy in humans (He et al. 2013).

1.3.1.2 Bi-specific T-cell engaging antibodies (BiTEs)

BiTEs simultaneously engage the TCR via the CD3ε chain and a selected surface antigen expressed on cancer cells. This process induces the formation of an "immunological synapse" between T-cells and cancer cells, thus allowing for targeted cell lysis. The main advantage of BiTEs is their ability to induce the lysis of target cells irrespective of TCR specificity and in a MHC-independent manner. A multitude of BiTEs have been developed, some of which have been shown to be efficacious for the treatment of multiple malignancies (Frankel and Baeuerle 2013).

Blinatumomab is a BiTE that has been developed for the treatment of multiple B-cell malignancies and thus possesses dual specificity for CD3 and CD19. Treatment of patients with non-Hodgkin lymphoma has been shown to induce the activation and expansion of $CD4^+$ and $CD8^+$ T-cells, specifically those of an effector memory phenotype. This coincides with the targeted killing of B-cells and in some patients complete and partial remissions were observed. Interestingly the treatment not only led to the depletion of peripheral tumour cells, but those located within lymph node lesions, the spleen and bone

marrow (Bargou et al. 2008). Blinatumomab has also shown efficacy in patients with acute lymphoblastic leukemia (ALL) (Topp et al. 2011).

This technology has also been applied to the treatment of solid tumours with multiple BiTEs currently in clinical development. AMG 211 (Micromet) is a BiTE that possesses dual specificity for CD3 and CEA. The latter is a cell adhesion molecule that is over expressed on multiple cancers such as breast and lung. AMG 212 (Bayer) possesses dual specificity for CD3 and PSMA which is over expressed on prostate cancer cells (Frankel and Baeuerle 2013).

1.3.2 Therapeutic vaccines

The use of therapeutic vaccines to induce a successful immune response against pre-existing disease has been investigated within a multitude of cancers, but has failed to yield many positive outcomes. Disappointingly it has been reported that >96% of patients who received vaccine therapy failed to exhibit evidence of cancer regression, using the standard oncological reporting criteria. However, it has been suggested that this may be not only due to lack of treatment efficacy, but in part, due to the limitations of the response criteria applied when evaluating of immunotherapies (Klebanoff et al. 2010).

1.3.2.1 Peptide vaccines

Peptide vaccines are typically made up of a single or multiple aa sequences derived from TAA administered in combination with an adjuvant. The aim of this treatment is to induce the activation of T-cells specific for known tumour antigens in the hope these T-cells will then be able to specifically target and kill tumour cells. Thus far they have failed to yield many positive results, which could be due to antigenic heterogeneity observed within patients and/or tumour-associated immune dysfunction. Additionally *in vivo* these peptides are susceptible to the rapid degradation by serum factors and can be tolerogenic when presented by non-professional APCs (Slingluff 2011).

Despite the mounting negative data, some successes has been achieved with the use of peptide vaccines, for example the treatment of melanoma patients with gp100 peptide vaccine in combination with IL-2 had an increased median survival of over six months when compared to patients who received IL-2 only (Schwartzentruber et al. 2011).

1.3.2.2 Dendritic cell vaccines

DCs are specialised APCs that have the capacity to capture, process, and present antigens to T-cells. Furthermore, they express essential co-stimulatory and adhesion molecules required for the formation of the immunological synapse and subsequent antigen specific T-cell activation (Adams et al. 2005; Banchereau and Steinman 1998).

DC vaccines can be divided into three categories, each with the goal of providing retrospective anti-tumour immunity to patients (Palucka and Banchereau 2013).

(1) Non-targeted peptide vaccines that are captured by DCs *in vivo*, as described above in section 1.3.2.1.

(2) Antigenic peptides coupled to antibodies specific for DC markers, such as the endocytic receptor DEC-205, administered in combination with a selected adjuvant to enhance DC maturation. Treatment of DCs derived from healthy individuals and cancer patients *in vitro* with DEC-205 targeting vaccines have been shown to induce enhanced antigen processing and presentation. This resulted in activation and proliferation of antigen specific T-cells and the induction of effector functions (Birkholz et al. 2010). The capacity of this strategy has been evaluated *in vivo* in murine systems. The treatment of mice with DEC-205 targeting vaccines in combination with agonistic anti-CD40 has been shown to stimulation T-cell mediated immunity, induced effector functions and prevented the development of antigen-specific tumours (Bonifaz et al. 2004). Treatment with DEC-205 targeting vaccines, in combination with adjuvants, in humans has been shown to induce humoral and cellular immunity against the tumour antigen NY-ESO-1. Furthermore, stabilisation of disease was observed in 13 patients and two patients experienced significant tumour shrinkage (Dhodapkar et al. 2014). While the clinically reported results are modest,

they highlight that DEC-205 targeting vaccines were well tolerated *in vivo*, induced both humoral and cellular immunity and exhibited some clinical effects. This supports their further development.

(3) *Ex vivo* loading of DCs with antigen peptides. This process involved in the *ex vivo* culture of monocytes/ peripheral blood mononuclear cells (PBMCs) in cytokine conditioned media to induce their differentiation and development into DCs, which can then be loaded with selected tumour antigens and re-infused in patients. Thus far DC vaccines of this nature have been shown to be well tolerated and induced the activation and expansion of antigen specific T-cells (Palucka and Banchereau 2012).

The greatest achievement thus far achieved with DC-based vaccines was the development of Sipuleucel-T, which in 2010 become the first cancer vaccine and cell based therapy approved by the FDA. Sipuleucel-T is an immunotherapy produced by the *ex vivo* treatment of autologous patients DCs with the recombinant fusion protein PA2024, which is made up of prostatic acid phosphatase fused to granulocyte–macrophage colony-stimulating factor. In a double-blind, placebo-controlled, multi-centre trial it was shown that Sipuleucel-T induced humoral and cellular immune responses and increased the median survival by 4.1 months, over the placebo controls (Kantoff et al. 2010). Collectively these findings highlight the efficacy of *in vivo* targeting or *ex vivo* manipulation of DCs to induce anti-tumour immune responses and highlight the importance of effective antigen presentation to mediate this effect.

1.3.3 Adoptive T-cell transfer (ACT)

ACT is an active immunotherapeutic approach that involves the identification, *ex vivo* expansion and re-infusion of autologous or allogeneic T-cells with anti-tumour activity. Various approaches have been shown to increase the efficacy of ACT, such as lympho-depletion before infusion, specifically targeting immunosuppressive cell types such as Tregs and complementing the transfusion with homeostatic cytokines. Furthermore, the differentiation state of the T-cells selected for reinfusion has been shown to be highly

important. While highly differentiated $CD8^+$ T-cells exhibit increased effector functions *in vitro* they have been shown to be up to 100-fold less effective *in vivo* than T-cells at an early stage of differentiation, such as CM T-cells, due to defects in proliferative potential and increased sensitivity to apoptosis (Rosenberg et al. 2008; June 2007; Gattinoni et al. 2006).

ACT has been shown to be successful in the treatment of patients with melanoma. In a clinical trial by Rosenberg *et al*, 20 out 93 patients (22%) showed complete tumour regression with ongoing regression beyond three years being observed in 19 patients (Rosenberg et al. 2011). Furthermore, melanoma specific ACT as been successful for the treatment of metastatic melanoma (Hong et al. 2010). In addition, ACT has shown varying degrees of efficacy in the treatment of other malignancies (June 2007) such as gastric cancer; patients that received ACT plus chemotherapy exhibited significantly longer survival (>3 months) when compared with chemotherapy alone (Kono et al. 2002).

1.3.3.1 Genetic modification of T-cells

Achieving successful T-cell engraftment, survival, proliferation and ultimately T-cell function can be hindered by the limitations associated with the cellular "starting material" and the hostile tumour microenvironment of the patients. Thus the genetic manipulation of T-cells to increase their efficacy and resistance to immunosuppressive strategies is an attractive option for cancer immunotherapy.

To enhance survival and *in vivo* longevity, CTLs can be transduced with chimeric GM-CSF-IL-2 receptors. These T-cells deliver IL-2 signalling as a consequence of GM-CSF binding, which results in an autocrine loop of proliferative signals (Evans et al. 1999). Other strategies include engineering T-cells to ubiquitously express the co-stimulatory receptor CD28 (Topp et al. 2003) and the catalytic subunit of telomerase reverse transcriptase (hTERT) to enhance replicative potential (Rufer et al. 2001). Additionally, the introduction of a chimeric protein expressing the extracellular PD-1 domain and the intracellular CD28 domain could redirect PD-1 signalling and overcome immunosuppression (Prosser et al. 2012). However, as many of these mechanisms redirect

"normal" T-cell processes to enhance activation, survival and proliferation, great care must to taken to not induce inappropriate T-cell responses, which could lead to the development of T-cell leukaemias. Furthermore, the specificity of T-cells can be redirected through TCR gene transfer and the use of chimeric antigen receptors.

1.3.3.1.1 TCR gene transfer

Under normal circumstances the antigen specificity of T-cells is dictated by the re-arrangement of specific TCR α and β chains. The genetic transfer of new TCR α and β chains, utilising retroviral or lentiviral constructs, allows for the redirection of T-cell specificity towards a selected TTAs. This process has the potential to be a promising immunotherapy strategy for the treatment of various malignances as well as viral infectious diseases (Thomas et al. 2010). It has been shown that TCR transduced cells can be activated by antigen *in vivo*, undergo significant expansion, home to effector sites and contribute to tumour clearance in murine models (Schumacher 2002).

For stable TCR expression the α and β chains must form a heterodimer and associate with the CD3 complex. However, the undesired pairing of introduced TCR chains with endogenous TCR chains could occur and result in the generation of TCRs of unknown specificity, which could potentially be auto-reactive (Kershaw et al. 2014). This highlights one of the main limitations of this approach.

1.3.3.1.2 Chimeric Antigen Receptors Therapy (CAR-T)

CAR-T is an immunotherapeutic strategy that involves manipulating and re-directing the specificity of autologous T-cells towards a selected cell-surface antigen. Chimeric antigen receptors (CARs) combine the antigen-recognition domain of a specific monoclonal antibody with an intracellular domain of the CD3-ζ chain or FcγRI, which allows the receptor to trigger T-cell activation. Furthermore, the lack of HLA specificity and MHC recognition required for recognition makes the process an attractive personalised 'off the shelf' immunotherapy (Maus et al. 2014).

The first generation of CAR-T trials involved the introduction of only a chimeric antigen receptor into prospective T-cells but had limited success as a treatment option as the absence of co-stimulatory signalling led to anergy and failure to expand *in vivo* (Heslop 2010). However, the addition of co-stimulatory signalling domains from molecules such as CD137 (4-1BB) and CD28 have been shown to enhance CAR-mediated T-cell responses and has led to the emergence of second and third generation CARs (Maus et al. 2014).

This approach has been applied to both solid tumours (Zhao et al. 2009) and haematological malignancies, in various *in vitro* and *in vivo* models and clinical trials including CLL (Porter et al. 2011; Kalos et al. 2011) and ALL (Grupp et al. 2013). Encouragingly it has been recently shown that CAR T-cells can be detected in patients 11 years post infusion at frequencies higher than expected for most vaccine approaches (Scholler et al. 2012).

1.4 Chronic lymphocytic leukaemia

CLL is a B-cell leukaemia that is characterised by the accumulation of mature B-cells in the blood, bone marrow, lymph nodes and lymphoid tissue. These cells can be phenotypically identified by their expression of CD19, CD5 and CD23, and the low expression of other markers such as CD22 (Zenz et al. 2010b).

1.4.1 Aetiology and epidemiology

CLL is most common type of leukaemia in the western world, representing 22-30% of all leukaemia cases with a worldwide incidence of between 1 and 5.5/100,000 people. The incidence of CLL increases with age, with the median age at diagnosis being 64-70 years of age. Furthermore, CLL has been shown to be more prevalent in males than females (approximately 2:1) and the highest incidence in Caucasians (Redaelli et al. 2004).

The specific cellular origin and the exact mechanisms that result in development of CLL are still unknown. However, it is widely accepted that CLL is derived from the development of a $CD19^{+}CD5^{+}$ pre-malignant B-cell (Seifert et al. 2012). Familial history

has been shown to be a risk factor associated with the development of CLL (Goldin et al. 2009), suggesting the role of inherited traits in the manifestation of the disease. Multiple genome-wide association studies have identified numerous single nucleotide polymorphisms (SNP) that are associated with an increased incidence of disease in CLL patients such as hTERT and protection of telomeres protein 1 (POT1) which are both important in telomere maintenance (Di Bernardo et al. 2008; Speedy et al. 2013).

1.4.2 Symptoms and diagnosis

Diagnosis is made based on the detection of a clonal population of B-cells within the bone marrow, lymphoid organs or the peripheral blood, that bears the phenotypic and morphological hallmarks associated with CLL. Furthermore, the presence of at least 5000 $CD19^{+}CD5^{+}$ B-cells/L is required for a diagnosis (Gribben 2010). At the time of diagnosis many patients present with few symptoms but this changes with disease progression. Common symptoms include hepatomegaly, splenomegaly, lymphadenopathy and a increase in lymphocyte doubling time, leading to the accumulation of malignant CLL cells (Hallek 2005). Furthermore, due to inherent abnormalities in humoral and cell mediated immunity, CLL patients are subject to numerous opportunistic infections (Morrison 2010).

1.4.3 Staging

Rai (Rai et al. 1975) and Binet (Binet et al. 1981) developed the current systems utilised for the clinical staging of CLL patients. The Rai staging system is based on the progressive accumulation of malignant CLL cells due to lymphocytosis, lymphadenopathy, splenomegaly and hepatomegaly. While the Binet staging systems is based upon the involvement of five specific lymphoid sites (cervical, axillary and inguinal lymph nodes, spleen and liver) with the disease. Collectively these two systems allow patients be divided into those that have early (Binet A, Rai 0), intermediate (Binet stage B, Rai I and II) or advanced (Binet stage C, Rai III and IV) disease. However, to obtain a comprehensive evaluation of an individual patient's disease, likelihood of progression, time to first

treatment (TTFT) and overall predicted survival, numerous molecular prognosis markers must be considered (Gribben 2010).

1.4.4 Prognostic markers

CLL is highly heterogeneous disease with some patients presenting with stable non-progressive disease, while other rapidly progress to develop an aggressive disease. These two forms of CLL can be stratified based on the presence of a combination of prognostic markers (Gribben 2010).

1.4.4.1 ZAP-70

ZAP-70 is a member of the protein-tyrosine kinase family that is typically expressed by T-cells and natural killer cells (Wang et al. 2010). Multiple independent studies have shown that the high expression of ZAP-70 (>20% ZAP-70^+ CLL cells) is associated with shorter PFS and OS (Del Principe et al. 2006; Dürig et al. 2003) as well as shorter TTFT (Rassenti et al. 2008).

The specific molecular mechanisms behind this have not yet been fully elucidated but the increased expression of ZAP-70 has been associated with enhanced signalling via the BCR in CLL cells (Chen et al. 2005). Furthermore, the expression of ZAP-70 has been shown to enhance nuclear factor-κB (NF-κB) signalling downstream of the BCR. Pede *et al* demonstrated that the induction of ZAP-70 in previously ZAP-70^- CLL cells induced the expression of NF-κB target genes (IL-1β, IL-6 and IL-8) at the mRNA and protein level, following BCR signalling. Furthermore, blockade of the NF-κB resulted in a complete knockdown of the expression of the NF-κB target genes described above (Pede et al. 2013). In addition, the increased expression of ZAP-70 has been shown to enhance cell survival and increase the expression of chemokine receptors, adhesion molecules and cell migration (Calpe et al. 2011; Richardson et al. 2006).

1.4.4.2 CD38

CD38 is a single chain type II transmembrane molecule involved in regulating the activation and proliferation of T-cells. However, it's expression on CLL cells can be utilised to differentiate patients into two sub-groups with different clinical outcomes (Damle et al. 1999; Del Poeta et al. 2001). Patients that have >30% $CD38^+$ CLL cells have been shown to have shorter OS, TTFT and higher absolute lymphocyte counts (Malavasi et al. 2011).

The exact cause of the poor prognosis associated with increased CD38 expression is still not fully known. However, $CD38^+$ CLL cells have been shown to more resistant to apoptosis in *in vitro* culture, suggesting they may have a survival advantage, over their $CD38^-$ counterparts. Furthermore, $CD38^+$ CLL cells exhibit a differential gene expression profile when compared to $CD38^-$ CLL isolated from the same monoclonal source. For example, $CD38^+$ CLL cells have relative over expression of genes associated with cytoprotection and resistance to apoptosis, such as MCL-1 and VEGF (Pepper et al. 2007).

CD38 has one known ligand, CD31 (Deaglio et al. 2010). The interaction between these molecules has been shown to induced the proliferation of CLL cells and induce a gene transcript signature associated with cell migration and lymph node homing (Deaglio et al. 2010). Furthermore, the expression and activation of CD38 has been shown to increase the migration of cells in response to the chemo-attractant CXCL12 (Vaisitti et al. 2010). Additionally, when compared to $CD38^-$ CLL cells, $CD38^+$ CLL cells have been shown to have higher levels of cGDPR and cADPR, both of which are associated with Ca^{2+} mobilisation. This indicates that CD38 is enzymatically active in CLL cells. Furthermore, transfection of the CLL-like cell line, Mec-1, with CD38 was shown to significantly increase the production of cADPR and induce proliferation and cell migration, when compared with $CD38^-$ Mec-1 cells and Mec-1 cells transfected with a enzymatically defective mutant CD38 (Vaisitti et al. 2015).

1.4.4.3 CD49d

The process of leukocyte migration from the periphery to second lymphoid organs is a 4 stage process that involves tethering and rolling across the endothelial surface, leukocyte stimulation, cell arrest, spreading and finally migration. At each stage α4 integrins play a critical role (Rose et al. 2002).

CD49d is an α subunit of the α4β1 lymphocyte homing receptor, which interacts with vascular cell adhesion molecule-1 (VCAM-1) and is key in the lymphocyte migration (Zucchetto et al. 2012). Furthermore, it has been shown that interaction between CD49d and its ligand can inhibit the process of apoptosis through the up-regulation of the anti-apoptotic molecule BCL-x_L (Koopman et al. 1994; Hayashida et al. 2000).

The expression of CD49d has been shown to be highly variable in CLL patients, however high expression has been shown to significant correlate with other CLL related prognostic markers, and is associated with shorter TTFT and OS (Nückel et al. 2009; Majid et al. 2011; Gattei et al. 2008). Additionally it has been shown the CD49d is the most powerful flow-based marker for the evaluation of CLL prognosis (Bulian et al. 2014).

Although the specific mechanism for these clinical correlations is unknown, it could be hypothesised that CLL cells with high CD49d expression are able to more readily undergo migration re-enter lymphoid tissue tumour microenvironments that are cytoprotective and drive proliferation. Interestingly the blockage of CD49d in a physiologically relevant model of the peripheral vasculature was shown to inhibit CLL cell migration (Walsby et al. 2014) This suggests that CD49d could be a useful therapeutic target for the treatment of CLL.

1.4.4.4 Immunoglobulin heavy chain variable (*IGHV*) mutation

The formation of Ig through the selection and recombination of the *V*, *D* and *J* domain gene segments occurs within the bone marrow. These genes can then be subject to somatic hypermutation within the germinal centres of secondary lymphoid organs, to

produce high affinity Ig. This process of somatic hypermutation, specifically within the *IGHV* region, has been shown to stratify CLL patients into two discrete subsets which exhibit significantly different clinical outcomes (Damle et al. 1999). Patients with unmutated *IGHV* regions (>98% homology to germline) have been shown to have a median survival time that is over three times shorter than patients with mutated *IGHV* status (Hamblin et al. 1999).

The specific cellular origin of unmutated and mutated CLL is still an area surrounded by a great deal of debate. Some suggest that both mutated and unmutated CLL is derived from same subset of marginal zone B-cells (Chiorazzi and Ferrarini 2011). While others support the concept that unmutated *IGHV* CLL is derived from naive "pre-germinal centre" B-cells and mutated *IGHV* CLL from antigen experienced B-cells presented within the germinal centres (Gribben 2010). Interestingly, transcriptome analyses of CLL cells and normal B-cells from healthy PBMCs has shown that mutated *IGHV* CLL cells were transcriptionally more similar to $CD5^+CD27^+$ memory B-cells while unmutated *IGHV* CLL cells were transcriptional more similar to $CD5^+CD27^-$ B-cells (Seifert et al. 2012). This suggests potential differences in the cellular origin of unmutated and mutated CLL.

1.4.4.5 Genetic aberrations

Analysis of CLL cells by fluorescent *in situ* hybridisation (FISH) has led to the identification of multiple genetic aberrations that can be associated with prognosis and patient outcome. Deletion of the short arm of chromosome 17 (del 17p) occurs in approximately 7% of CLL patients and has been associated with highly aggressive disease and is typically accompanied by loss of p53 function. p53 plays an intrinsic role in regulating the cell cycle, repairing DNA damage and initiating apoptosis when DNA repair fails, thereby preventing the introduction of mutations that may lead to cell transformation and cancer (Menendez et al. 2009). Unsurprisingly mutations of p53 have been widely associated with significantly shorter PFS and OS in CLL. Furthermore, patients with p53

mutations or deletions exhibit greater resistance to treatment and increased incidence of relapse (Zenz et al. 2010a; Rossi et al. 2014).

Deletion of the long arm on chromosome 11 (del 11q) occurs in approximately 15% of CLL patients and is associated with aggressive disease, shorter survival and unmutated *IGHV* status (Döhner et al. 2000). The presence of three copies of chromosome 12 (trisomy 12) occurs in approximately 15% of CLL patients and has also been associated with shorter survival (Döhner et al. 2000). Conversely deletion of the long arm of chromosome 13 (del 13q), which is the most common genetic aberration observed in CLL (approximately 50%), is associated with a favourable clinical outcome and mutated *IGHV* status (Döhner et al. 2000; Chiorazzi 2012).

1.4.4.6 CD4:CD8 ratio

Healthy middle-aged individuals have a CD4:CD8 T-cell ratio between 2-11, however with age it has been observed that there is a steady decrease in this ratio, which can sometimes result in an inversion (CD4:CD8 ≤1). The inversion in the CD4:CD8 ratio in "healthy" individuals has been associated with $CD4^+$ and $CD8^+$ T-cells of a highly differentiated or activated phenotype, and decreased survival in follow-up studies (Wikby et al. 2002; Strindhall et al. 2007; Olsson et al. 2000).

Within CLL patients this inversion has been associated with a highly differentiated memory phenotype in both the $CD4^+$ and $CD8^+$ T-cells, increased PD-1 expression as well as significantly shorter TTFT and PFS (Nunes et al. 2012). The specific mechanism behind this observation is unknown, however it could be related to phenotypic and potentially functional differences within the T-cell compartment of normal ratio (CLL^{NR}) and inverted ratio (CLL^{IR}) CLL patients.

1.4.5 The lymph node microenvironment

CLL cells derived from the peripheral blood are predominantly in G0/G1 "resting" phase of the cell cycle. This is in stark contrast to the cells located within the specialised

niche known as the lymph node microenvironment, where CLL cell survival and proliferation is supported by a host of accessory cells (Fig 1.6) (Messmer et al. 2005; Burger and Gribben 2014). Because of the reliance on external signals from the microenvironment, CLL cells express an array of adhesion molecules to facilitate migration and infiltration into the lymph nodes (Behr et al. 1998). In keeping with this statement, the recent development of a model *in vitro* circulating system has shown that CLL cells under sheer force up-regulate the expression of L-selectin (CD62L), CXCR4 and CD49d (Walsby et al. 2014), all of which are involved in cell migration and chemotaxis (Venturi et al. 2003; Burger et al. 1999).

Once within the lymph node mircroenvironment CLL cells are able to interact with bone marrow-derived stromal cells, nurse-like cells and T-cells, which collectively provide proliferative and cytoprotective support (Burger and Gribben 2014). However, it is T-cells, specifically $CD4^+$ helper cells that have been shown to be essential for the engraftment, survival and proliferation of CLL cells in *in vivo* murine systems (Bagnara et al. 2011). Furthermore, it has been shown that proliferating CLL cells co-localise with activated $CD4^+$ within lymph nodes of patients (Patten et al. 2008).

1.4.6 Immunological defects within CLL

T-cells from CLL patients have been shown to exhibit numerous defects in their ability to form IS with CLL cells. Co-culture of healthy allogeneic T-cells with CLL cells has been shown to significantly decrease the recruitment of key molecules involved in the formation of the IS and impair recruitment of Lck (Ramsay et al. 2008). Collectively, the data from this study indicates that direct interaction between CLL cells and T-cells interferes with recruitment of molecules essential for the formation of the IS and thus antigen-dependent activation. Therefore it could be suggested that CLL cells are able to evade the immune system by preventing the recognition of potential TAAs by inhibiting the successful formation of the IS and induction of T-cell activation. Additionally, it has

shown CLL cells have been shown to decrease the differentiation of Th1 cells and cause a skewing towards a Th2 response (Görgün et al. 2005).

Additionally, the increased expression of PD-1 has been observed within the $CD8^+$ T-cell populations, specifically within the effector population. This increased expression has been associated with the inversion of CD4:CD8, a known marker for poor prognosis (Nunes et al. 2012), suggesting a role of immunosuppressive receptors in disease progression. However, the increased expression of PD-1 has also been associated with the increased production of the effector cytokines IFN-γ and TNF-α (Riches et al. 2013) suggesting that PD-1^+ T-cells in CLL patients may represent an activated rather than an exhausted phenotype. Therefore investigations into the expression of multiple immunosuppressive receptors may be required to distinguish between activated and exhausted T-cells within CLL.

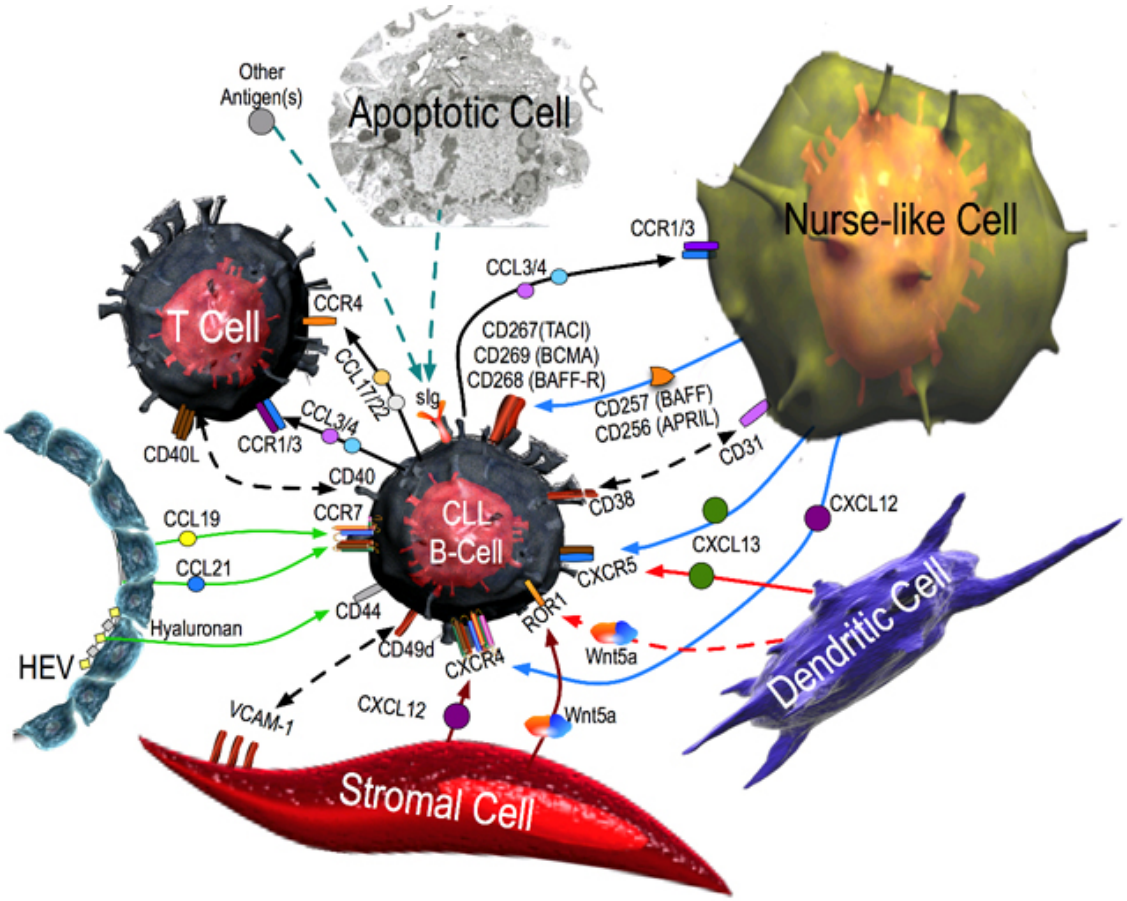

Figure 1.6 The CLL tumour microenvironment (Adapted from Fecteau and Kipps 2012). Accessory cells within the lymph node microenviroment provide proliferative and supportive signals to CLL cells in a contact dependent (receptor-ligand interactions) and independent manner (cytokines and chemokines).

1.4.7 Treatments

The treatment approaches used for CLL are extremely wide and varied, which is to be expected in such a heterogeneous disease. Over the past decades the treatment options for patients have dramatically improved and expanded to include chemotherapy, utilising established and novel compounds, immunotherapy and combinations of the two approaches, known as chemoimmunotherapy.

1.4.7.1 Chemotherapy

1.4.7.1.1 Alkylating agents

Generally cancer cells undergo more rapid proliferation and have defects within multiple DNA repair mechanisms, when compared to healthy cells. Thus making them more susceptible to DNA damage. Alkylating agents act though the transfer of alkyl carbon groups onto the DNA bases, resulting in covalent adducts and the formation of DNA lesions. Due to defects in the DNA repair processes in cancer cells, double-strand DNA breaks can accumulate and result in cell death (Fu et al. 2012).

The most widely used alkylating agents in the treatment of CLL are chlorambucil and cyclophosphamide. However, the exact mechanisms of action through which these drugs work still remains unclear. Chlorambucil has been shown to intercalate into numerous cellular components such as proteins, RNA and DNA; the intercalation with DNA, and the induction of cross-linking and subsequent DNA damage is thought to mediate the major anti-tumour effects (Begleiter et al. 1996). Cyclophosphamide is pro-drug that requires *in vivo* metabolism to produce active derivatives, such as 4-hydroxy-CTX. It has been suggested that cyclophosphamide derivatives can induce cytoskeleton alterations and the expression of anti-angiogenic and pro-apoptotic factors. Furthermore, cyclophosphamide has been suggested to have immunomodulatory effects (Penel et al. 2012).

Despite its use as a front line therapy, chlorambucil has been shown to have a low level of efficacy and no effect on OS (Dighiero et al. 1998). Therefore there remains a need for new and improved treatments. Bendamustine is a novel alkylating agent that received FDA approval for use in CLL in 2008. When compared to chlorambucil as first line treatment, bendamustine induced significantly higher response rates and longer PFS (Knauf et al. 2009).

1.4.7.1.2 Purine analogues

Purine analogues are a class of drugs that mimic the structure of metabolic purines, inhibit the function of multiple enzymes involved in DNA synthesis and repair, and ultimately induce cell death via apoptosis. There are currently several purine analogues used in the treatment of CLL, including fludarabine, cladribine and pentostatin (Pettitt 2003).

Fludarabine is the most extensively used purine analogue in the treatment of CLL. Fludarabine is a pro-drug that requires metabolism and dephosphorylation for successful entry into CLL cells. The metabolite must then undergo rephosphorylation in order to produce the active substance F-ara-ATP. F-ara-ATP inhibits enzymes involved in DNA synthesis, such as DNA polymerase, primase and ligase (Ricci et al. 2009). The clinical efficacy of fludarabine has been investigated in numerous studies and has been shown to have an overall response rate of 53-74% in patients and is more effective than cladribine and pentostatin. However, fludarabine is still not a curative option and numerous side effects have been associated with its use such as myelosuppression and the development of secondary malignancies (Lukenbill and Kalaycio 2013). Thus more research towards the development of specific and targeted therapy options is required.

1.4.7.2 Emerging pharmaceutical agents

Bruton tyrosine kinase (BTK) has been shown to play a key role in signalling downstream of the BCR and is expressed in multiple B-cell malignancies (Hendriks et al. 2014), including CLL, however the level of expression has been shown to be highly

variable among patients (Herman et al. 2011). Ibrutinib is a specific BTK inhibitor that inhibits the kinase activity through irreversibly binding to the cysteine at position 481 (Hendriks et al. 2014). *In vitro* treatment with ibrutinib has been shown to induce apoptosis and inhibit replication of CLL cells, even in the presence of pro-survival signals designed to mimic the *in vivo* microenvironment (Herman et al. 2011; Ponader et al. 2012). Ibrutinib treatment has been shown to inhibit disease progression *in vivo* in murine systems (Ponader et al. 2012) and inhibit *in vivo* proliferation in CLL patients (Cheng et al. 2014). Recently, a phase 3 multi-centre clinical trial showed that treatment with Ibrutinib increased PFS and OS in comparison to treatment with the anti-CD20 monoclonal antibody, Ofatumumab (Byrd et al. 2014).

PI3Ks are another family of molecules essential for transmitting signals from the BCR (Srinivasan et al. 2009). PI3Ks can be divided into 3 classes with class I containing four different isoforms. Of interest, PI3Kδ has been shown to be critical for B-cell survival and function (Fruman and Rommel 2014). Idelalisib is a PI3Kδ isoform-specific kinase inhibitor, *in vitro* treatment has been shown to inhibit cell migration in response to chemokine gradients and decrease cell viability even in the context of BCR activation. Additionally, treatment has been shown to inhibit the phosphorylation and activation of AKT and ERK (Hoellenriegel et al. 2011).

Idelalisib has been shown to be well tolerated and when used as a single agent has shown a 72% response rate in CLL patients. Additionally, it was shown that patients treated with ≥150mg had signifcantly longer PFS then those treated with a lower dose (32 months vs 7 months) (Brown et al. 2014). Futhermore, Idelalisib when used in combination with Rituximab resulted in signifcant improvements in PFS and OS, compared to Rituximab alone (Furman et al. 2014).

1.4.7.3 Haematopoietic stem cell transplantation (HSCT)

Allogeneic HSCT involves the transfer of HSCs from a HLA tissue-matched donor to a recipient. The aim is to use the donor immune system to induce a graft versus

leukaemia (GVL) effect and thereby promote the killing of the recipient's CLL cells. However, there is also the potential for the development of graft versus host disease (GVHD) (Dreger and Montserrat 2002). Generally HSCTs is not a suitable treatment strategy for many CLL patients due to the indolent nature of the disease and the age-related risks associated with transplantation. Furthermore, the efficacy of HSCT in comparison to other more suitable treatments is still unclear (Gribben 2009). A recent study has shown that HSCT can result in prolonged event-free survival for some patients, when compared to those who received no treatment. However, when compared to chemotherapy as a first-line therapy it offered no survival advantage (Dreger et al. 2010). Therefore further research is required to determine the efficacy and value of HSCT as a treatment option over immunotherapy, chemotherapy or combination of them both.

1.4.7.4 Immunotherapy

1.4.7.4.1 CLL specific monoclonal antibody therapy

CD20 is a phosphoprotein ubiquitously expressed by CLL cells making it an attractive target for mAb therapy. Rituximab is a chimeric CD20 antibody that when used as a single agent to treat CLL is able to induce the clearance of circulating malignant cells, but this effect can only be sustained with further treatment (Winkler et al. 1999). Furthermore, the rate of complete remission observed with rituximab treatment is extremely low (9%) (Hainsworth et al. 2003). However, when used in combination with standard chemotherapy, rituximab has proven to have greater clinical efficacy (Robak et al. 2010; Badoux et al. 2011). Since the development of rituximab, second and third generation CD20 antibodies have been developed which interact with different CD20 epitopes and contain different Fc fragments to enhance binding to Fc gamma receptors. Ofatumumab is a third generation type I, fully humanised CD20 antibody, which recognises a different region of the CD20 protein than rituximab, and has been shown to be effective in CLL patients that are refractory to fludarabine and alemtuzumab (Wierda et

al. 2011; Wierda et al. 2010). Obinutazumab is a third generation type II fully humanised CD20 antibody that has been shown to significantly prolong PFS and OS compared to chlorambucil alone or rituximab plus chlorambucil (Goede et al. 2014).

CD52 is a glycoprotein that is highly expressed on a variety of haematopoietic cells including normal and malignant B and T-cells, but not HSCs (Rodig et al. 2006). Alemtuzumab is a humanised CD52 antibody, which has been shown to be effective in the treatment of CLL patients, specifically fludarabine refractory patients (Keating et al. 2002; Montillo et al. 2008).

BiTE represent a novel antibody therapy, described in section 1.3.1.2, that involves the conjugation of Ab fragments that simultaneously engage the TCR and antigen on target cells. Blinatumomab is a BiTE that has dual specificity for the CD3 and CD19 and proven to be successful in the treatment of numerous hematological malignancies. To date blinatumomab has not been tested *in vivo* in the context of CLL. However, *in vitro* treatment of PBMCs from CLL patients was shown to induce the activation and expansion of T-cells, specifically of an effector memory phenotype. Furthermore, these T-cells released cytotoxic granules, expressed high levels of effector cytokines and induced apoptosis of CLL cells (Wong et al. 2013).

While antibody therapy has been shown to be beneficial in the treatment of CLL, this therapeutic option does have limitations such as high cost of production, limited access to tumour microenvironments and discrepancies between the *in vitro* and *in vivo* results have been observed (Chames et al. 2009).

1.4.7.4.2 T-cell based therapies

1.4.7.4.2.1 CLL associated tumor antigens

One of the key factors of any successful T-cell based therapy is the identification of TAAs expressed exclusively by malignant cells but absent on healthy tissue, to prevent off-target effects. One of the common sources of TAAs are proteins that are overexpressed

specifically by the malignant cells. Survivin (Schmidt et al. 2003), MDM2 (Mayr et al. 2006), CD23 (Bund et al. 2007), RHAMM (Giannopoulos et al. 2006) and CD229 (Bund et al. 2006) have all been shown to be relatively overexpressed by CLL cells. Moreover, peptide-specific CTL lines generated from healthy donors and CLL patients have been shown to be activated in response to CLL cells and induce their targeted lysis. However, in each of the reported cases T-cell clones specific to a defined peptide epitope were never generated. Vaccination with peptides derived from RHAMM has been investigated in a limited number of CLL patients. RHAMM vaccination appeared to increase the frequency of RHAMM-specific T-cell *in vivo* in CLL patients, which exhibited effector function *ex vivo* and could induce the lysis of autologous CLL cells. However, the data presented in the study was highly variable and the association with clinical efficacy was weak (Giannopoulos et al. 2010). Therefore further research on the identification of more immunogenic targets is clearly required.

Proteins that exhibit other irregularities in their expression can also be potential TAAs in CLL. For example the pro-apoptotic protein Bax has been shown to undergo enhanced proteasomal degradation in CLL (Agrawal et al. 2008). As the proteasome is instrumental in the generation of MHC-I/peptide complexes it could be hypothesised that peptides derived from the degradation of Bax could be presented to $CD8^+$ T-cells. This concept was confirmed in a proof-of-principle study by Nunes *et al,* in which Bax-specific $CD8^+$ T-cell clones, isolated from healthy individuals, were able to induce the targeted lysis of CLL cells (Nunes et al. 2011). However, the existence of these T-cells in CLL patients was not explored.

1.4.7.4.3 CLL specific CAR-T

CART-19 is lentiviral vector that expresses the chimeric antigen receptors specific for the B-cell antigen CD19, as well as the CD3-zeta chain and the signalling domain for CD137. Recognition of CD19 by CART-19 transduced T-cells has been shown to induce the temporal release of various cytokines and the lysis of leukaemia cells, as well as healthy

B-cells, *in vivo*. Furthermore, these modified T-cells have been shown to expand >1000-fold *in vivo* and persist in the peripheral blood and bone marrow of patients for up to six months. It has been hypothesised that after the elimination of the tumour cells, CART-19 T-cells may be stimulated by healthy B-cells within the bone marrow to generate "CAR memory", thus allowing for the maintenance of CART-19 T-cells *in vivo* and hence immunosurveillance (Kalos et al. 2011; Porter et al. 2011). While CART-19 has proven to be an extremely effective treatment, it has the major drawback of targeting normal healthy B-cells.

The receptor tyrosine kinase-like orphan receptor 1 (ROR1) was identified as a highly expressed gene in malignant $CD19^+$ $CD5^+$ CLL cells, but not normal B-cells ($CD19^+$ $CD5^-$), T-cells ($CD19^-$ $CD5^+$) or other components of PBMCs ($CD19^-$ $CD5^-$), isolated from CLL patients and healthy individuals. Furthermore, the expression of the protein in normal B-cells does not appear to be affected by activation status. This tight regulation and association with $CD19^+$ $CD5^+$ malignant CLL cells makes ROR1 a highly attractive target. Promisingly, ROR1-CAR T-cells from healthy donor and CLL patients have been shown to induce target lysis of CLL cells *in vitro*, while having no effect on resting, activated, and EBV-transformed B-cells (Hudecek et al. 2010).

Further refinement of this approach has shown that the addition of a shorter "hinge" section and a higher affinity mAb region can significantly improve ROR1-CAR T-cells effector function, their ability to lyse target cells and their *in vitro* proliferation. Additionally, in *in vivo* mice experiments ROR1-CAR T-cells were shown to have comparable efficacy to CD19-CAR transduced T-cells (Hudecek et al. 2013). Therefore the use of CAR T-cells targeting ROR1 appears to be a promising immunuotherapeutic strategy for the treatment of CLL. However, while CAR transduced T-cells appear to be highly promising option for the treatment of CLL, serious adverse effects, and in extreme cases patient deaths, associated with the release of pro-inflammatory cytokines, have been

reported in some clinical trials (Brentjens et al. 2009; Kochenderfer et al. 2012; Morgan et al. 2010).

1.4.7.5 Combination therapy

Due to the numerous varieties of treatment options available for CLL patients, the combination of different therapeutic strategies has been employed. The addition of monoclonal antibodies to "traditional" chemotherapy has been actively investigated. For example, the combination of fludarabine, cyclophosphamide and rituximab (FCR), is now generally regarded as the gold standard of treatment for CLL. This is because treatment with FCR resulted in improvement in overall response rates, PFS and OS when compared to FC or single agent therapy (Tam et al. 2008; Hallek et al. 2010; Badoux et al. 2011).

1.5 Hypothesis and Aim

1) The enhanced proteasomal degradation of Bax will render CLL cells susceptible to immune surveillance by $CD8^+$ T-cells
   a) Determine the existence of Bax-specfic T-cells in HLA-$A2^+$ patients
   b) Isolate and clone Bax-specfic T-cells
   c) Characterisation of Bax-specfic T-cells
   d) Determine the ability of Bax-specfic T-cells to recognise and kill HLA-$A2^+$ CLL cells.
2) The inversion in the CD4:CD8 ratio will be associated with phenotypic and transcriptional hallmarks of immune exhaustion.
   a) Investigation the expression of marker associated with immunological differentiation (CD57 / CD27) and immune suppression (PD-1 / TIM-3/ LAG-3) within the $CD4^+$ and $CD8^+$ T-cell compartments.
   b) Investigate the expression of the immunosuppressive ligands with the B-cell compartment

c) Investigation transcription differences in genes related to T-cell activation and anergy within the $CD4^+$ and $CD8^+$ T-cell compartments of CLL patients.

Chapter 2

Materials and Methods

2.1 Tissue culture basics

2.1.1 Media and buffers

FCS-RPMI

Roswell Park Memorial Institute (RPMI) 1640 (Sigma) was supplemented with L-Glutamine (2mM, Invitrogen), 4-(2-hydroxyethyl)-1-piperazineethanesulfonic acid (HEPES) buffer (25mM, Sigma), penicillin (100U/ml, Invitrogen), streptomycin (100μg/ml, Invitrogen) and foetal calf serum (FCS) (10%, Invitrogen).

Serum-free RPMI

RPMI 1640 was supplemented as above but without the addition of FCS.

AB-RPMI

RPMI 1640 was supplemented as above but without FCS. Instead 5% human AB serum was added (Welsh blood service).

FCS-DMEM

Dulbecco's Modified Eagle's Media (DMEM) (Sigma) was supplemented with L-Glutamine (2mM), HEPES buffer (25mM), penicillin (100U/ml), streptomycin (100μg/ml) and FCS (10%).

Cryopreservation solution

FCS (50%), RPMI 1640 (40%) and 10% dimethyl sulfoxide (DMSO) (Sigma). Cyropreservation solution was stored at -20°C or 4°C.

Magnetic-activated cell sorting (MACS) separation buffer

Sterile phosphate buffered saline (PBS) (Invitrogen) was supplemented with bovine serum albumin (BSA) (0.5%, Sigma) and ethylenediaminetetraacetic acid (EDTA) (2mM, Sigma). The buffer was then sterile filtered using a 0.2μm bottle top filter (Millipore).

Fluorescence-activated cell sorting (FACS) buffer

PBS was supplemented with FCS (1%).

2.1.2 Tissue culture plastics

All tissue culture flasks (T25 and T75) and plates (6, 48 and 96 wells) were obtained from Greiner Bio-one or Fisher.

2.1.3 Cell counts and viability

Cell counts and cell viability were assessed using a Vi-Cell XR (Beckman Coulter) or manually using trypan blue solution (Sigma) and a haemocytometer (Hycor). For the Vi-Cell XR, cells were diluted 1 in 10 in PBS and added to a cell counting cup (Beckman Coulter). The cups were loaded into the Vi-Cell XR, the cell suspension was taken up, mixed with trypan blue and the viable cells were counted. For manual counting the cell suspension was diluted 1 in 10 with trypan blue solution (Sigma) and loaded (10μl) into a haemocytometer slide. Viable cells were then counted using a high-resolution microscope and non-viable (stained dark blue) cells were excluded from the count. The number of cells/ml, was calculated by taking the average count as follows: (mean of 2-3 grids × 10) × 10000.

2.1.4 Routine maintenance of cell lines

Culturing established cell lines

Adherent and non-adherent cell lines were cultured in T25 or T75 flasks in FCS-RPMI or FCS-DMEM. Cells were routinely split 1:3 every 2-3 days using the following procedure. Adherent cells were first rinsed with sterile PBS (10ml) and then incubated at 37°C for 5-10 minutes with EDTA-trypsin (1ml - T25 or 5ml - T75, Invitrogen). After the cells had detached, an appropriate volume of FCS-RPMI was added to deactivate the trypsin (5ml for a T25; 15ml for a T75). The cells were harvested, centrifuged at 470×g for 5 minutes, resuspended in the appropriate media and split between new flasks.

Cryopreservation of cells

Selected cells were pelleted by centrifugation, before being resuspended in cryopreservation solution (2-10×10^6 cells/ml) and divided between cryovials (Greiner Bio-one). The cryovials were then placed in a Nalgene 5100 cryofreezing container (Merck Laboratory Supplies) at -80°C for 24 hours. The cells were then transferred to liquid nitrogen for long-term storage.

Thawing cryopreserved cells

Cells were rapidly thawed using a 37°C water bath and then aliquoted into a new sterile tube containing FCS-RPMI. The cells then centrifuged at 470×g for 5 minutes and resuspended in the appropriate media for further use.

2.2 Peptide Libraries

2.2.1 Bax peptide pool P601 – P623

The Bax peptide pool P601-P623 consisted of 23 peptides (9-mer and 10-mer) that originated from the Bax-α protein. These peptides were identified as potential antigens through the use of computer algorithms (BIMAS, SYFPEITHI, SMM, MHCpep, NET

MHC, EpiJen) that predict HLA binding. Within the pool there were fourteen peptides predicted to bind HLA-A*0201, one to HLA-A3, one to HLA-B7, two to HLA-A1, two to HLA-B8 and three to HLA-B44 (Table 2.1). The peptides were synthesised to a purity of greater than 35% (Mimotope) and dissolved in DMSO to produce stock solutions (10mg/ml and 50mg/ml) and peptide pools (10mg/ml). The individual peptides and peptide pools were stored at -80°C.

Table 2.1 Bax peptide pool P601-623

Number	Sequence	Position	HLA Restriction	Databases	Purity (%)
601	RMGGEAPEL	37	A2	6/6	73
602	QIMKTGALL	18	A2	4/6	37
603	LLSYFGTPT	161	A2	4/6	77
604	LLQGFIQDRA	26	A2	3/6	83
605	GLLSYFGTPT	160	A2	3/6	79
606	FVAGVLTASL	176	A2	3/6	67
607	ELQRMIAAV	75	A2	5/6	69
608	ALDPVPQDA	46	A2	4/6	65
609	LLLQFIQDR	25	A2	4/6	83
610	TIMGWTLDFL	135	A2	3/6	51
611	FLRERLLGWI	143	A2	3/6	76
612	KLSECLKRI	58	A2	6/6	36
613	IMGWTLDFL	136	A2	6/6	68
614	ALCTKVPEL	124	A2	6/6	64
615	DELDSNMEL	68	B44	3/3	51
616	MELQRMIAA	74	B44	3/3	77
617	SEQIMKTGAL	16	B44	3/3	68
618	CLKRIGDEL	62	B8	2/3	49
619	ASKLVLKAL	117	B8	3/3	37
620	GGWDGLLSY	156	A1	2/5	59
621	DTDSPREVF	84	A1	4/4	84
622	VALFYFASK	111	A3	5/5	78
623	SPREVFFRV	87	B7	3/5	84

2.2.2 Nonamer combinatorial peptide library (CPL)

The Nonamer CPL (Pepscan) was acquired from Professor Linda Wooldridge (Faculty of Medical and Veterinary Sciences, Bristol University) and contained a total of 5×10^{11} different nonamer peptides and was divided into 180 different peptide mixtures. In every peptide mixture, one position had a fixed L-amino acid residue and all other positions were degenerate, with the possibility of any one of 19 natural L-amino acids being incorporated at each position (cysteine was excluded, due to its high oxidative potential). Each library

mixture consisted of 1.7×10^{10} different nonamer peptides in approximately equimolar concentrations.

2.2.3 Peptides identified from the CPL screen

Three degenerate peptide sequences were utilised to probe the UniProt Knowledgebase peptide database, to identify potential antigenic peptides originating from multiple biological sources (self, viral, bacterial and fungal). Degenerate peptides searches were performed on 13/5/2013 using the ScanProsite (de Castro et al. 2006). Ten peptides (Table 2.2) were synthesised to purities of greater than 95% (Peptide synthetics) and dissolved in DMSO to produce stock solutions (10mg/ml and 100mg/ml). The peptides and were stored at -80°C.

Table 2.2: Candidate peptides identified from nonamer CPL

Type	Source	Sequence	Purity
Optimal	N/A	IIGWMWIPV	>95%
Self	Protein LYRIC	LLGYGWAAA	>95%
	Parathyroid hormone 2 receptor.	LIGWGFPAA	>95%
	Serine palmitoyltransferase small subunit B	YTAYVFIP	>95%
Viral	Influenza A virus	VVWYGGRPV	>95%
	Varicella-zoster virus	STGYGLARI	>95%
		FSPYGWSST	>95%
	Hepatitis C virus subtype 1a	KAAYGFTGI	>95%
Bacterial	Staphylococcus	FIAWGFIAA	>95%
Fungal	Candida dubliniensis	MIAWGFISV	>95%

2.3 Peptide binding assay

T2 cells (1×10^5) were cultured in serum-free media (100µl) supplemented with peptide (10µg/ml) overnight at 37°C in a 5% CO_2 atmosphere. MART-1 peptide (ELAGIGILTV, ProImmune), which is an analogue of the natural MART-1 peptide (AAGIGILTV), was used as a positive control due to its superior HLA-A2 binding properties. Cells were also treated with DMSO alone as a negative control. After the incubation period, the cells were washed and stained with anti-human HLA*A201-Fluorescein isothiocyanate (FITC) (Biolegend, Clone BB7.2). The cells were washed once and resuspended in FACS buffer

(200µl). The cells were analysed using an Accuri C6 flow cytometer (BD) and data analysis was performed using CFlow software (BD). HLA-A2 expression was quantified as the percentage increase according to the formula:

% change in MFI = [(mean fluorescence with peptide - mean fluorescence without peptide) / mean fluorescence without ×100].

2.4 Blood origin and preparation

2.4.1 Blood donors

Whole blood samples from CLL patients were obtained from outpatient clinics held at the University Hospital Wales and Llandough Hospital by Professor Chris Fegan. Dr Guy Pratt also provided additional CLL samples from Birmingham Heartlands Hospital. Professor Chris Fegan also provided age-matched control samples derived from healthy volunteers. In all cases informed consent and ethical approval was obtained in compliance with the ethical approval granted for this study [South East Wales Research Ethics Committee (02/4806)].

2.4.2 Isolation of PBMCs

Fresh blood samples from healthy donors were collected in falcon tubes containing heparin (10U/ml; LEO Pharma) and CLL blood samples were collected in EDTA tubes (BD). In both cases PBMCs were isolated by Ficoll-Hypaque density gradient centrifugation. The blood was carefully layered on top of the Histopaque (Sigma) at a 1:1 ratio and centrifuged at 840×g for 20 minutes with the centrifuge brake off. The PBMC monolayer formed at the interface between the plasma and Histopaque was carefully aspirated using a sterile pasteur pipette (Fisher Scientific). The cells were washed in PBS (at least three times the volume of the aspirated PBMC) and centrifuged at 470×g for 5 minutes with the brake on. The supernatant was aspirated; the cell pellet was resuspended in 1x red blood cell lysis buffer (Miltenyi, 1ml) and incubated at room temperature for 10 minutes. The cells were washed with PBS and centrifuged at 470×g for 5 minutes. The supernatant was aspirated;

the cells were resuspended in an appropriate volume of media and counted using the Vi-Cell XR.

2.5 Primary cell cultures

2.5.1 CLL cell co-culture

Irradiated (6000 rads) murine fibroblast expressing CD40L was cultured in 6-well (1×10^6 cells/well) or 24-well (1×10^5 cells/well) tissue culture plates in FCS-DMEM overnight at 37°C in a 5% CO_2 atmosphere to allow for cell adhesion. The media was aspirated the following day and the wells were washed with PBS (1ml). CLL cells was then placed on top of the fibroblast layer in FCS-RPMI supplemented with IL-4 (5μg/ml; Miltenyi), at a ratio of 10:1 CLL cells:fibroblast. CLL cells were harvested after two days for further use.

2.5.2 *In vitro* culture of T-cells and CLL cells

Enriched $CD8^+$ T-cells, as described in section 2.6.1, were cultured in a 48-well tissue culture plates in of AB-RPMI (1ml) supplemented with IL-7 (10ng/ml, Peprotech) for two days, to allow for the activation of CLL cells to serve as APC. $CD8^+$ T-cells ($\geq2\times10^6$) were cultured in the presence of irradiated (3000 rads) activated CLL cells at a ratio of 1:4 in AB-RPMI (1ml) supplemented with IL-2 (40U/ml, Proleukin) and Bax peptides (10μg/ml). The initial T-cell stimulation was performed with fresh CLL cells and all subsequent stimulations were done with cryopreserved cells. On day three, AB-RPMI (500μl) supplemented with IL-2 (120U/ml) and IL-7 (30ng/ml) was added to each well. The cultures were harvested on day seven, counted and re-stimulated. The cells were re-stimulated for five weeks and the immunogenicity of the Bax peptides was determined via IFN-γ ELISpot assays as described in section 2.8.1.

2.5.3 Nonamer CPL screen

C1R-A2 cells (6×10^5) were pre-incubated with each peptide mixture (1mM) in serum-free media (50μl) for two hours at 37°C in a 5% CO_2 atmosphere. After the peptide

pulsing phase, $CD8^+$ T-cells (3×10^5) in AB-RPMI (50µl) were added to each well. Phytohaemagglutinin (PHA) (10µg/ml, Sigma) was used as a positive control to determine the presence of viable responsive cells. The cells were incubated at 37°C in a 5% CO_2 atmosphere for 16-18 hours. Cell-free supernatants (75µl) were then harvested and stored at -20°C for further processing. C1R-A2 cells were acquired from Professor Linda Wooldridge and used as APC for experiments using macrophage inflammatory protein 1 beta (MIP-1β) as a functional readout, due to the low background production of M1β observed with C1R-A2 cells.

2.5.4 Expansion of T-cells using allogeneic feeder cells

T-cells (1×10^6) were placed in a T25 tissue culture flask with AB-RPMI media (25ml) supplemented with IL-2 (20U/ml), PHA (10µg/ml) and irradiated PBMC (4×10^5/ml, isolated from 2-3 allogeneic donors). The flasks were then incubated at a 45° angle to enhance the cell-to-cell contact for five days at 37°C in a 5% CO_2 atmosphere.

After five days AB-RPMI (1ml) supplemented with IL-2 (520U/ml) was added to each flask. The flasks were the returned to the original position for an additional 2-3 days. The cells were then harvested, counted and cultured (2×10^6 cells/ml) in 24-well tissue culture plates in AB-RPMI (1ml) supplemented with IL-2 (100U/ml) and IL-15 (50ng/ml). After 3-4 days the cells were split 1:2 and AB-RPMI (500µl) supplemented with IL-2 (100U/ml) and IL-15 (50ng/ml) as was added to each well. T-cells were then harvested and cryopreserved for future use.

2.6 Cell enrichment

2.6.1 Enrichment of T-cells and CLL cells using magnetic microbeads

$CD8^+$ and $CD4^+$ T-cells were enriched through positive selection using anti-human CD8 or CD4 microbeads (Miltenyi). Furthermore, $CD19^+$ CLL cells were enriched through positive selection using anti-human CD19 microbeads (Miltenyi).

PBMC were washed once in PBS and centrifuged at 470×g for 5 minutes. The supernatant was removed and the cells were resuspended in cold MACS buffer (80µl/10^7 cells) and CD8 or CD4 microbeads (20µl/10^7 cells). The cells were mixed thoroughly and incubated at 4°C for 15 minutes under rotation using a MACSmix (Miltenyi). The cells were then washed in cold MACS buffer (2ml/10^7 cells) and centrifuged at 470×g for 5 minutes. The supernatant was then poured off and the cells were resuspended in cold MACS buffer (500µl) for magnetic enrichment using the autoMACS Pro Separator or manually using MS columns (Miltenyi).

MS columns were washed with cold MACS buffer (500µl) and then the samples were then loaded on to the column. The unlabelled cells passed through the column, which was then washed three times with cold MACS buffer (500µl). The positively selected cells were then eluted from the column. The column was removed from the magnetic field and washed with cold MACS buffer (1ml). Rather than allowing the cells to pass through, the positively selected cells were forced through using a syringe plunger. The enriched fraction was then passed through a second column to maximise purity. The cells were counted and an aliquot was then assessed for purity by flow cytometry.

2.6.2 Enrichment of IFN-γ secreting T-cells

Peptide-specific IFN-γ production was induced by culturing the polyclonal $CD8^+$ T-cells with the Bax peptide pool (10µg/ml) presented on irradiated (3000 rad), autologous activated, CLL cells at a 1:1 ratio. The cells were cultured in AB-RPMI (500µl) in a 24-well tissue culture plate for five hours at 37°C in a 5% CO_2 atmosphere. The cells were then harvested, transferred to a 15ml falcon tube and washed with cold MACS buffer (10ml). The cells were centrifuged at 470×g for 5 minutes and the supernatant was carefully aspirated. The cells were resuspended in cold MACS buffer (80µl/10^7 cells), IFN-γ microbeads added (20µl/10^7 cells) and the mixture incubated on ice for 5 minutes.

To reinitiate the process of IFN-γ secretion the cells were resuspended in warm AB-RPMI and incubated under gentle rotation for 45 minutes. The volume of media was selected according to the expected number of IFN-γ positive cells (<5% 1-2×10^6 cells/ml or 5-20% 1-2×10^5 cells/ml). To terminate IFN-γ secretion the cells were then incubated at 4°C under gentle rotation for 10 minutes using a MACSmix (Miltenyi). The cells were subsequently centrifuged at 470×g for 5 minutes and the supernatant was carefully aspirated. The cells were then resuspended in cold MACS buffer (80µl/10^7 cells) containing detection antibody (20µl/10^7 cells) and incubated on ice in the dark for 10 minutes.

The cells were then washed in cold MACS buffer (10ml), centrifuged and the cell pellet was resuspended in cold MACS buffer (80µl/10^7 cells) and anti-Phycoerythrin (PE) microbeads (20µl/10^7 cells) and incubated at 4°C for 15 minutes. The cells were washed in cold MACS buffer (10ml), the cell pellet was resuspended in cold MACS buffer (500µl) and separated using the MS magnetic columns as described in section 2.6.1.

IFN-γ^+ $CD8^+$ T-cells were then "rested" overnight in AB-RPMI (200µl) supplemented with IL-2 (40U/ml) and IL-7 (10ng/ml) at 37°C in a 5% CO_2 atmosphere. The cells were then cloned using limiting dilution as described in section 2.7.1.

2.7 Generating peptide-specific T-cell clones

2.7.1 Generation of T-cell lines from peptide-specific T-cells under limited dilution

After IFN-γ enrichment and "resting", T-cells were counted using a haemocytometer and approximately 800 cells were recovered. The T-cells were diluted in varying volumes of cloning mixture to achieve either 0.5 cells/50µl or 10 cells/50µl. The cloning mixture consisted of AB-RPMI supplemented with IL-2 (20U/ml), PHA (10µg/ml) and irradiated PBMC (4×10^6/ml, isolated from 2-3 allogeneic donors). The combined T-cell/cloning mixture was then added to 96-well U bottom tissue culture plates (50µl/well) and the plates

were then incubated for 7 days at 37°C in a 5% CO_2 atmosphere. 6 plates of 0.5 cells/well were produced and 2/3 of a plate of 10 cells/well was produced.

On day seven the cells were "fed" with AB-RPMI (100µl) supplemented with IL-2 (100U/ml) and IL-15 (50ng/ml). On day 14 supernatant (100µl) was removed from each well and replaced with fresh cloning mixture (100µl). For the duration of this procedure the cells were checked regularly and cultures that showed a high level of growth (large pellet size and yellow media) were split 1:2 into new wells.

The process of alternating "feeding" with high dose IL-2 + IL-15 and replacement of cloning mixture was repeated for five weeks, after which the T-cell lines were tested for peptide specificity by IFN-γ ELISpot assay as described in section 2.8.1.

2.7.2 Screening of peptide-specific lines

T-cell lines were produced as described in section 2.7.1 and were tested for Bax peptide reactivity by IFN-γ ELISpot assays as described in section 2.8.1. To determine the average number of cells/culture, four wells were randomly selected and counted using a haemocytometer. The values ranged from 0.6×10^5 – 5.7×10^5 cells, with an average count of 2.47×10^5 cells/well.

Each T-cell line (~3×10^4 cells) was then cultured individually with T2 cells at a 1:1 ratio ± Bax peptide pool (10µg/ml) in AB-RPMI (150µl) at 37°C in a 5% CO_2 atmosphere for 16-18 hours. The ELISpot plates were then developed as described in section 2.8.1.

2.8 Detection of peptide-specific responses

2.8.1 IFN-γ ELISpot

The wells of MultiScreen$_{HTS}$ IP Filter Plates (Millipore) were coated with anti-human IFN-γ antibody (10µg/ml, Mabtech) for 24 hours at 4°C and then washed five times with PBS (150µl/well). FCS-RPMI (100µl) was then added to each well and the plates were incubated at room temperature for 1 hour. The washing process was then repeated.

T-cells (1×10^5 polyclonal T-cells or $1\text{-}3\times10^4$ T-cell clones) were cultured in AB-RPMI (150µl) in triplicate at 1:1 ratio with APC ± peptides (10µg/ml) for 16-18 hours at 37°C in a 5% CO_2 atmosphere. T-cells were also incubated in the absence of APC (negative control) or with mitogen (positive control).

The plates were washed three times with PBS (150µl/well) and were incubated with sterile water (100µl/well) at room temperature to lyse any remaining cells. The plates were washed a further two times with PBS and incubated with a secondary biotinylated antibody (50µl/well, 10µg/ml, Mabtech) at room temperature for two hours. The plates were protected from direct light by covering in metal foil for the duration of the incubation process. The plate was then washed five times with PBS and incubated with streptavidin (50µl/well, 10µg/ml, Mabtech) at room temperature for two hours.

Development solution was made by combining 25xAP colour development buffer (40µl, Bio-Rad) and AP conjugate substrate A (10µl, Bio-Rad) and B solution (10µl, Bio-Rad) with sterile water (1ml). Subsequently, 50µl of this solution was added to each well and incubated at room temperature for 10-50 minutes. Again, the plates were protected from direct light by covering in metal foil for the duration of the incubation process.

Plates were then washed four times with tap water and air dried in the dark. The numbers of spots/well were counted with an ELISpot reader (Oxford Biosystems Cadama). Wells were also checked by eye to correct for any machine counting errors e.g. false positive or false negative spot counts. Peptide-specific responses were calculated by subtracting the spot counts for T-cells + T2 (background response) from the T-cells + T2 + peptide wells.

2.8.2 IFN-γ Intracellular staining

T-cells (1×10^5) were cultured in AB-RPMI (180µl) at 1:1 ratio with T2 cells ± peptide or PHA (10µg/ml). GolgiStop™ (0.7µl, BD) and GolgiPlug™ (1.0µl, BD) were diluted in PBS (198.3µl) and the solution (20µl) was then added to each sample. The samples were

then spun down to increase the cell-to-cell contact and incubated for 5-6 hours at 37°C in a 5% CO_2 atmosphere. The cells were then washed once with FACS buffer and co-stained with anti-human CD3-FITC (Biolegend - clone UCHT1) and CD8-Peridinin chlorophyll protein (PerCP) (Biolegend – clone HIT8a) for 15 minutes at 4°C. The cells were then fixed with solution A (50µl) for 15 minutes at room temperature and permeabilised with solution B (50µl) for 15 minutes at room temperature using a Leucoperm™ kit (AbD Serotec). Intracellular IFN-γ was identified through the addition of anti-human IFN-γ-PE (eBioscience - clone 4S.B3) during the permeabilisation step. The cells were washed once, resuspended in FACS buffer (200µl) and then analysed using an Accuri C6 flow cytometer (BD). Data analysis was performed using CFlow software (BD).

2.8.3 IFN-γ enzyme-linked immunosorbent assay (ELISA)

T-cells (1×10^5) were cultured in AB-RPMI (200µl) at a 1:1 ratio with peptide pulsed T2 cells for 18 hours in U-bottomed tissue culture plates. T-cells were also cultured with unpulsed T2 cells (negative control) or PHA (10µg/ml). Cell-free supernatants (75µl) were harvested and analysed for human IFN-γ (Human IFN-γ ELISA^{PRO} kit, Mabtech)

The plates were pre-coated with IFN-γ capture antibody were equilibrated to room temperature and washed six times with ELISA wash solution (200µl/well). ELISA diluent (50µl) and either the standard or sample supernatant (50µl) were then added to each well. Plates were covered with an adhesive strip and incubated at room temperature for two hours followed by a further wash step. 1× IFN-γ detection antibody (100µl) was added to each well, the plates were covered and incubated at room temperature for one hour. The washing process was then repeated. 1x Streptavidin-horseradish peroxidase (SA-HRP) (100µl) was added to each well, the plates were covered and incubated at room temperature for one hour. The washing process was then repeated. 3,3′,5,5′-tetramethylbenzidine (TMB) substrate (100µl) was added to each well and the plates were incubated in the dark for 15 minutes. Stop solution (100µl) was then added to terminate the reaction. Plates were

then analysed using the iMark Microplate Absorbance Reader (Bio-Rad) and IFN-γ concentrations were calculated using a standard curve generated from the purified recombinant IFN-γ supplied in the kit.

2.8.4 MIP-1β ELISA

For the nonamer CPL screen, cell stimulation was performed as described in section 2.5.3. T-cells (1×10^5) were cultured in AB-RPMI (200µl) at a 1:1 ratio with peptide pulsed T2 cells for 18 hours in U-bottomed tissue culture plates. T-cells were also cultured with unpulsed T2 cells (negative control) or 10µg/ml PHA (positive control). Cell-free supernatants (75µl) were harvested and analysed by ELISA for human MIP-1β (R&D Systems).

MIP-1β capture antibody was diluted 1 in 200 in PBS and added to each plate (50µl/well), the plates were then incubated at room temperature overnight. The plates were then washed three times with ELISA wash solution (400µl/well) and blocked for one hour at room temperature with 1x ELISA diluent (50µl/well). The washing process was then repeated. MIP-1β standard or supernatant (50µl/well) was then added to each plate, which were then incubated at room temperature for one hour and 15 minutes. The washing process was then repeated. The detection antibody was diluted 1 in 200 in the reagent diluent and added to each plate (50µl/well), which were then incubated at room temperature for one hour and 15 minutes. The washing process was then repeated. SA-HRP was diluted 1 in 200 in reagent diluent and added to each plate (50µl/well), followed by incubation at room temperature in the dark for 20 minutes. Equal volumes of colour reagent A and B were combined together and the resulting solution was added to each plate (50µl/well). The plates were incubated for up to 20 minutes in the dark and the reaction was terminated by the addition of the stop solution (25µl/well). Plates were then analysed using the iMark Microplate Absorbance Reader (Bio-Rad) and MIP1-β concentrations were calculated using the standard curve.

2.8.5 CD107α surface staining

T-cells (1×10^5) were cultured in AB-RPMI (180µl) at 1:1 ratio with T2 cells ± peptide or PHA (10µg/ml) as a positive control. GolgiStop™ (0.7µl) and GolgiPlug™ (1.0µl) were diluted in PBS (198.3µl) and the solution (20µl) was then added to each sample. Changes in the surface expression of CD107α were determined after the addition of anti-human CD107α-PE (Biolegend – clone H4A3) to each culture. The samples were then spun down to increase the cell-to-cell contact and incubated for five hours at 37°C in a 5% CO_2 atmosphere. After five hours the cells were washed and co-stained with anti-human CD3-FITC (Biolegend – clone UCHT1) and CD8-PerCP (Biolegend – clone HIT8a). The cells were washed once and resuspended in FACS buffer (200µl). The cells were analysed using the Accuri C6 flow cytometer (BD) and data analysis was performed using CFlow software (BD).

2.9 Flow cytometry and Monoclonal Antibodies

2.9.1 Single and multi-colour immunophenotyping

To ensure optimal staining, the antibodies used in this study were tested at 100% and 50% of the manufactuers' recommendations prior to use. The antibodies were then incubated with the cells ($0.2 – 2\times10^6$) for 15-30 minutes at 4°C. The cells were then washed with FACS buffer and resuspended in FACS buffer or 1% PFA (100 - 400µl). The cells were analysed using the Accuri C6 flow cytometer or ARIA III FACS sorter (BD) and data analysis was performed using CFlow software (BD) or FlowJo (Tree star), respectively.

2.9.2 Antibody panels

Table 2.3 TCR Vβ chain antibodies

Antigen	Fluorochrome	Supplier	Description
TCR Vβ 1	FITC	Beckman Coulter	Rat IgG1, Clone BL37.2
TCR Vβ 2	FITC	Serotec	Mouse IgG1, Clone MPB2D5
TCR Vβ 3	FITC	Serotec	Mouse IgG1, Clone CH92
TCR Vβ 4	PE	Serotec	Rat IgM, Clone WJF24

TCR Vβ 5.1	FITC	Serotec	Mouse IgG2a, Clone IMMU157
TCR Vβ 5.2	PE	Beckman Coulter	Mouse IgG1, Clone 36213
TCR Vβ 5.3	PE	Beckman Coulter	Mouse IgG1, Clone 3D11
TCR Vβ 7.1	FITC	Serotec	Mouse IgG1, Clone ZOE
TCR Vβ 7.2	FITC	Beckman Coulter	Mouse IgG2a, Clone ZIZOU4
TCR Vβ 8	FITC	Serotec	Mouse IgG2a, Clone 56C5
TCR Vβ 9	FITC	Serotec	Mouse IgG2a, Clone FIN9
TCR Vβ 11	FITC	Serotec	Mouse IgG2a, Clone C21
TCR Vβ 12	FITC	Serotec	Mouse IgG2a, Clone VER2.3.2
TCR Vβ 13.1	FITC	Serotec	Mouse IgG2b, Clone IMMU222
TCR Vβ 13.2	PE	Beckman Coulter	Mouse IgG1, Clone H132
TCR Vβ 13.6	FITC	Serotec	Mouse IgG1, Clone JU-74
TCR Vβ 14	FITC	Serotec	Mouse IgG1, Clone CAS1.1.3
TCR Vβ 16	FITC	Serotec	Mouse IgG1, Clone TAMAYA1.2
TCR Vβ 17	FITC	Serotec	Mouse IgG1, Clone E17.5F3
TCR Vβ 18	FITC	Serotec	Mouse IgG1, Clone BA62
TCR Vβ 20	FITC	Serotec	Mouse IgG1, Clone ELL1.4
TCR Vβ 21.3	FITC	Serotec	Mouse IgG1, Clone IG125
TCR Vβ 22	FITC	Serotec	Mouse IgG1, Clone IMMU546
TCR Vβ 23	FITC	Serotec	Mouse IgG1, Clone AF-23
TCR Vα 24	FITC	Beckman Coulter	Mouse IgG1, Clone C15

Table 2.4 T-cell subsets and immunosuppressive receptors panel

Antigen	Fluorochrome	Supplier	Description
CD3	APC-H7	BD Biosciences	Mouse IgG1, Clone SK7
CD4	V500	BD Biosciences	Mouse IgG1, Clone RPA-T4
CD8	Alexa Fluor 700	BD Biosciences	Mouse IgG1, Clone RPA-T8
CCR7	PE-CY7	BD Biosciences	Rat IgG2a, Clone 3D12
CD45R0	ECD	Beckman Coulter	Mouse IgG2a, Clone UCHL1
CD57	FITC	BD Biosciences	Mouse IgM, Clone NK-1
CD27	QDOT605	Life Technologies	Mouse IgG2a, CloneCLB-27/1
PD-1	Brilliant Violet 421	Biolegend	Mouse IgG1, Clone EH12.2H7
LAG3	APC	R&D Systems	Goat IgG,
TIM3	PE	R&D Systems	Rat IgG2a, Clone 215008

Table 2.5 CLL and immunosuppressive ligands panel

Antigen	Fluorochrome	Supplier	Description
CD19	PE-CY7	Biolegend	Mouse IgG1, Clone HIB19
CD5	PerCP-Cy5.5	BD Biosciences	Mouse IgG2a, Clone L17F12
CD38	PE-CY7	eBiosciences	Mouse IgG1, Clone HIT2
PDL-1	APC	Biolegend	Mouse IgG2b, Clone 29E.2A3
HLA-DR	FITC	BD Biosciences	Mouse IgG2a, Clone G46-6
GAL-9	PE	Biolegend	Mouse IgG1, Clone 9M1-3

Table 2.6 General antibodies

Antigen	Fluorochrome	Supplier	Description
CD3	FITC	Biolegend	Mouse IgG1, Clone UCHT1
CD3	PerCP	Biolegend	Mouse IgG2a, Clone OKT3
CD4	PE	Biolegend	Mouse IgG1, Clone RPA-T4
CD8	APC	Biolegend	Mouse IgG1, Clone HIT8a
CD8	PerCp	Biolegend	Mouse IgG1, Clone HIT8a
CD107α	PE	Biolegend	Mouse IgG1, Clone H4A3
IFN-γ	PE	eBioscience	Mouse IgG1, Clone 4S.B3
HLA*A201	FITC	Biolegend	Mouse IgG2b, Clone BB7.2
HLA-DR	PE	R&D	Mouse IgG1, Clone L203
CD86	FITC	R&D	Mouse IgG1, Clone 37301

2.10 RT^2 polymerase chain reaction array

2.10.1 RNA extraction

RNA extraction was performed using the RNeasy kit (Qiagen). $CD4^+$ and $CD8^+$ T-cells were purified from PBMC as described in section 2.6.1. The cell pellets were resuspended in RLT lysis buffer (350µl) supplemented with β-mercaptoethanol (10µl/1ml) and stored at -80°C until further processing.

Samples were then thawed at room temperature, transferred to a QIAshedder spin column and centrifuged for 2 minutes at 11700×g. 70% ethanol (350µl) was added to the homogenised sample, which was then transferred to an RNeasy mini column. The sample was centrifuged for 15 seconds at 6900×g and the flow-through was discarded. RW1 buffer (350µl) was added to the RNeasy mini column, centrifuged for 15 seconds at 6900×g and the flow-through was then discarded.

The DNase mixture was formulated by combining DNase I stock (10µl) with RDD buffer (70µl). This was then transferred directly onto the RNeasy silica-gel membrane and incubated at room temperature for 15 minutes. RW1 buffer (350µl) was added to the RNeasy mini column, centrifuged for 15 seconds at 6900×g and the flow-through discarded. The RNeasy column was then transferred to a new 2ml collection tube. RPE buffer (500µl) was added to the column, centrifuged for 15 seconds at 6900×g and

the flow-through was discarded. This wash step was then repeated, however the column was centrifuged for 2 minutes at 6900×g. The RNeasy column was transferred to a new 1.5ml collection tube. RNase-free water (20µl) was added to the RNeasy mini column and centrifuged for 1 minute at 6900×g. To increase RNA yield the elution step was repeated by passing the flow-through through the column for a second time. The RNA was stored at -80°C until further processing.

2.10.2 RNA quantification and quality control

The RNA concentration was determined using a NanoDrop UV-Vis Spectrophotometer (Thermo scientific). The integrity of the RNA was determined using the RNA Analysis Kit (Agilent Technologies) by Central Biotechnology Services (Cardiff University). Before use, all the reagents were equilibrated to room temperature. The RNA 6000 pico dye concentrate was vortexed for 10 seconds and then centrifuged briefly at 300×g. The dye (1µl) was added to filtered gel (65µl), the mixture was vortexed thoroughly and centrifuged for 10 minutes at 13000×g. The gel-dye mix (9µl) was added to the well marked **(G)** on the RNA Pico chip. The chip was locked into the chip priming station; the plunger of the syringe was pushed down and held for 30 seconds to distribute the gel-dye mixture. The plunger was then released and the chip removed from the station. Additional gel-dye (9µl) was then added to the wells marked **(G)**.

The RNA ladder and samples were thawed at room temperature, heat denatured at 70°C for 2 minutes and placed on ice until use. The RNA ladder and RNA samples (1µl) were added to their designated wells and the chip was then vortexed for 60 seconds using an IKA vortex mixer. The chip was then analysed using the Agilent 2100 bioanalyser and the ratio between the 18S and 28S ribosomal RNA were used to determine the RNA Integrity Number (RIN).

2.10.3 Reverse transcription

RNA samples and all the reagents from the RT^2 first strand kit (Qiagen) were thawed at room temperature. RNA (60ng) was combined with 5× genomic DNA Elimination Buffer (4µl) and the solution was adjusted to a final volume (20µl) with RNase-free water. The samples were then incubated at 42°C for 5 minutes and then placed on ice for 1 minute. The reverse transcription mix (Table 2.7) was combined with the RNA and the sample was incubated at 42°C for 15 minutes. The reaction was terminated by incubating the sample at 95°C for 5 minutes. RNase-free water (182µl) was added to the sample, which was stored at -20°C until further processing.

Table 2.7 Reverse transcription mixture

Component	Volume
5x Buffer BC3	8µl
Control P2	2µl
RE3 Reverse Transcriptase Mix	4µl
RNase-free water	6µl

2.10.4 Real-time PCR

The real-time PCR mixture was formulated in accordance with Table 2.8 and was dispensed across the RT^2 Profiler PCR Array (25µl/well). The array was then sealed tightly with the Optical Thin-Wall 8-Cap Strips and centrifuged for 1 minute at 200×g. The arrays were then inspected for bubbles and then the PCR was performed using the Applied Biosystems 7900HT (Life technologies) in accordance with Table 2.9 by the Core Genomic Facility (University of Sheffield). The cycle threshold (CT) values were calculated for each gene (Table 2.10 and 2.11) and data analysis was performed using RT^2 Profiler PCR Array Data Analysis (SA Biosciences).

Table 2.8 Real-time PCR mixture

Component	Volume
2x RT² SYBR Green Mastermix	2700µl
cDNA synthesis reaction	204µl
RNase-free water	2496µl

Table 2.9 Real-time PCR programme

Cycles	Duration	Temperature
1	10 minutes	95°C
40	15 seconds	95°C
	1 minute	60°C

Table 2.10 T-cell & B-cell activation PCR array gene list

Symbol	Description
ADA	Adenosine deaminase
AICDA	Activation-induced cytidine deaminase
APC	Adenomatous polyposis coli
BCL2	B-cell CLL/lymphoma 2
BLM	Bloom syndrome, RecQ helicase-like
BLNK	B-cell linker
CCL3	Chemokine (C-C motif) ligand 3
CCR1	Chemokine (C-C motif) receptor 1
CCR2	Chemokine (C-C motif) receptor 2
CCR3	Chemokine (C-C motif) receptor 3
CCR4	Chemokine (C-C motif) receptor 4
CCR5	Chemokine (C-C motif) receptor 5
CD1D	CD1d molecule
CD2	CD2 molecule
CD27	CD27 molecule
CD274	CD274 molecule
CD276	CD276 molecule
CD28	CD28 molecule
CD3D	CD3d molecule, delta (CD3-TCR complex)
CD3E	CD3e molecule, epsilon (CD3-TCR complex)
CD3G	CD3g molecule, gamma (CD3-TCR complex)
CD4	CD4 molecule
CD40	CD40 molecule, TNF receptor superfamily member 5
CD40LG	CD40 ligand
CD47	CD47 molecule
CD5	CD5 molecule
CD7	CD7 molecule
CD80	CD80 molecule

CD81	CD81 molecule
CD86	CD86 molecule
CD8A	CD8a molecule
CD8B	CD8b molecule
CSF2	Colony stimulating factor 2
CX3CL1	Chemokine (C-X3-C motif) ligand 1
CXCR3	Chemokine (C-X-C motif) receptor 3
CXCR4	Chemokine (C-X-C motif) receptor 4
CXCR5	Chemokine (C-X-C motif) receptor 5
DPP4	Dipeptidyl-peptidase 4
EGR1	Early growth response 1
FAS	Fas
FASLG	Fas ligand
FOXP3	Forkhead box P3
ICOSLG	Inducible T-cell co-stimulator ligand
IFNG	Interferon, gamma
IL10	Interleukin 10
IL11	Interleukin 11
IL12A	Interleukin 12A
IL12B	Interleukin 12B
IL12RB1	Interleukin 12 receptor, beta 1
IL12RB2	Interleukin 12 receptor, beta 2
IL13	Interleukin 13
IL15	Interleukin 15
IL18	Interleukin 18
IL18R1	Interleukin 18 receptor 1
IL1B	Interleukin 1, beta
IL2	Interleukin 2
IL2RA	Interleukin 2 receptor, alpha
IL3	Interleukin 3
IL4	Interleukin 4
IL4R	Interleukin 4 receptor
IL5	Interleukin 5
IL6	Interleukin 6
IL7	Interleukin 7
IL8	Interleukin 8
IRF4	Interferon regulatory factor 4
LAG3	Lymphocyte-activation gene 3
LCK	Lymphocyte-specific protein tyrosine kinase
MAP3K7	Mitogen-activated protein kinase 7
MICB	MHC class I polypeptide-related sequence B
MS4A1	Membrane-spanning 4-domains, subfamily A, member 1
NCK1	NCK adaptor protein 1

NOS2	Nitric oxide synthase 2, inducible
PTPRC	Protein tyrosine phosphatase, receptor type, C
RAG1	Recombination activating gene 1
RIPK2	Receptor-interacting serine-threonine kinase 2
SOCS1	Suppressor of cytokine signalling 1
TGFB1	Transforming growth factor, beta 1
TLR1	Toll-like receptor 1
TLR2	Toll-like receptor 2
TLR4	Toll-like receptor 4
TLR6	Toll-like receptor 6
TLR9	Toll-like receptor 9
TNFSF14	Tumour necrosis factor (ligand) superfamily, member 14
VAV1	Vav 1 guanine nucleotide exchange factor
ACTB	Actin, beta
B2M	Beta-2-microglobulin
GAPDH	Glyceraldehyde-3-phosphate dehydrogenase
HPRT1	Hypoxanthine phosphoribosyltransferase 1
RPLP0	Ribosomal protein, large, P0

Table 2.11 Human T-cell Anergy and Immune Tolerance PCR Array gene list

Symbol	Description
BTLA	B and T lymphocyte associated
CBLB	Cas-Br-M (murine) ecotropic retroviral transforming sequence b
CCL3L1	Chemokine (C-C motif) ligand 3-like 1
CCR4	Chemokine (C-C motif) receptor 4
CD27	CD27 molecule
CD28	CD28 molecule
CD40	CD40 molecule, TNF receptor superfamily member 5
CD40LG	CD40 ligand
CD70	CD70 molecule
CDK2	Cyclin-dependent kinase 2
CDK4	Cyclin-dependent kinase 4
CMA1	Chymase 1, mast cell
CSF1	Colony stimulating factor 1 (macrophage)
CSF2	Colony stimulating factor 2 (granulocyte-macrophage)
CTLA4	Cytotoxic T-lymphocyte-associated protein 4
DGKA	Diacylglycerol kinase, alpha 80kDa
DGKZ	Diacylglycerol kinase, zeta
EGR2	Early growth response 2
EGR3	Early growth response 3
EOMES	Eomesodermin
FAS	Fas
FASLG	Fas ligand

FOS	FBJ murine osteosarcoma viral oncogene homolog
FOXP1	Forkhead box P1
FOXP2	Forkhead box P2
FOXP3	Forkhead box P3
GATA3	GATA binding protein 3
GZMB	Granzyme B
HDAC9	Histone deacetylase 9
ICAM1	Intercellular adhesion molecule 1
ICOS	Inducible T-cell co-stimulator
IFNG	Interferon, gamma
IL10	Interleukin 10
IL10RA	Interleukin 10 receptor, alpha
IL13	Interleukin 13
IL15	Interleukin 15
IL17A	Interleukin 17A
IL1A	Interleukin 1, alpha
IL2	Interleukin 2
IL2RA	Interleukin 2 receptor, alpha
IL2RB	Interleukin 2 receptor, beta
IL31	Interleukin 31
IL4	Interleukin 4
IL5	Interleukin 5
IL6	Interleukin 6
IL7R	Interleukin 7 receptor
ING4	Inhibitor of growth family, member 4
IRF4	Interferon regulatory factor 4
ITCH	Itchy E3 ubiquitin protein ligase homolog
ITGA1	Integrin, alpha 1
JAK1	Janus kinase 1
JAK3	Janus kinase 3
JUN	Jun proto-oncogene
LAT	Linker for activation of T cells
LEP	Leptin
LGALS3	Lectin, galactoside-binding, soluble, 3
LTA	Lymphotoxin alpha
MEF2A	Myocyte enhancer factor 2A
NFATC1	Nuclear factor of activated T-cells, cytoplasmic, calcineurin-dependent 1
NFATC2	Nuclear factor of activated T-cells, cytoplasmic, calcineurin-dependent 2
NFATC3	Nuclear factor of activated T-cells, cytoplasmic, calcineurin-dependent 3
NFKB1	Nuclear factor of kappa light polypeptide gene enhancer in B-cells 1
NHLH2	Nescient helix loop helix 2
NOTCH1	Notch 1
PDCD1	Programmed cell death 1
PRF1	Perforin 1 (pore forming protein)
PRKCG	Protein kinase C, gamma

PTGER2	Prostaglandin E receptor 2 (subtype EP2), 53kDa
PTGS2	Prostaglandin-endoperoxide synthase 2
RNF128	Ring finger protein 128
SELL	Selectin L
STAT3	Signal transducer and activator of transcription 3 (acute-phase response factor)
STAT6	Signal transducer and activator of transcription 6, interleukin-4 induced
TBX21	T-box 21
TGFB1	Transforming growth factor, beta 1
TNFRSF10A	Tumour necrosis factor receptor superfamily, member 10a
TNFRSF14	Tumour necrosis factor receptor superfamily, member 14
TNFRSF18	Tumour necrosis factor receptor superfamily, member 18
TNFRSF4	Tumour necrosis factor receptor superfamily, member 4
TNFRSF8	Tumour necrosis factor receptor superfamily, member 8
TNFRSF9	Tumour necrosis factor receptor superfamily, member 9
TNFSF10	Tumour necrosis factor (ligand) superfamily, member 10
TNFSF14	Tumour necrosis factor (ligand) superfamily, member 14
TNFSF8	Tumour necrosis factor (ligand) superfamily, member 8
ACTB	Actin, beta
B2M	Beta-2-microglobulin
GAPDH	Glyceraldehyde-3-phosphate dehydrogenase
HPRT1	Hypoxanthine phosphoribosyltransferase 1
RPLP0	Ribosomal protein, large, P0

2.11 Statistical analysis

Non-parametric Mann-Whitney U test or parametric student's t-test was used for comparison of two independent groups. Non-parametric Kruskal-Wallis ANOVA with the Dunn's multiple comparisons test or the parametric ANOVA with Tukey Post-hoc analysis was used for the comparison of three or more independent groups. The prognostic relevance of individual parameters was performed using the method of Kaplan and Meier and statistical significance was determined using a log-rank (Mantel Cox) test. Statistical analysis was carried out using Prism 6.0 (GraphPad Software) or SPICE (SPICE 5.35).

2.12 Pathway enrichment analysis

MetaCore Analytical Suite (https://portal.genego.com) was used to perform Gene Ontology (GO) term enrichment in order to interpret the results generated from the PCR array. This process involved comparing the input gene list with a database of manually curated pathways. To determine enrichment, a randomly generated list of genes of the

same size was simultaneously compared to the MetaCore pathways. Significance was evaluated based upon the size of the intersection between the input gene list and the corresponding pathway. This was determined through a variation of Fisher's exact test and that was adjusted for multiple testing using Benjamini-Hochberg false discovery rate (FDR) analysis, which was an inbuilt function within the MetaCore Analytical Suite.

Chapter 3

Generation and Characterisation of Bax-Specific $CD8^+$ T-cell Clones from CLL patients

The enhanced proteasomal degradation of the pro-apoptotic protein Bax is one mechanism utilised by CLL cells to resist apoptosis (Liu et al. 2008). However, usage of this pathway has the potential to result in the generation of Bax-derived peptides for presentation on the surface of CLL cells. These peptides could potentially serve as TAA, triggering the activation of $CD8^+$ cytotoxic T-cells and the subsequent killing of CLL cells. This concept has been confirmed in a proof of principle study utilising T-cells from healthy donors (Nunes et al. 2011), but the existence and function of Bax-specific T-cells from CLL patients is currently unknown. Therefore the main aim of this study was to establish whether it was possible to isolate and then characterise Bax-specific $CD8^+$ T-cells from CLL patients. A schematic diagram showing the experimental workflow for these assays is given in Figure 3.1.

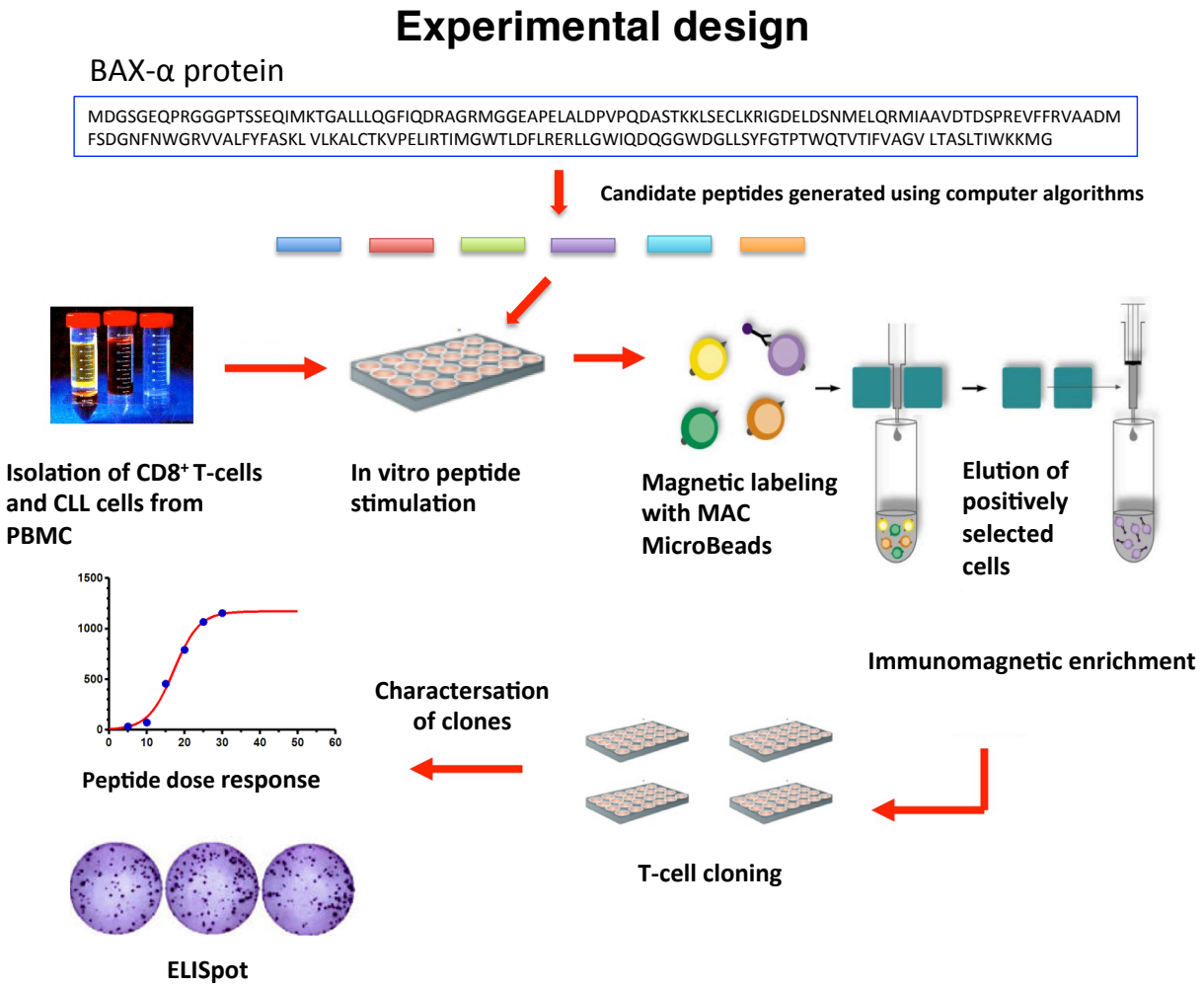

Figure 3.1 Experimental design for the cloning and characterisation of Bax-specific T-cells from CLL patients.

3.1 Activation of CLL cells

It is well established that resting CLL cells have extremely poor antigen presentation potential due to low expression of co-stimulatory and adhesion molecules. However, activation of the CD40 signalling pathway has been shown to enhance antigen presentation potential (Van den Hove et al. 1997; Os et al. 2013). Therefore it was investigated whether co-culture with CD40L-expressing fibroblasts would result in the activation of CLL cells and enhance antigen presentation potential.

The expression of the activation marker HLA-DR and co-stimulatory ligand CD86 were determined by flow cytometry. In the resting state HLA-DR was constitiutively expressed on the surface of all CLL cells (Fig 3.2a), therefore changes in the mean fluorescence intensity (MFI) of HLA-DR were investigated. A significant increase in the level of expression of HLA-DR was observed in response to CD40L stimulation (Fig 3.2b) when compared to baseline (Time 0) and cultures with non-transfected murine fibroblasts (NTL) ($P \leq 0.01$) as well as liquid culture (LC) conditions ($P \leq 0.001$).

Co-culture of the CLL cells with CD40L-expressing fibroblasts resulted in a significant increase in the precentage of cells expressing CD86 ($P<0.0001$) (Fig 3.2c) and the level of expression as determined by the increase in MFI ($P \leq 0.001$) (Fig 3.2d). These changes were observed in comparsion with Time 0, LC and NTL and confirmed that CD40L activation of CLL cells up-regulated HLA-DR and CD86.

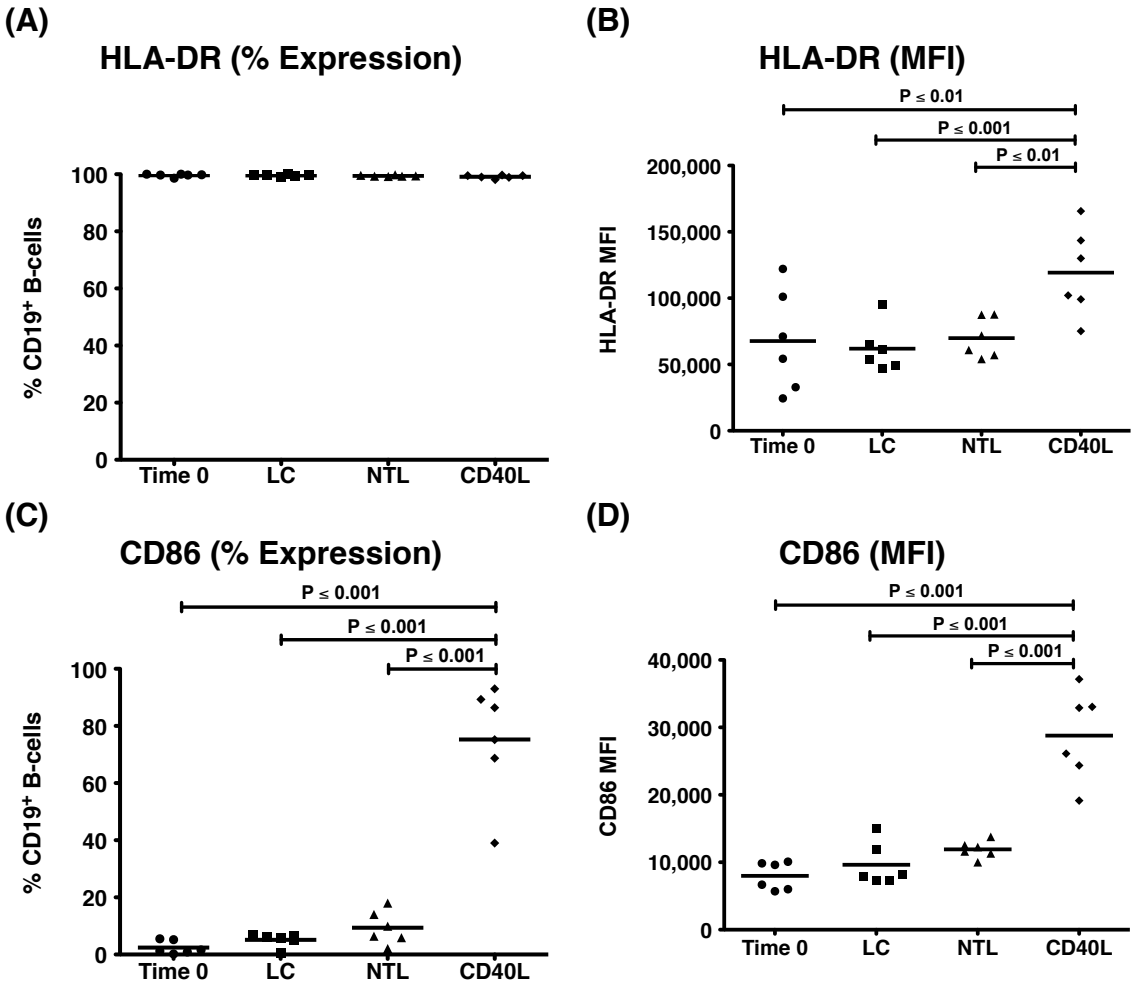

Figure 3.2 Analysis of the expression of the activation maker HLA-DR and co-stimulatory ligand CD86. PBMC (1×10^6) from CLL patients were cultured alone (LC) or co-cultured with either non-transfected murine fibroblasts (NTL) or CD40 ligand (CD40L) expressing fibroblasts. For each condition the cells were cultured in FCS-RPMI (1ml) supplemented with IL-4 (5ng/ml) for 48 hours. **(A)** and **(B)** show the analysis of HLA-DR expression as a percentage of $CD19^+$ B-cells and MFI, respectively. **(C)** and **(D)** show the analysis of CD86 expression as percentage of $CD19^+$ B-cells and MFI, respectively. Mean ± SD of 6 individual patient samples. Statistical analysis (Repeat measure ANOVA with Tukey Post-hoc analysis) was carried out using GraphPad Prism 5.0.

3.2 Donor response

PBMC were isolated from whole blood by ficoll density centrifugation of a CLL patient (R6A8R89). $CD8^+$ T-cells were isolated by immunomagnetic separation and the remaining PBMC were co-cultured with CD40L-expressing murine fibroblasts. $CD19^+$ B-cells were then isolated by immunomagnetic separation to exclude other cell types for the *in vitro* stimulation process. The activated CLL cells were then utilised to present the full Bax peptide pool (P601- P623) to the autologous $CD8^+$ T-cells, which were then subjected to five rounds of stimulation over five weeks. T-cell reactivity against Bax peptides was then tested by IFN-γ ELISpot and a highly significant Bax peptide-specific response was observed (P=0.0008) (Fig 3.3), indicating the presence of Bax-specific T-cells.

3.3 Cloning by limiting dilution

Immunomagnetic enrichment of Bax-specific T-cells was carried out utilising the process of IFN-γ secretion, in response to peptide-specific T-cell activation. After the enrichment process the T-cells were "rested" overnight in AB-RPMI supplemented with IL-2 (40U/ml) and IL-7 (10ng/ml). The cells were counted the following day and approximately 800 cells were recovered and used to establish T-cell lines by limiting dilution. Six plates of 0.5 cells/well, 2/3 of a plate of 10 cells/well and half a plate of "cloning mix"(containing irradiated stimulator cells) alone were established. After 4 weeks of antigen independent expansion, the cultures that showed a high level of growth were assessed for Bax peptide immunogenicity by IFN- γ ELISpot.

From the 0.5 cells/well plate, 19/576 cultures showed significant growth and were selected for testing. Six cultures (6C2, 6E2, 6C5, 8C9, 7F7 and 9D7) showed potential Bax-specific responses (>20 SFC/ 3×10^4) varying from 42 to 770 SFC/3×10^4 cells and were selected for antigen independent expansion and further characterisation (Fig 3.4).

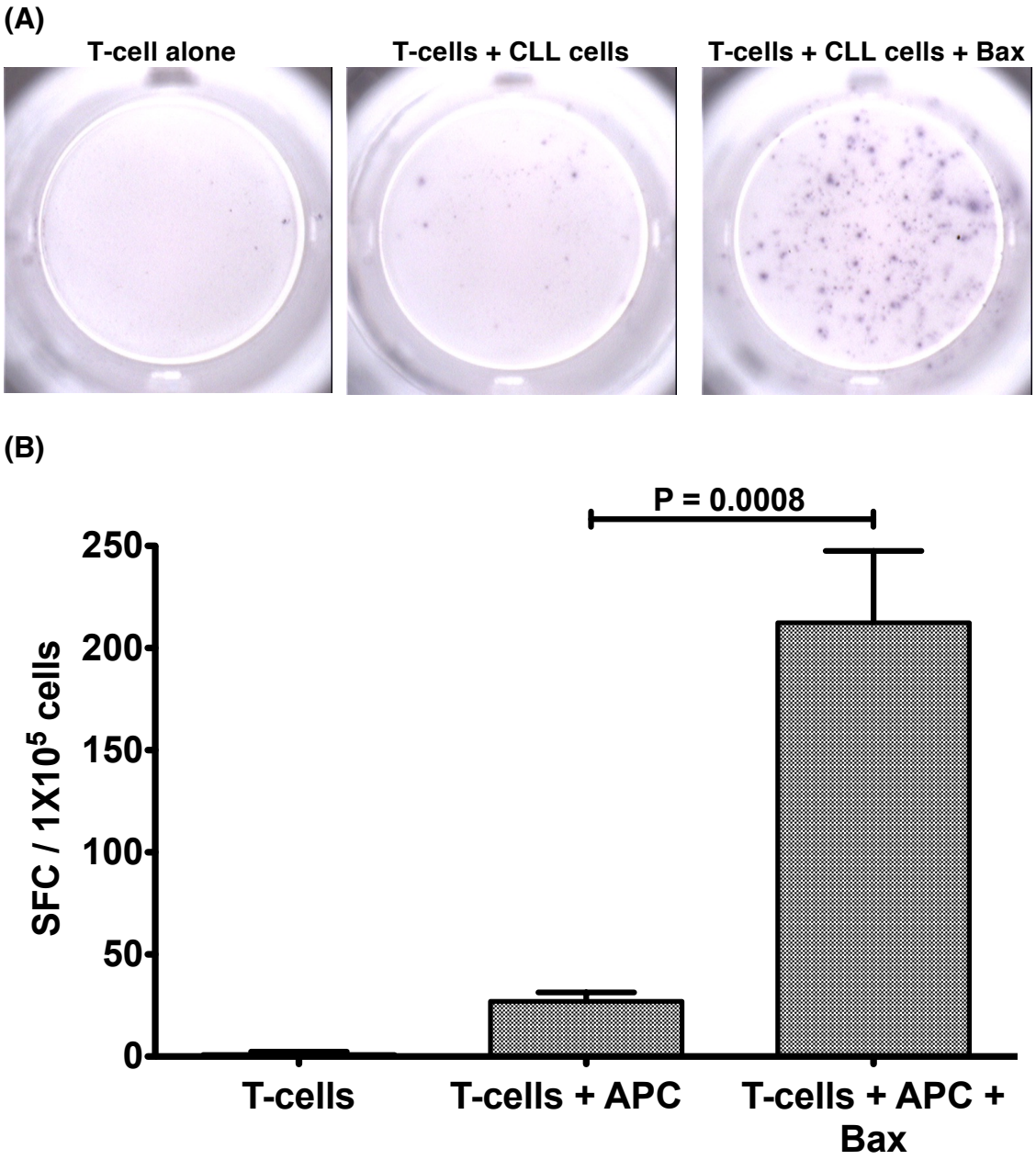

Figure 3.3 Bax T-cell response in CLL Patient samples after five weeks of stimulation. $CD8^+$ T-cells were repeatedly stimulated with irradiated activated autologous CLL cells at a ratio of 4 T-cells : 1 CLL cell, in AB-RPMI (1ml) supplemented with the Bax peptide pool (10μg/ml) and IL-2 (40U/ml). On day 3 the cells were "fed" with AB-RPMI (500μl) supplemented with IL-2 (120U/ml) and IL-7 (30ng/ml). On day 7 the cells were harvested, counted and re-stimulated. After 5 weeks of *in vitro* stimulation a significant Bax specific response was observed by IFN-γ ELISpot (P=0.0008). T-cells (1×10^5 cells/well) were plated in triplicate in ELISpot plates with CLL cells ± Bax peptide pool (10μg/ml) at a ratio of 1:1. The spots were counted and the background response (T-cells + CLL cells) was subtracted from the data. Mitogen control wells were also set up which resulted in a completely dark well, which could not be accurately counted but indicated the presence of viable T-cells. **(A)** A representative example of the response observed in a single set of wells. **(B)** Mean ± SD of triplicate wells for each condition. Statistical analysis (unpaired two-tailed t-test) was carried out using GraphPad Prism 5.0.

3.4 Epitope mapping of Bax-specific T-cells

For the process of *in vitro* stimulation the full Bax peptide pool was utilised, therefore the putative T-cell clones had the potential to be reactive to any of the 23 candidate peptides. These T-cell clones were first tested against the full peptide pool to reaffirm Bax specificity; then against four smaller peptide pools (Bax P601-606, Bax P607-612, Bax P613-618 and Bax P619-623) to narrow down the response, followed by individual peptides for epitope identification. The putative T-cell clones 6C5 and 8C9 both exhibited positive responses against the full Bax peptide pool and the sub pool Bax P601-606. Of the peptides within the Bax P601-606 pool, only P603 and P605 induced an ELISpot response (Fig. 3.5). Interestingly, these two peptides shared an overlapping nine amino acid sequence: Bax P603 was a 9mer ($Bax_{161-170}$; LLSYFGTPT) and Bax P605 was a 10mer ($Bax_{160–170}$; GLLSYFGTPT). Furthermore, as HLA-A2 is the only functional MHC molecule expressed by T2 cells, and as the T-cell clones were isolated from an HLA-$A2^+$ patient, it would suggest that the peptide and its activity was restricted to this specific MHC molecule. It should be noted that for this experiment and all subsequent peptide stimulation experiments T2 cells were used as source of APC, due the lack of available autologous CLL cells.

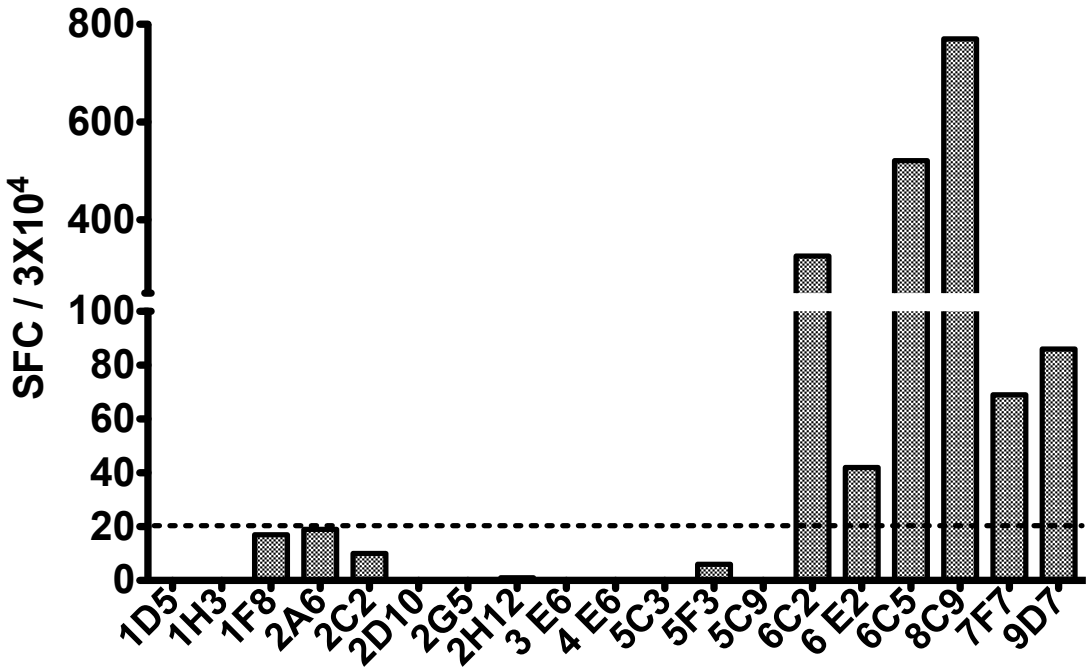

Figure 3.4 T-cell cultures generated under limiting dilution conditions were tested for Bax immunogenicity by IFN-γ ELISpot. To determine the average number of cells per culture, four cultures were selected at random, counted and averaged. T-cells (~3×10^4) were cultured at an approximate 1:1 ratio with T2 cells ± Bax peptide pool (10μg/ml) in ELISpot plates. For each culture tested, only one well was set up per culture condition. The spots were counted and the background response (T-cells + APC) was subtracted from the experimental data (T-cells+APC+peptide). Mitogen control wells were also set up which resulted in a completely dark well, which could not be accurately counted but indicated the presence of viable T-cells. Six cultures showed positive responses against the Bax peptide pool (>20 SFC/ 3×10^4).

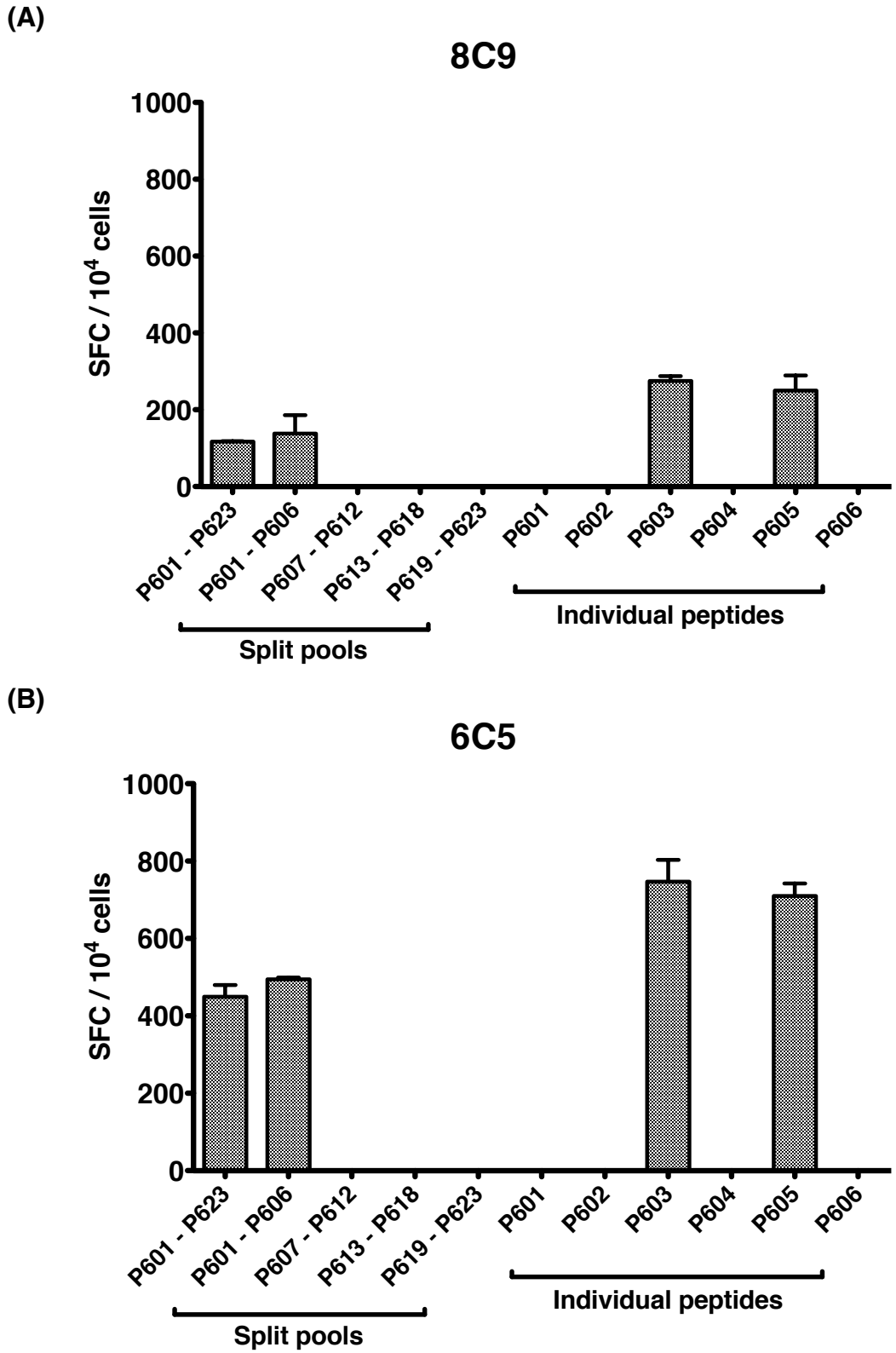

Figure 3.5 Epitope mapping of T-cell clones 6C5 and 8C9. The putative T-cell clones 8C9 and 6C5 were tested by IFN-γ ELISpot against the full Bax peptide pool, four split pools and individual peptides, to determine the T-cells epitope specificity. T-cells (1×10^4 cells/well) were plated in duplicate in ELISpot plates with T2 cells ± Bax peptide pool (10μg/ml) at a ratio of 1:1. The spots were counted and the background response (T-cells + T2) was subtracted from the experimental data (T-cells+T2+peptide). Mitogen control wells were also set up which resulted in a completely dark well, which could not be accurately counted but indicated the presence of viable T-cells. Data are presented as the mean ± SD and are representative of two independent experiments.

3.5 Avidity of 6C5 and 8C9 for Bax P603 and P605

Peptide dose-response experiments were performed to validate the activity of the peptides P603 and P605 and to determine the functional avidity between peptides and the respective T-cell clones. Both 6C5 and 8C9 were able to recognise P603 at a higher functional avidity than P605. Furthermore, 6C5 appeared to have higher functional avidity then 8C9; the half maximal effective concentration (EC_{50}) values in response to P603 were 4.92μM for 6C5 and 8.56μM for 8C9. For P605 a suitable EC_{50} value could not be calculated due to the limitations of the range of the dose-response curve. However, this was estimated to be ~100μM (Fig 3.6). These results indicated that P603 was the optimum epitope for both 6C5 and 8C9. Furthermore, of the two clones identified, 6C5 was selected for further characterisation due to higher functional avidity and superior growth kinetics.

3.6 Analysis of the TCR Vβ chain used by 6C5

The TCR of αβ T-cells is formed by the association of a single alpha and a single beta chain on the cell surface. Historically, the expression of a single TCR Vβ chain, in combination with consistent antigen specificity, function and phenotype has been used to infer T-cell clonality (Evans et al. 2001; Nunes et al. 2011).

The initial TCR analysis of 6C5 using TCR Vβ specific monoclonal antibodies indicted that 95.2% of the T-cells expressed TCR Vβ 13.1, 38.6% expressed TCR Vβ 18 and 27.8% expressed TCR Vβ 5.3 (Fig 3.7a). In light of these puzzling results, 6C5 was re-analysed using a different panel of TCR Vβ antibodies provided by Professor Linda Wooldridge (Faculty of Medical and Veterinary Sciences, Bristol University). The second analysis indicated that 6C5 comprised T-cells expressing mainly TCR Vβ 13.1 and TCR Vβ 5.2 (46.9% and 31.1%, respectively) (Fig 3.7b). Although dominant Vβ 13.1 expression was common to both analyses, it was not clear whether 6C5 was truly monoclonal or comprised a mixture of T-cell clones.

To resolve this, 6C5 was flow-sorted based on the expression of either TCR Vβ5.2 or Vβ 13.1, the T-cells were collected, subjected to antigen independent expansion and analysed for the expression of TCR Vβ 5.2 and Vβ 13.1. The analysis indicated that both expanded T-cell cultures expressed TCR Vβ 13.1 and not Vβ5.2, regardless of which TCR Vβ chain they were sorted on (Fig 3.7c). Based on pre and post flow sorting expression of Vβ 13.1, the consistent expression of TCR Vβ13.1 in two separate TCR Vβ panels, and the cloning protocol employed to establish 6C5, it seemed highly likely that 6C5 was a single $CD8^+$ T-cell clone.

3.7 Recongition of primary CLL cells by 6C5

It has been reported that Bax undergoes abnormal and enhanced proteasomal degradation in CLL cells (Agrawal et al. 2008). It was therefore hypothesised that this enhanced proteasomal processing would result in the presentation of Bax-derived peptides on the surface of CLL cells but not healthy cells. This hypothesis was supported by a proof of principle study that demonstrated that $CD8^+$ T-cells specific for Bax-derived peptides could recognise and kill CLL cells (Nunes et al. 2011). However, in that study the T-cells were sourced from healthy donors and restricted to a different epitope (IMGWTLDFL) to the one recognised by $CD8^+$ T-cell clone 6C5 (LLSYFGTPT).

The ability of the 6C5 to recognise primary CLL cells from HLA-$A2^+$ and HLA-$A2^-$ CLL patients was investigated by IFN-γ ELISpot. Initially recognition of "resting" CLL cells was investigated. However, no response above background was observed for any of the patient samples tested, regardless of HLA-A2 status. Therefore CLL cells were activated by co-culture on CD40L-expressing fibroblasts to induce the up-regulation of co-stimulatory molecules to assist with T-cell activation. Variable responses were observed from both HLA-$A2^-$ patients (11-31 SFC/10^4) and HLA-$A2^+$ (1-88 SFC/10^4) but no difference was observed between HLA-$A2^+$ and HLA-$A2^-$ patients (Fig. 3.8). This suggests that either CLL cells do not present the Bax-derived peptide epitope LLSYFGTPT or that

the avidity of 6C5 for P603 was too low to induce T-cell activation in response to LLSYFGTPT expressed by CLL cells.

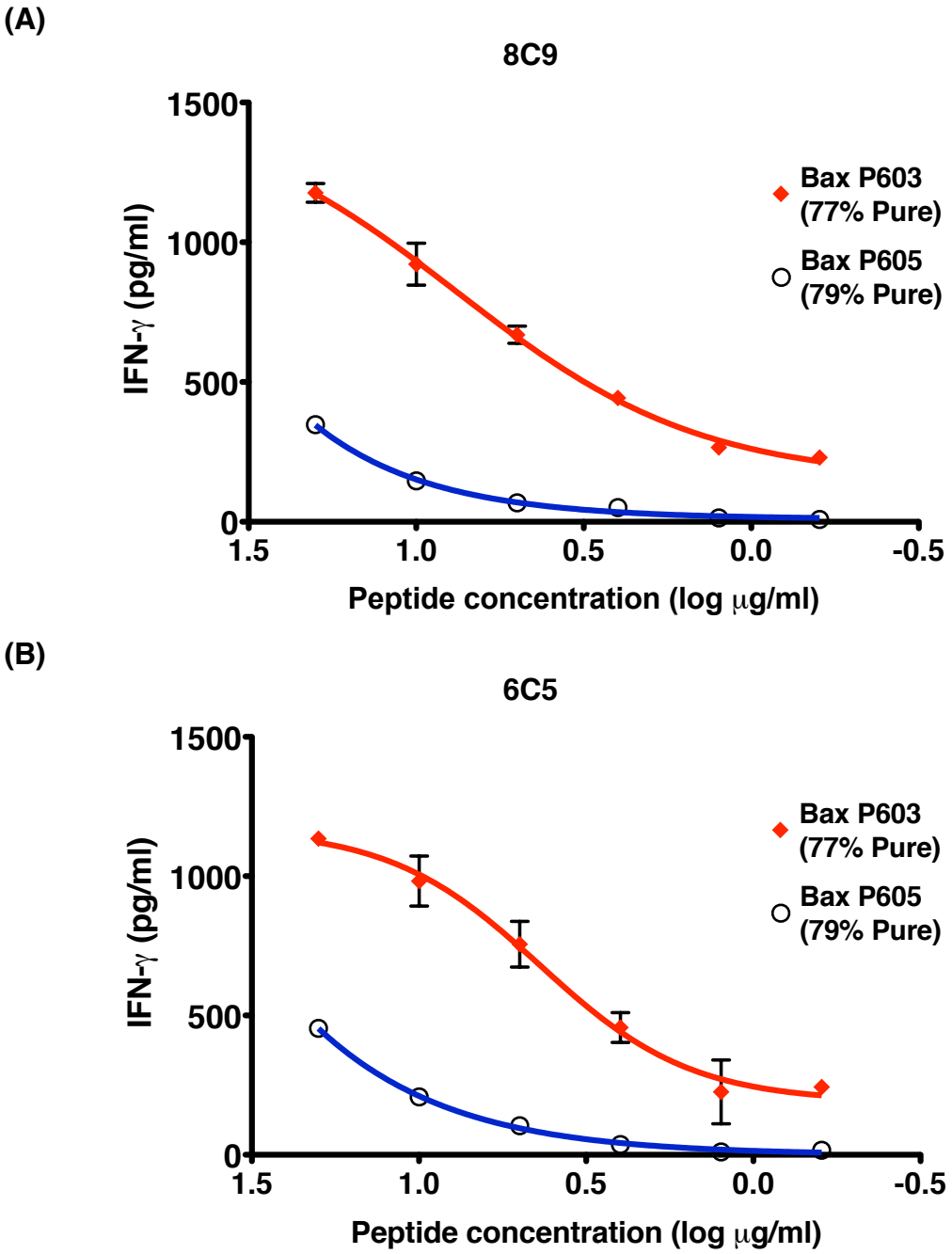

Figure 3.6 Peptide dose-response for 8C9 and 6C5 recognition for P603 and P605 pulsed target cells. T2 cells (5×10^5) pulsed with varying concentrations of **P603** (77% Pure, 20μg/ml to 6.25 μg/ml) and **P605** (79% Pure, 20μg/ml to 6.25μg/ml). T2 cells were incubated in the presence of DMSO alone were used as negative control to determine background production of IFN-γ. After one hour any unbound peptide was washed off and the T2 cells (1×10^5) were cultured overnight at a 1:1 ratio with 8C9 or 6C5 at 37°C / 5% CO_2. Furthermore, PHA (10μg/ml) was used as a positive control. Cell-free supernatants were harvested and evaluated for the presence of IFN-γ by ELISA. Taking into consideration the molecular weight of P603 (885), the molar EC_{50} values were calculated from the curve of best fit; 6C5 was 4.92μM and 8C9 was 8.56μM. For P605 a suitable EC_{50} value could not be calculated due to the limitations of the curve, however was ~100μM. Data are presented as the mean ± SD and are representative of three independent experiments.

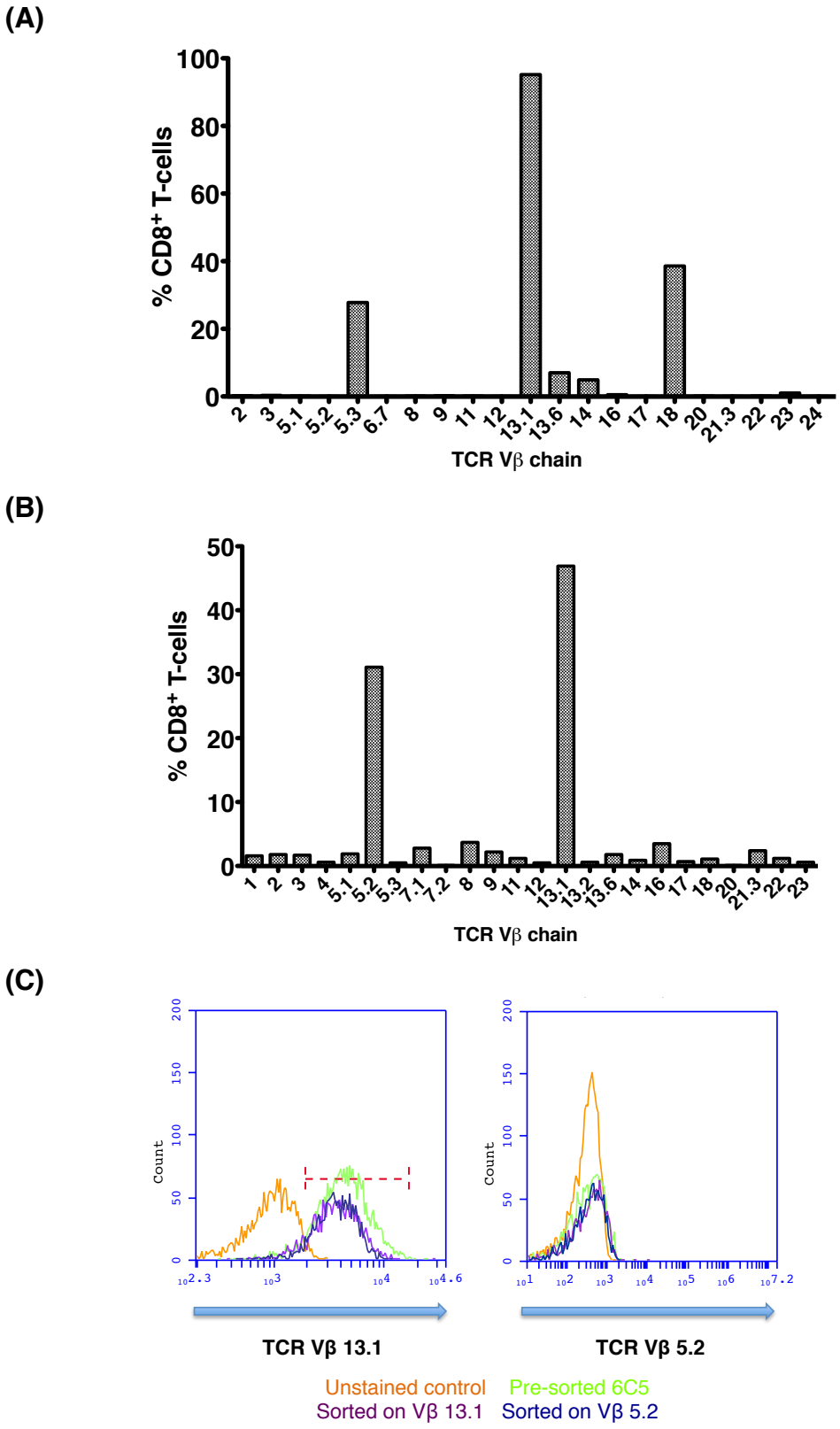

Figure 3.7 Analysis of the TCR Vβ chain used by Bax specific T-cell line. Initially **(A and B)** 6C5 T-cells (1×10^5) were co-stained with anti-human CD8 and two different panels of TCR Vβ chain antibodies, to determine TCR Vβ chain usage. Due to the puzzling results, 6C5 was cell sorted based on the expression of either TCR Vβ 13.1 or TCR Vβ 5.2. After antigen independent expansion, the pre and post sorted T-cells (1×10^5) were then **(C)** co-stained with anti-human CD8 and either anti-human TCR Vβ 13.1 or TCR Vβ 5.2.

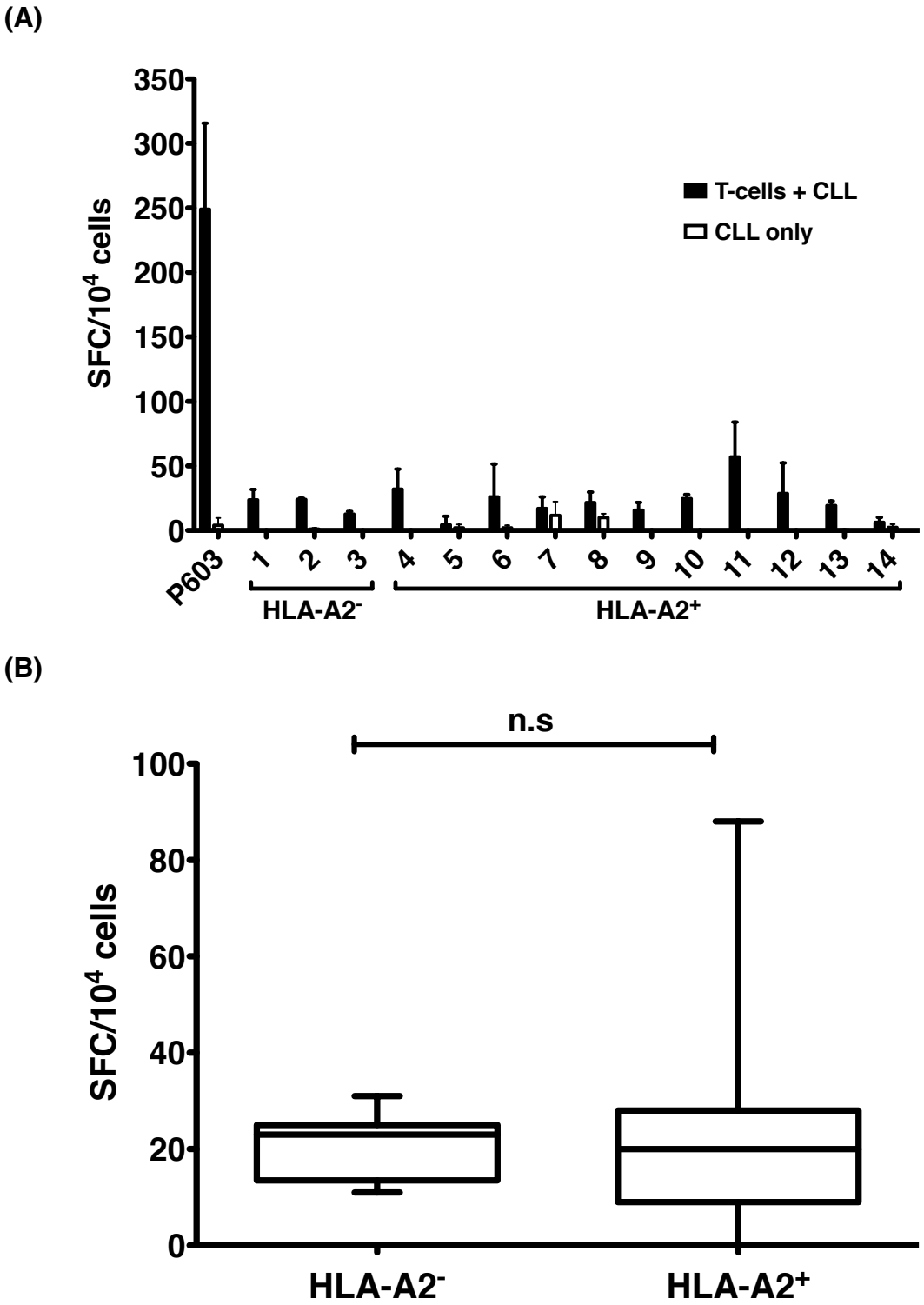

Figure 3.8 6C5 recognition of HLA-A2$^-$ and HLA-A2$^+$ activated CLL cells. CLL PBMC (1×10^6) was co-cultured with CD40L transfected murine fibroblasts at a ratio of 10:1 in FCS-RPMI (1ml) supplemented with IL-4 (5ng/ml) for 48 hours at 37°C / 5% CO_2. The cells were the harvested, resuspended in fresh FCS-RPMI and counted. The activated CLL PBMC (1×10^4) was cultured in triplicate ± CD8$^+$ T-cell clone 6C5 at 1:1 ratio for 18 hours at 37°C / 5% CO_2 in ELISpot plates. T2 cells pulsed with P603 was used as a positive control. Mitogen control wells were also set up which resulted in a completely dark well, which could not be accurately counted but indicated the presence of viable T-cells. Data are presented as the mean ± SD and are representative of 3 HLA-A2$^-$ and 11 HLA-A2$^+$ patients. Statistical analysis (unpaired two-tailed t-test) was carried out using GraphPad Prism 5.0.

3.8 Recognition of crude P603 (77% pure) but not pure P603 (>95%) by 6C5

Initial results using crude peptides (77% purity) suggested that the T-cell clone 6C5 recognised the 9aa sequence (LLSYFGTPT) common to P603 and P605 (Fig. 3.5b). To confirm this observation and to obtain a more accurate estimate of functional avidity, 6C5 was tested against higher purity P603 peptides (>95% purity) from two different commercial sources (Proimmune and Peptide Synthetics). 6C5 failed to respond to the purified forms of P603 (>95% purity), however the original P603 preparation (77% purity) induced a robust and highly significant IFN-γ response ($P<0.0001$) (Fig. 3.9). These results suggested that the immunogenicity associated with the original P603 (77% purity) was not due to the main peptide sequence (LLSYFGTPT). Furthermore, it was likely that the active component recognised by 6C5 was present in the remaining 23% of the peptide preparation.

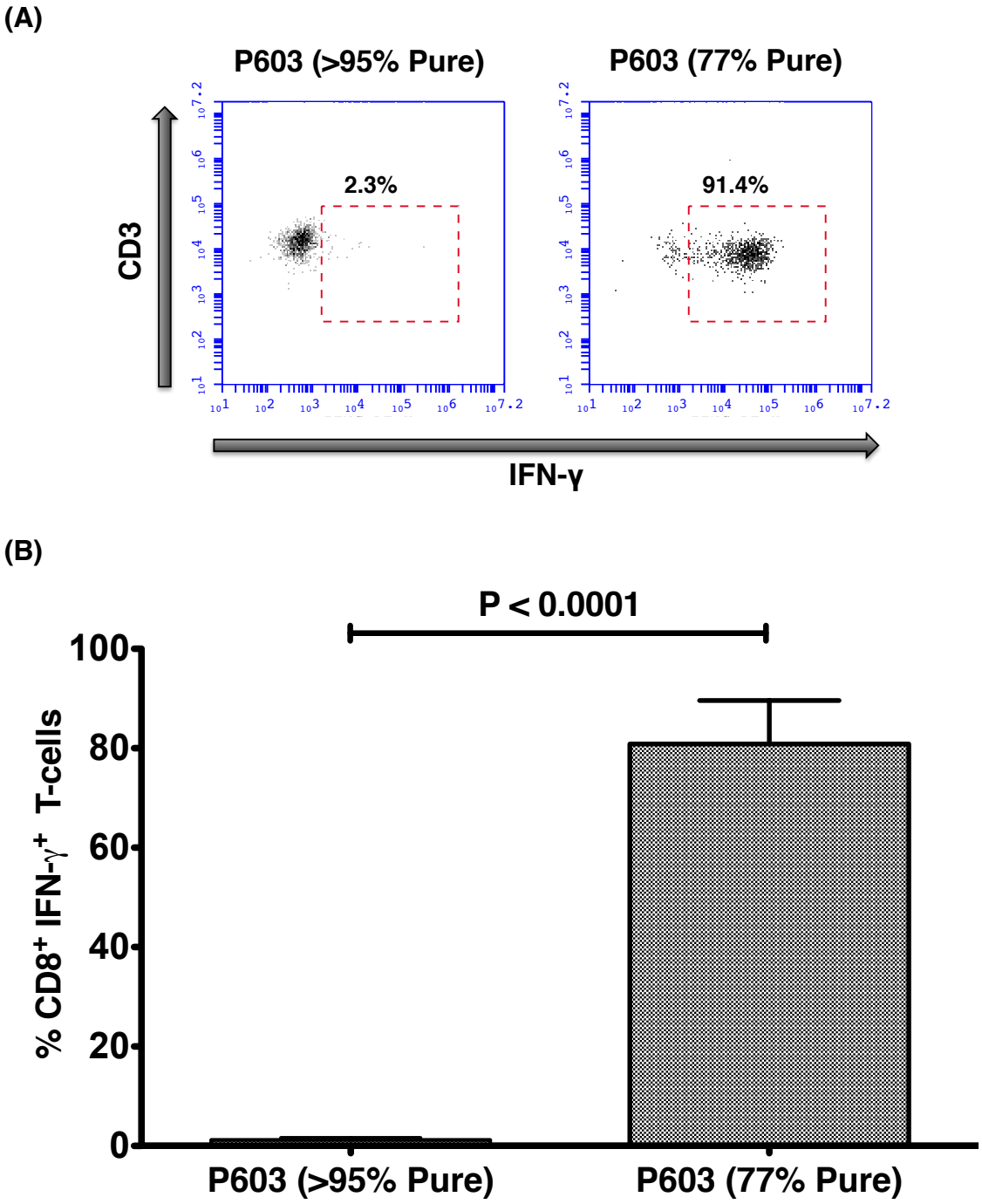

Figure 3.9 6C5 recognition of crude P603 but not pure P603. 6C5 T-cells (1×10^5) were cultured with T2 cells ± P603 (>95% Pure, 10μg/ml) or P603 (77% Pure, 10μg/ml) at 1:1 for 5 hours. T2 cells + DMSO was used as a negative control to determine background production of IFN-γ and PHA (10μg/ml) was used a positive control. IFN-γ production was assessed through intracellular staining of T-cells ($CD3^+CD8^+$) with anti-IFN-γ antibody **(A)** Raw data showing IFN-γ production in response to P603 (77% Pure) but not P603 (>95% Pure). **(B)** Significant production of IFN-γ in response to P603 (P<0.0001); 77% Pure) when compared to P603 (>95% Pure). Data are presented as the mean ± SD and represent three independent experiments**.** Statistical analysis (unpaired two-tailed t-test) was carried out using GraphPad Prism 5.0.

3.9 Identification of active component within crude P603 (77% pure)

Samples of crude and purified P603 peptide were analysed by ion trap Liquid chromatography-mass spectrometry (LCMS), by Dr James Redman (School of Chemistry, Cardiff University). The analysis of the both the 77% and >95% pure peptide preparations revealed the presence of minor/trace amounts of 8mer, 10mer and modified 9mer peptides (Table 3.1).

The potential immunogenicity of 8mer and 10mer peptides was initially investigated by synthesising a small library of crude peptides (Dr James Redman). The library consisted of four peptide preparations: (1) full length 9mer, LLSYFGTPT, (2) enhanced deletions in the *C*-terminal residues (deletion of G/T/P/T), (3) enhanced deletions in the *N*-terminal residues (deletion of L/S/Y/F) and (4) 10mer LLLSYFGTPT (additional *N*-terminal leucine). Assessment of all four peptide preparations induced similar levels of IFN-γ secretion suggesting that neither a truncated nor an extended peptide were solely responsible for the activation of 6C5. Furthermore, 6C5 remained unresponsive to P603 (>95% purity) while producing a robust IFN-γ response when challenged with P603 (>77% purity). These results suggest that a peptide common to all four preparations and P603 (>77% purity) was responsible for the activation of 6C5 (Fig. 3.10).

Peptide preparation 1 (crude full length 9mer, LLSYFGTPT) was fractionated by reverse phase HPLC, with fraction collection guided by UV absorbance (Dr James Redman) (Fig. 3.11a). Individual fractions (F1-F8) were collected, lyophilised and assayed to determine their capacity to induce T-cell activation (Fig 3.11b). Fraction 8 resulted in T-cell activation, suggesting that this fraction contained the peptide responsible for the activation of 6C5. Fractions 6 and 7 induced significant but minor T-cell activation, which may have been due to contamination from fraction 8 that occurred during the fractionation process. Furthermore, 6C5 remained unresponsive to the purified P603 (>95% purity) while producing a robust IFN-γ response when challenged with P603 (>77% purity) and peptide preparation 1.

LCMS analysis of the active fraction 8 (Dr James Redman) revealed the presence of a peptide with a fragmentation pattern associated with tyrosine tertiary butyl (Tyr(3-*t*Bu)) modification. Furthermore, a peptide with an identical fragmentation pattern was identified within the original crude P603 preparation (Fig 3.12).

Table 3.1 Comparison of purified and crude P603 peptide samples by LCMS.

Peptide	r.t. (min)	Transition	Crude P603	Purified P603
LLSYGTPT	5.5	851.5 ➔ 617.3 (b_6-H_2O)	✓	✓
LSYFGTPT	6.3	885.4 ➔ 651.3 (b_6-H_2O)	✓	✓
LLSFGTPT	6.8	835.5 ➔ 601.3 (b_6-H_2O)	✓	✓
LLSYFGTT	7.0	901.5 ➔ 764.4 (b_7-H_2O)	✓	✓
LLSYFGTPT	7.1	998.5 ➔ 764.4 (b_7-H_2O)	✓	✓
LLSYFTPT	7.1	941.5 ➔ 707.4 (b_6-H_2O)	×	✓
LLSYFGTP	7.2	897.5 ➔ 764.4 (b_7-H_2O)	✓	×
LLYFGTPT	7.4	911.5 ➔ 677.4 (b_6-H_2O)	✓	✓
LLLSYFGTPT	8.0	1111.6 ➔ 877.5 (b_8-H_2O)	✓	×
LLSY(3-*t*Bu)FGTPT	9.3	1054.6 ➔ 820.5 (b_7-H_2O)	✓	×

Chromatography was performed on an Ace Excel 2 C18 column (100×2.1mm), eluting with a linear gradient of 5-95 % acetonitrile (0.1 % formic acid) at 0.5 ml/min over 20 minutes. MS/MS spectra were measured on a Bruker amaZon SL ion trap spectrometer. The sequence and retention times (r.t.) of each of the peptides identified are indicated. The presence (✓) or absence (×) of the peptides in each sample was assessed using extracted ion chromatograms for the indicated transition.

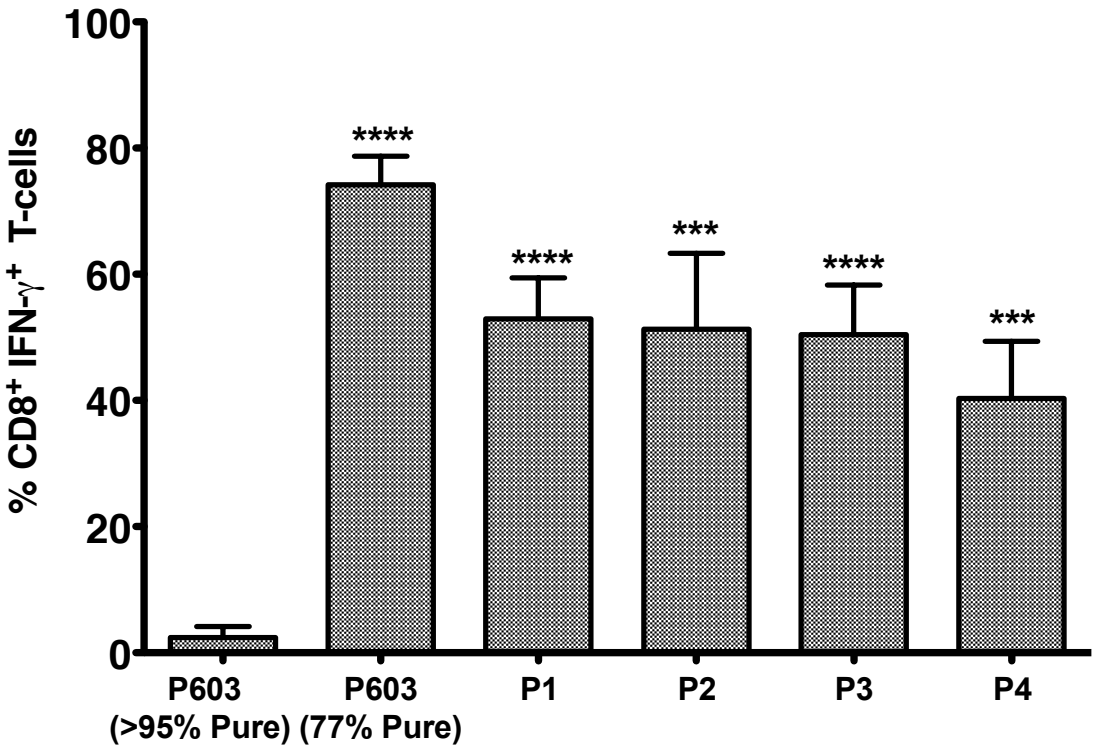

Figure 3.10 Mapping 6C5 response to peptide preparation representing potentially active contaminates identified from crude P603. 6C5 T-cells (1×10^5) were cultured with T2 cells ± P603 (>95% Pure, 10μg/ml), P603 (77% Pure, 10μg/ml) or 4 separate peptide presentation (P1-P4, 10μg/ml) at 1:1 ratio for 5 hours. T2 cells + DMSO was used as a negative control to determine background production of IFN-γ, and PHA (10μg/ml) was used as a positive control. IFN-γ production was assessed through intracellular staining of T-cells ($CD3^+CD8^+$) with anti-IFN-γ antibody. Data are presented as the mean ± SD and are representative of three independent experiments**.** Statistical analysis (unpaired two-tailed t-test, in comparison to P603 >95% Pure) was carried out using GraphPad Prism 5.0; significance was indicated by asterisks **** < 0.0001 and *** 0.0001 to 0.001.

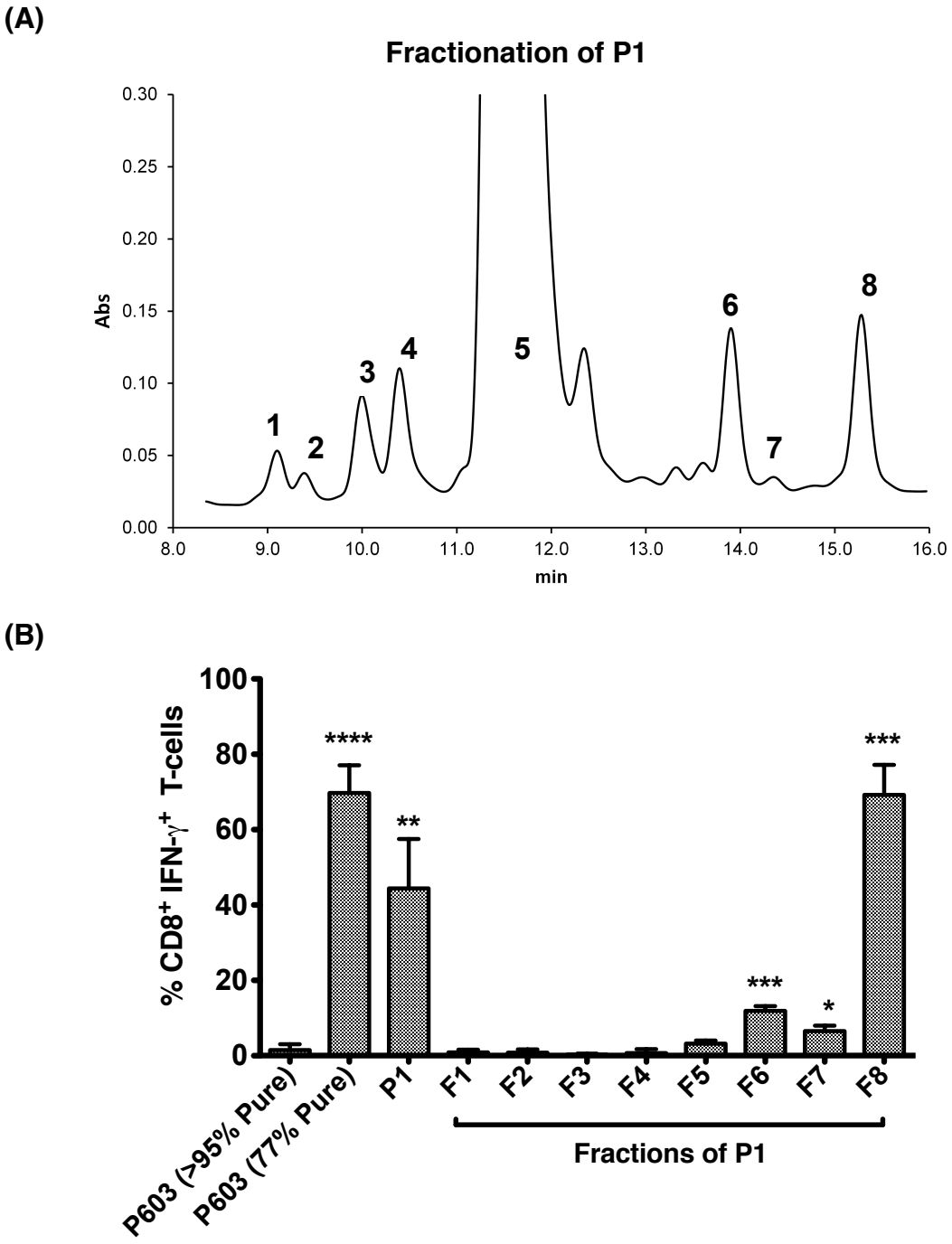

Figure 3.11 Mapping 6C5 response to the fractions generated from peptide preparation 1. (A) P1 was the most abundant peptide preparation available and was selected for fractionation by reverse phase HPLC and eight fractions were obtained. **(B)** Each fraction was reconstituted in 30µl of 100% DMSO and tested for activity against 6C5. 6C5 T-cells (1×10^5) were cultured at 1:1 ratio with T2 cells in the presence of each fraction F1-F8 (unknown concentration), P603 (>95% Purity, 10µg/ml) or P603 (77% Purity, 10µg/ml). T2 cells + DMSO were used as a negative control to determine background production of IFN-γ and PHA (10µg/ml) was used as a positive control. IFN-γ production was assessed through intracellular staining of T-cells ($CD3^+CD8^+$) with anti-IFN-γ antibody. A significant production of IFN-γ in response to P603 (77% Purity), P1, F6, F7 and F8 in comparison to P603 (>95% Pure) was observed. Data are presented as the mean ± SD and are representative of three independent experiments**.** Statistical analysis (unpaired two-tailed t-test, in comparison to P603 >95% Purity) was carried out using GraphPad Prism 5.0; significance was indicated by asterisks **** < 0.0001, *** 0.0001 to 0.001, ** 0.001 to 0.01 and * 0.01 to 0.05.

(A)

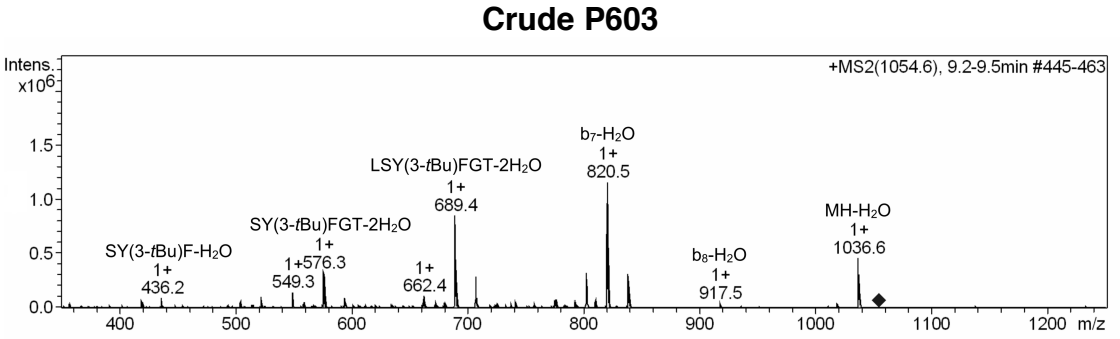

(B)

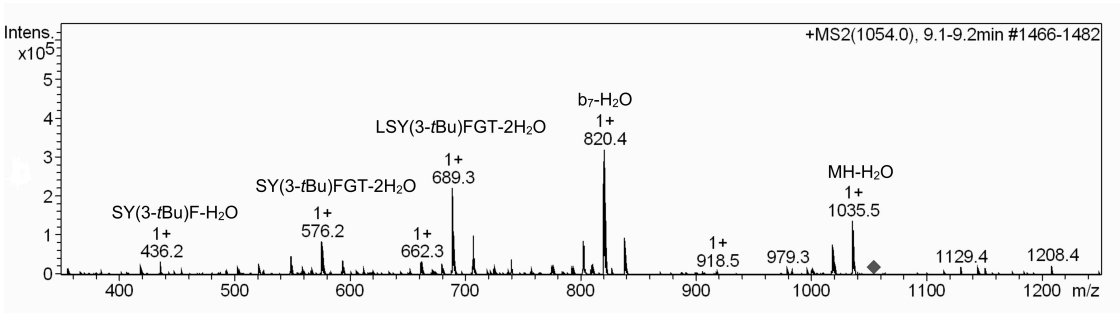

Figure 3.12 LCMS analysis of purified and crude P603 peptide samples. Chromatography was performed on an Ace Excel 2 C18 column (100×2.1mm), eluting with a linear gradient of 5-95% acetonitrile (0.1% formic acid) at 0.5 ml/min over 20 minutes. MS/MS spectra are shown with the m/z of the precursor ion indicated with a diamond, ◆. **(A)** Crude P603, retention time (r.t.) 9.5 min, precursor m/z 1054.6, **(B)** Fraction 8, r.t. 9.2 min, precursor m/z 1054.6.

3.10 Recognition of P603 *t*Bu by 6C5

The previous data (Fig 3.11 and 3.12) suggested that a peptide species containing Tyr(3-*t*Bu) was responsible for the observed activation of 6C5. To investigate this further the inactive wt P603 peptide (95% purity) was subjected to conditions intended to generate *t*Bu cations. It was predicted that this treatment would re-introduce the alkylated side products and confer activity to the previously inactive wt sequence. Peptide samples were treated under differing conditions, methylpropene with trifluoroacetic acid (TFA) or di-*tert*-butyl dicarbonate (BoC20) with TFA (Dr James Redman) (Fig. 3.13a). Analysis of the reaction products by HPLC and LCMS indicated the presence of peptides carrying the Tyr(3-*t*Bu) (Dr James Redman). Both of the Tyr(3-*t*Bu) modified preparations were able to induce IFN-γ secretion; strongly suggesting that modification of Tyr by *t*Bu was sufficient to mimic the activity associated with the crude P603 peptide preparation (Fig. 3.13b).

To confirm that P603 Tyr(3-*t*Bu) was responsible for the activation of 6C5, a highly purified (>98%) preparation of this modified peptide, was obtained from a commercial supplier (PolyPeptide Group). This peptide was able to stimulate robust and highly significant IFN-γ and CD107α responses from 6C5 ($P<0.0001$). However, the unmodified wt P603 (95% pure) failed to induce T-cell activation under the same conditions (Fig. 3.14 and 3.15). Peptide dose-response experiments were performed to validate the activity of P603 Tyr(3-*t*Bu) and to compare the activity of this peptide against the original crude (77% purity) P603 preparation. P603 Tyr(3-*t*Bu) (>98% purity) was more potent than P603 (77% purity) as determined by comparison of the calculated EC_{50} values (Fig. 3.16a and b). Using IFN-γ production as a functional read-out, the EC_{50} values were 0.2 μM for P603 Tyr(3-*t*Bu) (>98% purity) and 1.4 μM for P603 (77% purity). By contrast, using CD107α expression as a read-out, the EC_{50} values were 0.52 nM for P603 Tyr(3-*t*Bu) (>98% purity) and 610 nM for P603 (77% purity). For both assays the highly purified P603 Tyr(3-*t*Bu) peptide induced 1-3 log greater activity than the crude P603 (77% purity). These results were consistent with the chemical analysis data, as HPLC analysis of the crude P603 (77%

pure) preparation indicated that the Tyr(3-*t*Bu) modified form of the peptide comprised less than 1% of the crude P603 (77% pure) preparation (Dr James Redman).

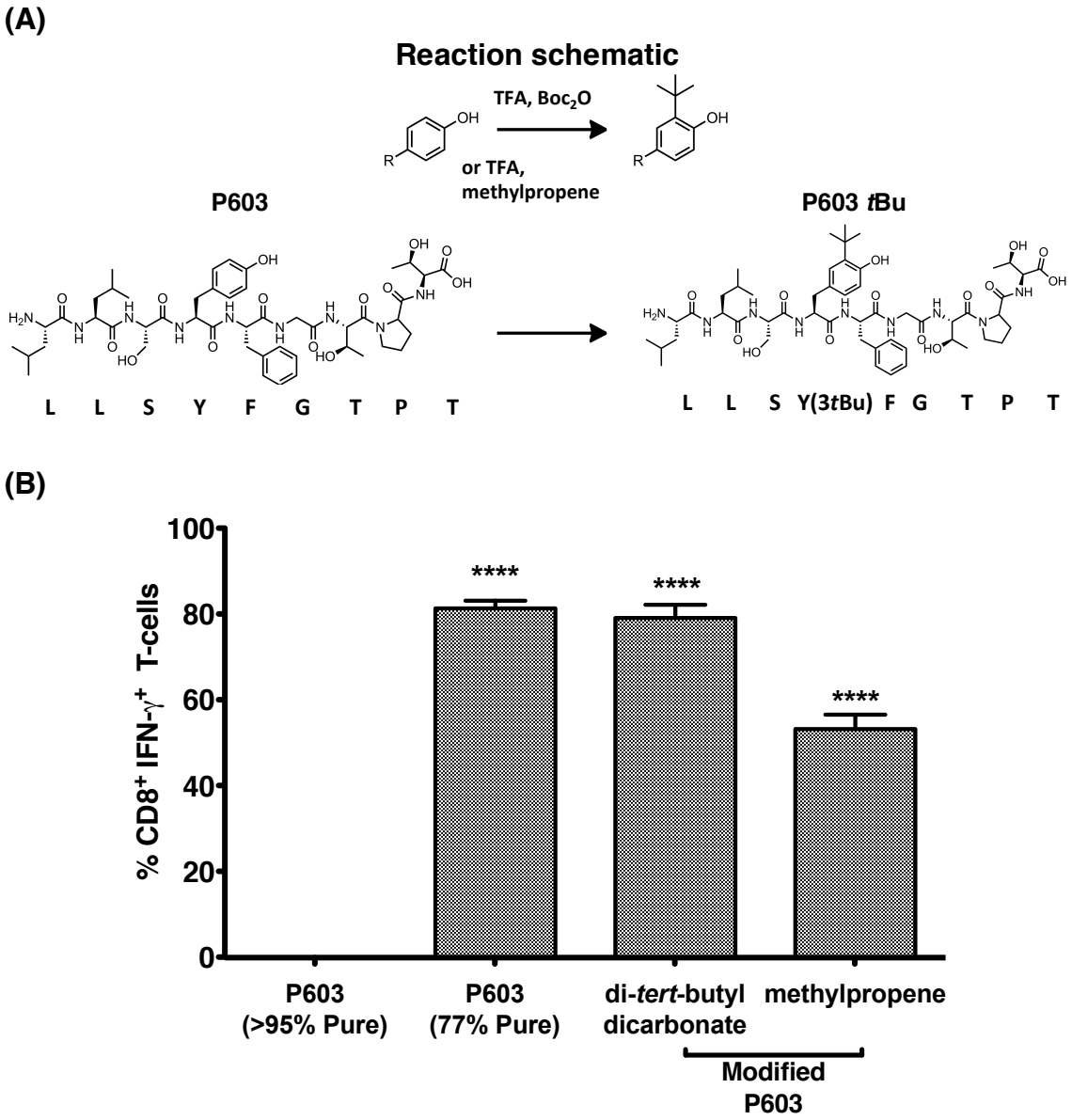

Figure 3.13 Recognition of butylated P603 by 6C5 T-cells. (A) P603 (>95% Purity), which exhibited no activity in respect to 6C5, was reacted with methylpropene and TFA, or Boc_2O and TFA to induce butylation of P603. The modified peptides were collected and reconstituted in 100% DMSO. **(B)** 6C5 T-cells (1×10^5) were cultured at 1:1 ratio with T2 cells in the presence of P603 (>95% Purity, 10μg/ml), P603 (77% Purity, 10μg/ml) or the two modified P603 peptides (di-*tert*-butyl dicardonate and methylpropene, 10μg/ml) for 5 hours at 37°C / 5% CO_2. T2 cells + DMSO were used as a negative control to determine background production of IFN-γ and PHA (10μg/ml) was used as a positive control. IFN-γ production was assessed through intracellular staining of T-cells ($CD3^+CD8^+$) with anti-IFN-γ antibody. Significantly increased production of IFN-γ was observed in response to P603 (77% Purity) and the two modified P603 peptides when comparison with P603 (>95% Purity). Data are presented as the mean ± SD and are representative of three independent experiments. Statistical analysis (unpaired two-tailed t-test, in comparison to P603 >95% Purity) was carried out using GraphPad Prism 5.0; significance was indicted by asterisks **** < 0.0001.

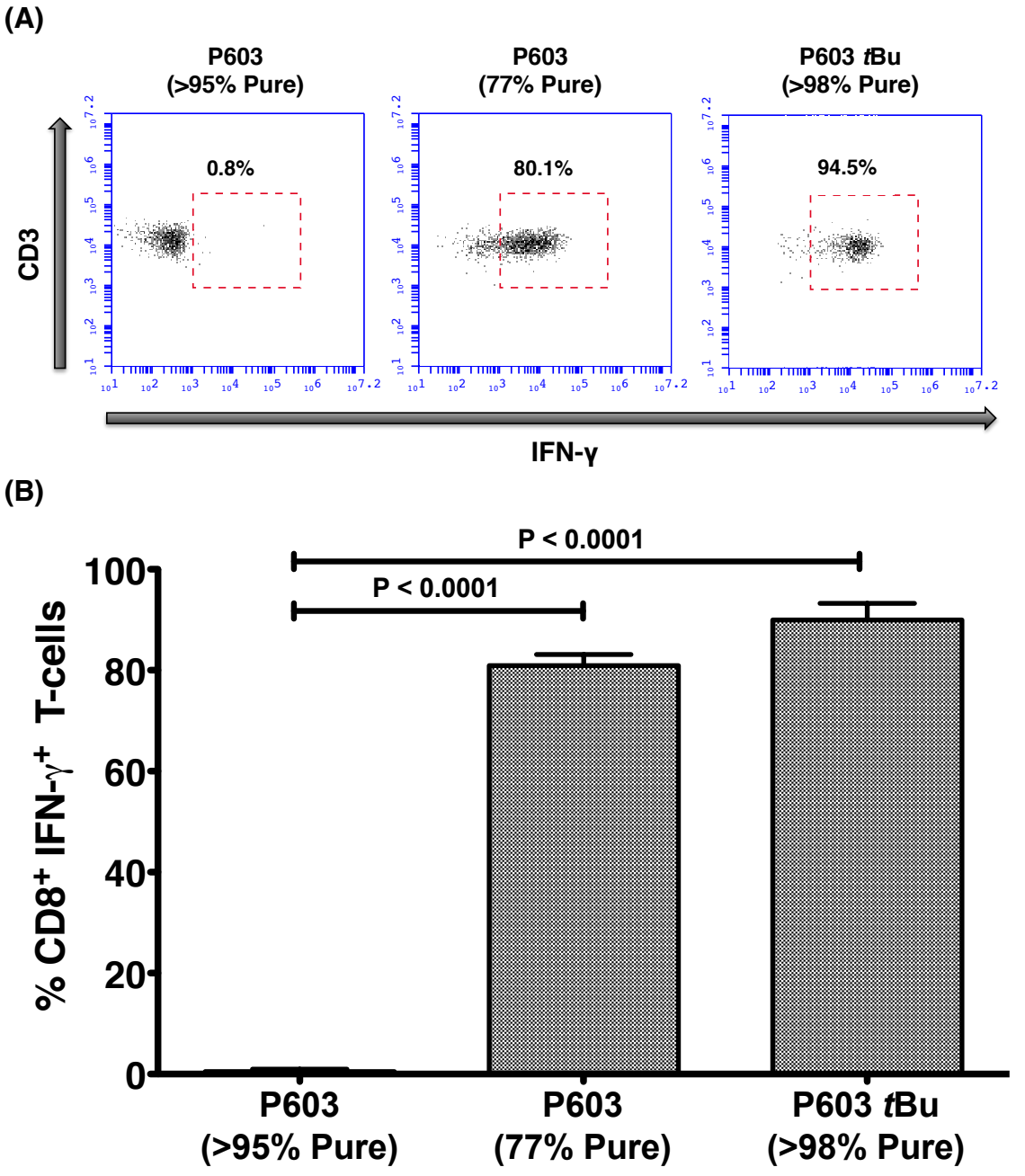

Figure 3.14 Production of IFN-γ by 6C5 T-cells in response to P603 *t*Bu. 6C5 T-cells (1×10^5) were cultured at 1:1 ratio with T2 cells in the presence of P603 (>95% Purity, 10μg/ml), P603 (77% Purity, 10μg/ml) or P603 *t*Bu (>98% Purity, 10μg/ml) for 5 hours at 37°C / 5% CO_2. T2 cells + DMSO were used as a negative control to determine background production of IFN-γ and PHA (10μg/ml) was used as a positive control. IFN-γ production was assessed through intracellular staining of T-cells ($CD3^+CD8^+$) with anti-IFN-γ antibody. A significant production of IFN-γ in responses to P603 (77% Purity) and P603 *t*Bu (>98% Purity) in comparison to P603 (>95% Purity) was observed. (A) Representative example of the flow cytometry analysis. (B) Data are presented as the mean ± SD and are representative of three independent experiments. Statistical analysis (unpaired two-tailed t-test, in comparison to P603 >95% Purity) was carried out using GraphPad Prism 5.0.

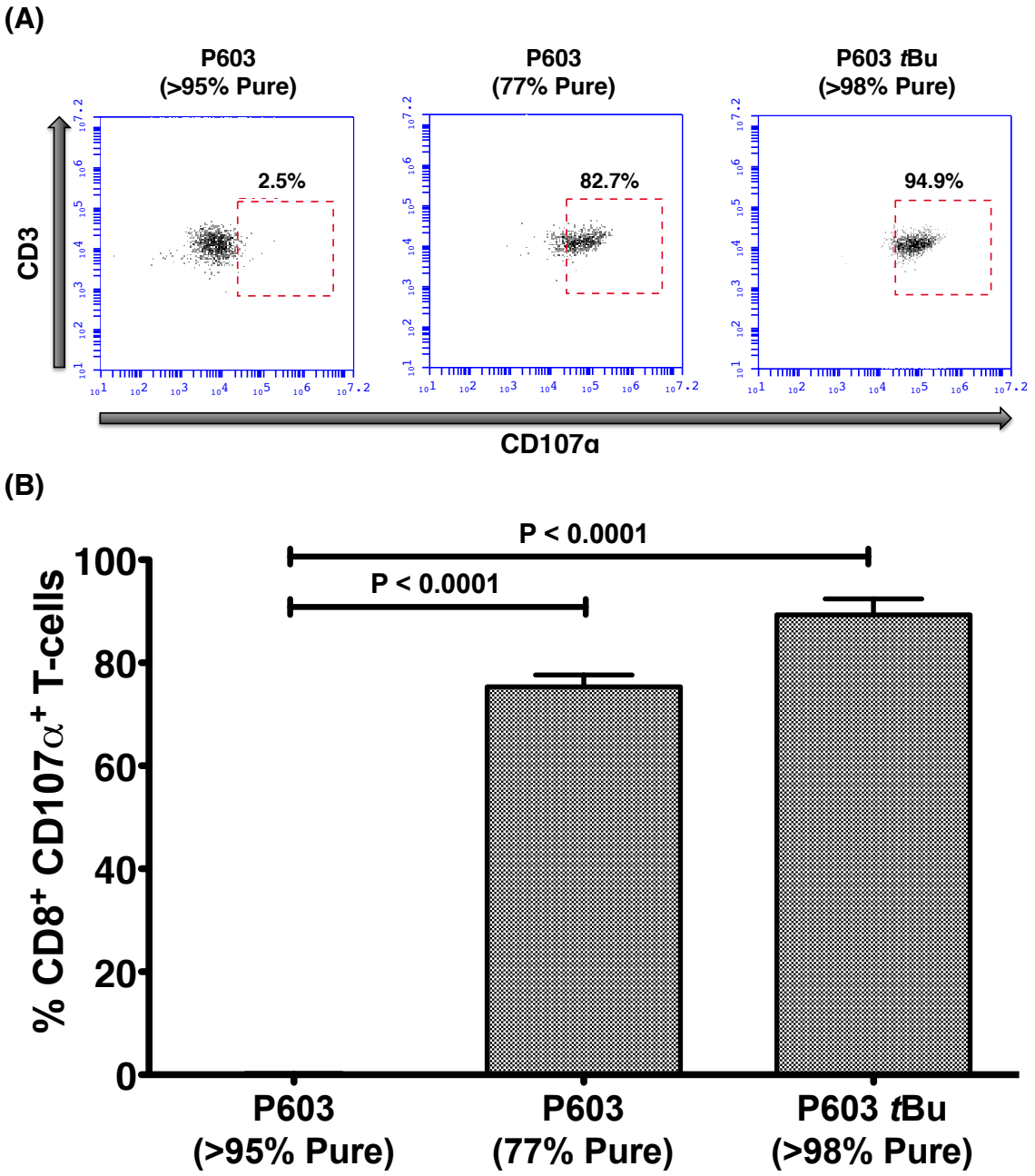

Figure 3.15 Expression of CD107α in 6C5 T-cells in response to P603 *t*Bu. 6C5 T-cells (1×10^5) were cultured at 1:1 ratio with T2 cells in the presence of P603 (>95% Purity, 10μg/ml), P603 (77% Purity, 10μg/ml) or P603 *t*Bu (>98% Purity, 10μg/ml) for 5 hours at 37°C / 5% CO_2. T2 cells + DMSO was used as a negative control to determine background expression of CD107α and PHA (10μg/ml) was used as a positive control. Changes in the surface expression of CD107α on T cells ($CD3^+CD8^+$) were determined through culturing the cells in the presence of anti-CD107α. A significant increase in the expression of CD107α in responses to P603 (77% Purity) and P603 tBu (>98% Purity) in comparison to P603 (>95% Purity) was observed. **(A)** Representative sample of flow cytometry analysis. **(B)** Data are presented as the mean ± SD and are representative of three independent experiments. Statistical analysis (unpaired two-tailed t-test, in comparison to P603 >95% Purity) was carried out using GraphPad Prism 5.0.

(A)

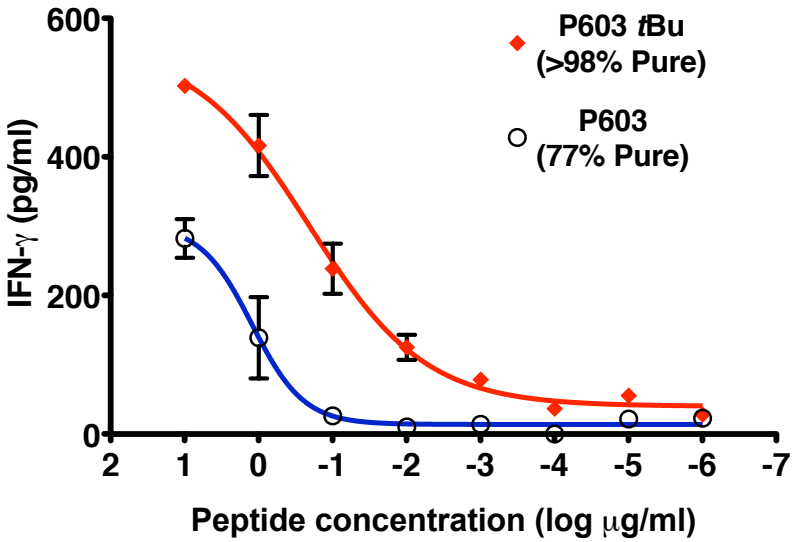

(B)

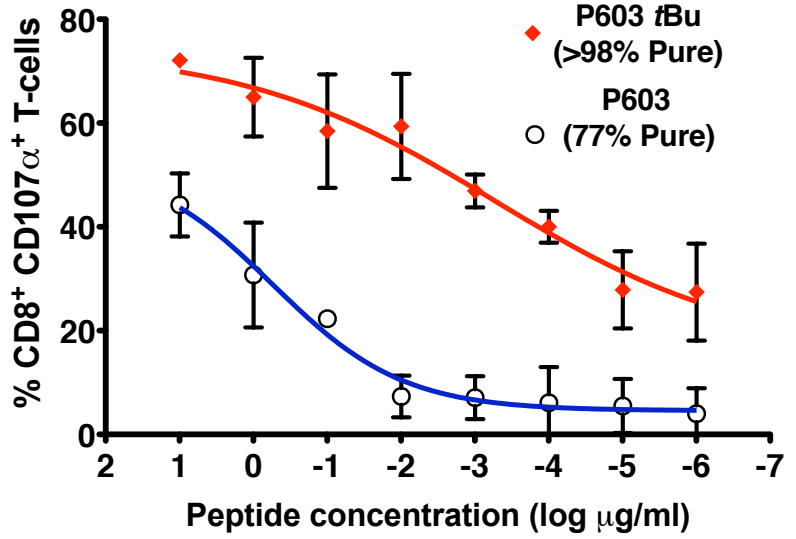

Figure 3.16 Peptide dose-response for 6C5 recognition of crude P603 and P603 *t*Bu pulsed target cells. (A) T2 cells (5×10^5) pulsed with varying concentrations of **P603** (77% Purity, 10μg/ml to 1×10^{-6} μg/ml) and **P603 *t*Bu** (>98% Purity, 10μg/ml to 1×10^{-6}μg/ml). T2 cells incubated in the presence of DMSO were used as a negative control to determine background production of IFN-γ. After 1 hour any unbound peptide was washed off and the pulsed T2 cells (1×10^5) were cultured overnight at 37°C / 5% CO_2 with 6C5 T-cells at a 1:1 ratio. Furthermore, PHA (10μg/ml) was used as a positive control. Cell-free supernatants were harvested and evaluated for the presence of IFN-γ by ELISA. **(B)** 6C5 T-cells (1×10^5) were cultured at 1:1 ratio with T2 cells in the presence of varying concentrations of P603 (77% Pure, 10μg/ml to 1×10^{-6} μg/ml) and P603 *t*Bu (>98% Pure, 10μg/ml to 1×10^{-6} μg/ml) for 5 hours at 37°C / 5% CO_2. T2 cells + DMSO was used as a negative control to determine background expression of CD107α and PHA (10μg/ml) was used as a positive control. Change in the surface expression of CD107α on T-cells ($CD3^+CD8^+$) was determined by culturing the cells in the presence of anti-CD107α. Data are presented as the mean ± SD and are representative of three independent experiments. Taking into consideration the molecular weight of P603 (885) and P603 *t*Bu (1053.6), the molar EC_{50} values were calculated from the curve of best fit. For IFN-γ production P603 (77% Purity) had an EC_{50} of 1.4μM and P603 *t*Bu had an EC_{50} of 0.2μM For CD107α expression P603 (77% Purity) had a EC_{50} of 610 nM and P603 *t*Bu had an EC_{50} of 0.52nM.

3.11 Peptide binding to HLA-A2 on the T2 cell line

One potential explanation for the difference observed between P603 *t*Bu (>98% Purity) and P603 (>95% Purity) could be related to a differential ability to bind to HLA-A2 and thus be presented to the TCR. Typically nine amino acid peptides are anchored to MHC-I molecules using the amino acids at position 2 and 9 (Denkberg et al. 2002). Since the modified tyrosine is at position 4 it unlikely that the modification would directly affect peptide binding. However, the presence of the Tyr(3-*t*Bu) residue could potentially alter the tertiary structure of the peptide and thus alter its interactions with HLA-A2. This hypothesis was tested by incubating each peptide in the presence of the TAP-deficient and HLA-$A2^+$ T2 cell line. This cell line's inherent inability to process and present endogenous peptide results in the expression of empty and unstable HLA-A2 molecules. These unstable HLA-A2 molecules are thus rapidly endocytosed, but the presence of an exogenous source of HLA-A2 binding peptide would result in the stability of the molecules and the maintance of their surface expression.

The surface expression of HLA-A2 was assessed by flow cytometry and changes in the percentage expression were compared to the negative control (DMSO alone). MART-1 peptide (ELAGIGILTV), which is an analogue of the natural MART-1 peptide (AAGIGILTV), was used as a positive control due to its superior HLA-A2 binding properties (Maeurer et al. 2002). Culturing T2 cells with ELAGIGILTV resulted in the successful up-regulation of HLA-A2. However, neither P603 *t*Bu (>98% Purity) nor P603 (>95% Purity) were able to induce an up-regulation in the expression of HLA-A2 (Fig 3.17). This suggested that neither peptide was a strong binder, but did not rule out weak or transient binding. It should be noted that HLA-A2 binding is not always an indicator of peptide activity, as peptides that exhibit poor HLA binding can successfully activate and expand peptide-specific T-cells (Khanna 2004). Nevertheless, these results show that the *t*Bu modification did not substantially improved the binding of P603 to HLA-A2, therefore

suggesting that the differences in the T-cell response induced by the two peptides may occur due to TCR recognition rather than HLA-A2 binding.

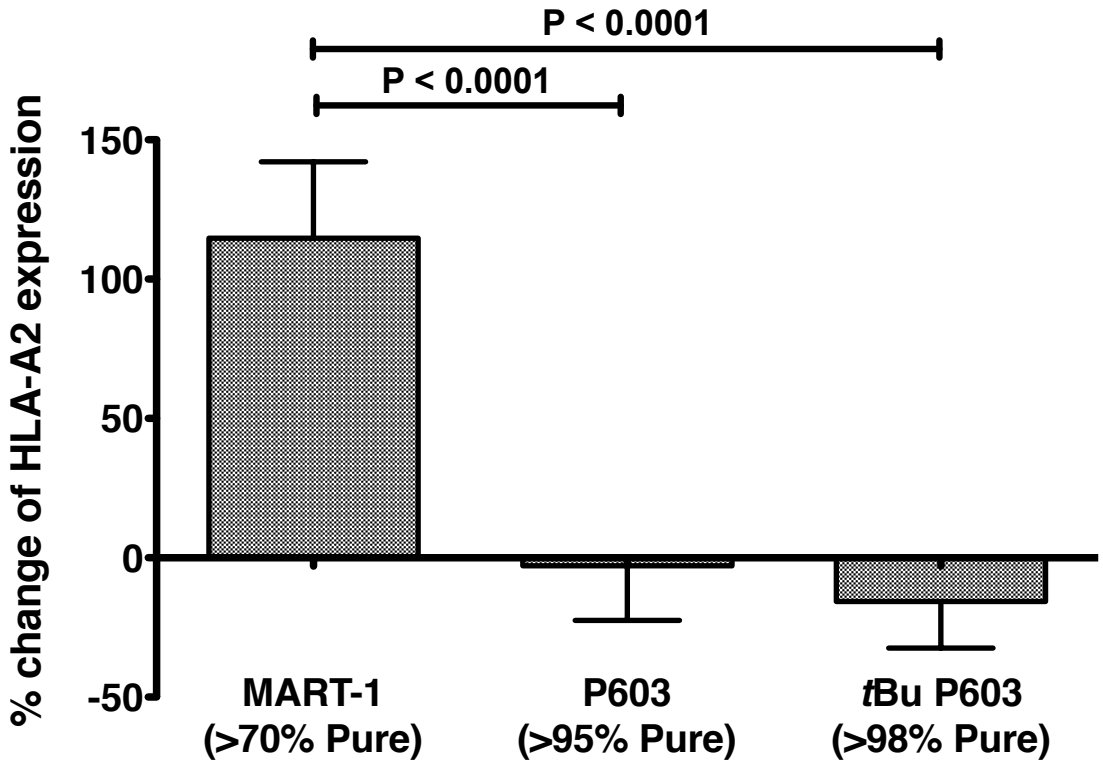

Figure 3.17 Binding of candidate peptides to HLA-A2. T2 cells (1×10^5) were incubated in the presence of P603 (>95% Purity, 10μg/ml), P603 *t*Bu (>98% Purity, 10μg/ml) or MART-1 (70% Purity, 10μg/ml) overnight at 37°C / 5% CO_2. Due to its known superior HLA-A2 binding, the MART-1 peptide was used as a positive control and T2 cells treated with DMSO-only were used as a negative control in order to determine background HLA-A2 expression. After culturing, the cells were then stained with anti-HLA-A2 and expression was determined by flow cytometry. As T2 cells ubiquitously express HLA-A2, changes in the mean fluorescence intensity (MFI) were investigated. The percentage change in HLA-A2 expression was determined according to the formula: % change = [(mean fluorescence with peptide – mean fluorescence without peptide) / mean fluorescence without peptide x 100]. Culturing with MART-1 resulted in an increase in the expression of HLA-A2, while P603 (>95% Purity) and P603 *t*Bu (>98% purity) resulted in a decrease in the expression of HLA-A2. Data are presented as the mean ± SD and are representative of three independent experiments.

3.12 Peptide:MHC computer modelling

Investigation of HLA-A2 binding suggested that the presence of the Tyr(3-*t*Bu) residue did not alter the HLA-A2 binding potential of the P603 peptide (Fig 3.17). To investigate this further, MHC/peptide complex computer modelling was performed by Dr Pierre Rizkallah (School of Medicine, Cardiff University). The molecular modelling of the two peptides suggested that the presence of the Tyr(3-*t*Bu) would not alter the interaction between the peptide and the MHC molecules. However, the modification was predicted to result in an extension of the tyrosine side chain out of the MHC towards the TCR and produce a peptide with the capacity to adopt two different conformations due to the rotation of the aryl ring (Fig 3.18). The predicted similarity between the peptide and MHC interactions supports the hypothesis that differential activity of the *t*Bu modified vs unmodified peptides is due to differential recognition by the TCR, rather than differences in HLA-A2 binding capacity.

3.13 Nonamer Combinatorial Peptide Library (CPL) screen

In summary, the data presented indicates that the $CD8^+$ T-cell clone 6C5 was unable to recognise $HLA\text{-}A2^+$ CLL (Fig 3.8) or the predicted Bax sequence (LLSYFGTPT) but was able to recognise a chemically modified peptide (LLSY(3-*t*Bu)FGTPT) (Fig 3.14-3.16). Since *t*Bu modifications do not occur naturally, it is unlikely that this artificial epitope is the source of the TCR specificity of 6C5. CPL screens have been successfully used to map the specificity of expanded T-cell populations of unknown specificity in leukaemia (L, Wooldridge, personal communication). Therefore, a CPL screen was performed to probe the molecular landscape recognised by the 6C5 TCR, which allowed for the identification of potential "naturally occurring" antigenic targets. 6C5 exhibited varying degrees of degeneracy at each position, however the greatest degrees of degeneracy were observed outside of central region (position 4-6), suggesting that these residues were important for TCR recognition of 6C5. Additionally, the index peptide (LLSY(3-*t*Bu)FGTPT) appeared to be suboptimal at every position, except position 8 (Fig 3.19 and Table 3.2). Collectively

these findings suggest that 6C5 could recognise a multitude of peptide sequences, with potentially greater affinity than its index peptide. This supports the notion that the modified peptide LLSY(3-*t*Bu)FGTPT is not the natural peptide epitope recognised by 6C5.

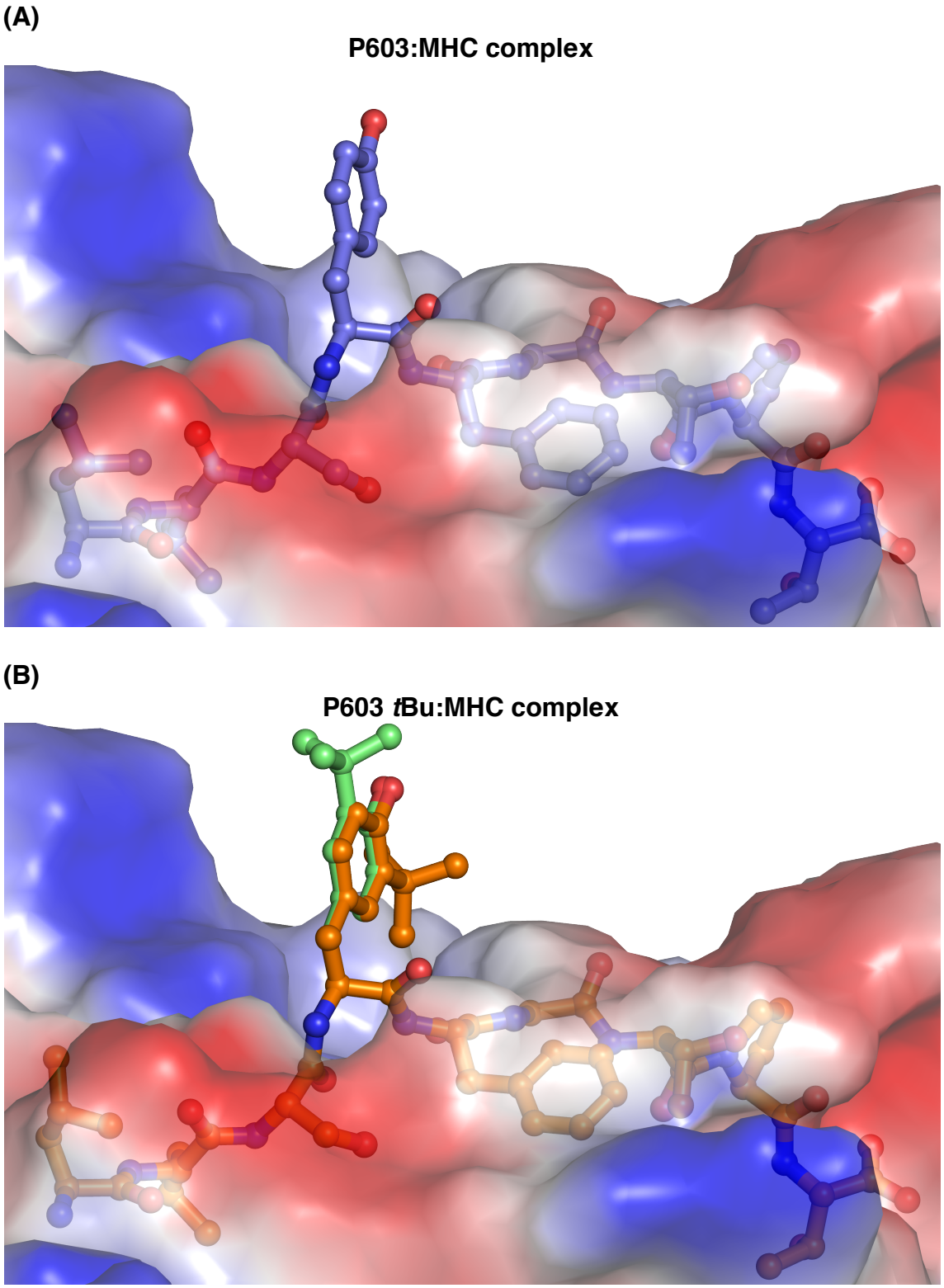

Figure 3.18 Peptide/MHC modelling of unmodified and Tyr(3-*t*Bu) modified peptide bound to HLA-A*0201. Computer models of Peptide:/HLA*0201 complexes were generated using entry 4I4W from the Protein Data Bank (PDB). Crystallographic Object-Oriented Toolkit (COOT) was used to modify the sequence of the peptide to be LLSYFGTPT. **(A)** and **(B)** show that for both peptides the anchor residues at either end of the peptide were buried in the MHC molecular groove. However, the presence of the Tyr(3-*t*Bu) resulted in the extension of the tyrosine side chain out of the MHC and towards the TCR.

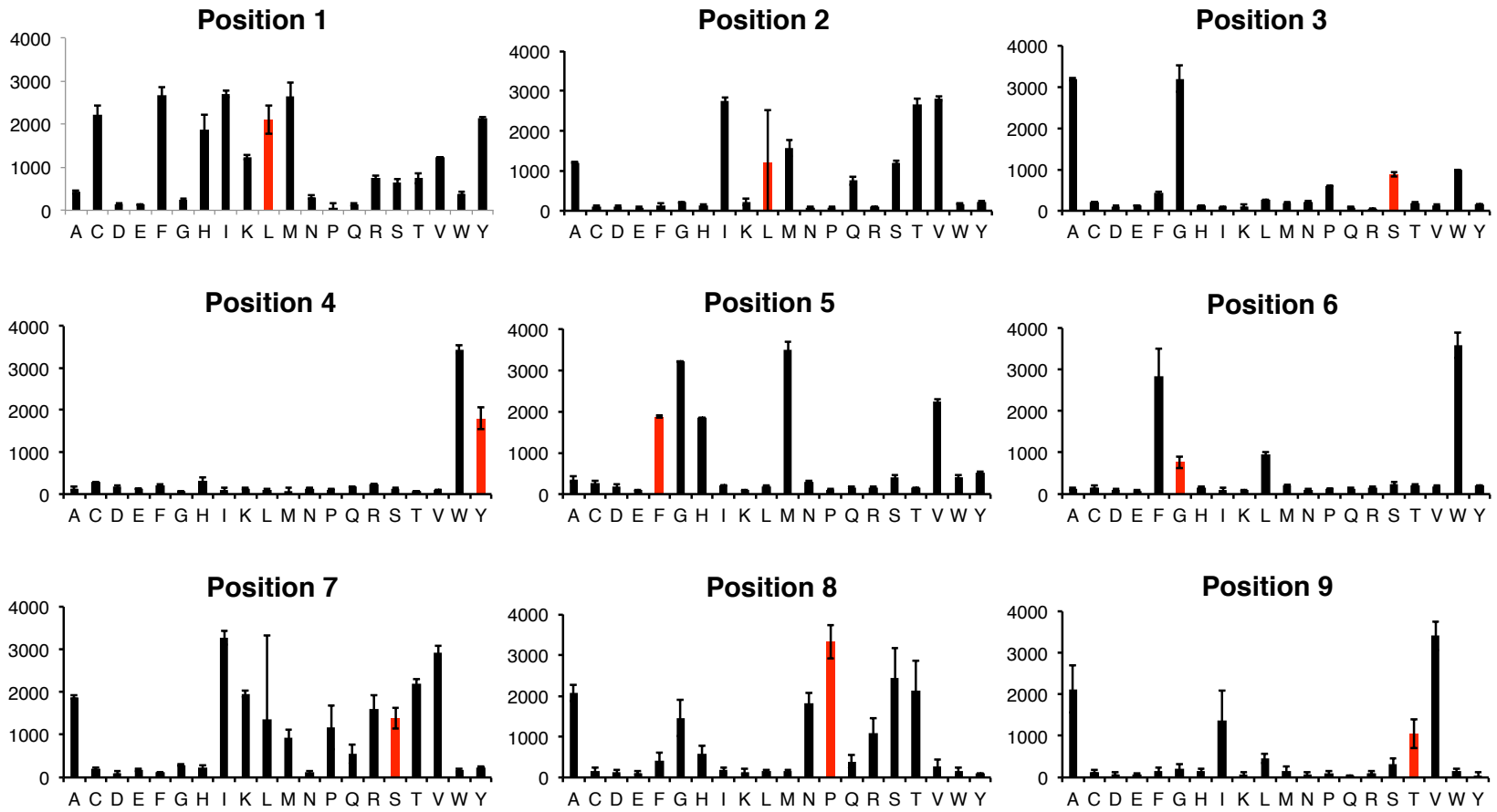

Figure 3.19 Nonamer CPL screen. The nonamer library contained a total of 5×10^{11} different nonamer peptides and was divided into 180 different peptide mixtures. In every peptide mixture, one position has a fixed L-amino acid residue and all other positions were degenerate, thus allowing for any one of 19 natural L-amino acids to being incorporated at each position (cysteine is excluded). C1R-A2 cells (6×10^4) were pulsed in duplicate with each mixture from a nonamer CPL (100 µg/ml). After 2 hours, 6C5 T-cells were added at a ratio of 2:1 and incubated overnight at 37°C / 5% CO_2. Cell free supernatants were harvested and evaluated for MIP-1β by ELISA. Data presented as the mean ± SD and is representative of 2 independent experiments.

Table 3.2 Summary of data from the nonamer CPL screen performed on 6C5.

1L	2L	3S	4Y*	5F	6G	7T	8P	9T
I H R A	V M Q	G W F	W Y H	M F Y W	W G S	I K M G	P N H F	V I L
F K T W	I L	A S L	C	G H S	F L	T A Q	S G Q	A T S
M V S N	T A	P		V A		V R	T R V	
C	S			N		L	A	
L				C		S		
						P		

MIP-1β(pg/ml) - **RED (2000 - 3600)** **BLUE (1000 - 2000)** **GREEN (500 - 1000)** **BLACK (250 - 500)**

The amino acid residues at each position were grouped based the quantity of the MIP-1β produced. For ease of interpretation the amino acids were coloured, sized and arranged in descending order based on the amount of MIP-1β produced.

3.14 Identification and screening of cross-reactive peptides

Three degenerate peptide sequences were identified based on MIP-1β production (Table 3.3) and were utilised to probe the UniProt Knowledgebase peptide database on 13/5/2013 using the ScanProsite (de Castro et al. 2006). This was an attempt to identify antigenic peptides originating from multiple biological sources (self, viral, bacterial and fungal) that could be recognised by 6C5. Twenty five peptide sequences of interest were identified and subsequently 10 were selected for synthesis and further testing (Table 3.4). The selection criteria were based on the likelihood of the peptides to induce T-cell activation (as determined by the MIP-1β production profile of the sequence), and to provide candidates from the four biological sources sampled (self, viral, bacterial and fungal). All of these were synthesised together with the "optimal peptide" identified from the CPL screen. This peptide comprised the amino acid sequence that resulted in the greatest MIP-1β production for each given position.

Of the 10 peptides selected for testing only four produced T-cell responses above background (Fig 3.20). Of these peptides only two, IIGWMWIPV (optimal peptide) and YTAYVFIPI (originated from serine palmitoyltransferase, SPT), resulted in responses greater than the index peptide (Fig 3.20 and Table 3.5). Analysis of the EC_{50} values indicated that the IIGWMWIPV peptide (5.45×10^{-9}M) out-performed the index peptide (LLSY(3-*t*Bu)FGTPT) by approximately two logs and the YTAYVFIPI (7.16×10^{-8}M) out-performed the index peptide by approximately one log. The two peptides that produced responses below the index peptide were MIAWGFISV (4.20×10^{-5}M) and FIAWGFIAA (1.23×10^{-5}M), which originated from *Candida dubliniensis* and multiple strains of *Staphylococcus*, respectively.

The CPL screen indicated that the index peptide for 6C5 was suboptimal at each position except position 8, which provided the potential for multiple peptide sequences to be generated that could be recognised by 6C5 and out-perform the index peptide. This concept was validated through the superior T-cell activation observed with the "optimal

peptide". Additionally, the CPL screen indicated that the 6C5 was capable of recognising peptides in which the modified tyrosine was substituted for a naturally occurring amino acid in combination with other changes to the peptide sequence.

Table 3.3 Degenerate peptide seqeunces produced from the nonamer CPL

MIP-1β production	Sequence
≥500µg/ml	[IFMCYLHKVRTS]-[VITMLAS]-[AGWSP]-[WY]-[FGHMVY]-[FGLW]-[IVTKARLSPMQ]-[PSTANGRH]-[AITV]
≥1000µg/ml	[IFMCYLHKV]-[VITMLAS]-[GA]-[WY]-[MGVFH]-[WF]-[IVTKARLSP]-[PSTANGR]-[VAIT]
≥2000µg/ml	[IFMCYL]-[VIT]-[GA]-W-[MGV]-[WF]-[IVT]-[PSTA]-[VA]

Table 3.4 Candidate peptides identified from the nonamer CPL

Type	Source	Sequence
Optimal	N/A	IIGWMWIPV
Self	Protein LYRIC	LLGYGWAAA
	Parathyroid hormone 2 receptor.	LIGWGFPAA
	Serine palmitoyltransferase small subunit B	YTAYVFIP
Viral	Influenza A virus	VVWYGGRPV
	Varicella-zoster virus	STGYGLARI
		FSPYGWSST
	Hepatitis C virus subtype 1a	KAAYGFTGI
Bacterial	Staphylococcus	FIAWGFIAA
Fungal	Candida dubliniensis	MIAWGFISV

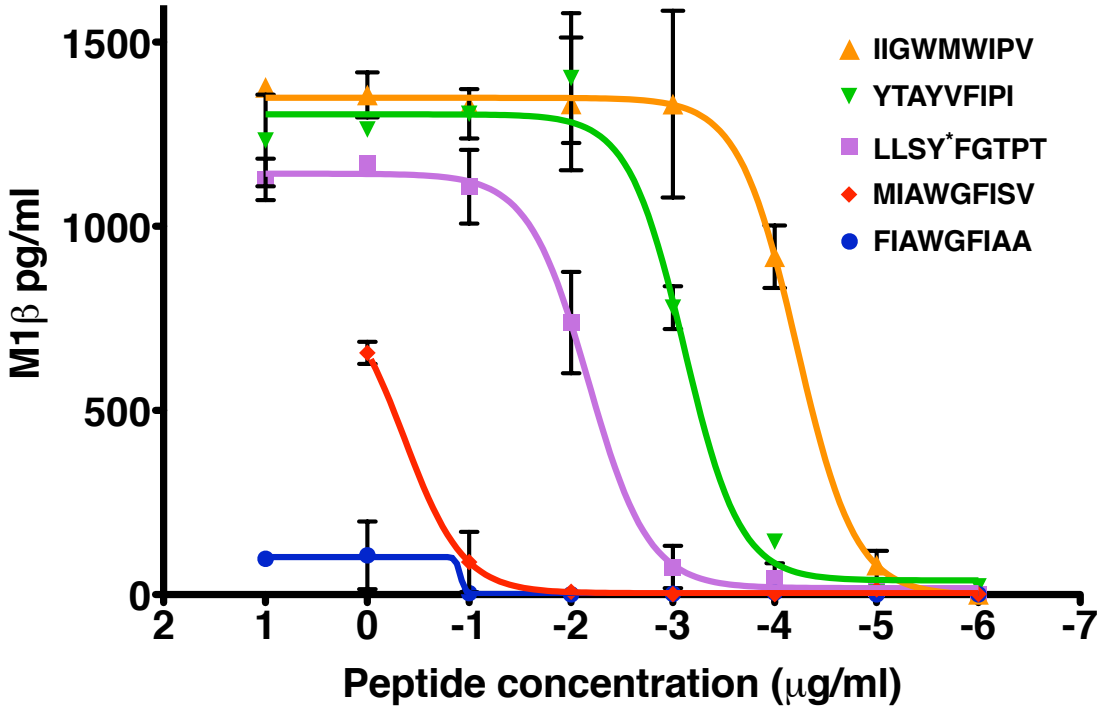

Figure 3.20 Peptide dose-response for 6C5 recognition of candidate peptide identified from CPL. C1R-A2 cells (1×10^5) were pulsed with varying concentrations (10μg/ml to 1×10^{-6} μg/ml) of the selected peptides. After 1 hour 6C5 T-cells were added at a 1:1 ratio and cultured overnight at 37°C / 5% CO_2. Cell-free supernatants were harvested and evaluated for the presence of MIP-1β by ELISA. C1R-A2 and 6C5 T-cells incubated in the presence of DMSO alone were used as a negative control to determine background production of MIP-1β. Furthermore, PHA (10 μg/ml) was used as a positive control. Taking into consideration the differing molecular weights of each peptide the molar EC_{50} values were calculated from the curve of best fit. Data are presented as the mean ± SD and are representative of three independent experiments.

Table 3.5 Candidate peptides that produced MIP-1β responses above background.

Sequence	Source	EC_{50} M
IIGWMWIPV	Optimal peptide	5.45×10^{-9}
YTAYVFIPI	Serine palmitoyltransferase	7.16×10^{-8}
LLSY*FGTPT	Index	6.44×10^{-7}
MIAWGFISV	Candida dubliniensis	4.20×10^{-5}
FIAWGFIAA	Staphylococcus	1.23×10^{-5}

3.15 Discussion

The initial phase of this study centred on generating $CD8^+$ T-cell clones from CLL patients that were specific for peptides derived from the pro-apoptotic protein Bax. Based on previous work, this had been proposed as a TAA for CLL (Agrawal et al. 2008; Nunes et al. 2011). However, the existence of Bax-specific $CD8^+$ T-cells had not been previously investigated in primary CLL patient samples.

To investigate this 23 candidate peptides were identified from the Bax-α protein using a computer algorithm to predict HLA binding. A pool of these peptides was used to stimulate $CD8^+$ T-cells from a CLL patient (R6A8R89) *in vitro* using CD40L-activated autologous CLL cells as APC (Rodríguez-Pinto 2005; Van den Hove et al. 1997). CD40L activation was shown to induce CLL expression of molecules important for T-cell activation such as CD86 and HLA-DR (Fig 3.1).

Repeated Bax peptide stimulation of $CD8^+$ T-cells from CLL patient R6A8R89 allowed detection of Bax-specific T-cells. This showed that it was possible to generate an apparent T-cell response against a "self" protein from a CLL patient using a similar procedure as previously described for healthy donors (Nunes et al. 2011). Limiting dilution cloning generated a T-cell clone 6C5 that recognised two peptides from the peptide pool: P603 ($Bax_{161-170}$; LLSYFGTPT) and P605 ($Bax_{160-170}$; GLLSYFGTPT), which shared an overlapping 9 amino acid sequence. The superior IFN-γ response observed with P603 indicated that 6C5 had a preference of nonamer peptides. The concept of a TCR having a preference for a specific length peptide, while demonstrating recognition of shorter or longer peptides, is not uncommon and has been observe with numerous T-cell clones (Ekeruche-Makinde et al. 2013). Furthermore, it has been suggested that the variation in the quality of response to similar peptides of different lengths is not due to effects on MHC binding but presentation at the level of the TCR (Ekeruche-Makinde et al. 2013).

While the process of generating T-cell clones utilised in this study (peptide pool stimulation and limiting dilution) is common practice (Mariotti and Nisini 2009; Gallagher

and Man 2007; Yee et al. 2002; Nunes et al. 2011), alternative approaches to the generation of clonal populations of T-cells have been used by others. For example, the *ex vivo* culturing and expansion of tetramer sorted T-cells (Dunbar et al. 1999). However, this approach was not utilised in this study for the following reasons:

1. Several Cardiff laboratories, including ours, had failed to generate long-lived T-cell clones using tetramer sorting (S Man, C Pepper, personal communication).
2. The proof of principle study (Nunes et al. 2011) indicated that a $CD8^+$ T-cell restricted to the Bax epitope P613 (IMGWTLDFL) was capable of recognising and killing CLL cells. However, it was unknown whether T-cells with the same specificity actually existed in CLL patients or whether this was indeed the optimal epitope in patients.
3. The high production costs associated with manufacturing multiple tetramers made this approach financially unfeasible.
4. Activation-induced cell death is a common side-effect of tetramer sorting thereby decreasing the efficacy of isolating and growing specific clones (Cebecauer et al. 2005).

The use of IFN-γ ELISpot to determine T-cell recognition of target cells has been successfully used to validate $CD8^+$ T-cells specific for epitopes associated with CLL (Nunes et al. 2011; Foster et al. 2010). Furthermore, as chromium release CTL assays are not suitable with CLL targets due to inherent instability associated with CLL cell membranes (S Man, C Pepper, personal communication), IFN-γ ELISpot was used to investigate the recognition of primary CLL cells by 6C5. It was observed that the 6C5 was unable to specifically recognise resting or activated HLA-$A2^+$ CLL cells. This suggested that the Bax-derived epitope P603 was not expressed on either resting or activated CLL cells. Alternatively, the affinity of 6C5 may be too weak to induce cellular activation in response to the quantity peptide expressed on the CLL cells.

An unexpected finding from the epitope mapping indicated the 6C5 was not actually specific for P603. By utilising an immunological and chemical approach it was determined that 6C5 was actually specific for a modified version of P603, which contained a tertiary butyl on the tyrosine residue (LLSY(3-*t*Bu)FGTPT). It is likely that the modified P603 peptide identified in this study was generated during the peptide synthesis process due to the alkylation of tyrosine by *t*Bu cations under peptide deprotection conditions. This reaction has been reported during model deprotection conditions (Lundt et al. 1979) and for preparative scale synthesis (Taka et al. 2009) of Tyr(3-*t*Bu). Therefore the observation of a peptide containing Tyr(3-*t*Bu) as a minor constituent of the crude P603 preparation was perhaps not surprising.

Peptide modifications can alter MHC binding kinetics (Parkhurst et al. 1996), the TCR contact residues of the peptides (de Haan et al. 2005a; de Haan et al. 2005b) and ultimately peptide immunogenicity. While it is clear that the presence of the Tyr(3-*t*Bu) dictated the peptide recognition of 6C5, the precise mechanism by which this modification modulates peptide immunogenicity was unknown e.g. altered MHC binding or differential TCR contact.

HLA-A2 binding assays were performed to determine if the presence of Tyr(3-*t*Bu) allowed for enhanced MHC binding and thus superior peptide presentation. This was determined by investigating changes in the stability of HLA-A2 on T2 cells, in presence of peptides by flow cytometry. The results suggested that the presence of Tyr(3-*t*Bu) had little or no influence on peptide binding. However, these results were inconclusive as no clear difference could be determined between the two peptides. Additionally only a single peptide concentration was tested, to provide an extensive evaluation of the interaction between the peptides of interest and MHC, it would be desirable to test multiple peptide concentrations. To fully assess the differences in MHC binding between the two peptides a more sensitive and efficient assay would be required e.g. a chemiluminescence HLA

binding assay such as the one used by the human MHC project (Harndahl et al. 2009) or a Biacore-based assay (Fayad et al. 2001).

However, as these techniques were not available at the time of this study, peptide/MHC models (Dr Pierre Rizkallah) were computer generated based on known peptide/MHC structures 4I4W (Ekeruche-Makinde et al. 2013). These models predicted that the presence of the Tyr(3-*t*Bu) would not change the peptide/MHC interactions involved in binding, but would result in an extension of the tyrosine side chain out of the MHC towards the TCR. This would potentially alter the peptide structure "observed" by the TCR. However, as this is only a computer model, based on previously described "natural" sequences, it remains uncertain whether the presence of the Tyr(3-*t*Bu) would actually alter the tertiary structure of the P603 thereby influencing MHC binding and/or the TCR contact residues. This could be investigated further by crystallisation of HLA-A2 complexed with the wild type and modified P603 peptides, but this was beyond the scope of this project.

Encouragingly it has been shown the chemical modification of amino acid side chains involved in TCR contact can result in the loss of peptide immunogenicity, whilst have no significant influence on MHC binding (de Haan et al. 2005a; de Haan et al. 2005b). Furthermore, it has been observed that a minor change in tyrosine, the conversion of tyrosine to nitrotyrosine, can abrogate peptide recognition in both $CD4^+$ (Birnboim et al. 2003) and $CD8^+$ T-cells (Hardy et al. 2008), whilst not affecting MHC binding. Conversely, it has been shown that alterations of MHC binding residues, which have positive effects on MHC binding, can have a negative effect on peptide recognition and T-cell responses (Cole et al. 2010). Thus highlighting the complexity involved in the relationships between peptide binding, TCR recognition and subsequent T-cell responses.

Since peptides containing Tyr(3-*t*Bu) are synthetic entities and do not occur in nature, it is unclear how a $CD8^+$ T-cell with specificity for LLSY(3-*t*Bu)FGTPT could have arisen. There are two possibilities for the origin of $CD8^+$ T-cell clone 6C5. Firstly, it could

be a memory T-cell generated *in vivo* against a naturally occurring epitope that is able to cross-react with LLSY(3-*t*Bu)FGTPT. Theoretically, a different, naturally occurring residue that possessed an extended side chain with similar properties to the (3-*t*Bu) group could result in a suitable peptide confirmation allowing for TCR contact and activation. Secondly, 6C5 could have been generated from naïve T-cells primed against P603 *t*Bu *in vitro*, which expanded to functionally detectable levels during the 5-week culturing period. This possibility could be tested by culturing flow sorted naïve T-cells in the presence of LLSY(3-*t*Bu)FGTPT (van der Burg et al. 2001).

Thus far it has been shown that the specificity of 6C5 is restricted to a modified version of P603 (LLSY(3-*t*Bu)FGTPT) rather then the original wild type Bax-derived peptide, P603 (LLSYFGTPT). This difference in specificity could therefore explain the inability of 6C5 to recognise primary HLA-A2$^+$ CLL cells. However, in the absence of T-cell clones specific for the wild type P603 it is still unknown whether this epitope could be generated and presented on the CLL cells.

To investigate the potential for 6C5 to cross-react with naturally occurring peptides a CPL screen was performed. This revealed that the 6C5 showed varying degrees of degeneracy across all 9 amino acids, but the greatest degeneracy were observed outside of central region (positions 4-6), suggesting that conservation of these residues is important for T-cell activation. Position 4 showed the least degeneracy with only four different amino acids being successfully recognised (W > Y > H > C). Interestingly the CPL screen suggested that the unmodified form of tyrosine would be successful recognised by 6C5. It is possible that the unmodified tyrosine may need to be "paired" with specific residues within the central region to allow for successful T-cell activation. This hypothesis could be tested through synthesis and assaying of a series of analogues of the P603 peptide that are fixed at all positions apart from 5 and 6.

Four out of the 10 peptides generated from the data produced by the CPL screen exhibited activity above the background, but only two showed activity above the index

peptide; the optimal peptide (IIGWMWIPV) and a peptide sequence originating from the enzyme SPT (YTAYVFIPI). SPT is the initial and rate-limiting enzyme in the sphingolipid synthesis process and is made up of two subunits SPT1 and SPT2. Immunocytochemistry analysis showed enhanced expression of both subunits in colon, ovarian, pancreas and thyroid carcinomas as well as Leiomyosarcoma (Carton et al. 2003). Therefore, it could be hypothesised that the enhanced expression of SPT in these malignancies could lead to the expression of SPT-derived peptides, which could serve as targets for T-cells that express TCRs specific for SPT-derived peptides, such as 6C5. However, investigation of this hypothesis was beyond the scope of this project.

In summary, this study highlights how the chemical modification of a single amino acid, Tyr ➔ Tyr(3-*t*Bu), could affect the activation of the $CD8^+$ T-cell clone 6C5. This modified P603 *t*Bu peptide arose as a byproduct of the peptide synthesis process and formed <1% of the original P603 crude (77% Purity) peptide preparation and <0.05% of the original 23 peptide mixture used during *in vitro* T-cell stimulation. These statistics emphasise the acute specificity and sensitivity of TCR and their ability to discriminate between peptides with identical primary amino sequence but which differ by a single chemical modification (de Haan et al. 2005a; de Haan et al. 2005b; Birnboim et al. 2003; Hardy et al. 2008). Additionally, this study highlights how minor peptide contaminants can potentially cause misleading results within immunological research (Mannering et al. 2003; Brezar et al. 2011). Given the standard methodology that is currently employed for peptide synthesis, this data could have wider implications in relation to the interpretation of results derived from the *in vivo* use of synthetic peptides for vaccination. The use of a CPL screen provided insight in which naturally occurring amino acids could function in place of the modified tyrosine and indicated that 6C5 could potentially cross-react with several "natural" peptides.

While this chapter ultimately failed to address the original aim of generating Bax-specific $CD8^+$ T-cells from CLL patients, it showed that activated CLL cells can serve as

effective source of APCs to expand low frequency peptide-specific T-cells. Furthermore, the study demonstrated that long-lived and functionally competent $CD8^+$ T-cell clones could be isolated from CLL patients. Therefore, although the investigation into the existence and function of Bax-specific T-cells within CLL patients was not further investigated within this thesis, the techniques and the knowledge acquired have proved invaluable for further work.

Chapter 4

Immunophenotyping of CLL patients

CLL has been widely characterised as a disease that exhibits multiple T-cell defects (Ramsay et al. 2008; Nunes et al. 2012; Riches et al. 2013), which could limit the immunological control of the tumour and increase susceptibility to opportunistic infections. Additionally, these immunological defects could limit the efficacy of T-cell based immunotherapies for the treatment of CLL such as adoptive T-cell therapy and bi-specific antibodies. Moreover it has become increasing apparent that T-cells may play a role in the survival of CLL cells *in vivo* (Bagnara et al. 2011) and may even influence the pathology of the disease (Nunes et al. 2012). Therefore the acquisition of knowledge regarding T-cell immunophenotype from CLL patients might identify patients who are most suitable for T-cell therapies and provide evidence for the involvement of specific T-cell populations in the pathology of the disease.

The objective of this study was to use polychromatic flow cytometry to perform a phenotypic analysis of T-cells and B-cells from the peripheral blood of 97 CLL patients (Appendix 1) and 21 healthy donor (HD) age-matched controls (Appendix 2) to identify potential immunological abnormalities. Patients were either analysed as whole cohort or divided into two groups based on their CD4:CD8 ratio: normal (<1) or inverted (>1). Additionally due to overwhelming dominance of CLL cells in peripheral blood samples, partial enrichment of the T-cell compartment was performed by the removal of $CD19^+$ leukaemic B-cells to allow for a more detailed analysis of T-cell populations expressing multiple markers in combination.

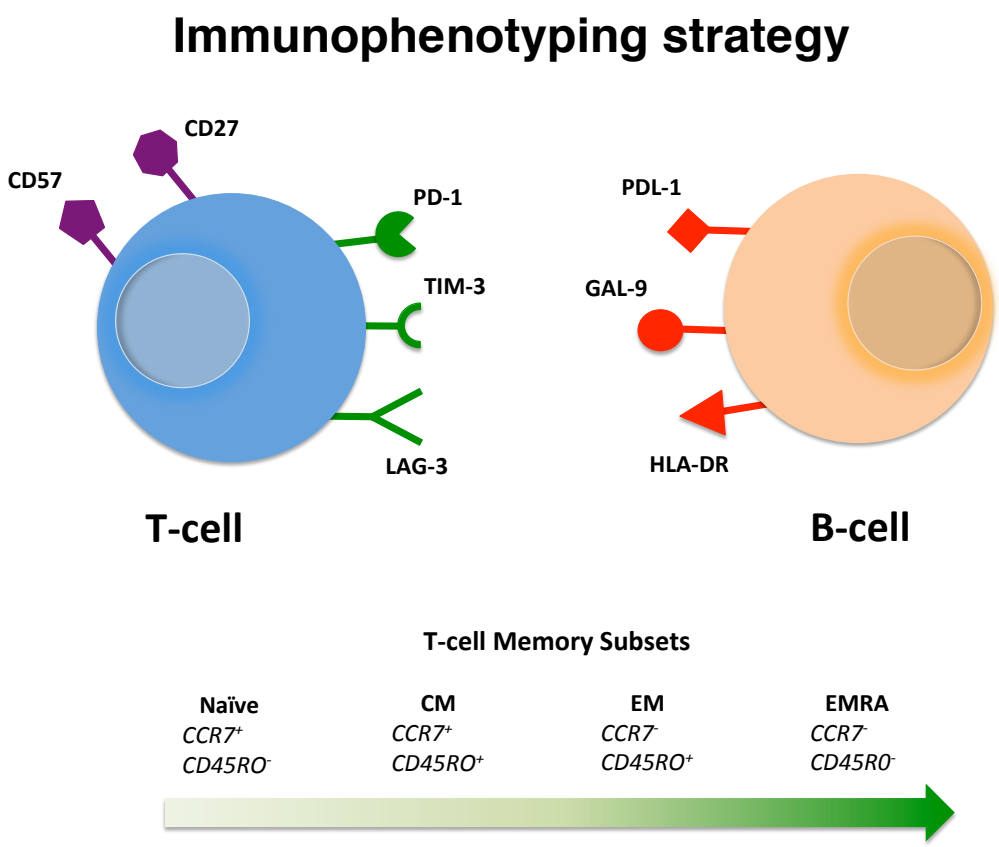

Figure 4.1 Immunophenotyping strategy. Schematic showing the markers investigated in this study and the potential interactions that could occur between the T-cells and B-cells.

Gating strategy

(A)

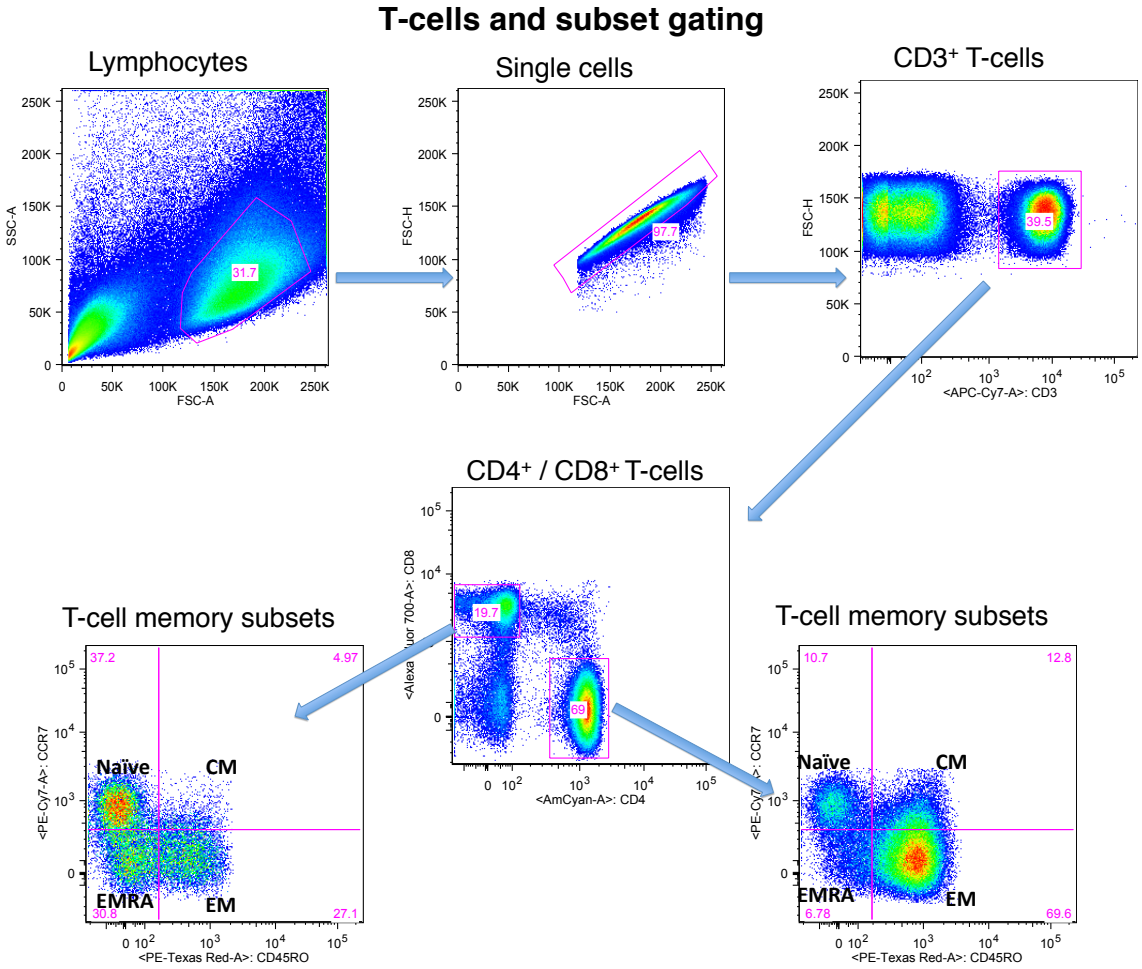

(B)

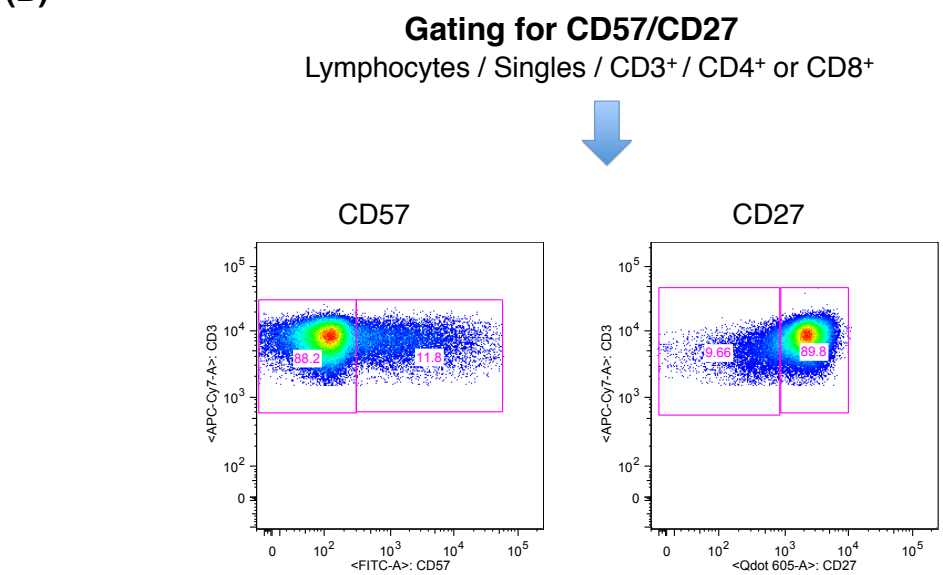

(C)

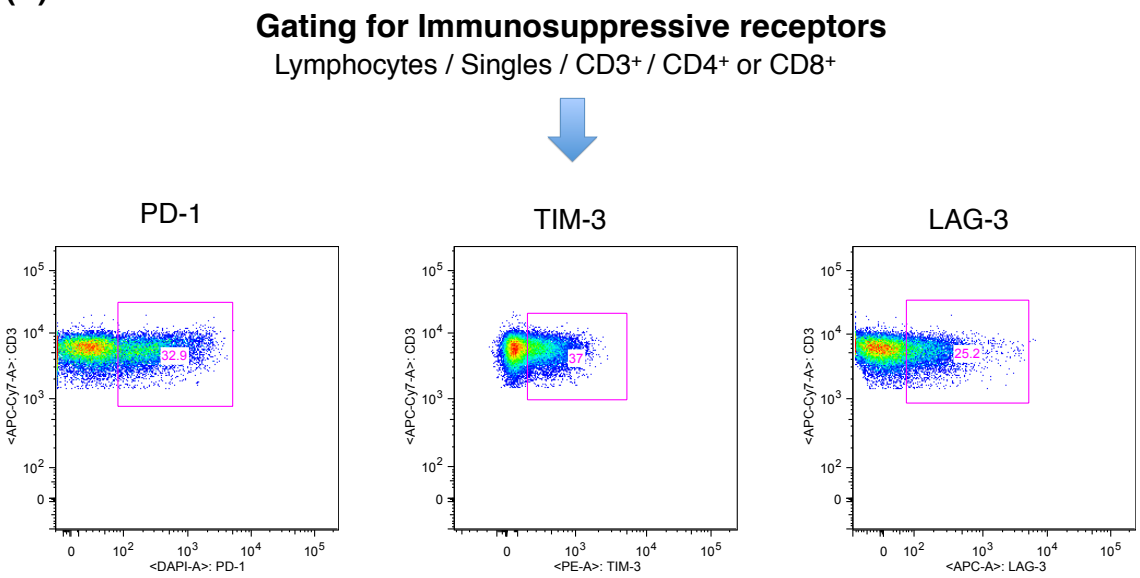

Figure 4.2 Representative results of T-cell phenotypic analysis. The percentage of positive cells was determined by flow cytometry (FACSAria) and analysis was carried out using FlowJo software. **(A)** The gating strategy used to identify the $CD4^+$ and $CD8^+$ T-cells as well as T-cell memory subsets, which were defined using CCR7 and CD45RO labelling: $CCR7^+$ $CD45RO^-$ (Naïve), $CCR7^+$ $CD45RO^+$ (CM), $CCR7^-$ $CD45RO^+$ (EM) and $CCR7^-$ $CD45RO^-$ (EMRA). **(B)** Gating strategy used to characterise the expression of CD27 and CD57 within the $CD4^+$ and $CD8^+$ T-cell compartments. **(C)** Gating strategy used to characterise the expression of PD-1, TIM-3 and LAG-3 within the $CD4^+$ and $CD8^+$ T-cell compartments. To assist with the gating of positive cell populations fluorescence minus one (FMO) controls were applied where necessary.

4.1 $CD4^+$ T-cells

4.1.1 Memory subsets

T-cells can be sub-divided into 4 main subsets (Naïve, CM, EM and EMRA) based on the expression of CCR7 and CD45RO (Fig 4.1 and 4.2a). As well as displaying phenotypic differences these subsets have been shown to exhibit functional distinctions both *in vitro* and *in vivo* (Sallusto et al. 2004; Klebanoff et al. 2006; Geginat et al. 2003).

When the 97 CLL patients were analysed as a group, no significant differences in the frequencies of $CD4^+$ T-cell subsets were observed when compared with age-matched healthy donors (HD) (Fig 4.3). However, when CLL patients were stratified into two groups based on CD4:CD8 ratios (normal ratio, CLL^{NR} and inverted ratio, CLL^{IR}) it was observed that there was a significant decrease in the percentage of naïve $CD4^+$ T-cells within the CLL^{IR} patient group when compared to the CLL^{NR} ($P \leq 0.001$) and the HD controls ($P \leq 0.01$). Furthermore, there was a significant increase in the percentage of EM $CD4^+$ T-cells within the CLL^{IR} patient group when compared to the CLL^{NR} ($P \leq 0.001$) and HD controls ($P \leq 0.01$). In contrast, no significant difference in the frequency of naïve or EM $CD4^+$ T-cells was observed between CLL^{NR} and HD controls (Fig 4.4). These results highlight that the distribution of the $CD4^+$ T-cell subsets within CLL patients is heterogeneous, with the CLL^{IR} patient group displaying a reduced naïve T-cell pool and an increased EM compartment.

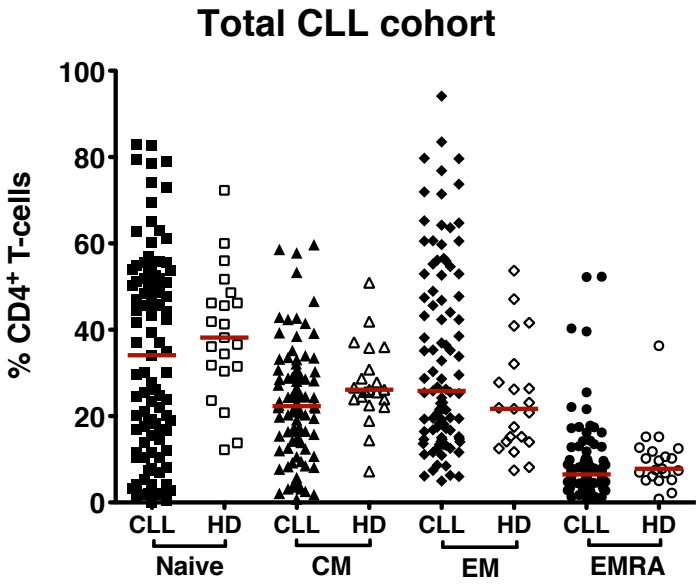

Figure 4.3 CD4$^+$ T-cell memory subsets in the total CLL cohort (n=97) and age-matched healthy donor (HD) controls (n=21). The percentages of positive cells were quantified using 10-colour flow cytometry (FACSAria). Live lymphocytes were gated based on forward and side scatter profile and T-cell memory subsets were defined using CCR7 and CD45RO, Naïve (CCR7$^+$ CD45RO$^-$), CM (CCR7$^+$ CD45RO$^+$), EM (CCR7$^-$ CD45RO$^+$) and EMRA (CCR7$^-$ CD45RO$^-$). Data are represented as dot plots with the median (red bar) shown for each distribution. Statistical analysis (Mann-Whitney U test) was performed using GraphPad Prism 5.0.

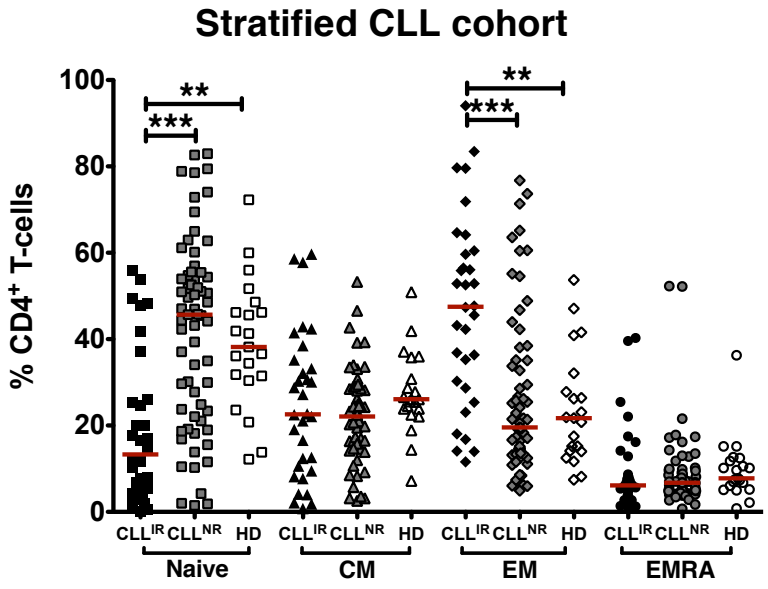

Figure 4.4 CD4$^+$ T-cell memory subsets in the stratified CLL cohort (CLL^{IR}, n=32 and CLL^{NR}, n=65) and age-matched healthy donor (HD) controls (n=21) The percentages of positive cells were quantified using 10-colour flow cytometry (FACSAria). Live lymphocytes were gated based on forward and side scatter profile and T-cell memory subsets were defined using CCR7 and CD45RO, Naïve (CCR7$^+$ CD45RO$^-$), CM (CCR7$^+$ CD45RO$^+$), EM (CCR7$^-$ CD45RO$^+$) and EMRA (CCR7$^-$ CD45RO$^-$). Data are represented as dot plots with the median (red bar). Statistical analysis (Kruskal-Wallis ANOVA with the Dunn's Multiple Comparison Test) was performed using GraphPad Prism 5.0. The level of statistical significance is denoted by asterisks (** $P \leq 0.01$, *** $P \leq 0.001$).

4.1.2 Expression of CD57 and CD27

The expression of CD57 has been historically associated with a "highly differentiated" T-cell phenotype, as $CD57^+$ T-cells have been shown to be more susceptible to apoptosis, and exhibit reduced proliferative potential and diminished effector function (Dolfi et al. 2008; Brenchley et al. 2003; Focosi et al. 2010). However, the specific fate bestowed upon a T-cell due to the expression of CD57 is still under debate (Chong et al. 2008). Additionally, the loss of expression and/or effective signalling via the co-stimulatory T-cell receptor CD27 has been associated with immune dysfunction and differentiation (Dolfi et al. 2008; Plunkett et al. 2007; Hendriks et al. 2000). The development of the described phenotypes typically coincide with a stepwise transition from the acquisition of CD57 and the loss of co-stimulatory receptors such as CD27 and CD28 (Klebanoff et al. 2006). Therefore because of their association with T-cell differentiation and function, the expression of CD57 and CD27 on T-cells was investigated.

When considering the total CLL cohort, no significant differences regarding the frequency of $CD57^+$ (Fig 4.5) or $CD27^-$ T-cells were observed (Fig 4.7) when compared with the HD controls. However, when CLL patients were stratified into two groups (CLL^{IR} and CLL^{NR}) there was a significant increase in the frequency of $CD57^+$ T-cells within the CLL^{IR} patient group when compared to the CLL^{NR} ($P \leq 0.001$) and the HD controls ($P \leq 0.001$). In contrast, no significant differences were observed between CLL^{NR} and the HD controls (Fig 4.6). Additionally, there was a significant increase in the frequency of $CD27^-$ T-cells within the CLL^{IR} patient group when compared to the CLL^{NR} ($P \leq 0.001$) with a trend towards an increase in the frequency of a $CD27^-$ phenotype within the CLL^{IR} patient group when compared to the HD controls (Fig 4.8).

These results indicated that CLL patients exhibit a diverse range of expression of CD57 and CD27 within the $CD4^+$ T-cell compartments. However, distinct differences were observed between subsets of patients with increased frequencies of $CD57^+$ and $CD27^-$

expression being associated with the CLL^{IR} patient group. This suggests that individuals within this group exhibit features associated with augmented immunological differentiation.

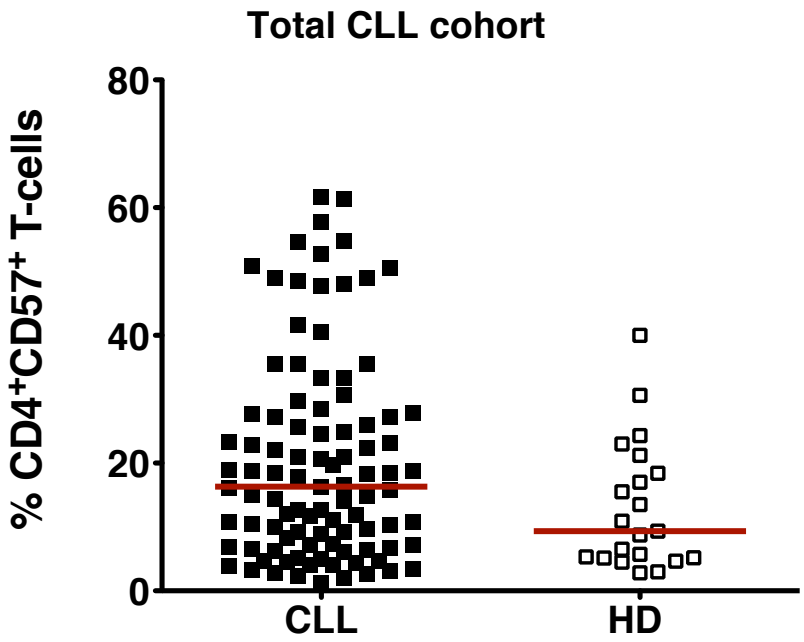

Figure 4.5 CD57 expression within CD4⁺ T-cells of the total CLL cohort (n=97) and age-matched healthy donor (HD) controls (n=21). The percentages of positive cells were quantified using 10-colour flow cytometry (FACSAria). Live lymphocytes were gated based on forward and side scatter profile. CD57 expression was measured in the total CD4⁺ T-cell population. Data are represented as dot plots with the median (red bar) shown for each distribution. Statistical analysis (Mann-Whitney U test) was performed using GraphPad Prism 5.0.

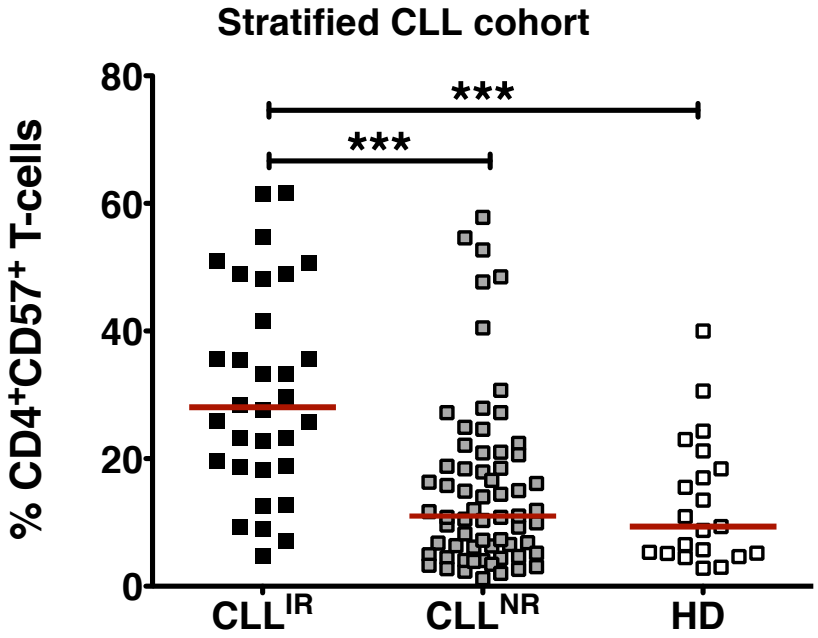

Figure 4.6 CD57 expression within CD4⁺ T-cells of the stratified CLL cohort (CLL^{IR}, n=32 and CLL^{NR}, n=65) and age-matched healthy donor (HD) controls (n=21). The percentages of positive cells were quantified using 10-colour flow cytometry (FACSAria). Live lymphocytes were gated based on forward and side scatter profile. CD57 expression was measured in the total CD4⁺ T-cell population. Data are represented as dot plots with the median (red bar) shown for each distribution. Statistical analysis (Kruskal-Wallis ANOVA with the Dunn's Multiple Comparison Test) was performed using GraphPad Prism 5.0. Statistical significance is denoted by asterisks (*** $P \leq 0.001$).

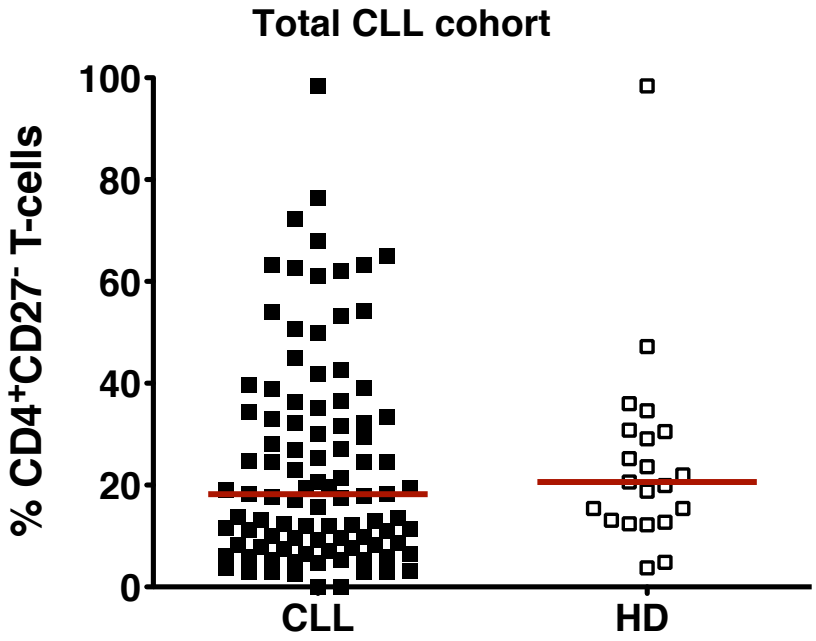

Figure 4.7 CD27 expression within CD4$^+$ T-cells of the total CLL cohort (n=97) and age-matched healthy donor (HD) controls (n=21). The percentages of positive cells were quantified using 10-colour flow cytometry (FACSAria). Live lymphocytes were gated based on forward and side scatter profile. CD27 expression was measured in the total CD4$^+$ T-cell population and was presented as CD27$^-$ CD4$^+$ T-cells. Data represented as dot plots with the median (red bar) shown for each distribution. Statistical analysis (Mann-Whitney U test) was performed using GraphPad Prism 5.0.

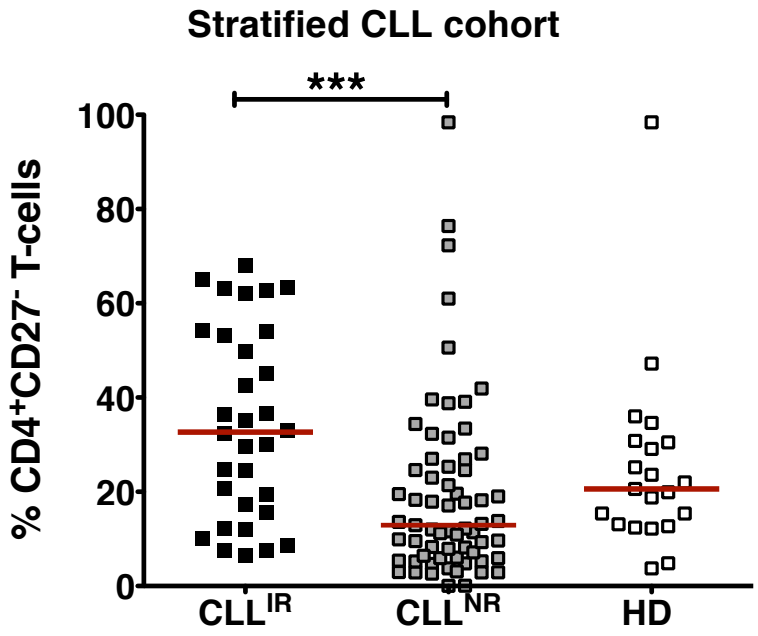

Figure 4.8 CD27 expression within CD4$^+$ T-cells of the stratified CLL patients (CLL^{IR}, n=32 and CLL^{NR}, n=65) and age-matched healthy donor (HD) controls (n=21). The percentages of positive cells were quantified using 10-colour flow cytometry (FACSAria). Live lymphocytes were gated based on forward and side scatter profile. CD27 expression was measured in the total CD4$^+$ T-cell population and was presented as CD27$^-$ CD4$^+$ T-cells. Statistical analysis (Kruskal-Wallis ANOVA with the Dunn's Multiple Comparison Test) was performed using GraphPad Prism 5.0. Statistical significance is denoted by asterisks (*** $P \leq 0.001$).

4.1.3 Immunosuppressive receptors

The expression of immunosuppressive receptors has been observed in numerous haematological (Nunes et al. 2012; Riches et al. 2013) and solid malignancies (Matsuzaki et al. 2010; Fourcade et al. 2009) as well as viral infections (McMahan et al. 2010; Day et al. 2006). The expression and activation of these receptors has been associated with reduced T-cell effector functions, diminished proliferative potential and increased sensitivity to apoptosis. Ultimately this can result in the development of an "exhausted" T-cell phenotype, loss of immunological control and the inability to induce tumour and viral clearance (Keir et al. 2008; Woo et al. 2012; Wei et al. 2013; McMahan et al. 2010). This investigation focused on PD-1 (Chemnitz et al. 2004; Yokosuka et al. 2012; Okazaki et al. 2001; Parry et al. 2005), TIM-3 (Rangachari et al. 2012) and LAG-3 (Workman et al. 2002; Workman and Vignali 2003) due to each receptor mediating immunosuppression and T-cell dysfunction through the activation of divergent signalling pathways, thus allowing for the potential evaluation of multiple immunosuppressive mechanisms.

4.1.3.1 PD-1

The expression of PD-1 was investigated due to its association with immunosuppression and T-cell exhaustion (Wei et al. 2013; Parry et al. 2005; Keir et al. 2008). When CLL patients were grouped as a whole no significant difference in the frequency of $CD4^+PD\text{-}1^+$ T-cells were observed in comparison with HD controls (Fig 4.9). However, the data were heterogeneous and a proportion of CLL patients appeared to exhibit higher percentages of $CD4^+PD\text{-}1^+$ T-cells than the HD controls. When the CLL patients were stratified into two groups (CLL^{IR} and CLL^{NR}) it was observed that there was a significant increase in the percentage of $CD4^+PD\text{-}1^+$ T-cells within the CLL^{IR} patient group when compared to the CLL^{NR} ($P \leq 0.001$) and the HD controls ($P \leq 0.001$) (Fig 4.10). These data indicate that although PD-1 expression was heterogeneous in CLL patients, a high proportion of the patients with high frequencies of $CD4^+PD\text{-}1^+$ T-cells were in the CLL^{IR} group.

4.1.3.2 TIM-3

The expression of TIM-3 was investigated due to its association with immunosuppression and T-cell exhaustion (Zhu et al. 2005; Wherry 2011). When considering the total CLL cohort there was a small but significant ($P \leq 0.05$) increase in the frequency of $CD4^+TIM\text{-}3^+$ T-cells when compared to the HD controls (Fig 4.11). As with PD-1, when CLL patients were stratified into two groups (CLL^{IR} and CLL^{NR}), there was a more obvious, significant increase in the frequency of $CD4^+TIM\text{-}3^+$ T-cells within the CLL^{IR} patient group when compared to the CLL^{NR} ($P \leq 0.01$) and the HD controls ($P \leq 0.001$) (Fig 4.12). These results indicated that the expression of TIM-3 within the $CD4^+$ T-cell compartment of CLL patients was significantly increased when compared with HD controls. Additionally, the elevated expression of TIM-3 appeared to be more pronounced within the CLL^{IR} patient group.

4.1.3.3 LAG-3

The expression of LAG-3 was investigated due to its association with immunosuppression and T-cell exhaustion (Hannier et al. 1998; Wherry 2011). The data obtained was highly heterogeneous (as observed with the other markers under investigation). However, no statistically significant differences in the frequencies $CD4^+LAG3^+$ T-cells were observed between CLL patients and the HD controls, either when patients were analysed as a total cohort (Fig 4.13) or stratified into CLL^{IR} and CLL^{NR} patient groups (Fig 4.14).

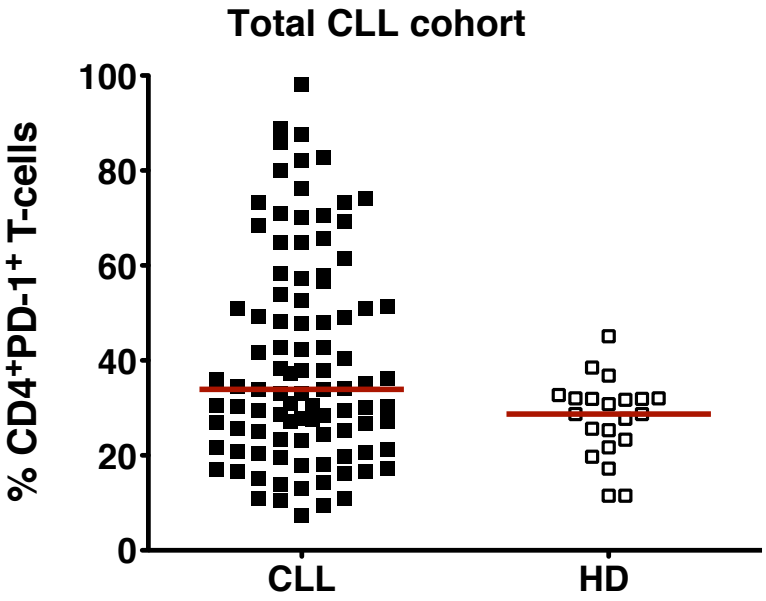

Figure 4.9 PD-1 expression within CD4⁺ T-cells of the total CLL cohort (n=97) and age-matched healthy donor (HD) controls (n=21). The percentages of positive cells were quantified using 10-colour flow cytometry (FACSAria). Live lymphocytes were gated based on forward and side scatter profile. PD-1 expression was measured in the total CD4⁺ T-cell population. Statistical analysis (Mann-Whitney U test) was performed using GraphPad Prism 5.0.

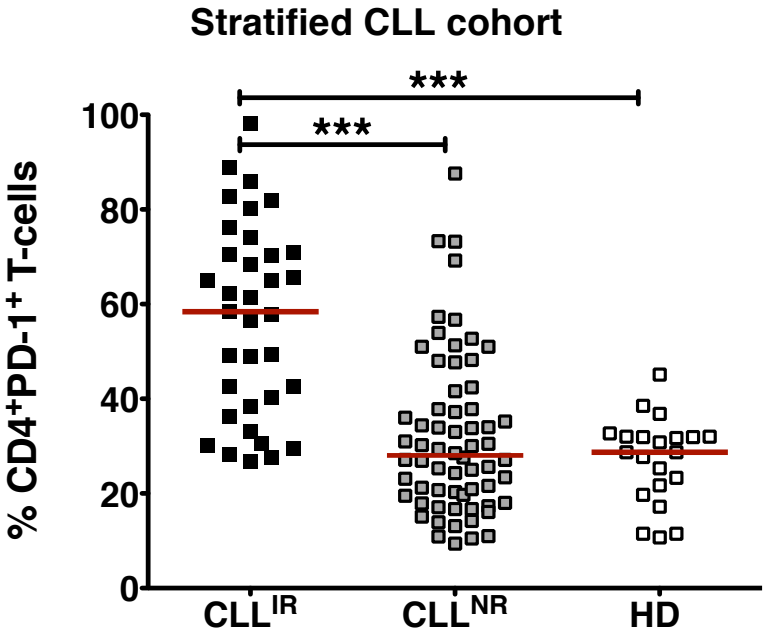

Figure 4.10 PD-1 expression within CD4⁺ T-cells of the stratified CLL cohort (CLL^{IR}, n=32 and CLL^{NR}, n=65) and age-matched healthy donor (HD) controls (n=21). The percentages of positive cells were quantified using 10-colour flow cytometry (FACSAria). Live lymphocytes were gated based on forward and side scatter profile. PD-1 expression was measured in the total CD4⁺ T-cell population. Statistical analysis (Kruskal-Wallis ANOVA with the Dunn's Multiple Comparison Test) was performed using GraphPad Prism 5.0. Statistical significance is denoted by asterisks (*** $P \leq 0.001$).

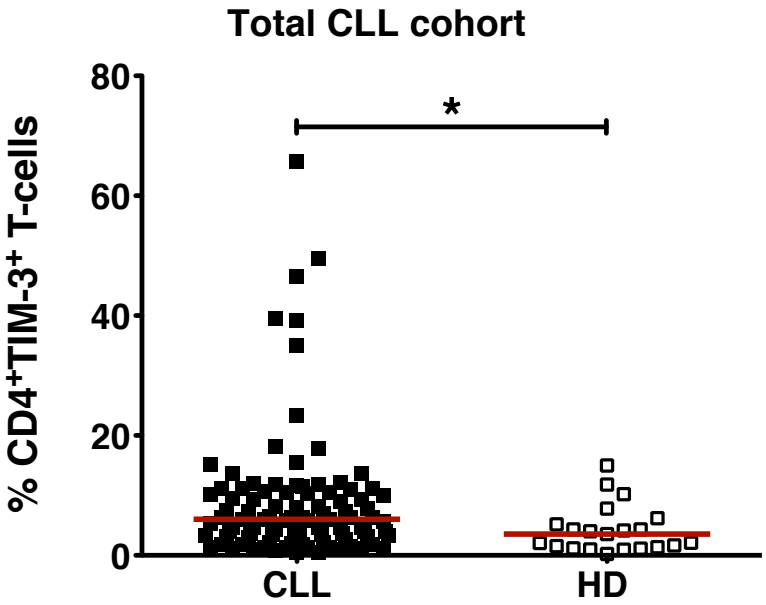

Figure 4.11 TIM-3 expression within CD4⁺ T-cells of the total CLL cohort (n=97) and age-matched healthy donor (HD) controls (n=21). The percentages of positive cells were quantified using 10-colour flow cytometry (FACSAria). Live lymphocytes were gated based on forward and side scatter profile. TIM-3 expression was measured in the total CD4⁺ T-cell population. Statistical analysis (Mann-Whitney U test) was performed using GraphPad Prism 5.0. Statistical significance is denoted by asterisks (* $P \leq 0.05$).

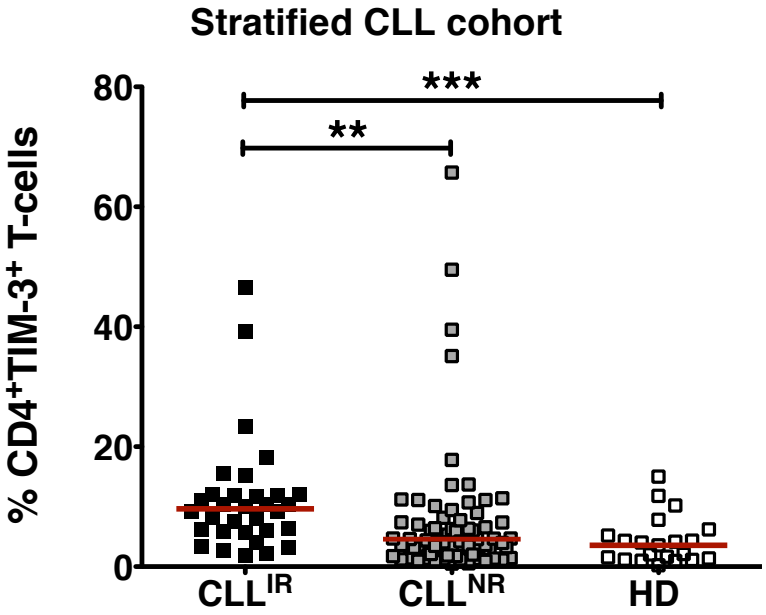

Figure 4.12 TIM-3 expression within CD4⁺ T-cells of the stratified CLL cohort (CLL^{IR}, n=32 and CLL^{NR}, n=65) and age-matched healthy donor (HD) controls (n=21). The percentages of positive cells were quantified using 10-colour flow cytometry (FACSAria). Live lymphocytes were gated based on forward and side scatter profile. TIM-3 expression was measured in total CD4⁺ T-cell population. Statistical analysis (Kruskal-Wallis ANOVA with the Dunn's Multiple Comparison Test) was performed using GraphPad Prism 5.0. Statistical significance is denoted by asterisks (** $P \leq 0.01$, *** $P \leq 0.001$).

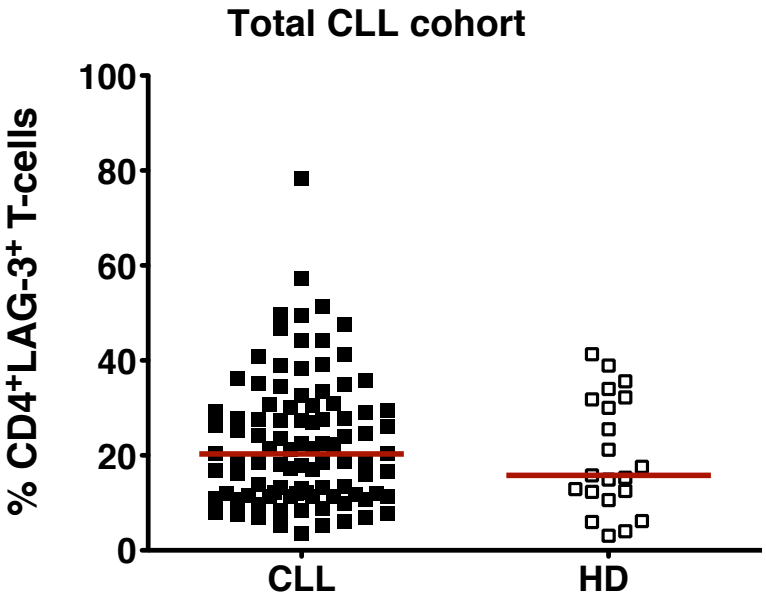

Figure 4.13 LAG-3 expression within CD4 T-cells of the total CLL cohort (n=97) and age-matched healthy donor (HD) controls (n=21). The percentages of positive cells were quantified using 10-colour flow cytometry (FACSAria). Live lymphocytes were gated based on forward and side scatter profile. LAG-3 expression was measured in total $CD4^+$T-cell population. Data represented as dot plots with the median (red bar) shown for each distribution. Statistical analysis (Mann-Whitney U test) was performed using GraphPad Prism 5.0.

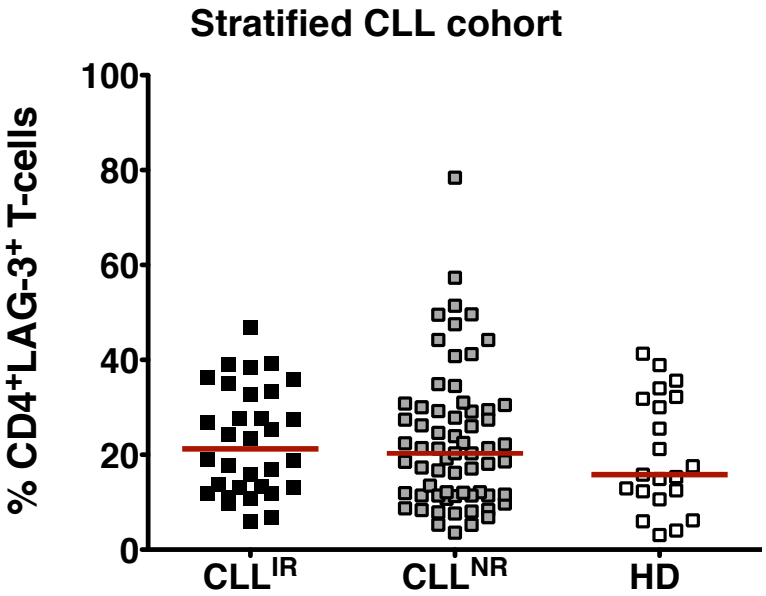

Figure 4.14 LAG-3 expression within $CD4^+$ T-cells of the stratified CLL patients (CLL^{IR}, n=32 and CLL^{NR}, n=65) and age-matched healthy donor (HD) controls (n=21). The percentages of positive cells were quantified using 10-colour flow cytometry (FACSAria). Live lymphocytes were gated based on forward and side scatter profile. **(A)** LAG-3 expression was measured in total $CD4^+$ T-cell population. Data represented as dot plot with the median (red bar) shown for each distribution. Statistical analysis (Kruskal-Wallis ANOVA with the Dunn's Multiple Comparison test) was performed using GraphPad Prism 5.0.

4.1.4 Combined expression of immunosuppressive receptors

Numerous reports have suggested that T-cells expressing multiple immunosuppressive receptors may represent populations, which exhibit the most profound impairments in T-cell function (Sakuishi et al. 2010; McMahan et al. 2010; Fourcade et al. 2010). Thus these T-cell populations may be more indicative of an "exhausted" T-cell phenotype and exhibit the greatest immune dysfunction.

To determine the frequency of combined expression of PD-1, TIM-3 and LAG-3 in the $CD4^+$ T-cells, Boolean gating was performed and the subsequent data was analysed and presented using SPICE 5.35 software. When CLL patients were grouped as a whole and compared to the HD controls, significant differences ($P = 0.047$) in the frequencies of T-cells expressing multiple immunosuppressive receptors were observed between the two groups (Fig 4.15 and Table 4.1). Further analysis indicated that the main differences were due to a significant increase in the frequency of the $PD\text{-}1^+TIM\text{-}3^+LAG\text{-}3^+$ ($P=0.011$) and $PD\text{-}1^+TIM\text{-}3^+LAG\text{-}3^-$ ($P < 0.001$) T-cells within the $CD4^+$ T-cell compartment of CLL patients when compared to HD controls (Table 4.2).

Stratification of CLL patients into two groups (CLL^{IR} and CLL^{NR}) revealed significant differences between CLL^{IR} and CLL^{NR}, and CLL^{IR} and HD groups (Fig 4.16 and Table 4.3). Further analysis revealed that this was due to the differences in the frequency of multiple cell populations, each expressing different combinations of immunosuppressive receptors. In terms of combined expression, significant increases in the frequency of $PD\text{-}1^+TIM\text{-}3^+LAG\text{-}3^+$, $PD\text{-}1^+TIM\text{-}3^+LAG\text{-}3^-$ and $PD\text{-}1^+TIM\text{-}3^-LAG\text{-}3^+$ T-cell were observed in the CLL^{IR} patient group, when compared to either CLL^{NR} or the HD controls (Table 4.4). In addition there was a significant decrease in the frequency of $PD\text{-}1^-TIM\text{-}3^-LAG\text{-}3^-$ $CD4^+$ T-cells in the CLL^{IR} patient group when compared to either CLL^{NR} or the HD controls (Table 4.4). These findings suggested that the increased frequency of $CD4^+$ T-cells expressing multiple immunosuppressive receptors is particularly associated with the CLL^{IR} patient group.

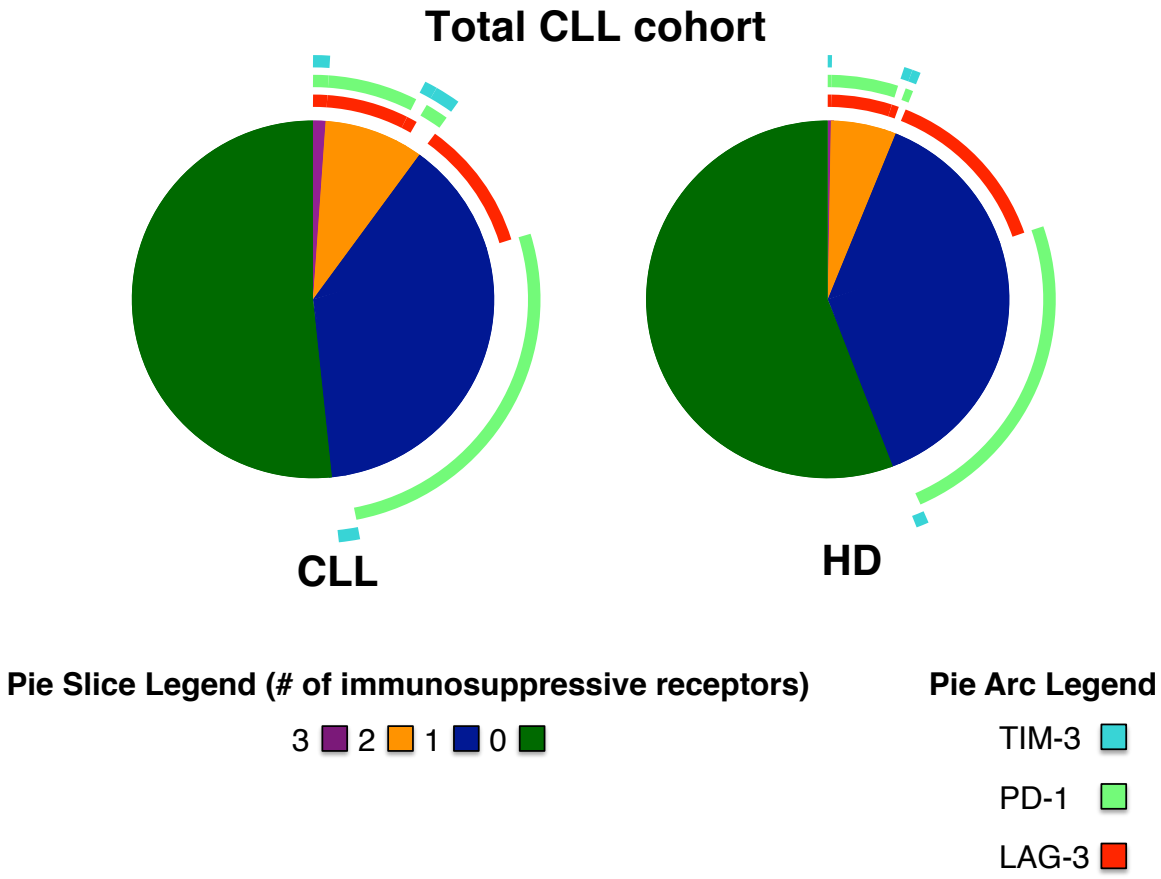

Figure 4.15 Combined expression of immunosuppressive receptors within CD4⁺ T-cells of the total CLL cohort (n=97) and age-matched healthy donor (HD) controls (n=21). The percentage of positive cells was quantified using 10-colour flow cytometry (FACSAria). Live lymphocytes were gated based on forward and side scatter profile. Combined expression of PD-1, TIM-3 and LAG-3 were determined using Boolean gating. Colours of the pie arcs depict the expression of individual inhibitory receptors, while the colour in the pie depicts the number of co-expressed inhibitory receptors. Data representation and statistical analyses (Mann-Whitney U test) were performed using SPICE 5.35 software.

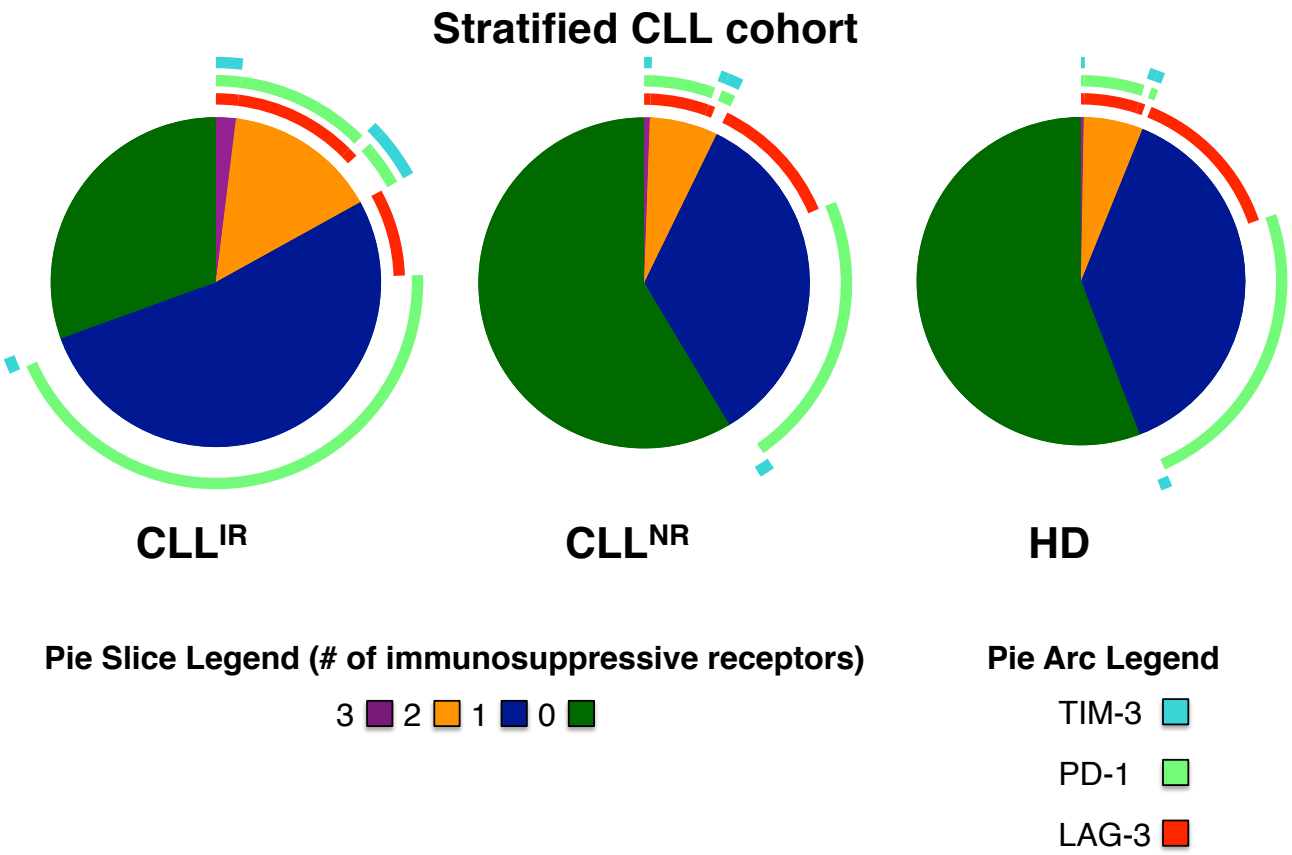

Figure 4.16 Combined expression of immunosuppressive receptors within CD4$^+$ T-cells of the stratified CLL cohort (CLL^{IR}, n=32 and CLL^{NR}, n=65) and age-matched healthy donor (HD) controls (n=21). The percentage of positive cells was quantified using 10-colour flow cytometry (FACSAria). Live lymphocytes were gated based on forward and side scatter profile. Combined expression of PD-1, TIM-3 and LAG-3 were determined using Boolean gating. Colours of the pie arcs depict the expression of individual inhibitory receptors, while the colour in the pie depicts the number of co-expressed inhibitory receptors. Data representation and statistical analyses (Mann-Whitney U test) were performed using SPICE 5.35 software.

Table 4.1 Overall CD4+ T-cell pie chart analysis (CLL vs HD)[1]

Pie Type	CLL	HD
CLL		0.0466
HD	0.0466	

Table 4.2 Detailed CD4+ T-cell pie chart analysis (CLL vs HD)[1]

Category	TYPE: HD
PD-1$^+$LAG-3$^+$TIM-3$^+$	0.011
PD-1$^+$LAG-3$^+$TIM-3$^-$	0.350
LAG-3$^+$TIM-3$^+$PD-1$^-$	0.399
PD-1$^+$TIM-3$^+$LAG-3$^-$	<0.0001
PD-1$^-$TIM-3$^-$LAG-3$^-$	0.103
Compared to CLL	

Table 4.3 Overall CD4+ T-cell pie chart analysis (CLL^{NR} vs CLL^{IR} vs HD)[1]

Pie Type	CLL^{IR}	CLL^{NR}	HD
CLL^{IR}		<0.0001	<0.0001
CLL^{NR}	<0.0001		0.7093
HD	<0.0001	0.7093	

Table 4.4 Detailed CD4+ T-cell pie chart analysis (CLL^{NR} vs CLL^{IR} vs HD)[1]

Category	CLL^{NR}	HD
PD-1$^+$LAG-3$^+$TIM-3$^+$	<0.0001	<0.0001
PD-1$^+$LAG-3$^+$TIM-3$^-$	<0.0001	0.007
LAG-3$^+$TIM-3$^+$PD-1$^-$	0.945	0.469
PD-1$^+$TIM-3$^+$LAG-3$^-$	<0.0001	<0.0001
PD-1$^-$TIM-3$^-$LAG-3$^-$	<0.0001	<0.0001
Compared to CLL^{IR}		

[1] Statistical analysis (Mann-Whitney U test) was performed using SPICE 5.35. Statistically significant differences were highlighted in red.

4.2 $CD8^+$ T-cells

Since $CD8^+$ T-cells have a distinctly different functional role to $CD4^+$ T-cells (Janeway 2012). Therefore, this T-cell subset was analysed separately to investigate potential phenotypic differences within our CLL and healthy donor populations using a similar gating strategy to that described in section 4.1.

4.2.1 Memory subset

In contrast to $CD4^+$ T-cells, there were significant differences in the frequencies of $CD8^+$ T-cell subsets when CLL patients were compared to age-matched HD controls (Fig 4.17). Significant decreases in the naïve ($P \leq 0.05$) and CM ($P \leq 0.01$) $CD8^+$ T-cells in CLL patients was observed when compared to the HD controls (Fig 4.17). These differences were more pronounced when the CLL patients were stratified. For example, naïve and CM $CD8^+$ T-cell subsets were decreased in the CLL^{IR} patient group when compared with either CLL^{NR} or HD controls (Fig 4.18). However, there were no significant differences when $CD8^+$ T-cell subsets were compared between CLL^{NR} and the HD control.

In contrast to $CD4^+$ T-cells (Fig 4.2 and 4.3), there was a marked skewing towards EMRA in $CD8^+$ T-cells in both CLL patients and HD controls (Fig 4.17 and 4.18). Comparisons between CLL patients and HD control showed no statistically significance differences, however stratification of the CLL patients indicated a significant increase in the percentage of EMRA $CD8^+$ T-cells within the CLL^{IR} patient group when compared to the CLL^{NR} ($P \leq 0.05$) and a trend towards an increase when compared to the HD controls (Fig 4.18). These results demonstrated that the distribution of the T-cell memory subsets within CLL patients was heterogeneous, but the CLL^{IR} patient group displayed a marked skewing in the naïve, CM and EMRA subsets.

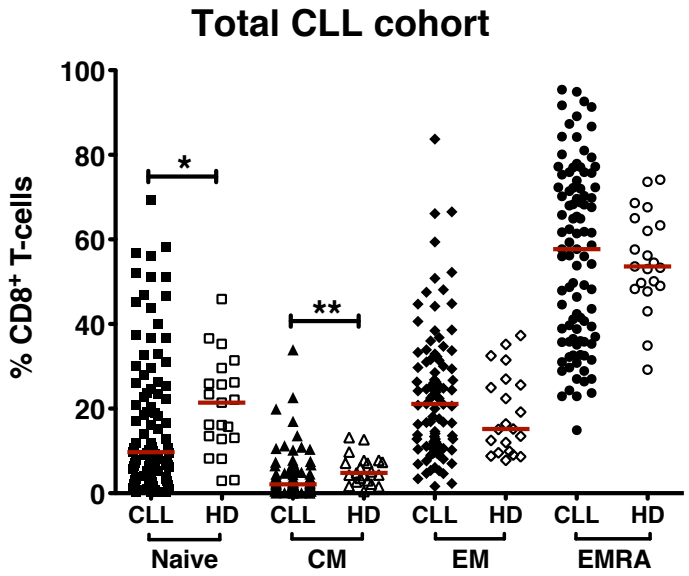

Figure 4.17 CD8$^+$ T-cell memory subsets in the total CLL cohort (n=97) and age-matched healthy donor (HD) controls (n=21). The percentages of positive cells were quantified using 10-colour flow cytometry (FACSAria). Live lymphocytes were gated based on forward and side scatter profile and T-cell memory subsets were defined using CCR7 and CD45RO, Naïve (CCR7$^+$ CD45RO$^-$), CM (CCR7$^+$ CD45RO$^+$), EM (CCR7$^-$ CD45RO$^+$) and EMRA (CCR7$^-$ CD45RO$^-$). Data represented as dot plots with the median (red bar) shown for each distribution. Statistical analysis (Mann-Whitney U test) was performed using GraphPad Prism 5.0. Statistical significance is denoted by asterisks (* $P \leq 0.05$, ** $P \leq 0.01$).

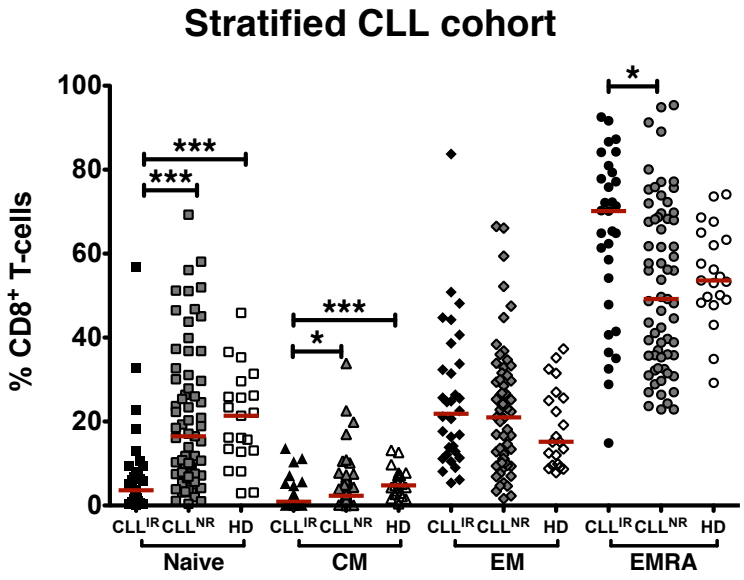

Figure 4.18 CD8$^+$ T-cell memory subsets in the stratified CLL cohort (CLL^{IR}, n=32 and CLL^{NR}, n=65) and age-matched healthy donor (HD) controls (n=21). The percentages of positive cells were quantified using 10-colour flow cytometry (FACSAria). Live lymphocytes were gated based on forward and side scatter profile and T-cell memory subsets were defined using CCR7 and CD45RO, Naïve (CCR7$^+$ CD45RO$^-$), CM (CCR7$^+$ CD45RO$^+$), EM (CCR7$^-$ CD45RO$^+$) and EMRA (CCR7$^-$ CD45RO$^-$). Data represented as dot plots with the median (red bar) shown for each distribution. Statistical analysis (Kruskal-Wallis ANOVA with the Dunn's Multiple Comparison Test) was performed using GraphPad Prism 5.0. Statistical significance is denoted by asterisks (* $P \leq 0.05$, *** $P \leq 0.001$).

4.2.2 Expression of CD57 and CD27

Due to the association between T-cell differentiation status and function (Dolfi et al. 2008; Brenchley et al. 2003; Focosi et al. 2010; Plunkett et al. 2007; Hendriks et al. 2000), the expression of the late differentiation markers CD57 and CD27 were investigated within the $CD8^+$ T-cell compartment. When the total CLL cohort was analysed for the frequencies of $CD8^+CD57^+$ (Fig 4.19) or $CD8^+CD27^-$ (Fig 4.21) T-cells, there were no significant differences when compared to the HD control group. However, when CLL patients were stratified into two groups (CLL^{IR} and CLL^{NR}) there was a significant increase in the percentage of $CD8^+CD57^+$ T-cells within the CLL^{IR} patient group when compared to CLL^{NR} ($P \leq 0.001$) and the HD controls ($P \leq 0.001$) (Fig 4.20). When the loss of CD27 was investigated in the $CD8^+$ T-cell compartment, a significant increase in the $CD8^+CD27^-$ phenotype was observed within the CLL^{IR} patient group when compared to CLL^{NR} ($P \leq 0.001$); no other significant differences were observed between the groups (Fig 4.22). These results suggested that the CLL^{IR} patient group manifested higher frequencies of $CD8^+$ T-cells with a "highly" differentiated memory T-cell phenotype when compared to either CLL^{NR} or HD controls.

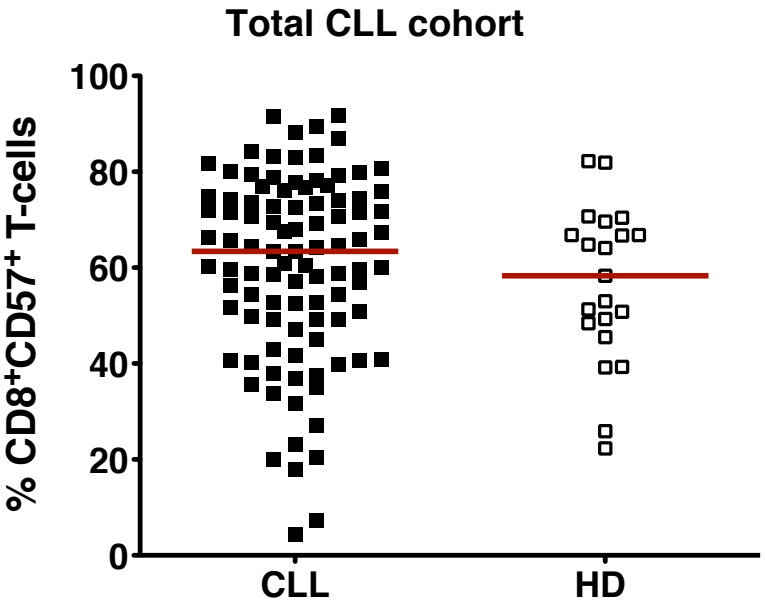

Figure 4.19 CD57 expression within the CD8$^+$ T-cells of the total CLL cohort (n=97) and age-matched healthy donor (HD) controls (n=21). The numbers of positive cells were quantified using 10-colour flow cytometry (FACSAria). Live lymphocytes were gated based on forward and side scatter profile. CD57 expression was measured in total CD8$^+$ T-cell population. Data are represented as dot plots with the median (red bar). Statistical analysis (Mann-Whitney U test) was performed using GraphPad Prism 5.0.

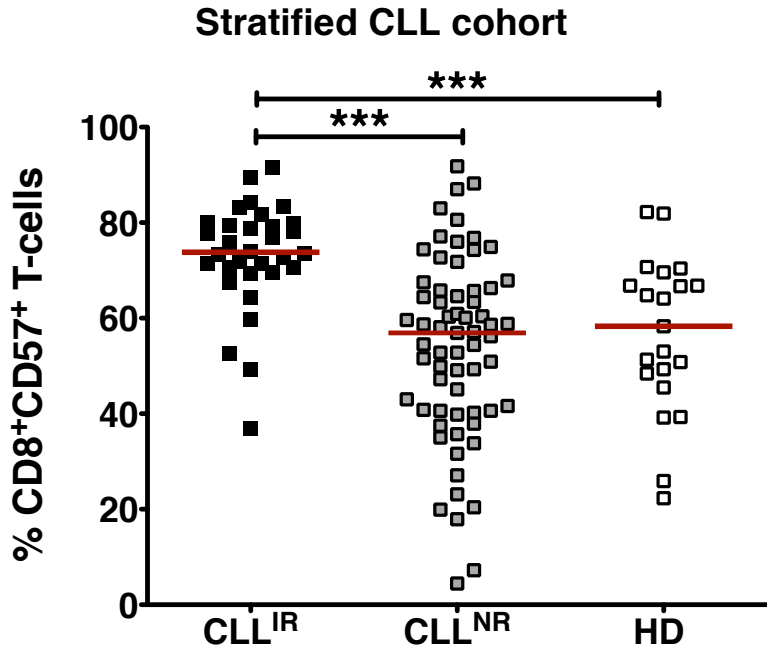

Figure 4.20 CD57 expression within the CD8$^+$ T-cells of the stratified CLL cohort (CLL^{IR}, n=32 and CLL^{NR}, n=65) and age-matched healthy donor (HD) controls (n=21). The numbers of positive cells were quantified using 10-colour flow cytometry (FACSAria). Live lymphocytes were gated based on forward and side scatter profile. CD57 expression was measured in total CD8$^+$ T-cell population. Data are represented as dot plots with the median (red bar). Statistical analysis (Kruskal-Wallis ANOVA with the Dunn's Multiple Comparison Test) was performed using GraphPad Prism 5.0. Statistical significance is denoted by asterisks (*** $P \leq 0.001$).

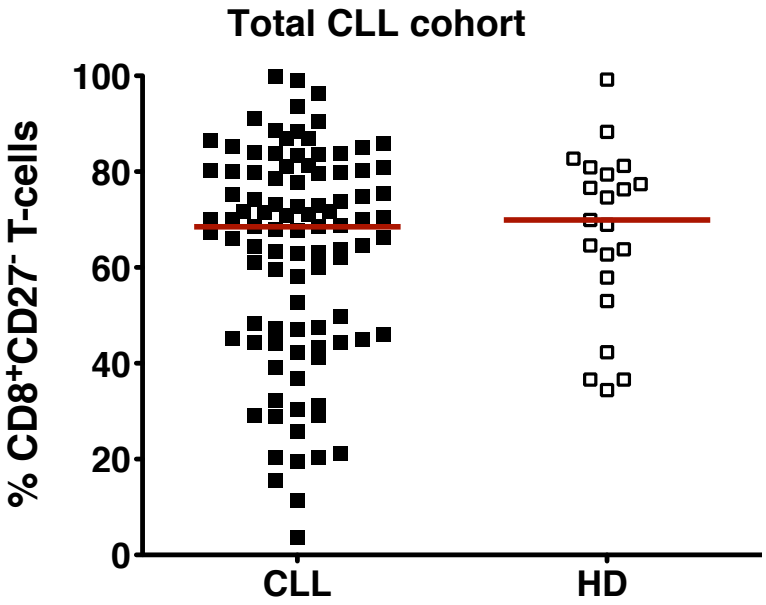

Figure 4.21 CD27 expression within the CD8⁺ T-cells of the total CLL cohort (n=97) and age-matched healthy donor (HD) controls (n=21). The percentages of positive cells were quantified using 10-colour flow cytometry (FACSAria). Live lymphocytes were gated based on forward and side scatter profile. CD27 expression was measured in total CD8⁺ T-cell population and was presented at CD27⁻ CD8⁺ T-cells. Data represented as dot plots with the median (red bar). Statistical analysis (Mann-Whitney U test) was performed using GraphPad Prism 5.0.

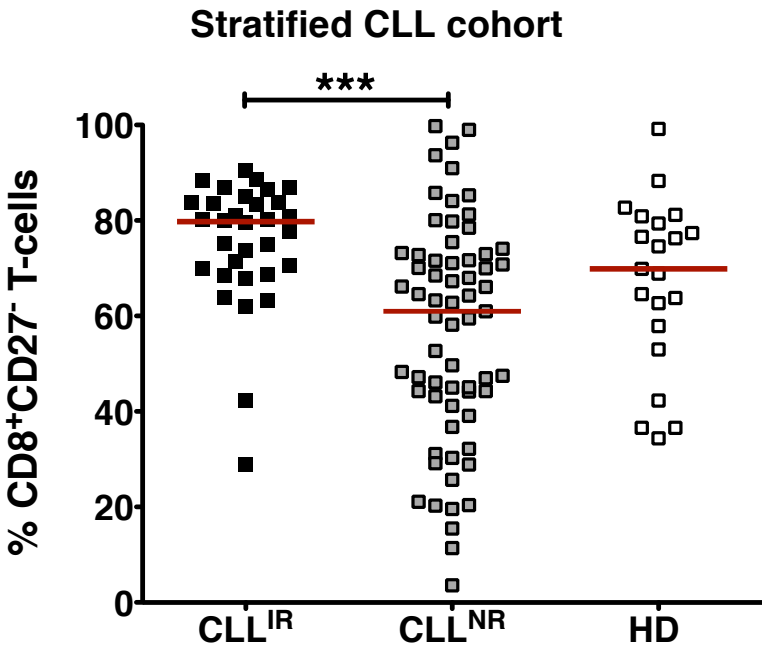

Figure 4.22 CD27 expression within the CD8⁺ T-cells of the stratified CLL cohort (CLL^{IR}, n=32 and CLL^{NR}, n=65) and age-matched healthy donor (HD) controls (n=21). The percentage of positive cells were quantified using 10-colour flow cytometry (FACSAria). Live lymphocytes were gated based on forward and side scatter profile. CD27 expression was measured in total CD8⁺ T-cell population and was presented at CD27⁻ CD8⁺ T-cells. Statistical analysis (Kruskal-Wallis ANOVA with the Dunn's Multiple Comparison test) was performed using GraphPad Prism 5.0. Statistical significance is denoted by asterisks (*** $P \leq 0.001$).

4.2.3 Immunosuppressive receptors

As previously described, the expression of immunosuppressive receptors such as PD-1, TIM-3 and LAG-3 has been associated with immune dysfunction and "exhausted" T-cells (Wherry 2011). The expression of PD-1, TIM-3 and LAG-3 were investigated within the $CD8^+$ T-cell compartment of CLL patients and the HD control group.

No differences in the frequency of $CD8^+PD\text{-}1^+$ (Fig 4.23) or $CD8^+TIM\text{-}3^+$ T-cells (Fig 4.25) were observed when the total CLL cohort was compared to the HD controls. This was also the case when CLL patients were stratified into two groups (CLL^{IR} and CLL^{NR}) (Fig 4.24 and Fig 4.26). Unexpectedly when the expression of LAG-3 was investigated within the $CD8^+$ T-cell compartment, a significant increase in $CD8^+LAG\text{-}3^+$ T-cells ($P \leq 0.01$) was observed within the HD controls when compared to CLL patients (Fig 4.27), as well as when compared to stratified CLL^{IR} ($P \leq 0.05$) and CLL^{NR} ($P \leq 0.01$) patients (Fig 4.28). Comparison between CLL^{IR} and CLL^{NR} indicated no difference with respect to the frequency of $CD8^+LAG\text{-}3^+$ T-cells.

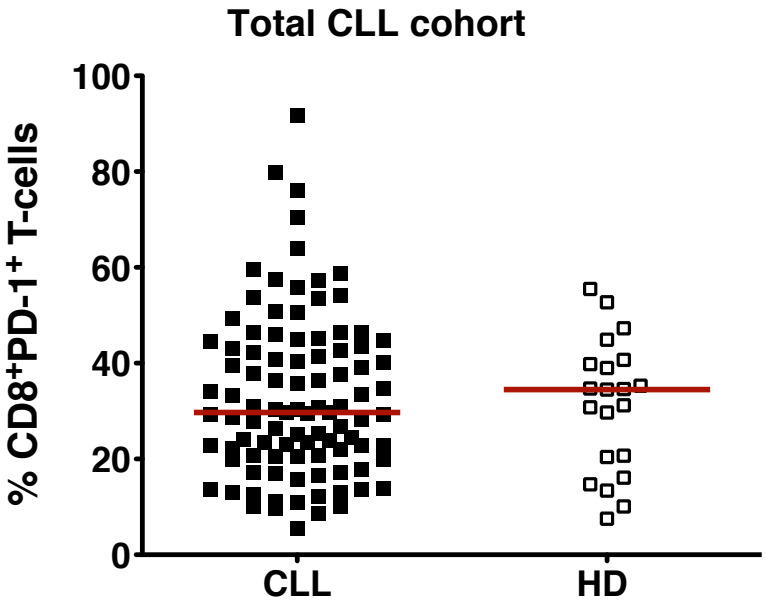

Figure 4.23 PD-1 expression within CD8⁺ T-cells of the total CLL cohort (n=97) and age-matched healthy donor (HD) controls (n=21). The numbers of positive cells were quantified using 10-colour flow cytometry (FACSAria). Live lymphocytes were gated based on forward and side scatter profile. PD-1 expression was measured in the total CD8⁺ T-cell population. Data are represented as dot plots with the median (red bar) shown for each distribution. Statistical analysis (Mann-Whitney U test) was performed using GraphPad Prism 5.0.

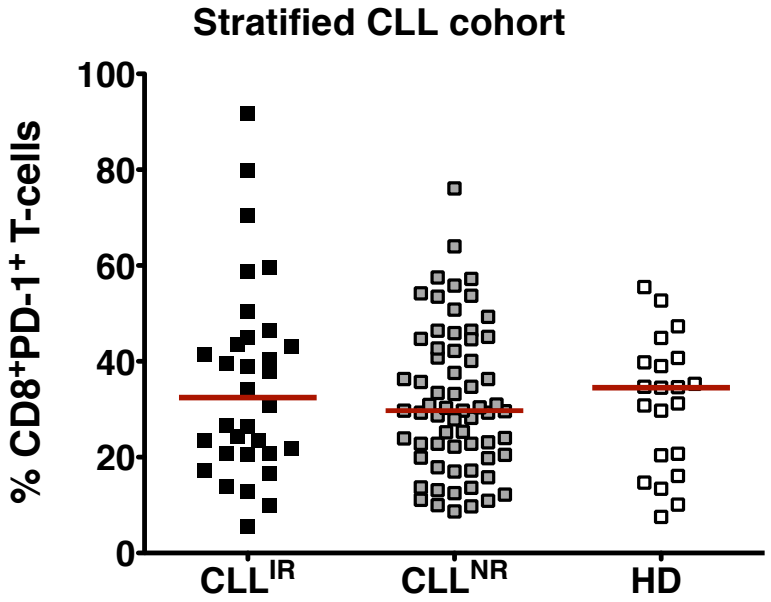

Figure 4.24 PD-1 expression within CD8⁺ T-cells of the stratified CLL cohort (CLL^{IR}, n=32 and CLL^{NR}, n=65) and age-matched healthy donor (HD) controls (n=21). The numbers of positive cells were quantified using 10-colour flow cytometry (FACSAria). Live lymphocytes were gated based on forward and side scatter profile. PD-1 expression was measured in total CD8⁺ T-cell population. Data are represented as dot plots with the median (red bar) shown for each distribution. Statistical analysis (Kruskal-Wallis ANOVA with the Dunn's Multiple Comparison test) was performed using GraphPad Prism 5.0.

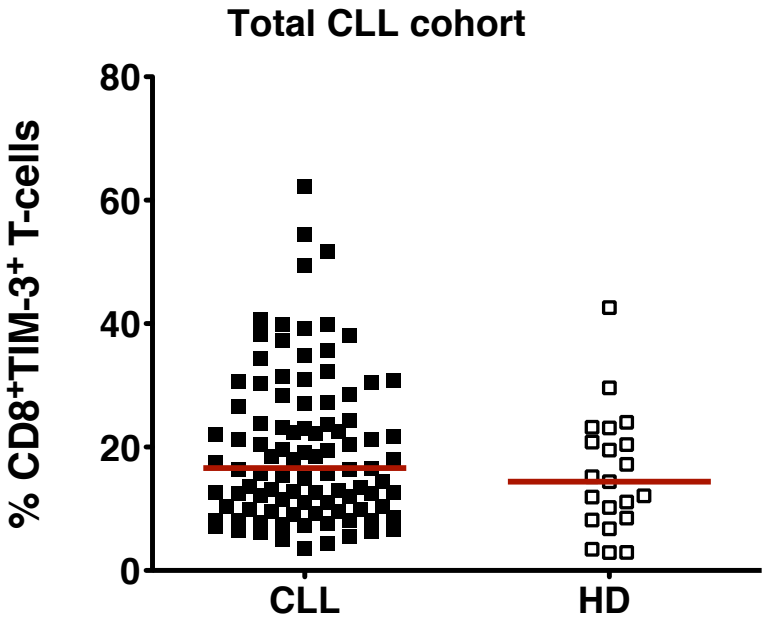

Figure 4.25 TIM-3 expression within the CD8⁺ T-cells of the total CLL cohort (n=97) and age-matched healthy donor (HD) controls (n=21). The numbers of positive cells were quantified using 10-colour flow cytometry (FACSAria). Live lymphocytes were gated based on forward and side scatter profile. TIM-3 expression was measured in total CD8⁺ T-cell population. Data are represented as dot plots with the median (red bar) shown for each distribution. Statistical analysis (Mann-Whitney U test) was performed using GraphPad Prism 5.0.

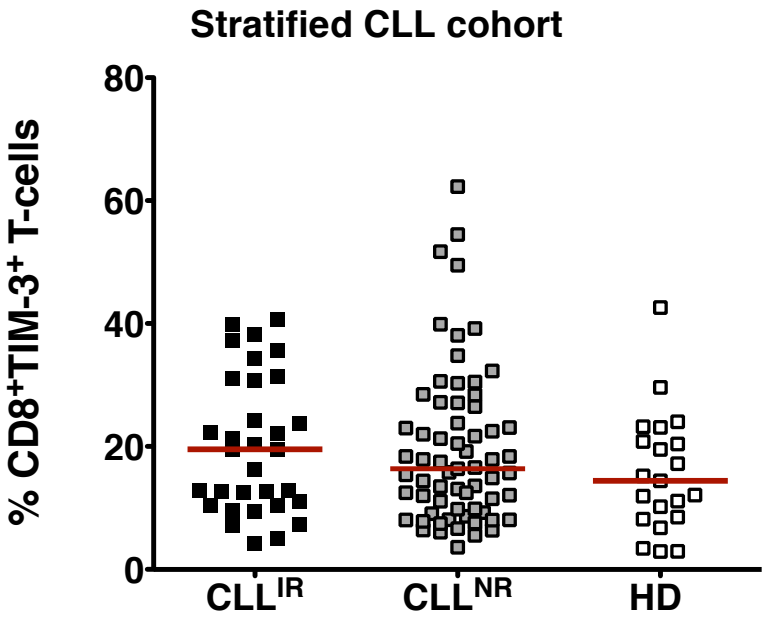

Figure 4.26 TIM-3 expression within the CD8⁺ T-cells of the stratified CLL cohort (CLL^{IR}, n=32 and CLL^{NR}, n=65) and age-matched healthy donor (HD) controls (n=21). The numbers of positive cells were quantified using 10-colour flow cytometry (FACSAria). Live lymphocytes were gated based on forward and side scatter profile. TIM-3 expression was measured in total CD8⁺ T-cell population. Data are represented as dot plots with the median (red bar) shown for each distribution. Statistical analysis (Kruskal-Wallis ANOVA with the Dunn's Multiple Comparison Test) was performed using GraphPad Prism 5.0.

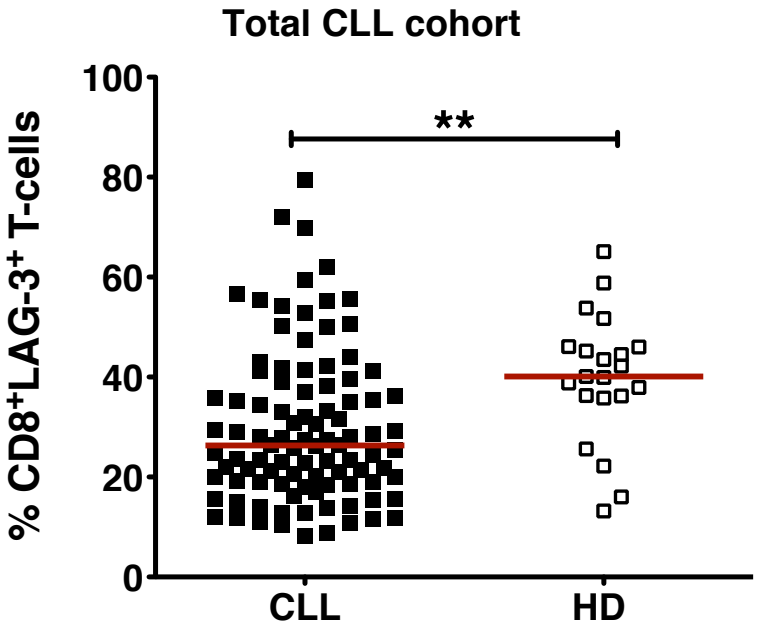

Figure 4.27 LAG-3 expression within CD8 T-cells of CLL patients (n=97) and age-matched healthy donor (HD) controls (n=21). The percentage of positive cells were quantified using 10-colour flow cytometry (FACSAria). Live lymphocytes were gated based on forward and side scatter profile. LAG-3 expression was measured in total $CD8^+$ T-cell population. Data are represented as dot plots with the median (red bar) shown for each distribution. Statistical analysis (Mann-Whitney U test) was performed using GraphPad Prism 5.0. Statistical significance is denoted by asterisks (** $P \leq 0.01$)

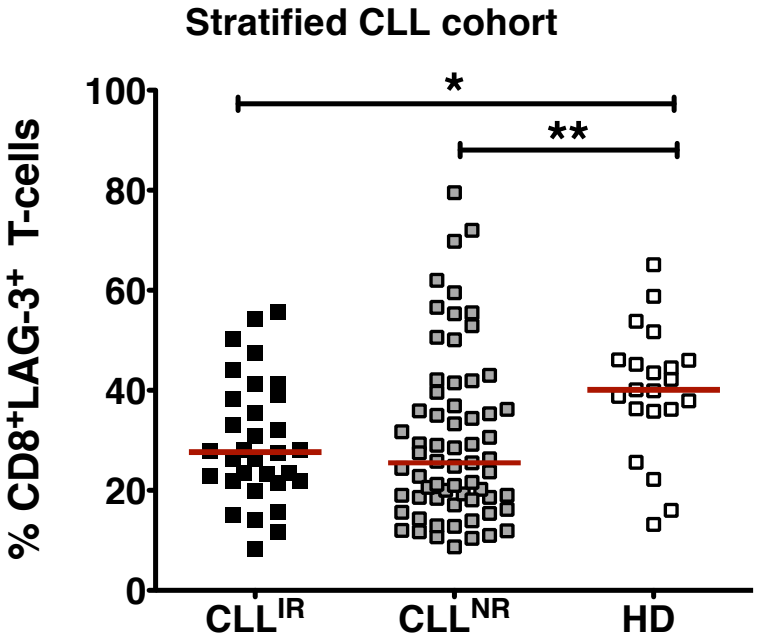

Figure 4.28 LAG-3 expression within $CD8^+$ T-cells of stratified CLL patients (CLL^{IR}, n=32 and CLL^{NR}, n=65) and age-matched healthy donor (HD) controls (n=21). The percentage of positive cells were quantified using 10-colour flow cytometry (FACSAria). Live lymphocytes were gated based on forward and side scatter profile. LAG-3 expression was measured in total $CD8^+$ T-cell population. Data are represented as dot plots with the median (red bar). Statistical analysis (Kruskal-Wallis ANOVA with the Dunn's Multiple Comparison Test) was performed using GraphPad Prism 5.0**.** Statistical significance is denoted by asterisks (* $P \leq 0.05$, ** $P \leq 0.01$).

4.2.4 Combined expression of immunosuppressive receptors

Previously published observations have suggested that T-cells, which expressed multiple immunosuppressive receptors, represent populations that exhibit greater functional defects and thus may be more representative of an "exhausted" T-cell phenotype (Sakuishi et al. 2010; McMahan et al. 2010; Fourcade et al. 2010).

To assess T-cell populations with expression of multiple immunosuppressive receptors, Boolean gating was performed and the subsequent data was presented and analysed using SPICE 5.35 software. When the CLL cohort was considered as a whole, a significant difference in the proportion of $CD8^+$ T-cells expressing multiple immunosuppressive receptors was observed when compared to the HD controls ($P = 0.0384$) (Fig 4.29 and Table 4.5). Further analysis indicated that the main differences concerning combined expression were due to a significant increase in the frequency of PD-1^+TIM-3^+LAG-3^- T-cells within the CLL patient group when compared to HD controls. In addition, a decrease in the frequency of PD-1^+TIM-3^-LAG-3^+ $CD8^+$ T-cells ($P = 0.004$) within the CLL group was seen in comparison to the HD group (Table 4.6). When patients were stratified, similar results were observed when CLL^{IR} patients were compared to the HD controls (Table 4.8).

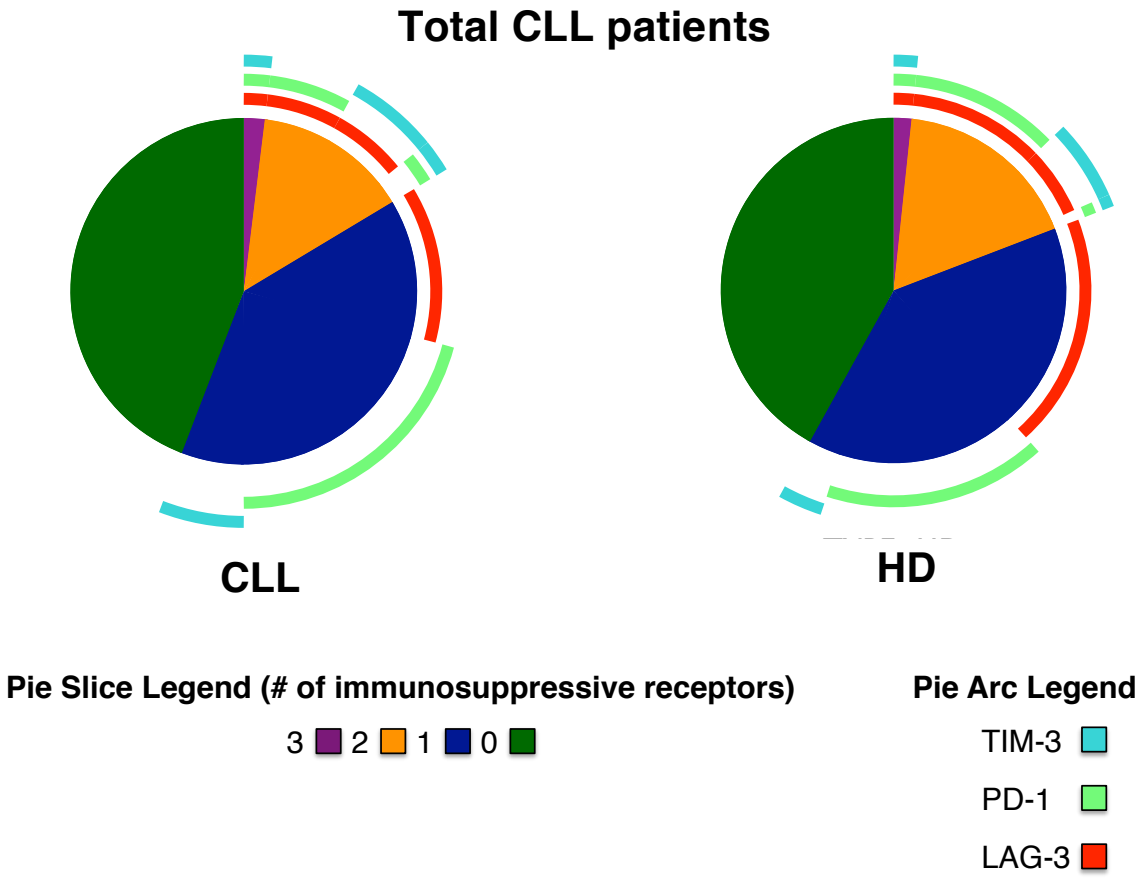

Figure 4.29 Combined expression of immunosuppressive receptors within the CD8⁺ T-cells of the total CLL cohort (n=97) and age-matched healthy donor (HD) controls (n=21). The percentage of positive cells was quantified using 10-colour flow cytometry (FACSAria). Live lymphocytes were gated based on forward and side scatter profile. Combined expression of PD-1, TIM-3 and LAG-3 were determined using Boolean gating. Colours of the pie arcs depict the expression of individual inhibitory receptors, while the colour in the pie depicts the number of co-expressed inhibitory receptors. Data representation and statistical analysis (Mann-Whitney U test) were performed using SPICE 5.35.

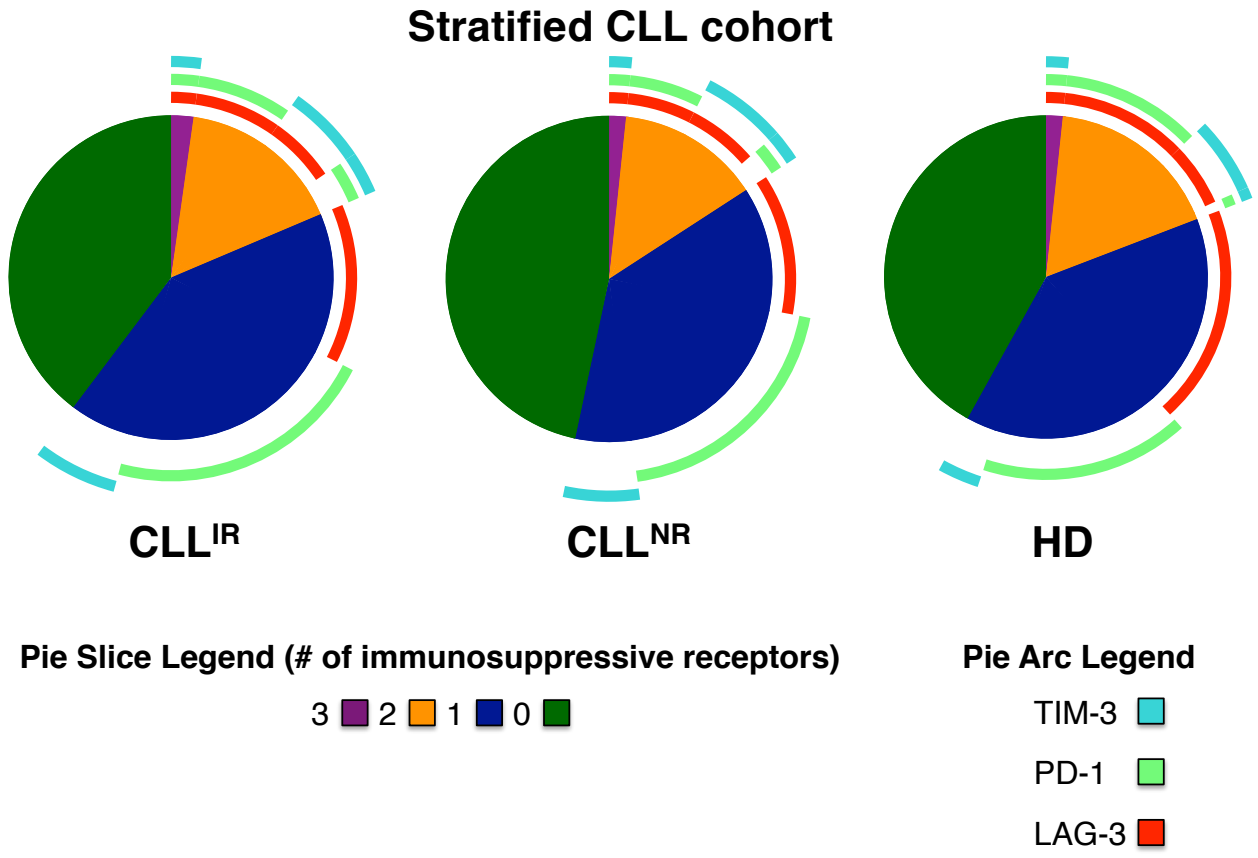

Figure 4.30 Combined expression of immunosuppressive receptors within the CD8⁺ T-cells of the stratified CLL cohort (CLL^{IR}, n=32 and CLL^{NR}, n=65) and age-matched healthy donor (HD) controls (n=21). The percentage of positive cells was quantified using 10-colour flow cytometry (FACSAria). Live lymphocytes were gated based on forward and side scatter profile. Combined expression of PD-1, TIM-3 and LAG-3 were determined using Boolean gating. Colours of the pie arcs depict the expression of individual inhibitory receptors, while the colour in the pie depicts the number of co-expressed inhibitory receptors. Data representation and statistical analysis (Mann-Whitney U test) were performed using SPICE 5.35.

Table 4.5 Overall CD8$^+$ T-cell pie chart analysis (CLL vs HD)[2]

Pie Type	CLL	HD
CLL		0.0384
HD	0.0384	

Table 4.6 Detailed CD8$^+$ T-cell pie chart analysis (CLL vs HD)[2]

Category	TYPE: HD
PD-1$^+$LAG-3$^+$TIM-3$^+$	0.0574
PD-1$^+$LAG-3$^+$TIM-3$^-$	0.004
LAG-3$^+$TIM-3$^+$PD-1$^-$	0.836
PD-1$^+$TIM-3$^+$LAG-3$^-$	<0.0001
PD-1$^-$TIM-3$^-$LAG-3$^-$	0.513
Compared to CLL	

Table 4.7 Overall CD8$^+$ T-cell pie chart analysis (CLL^{NR} vs CLL^{IR} vs HD)[2]

Pie Type	CLL^{IR}	CLL^{NR}	HD
CLL^{IR}		0.5686	0.0705
CLL^{NR}	0.5686		0.0814
HD	0.0705	0.0814	

Table 4.8 Detailed CD8$^+$ T-cell pie chart analysis (CLL^{IR} vs CLL^{NR} vs HD)[2]

Category	CLL^{NR}	HD
PD-1$^+$LAG-3$^+$TIM-3$^+$	0.334	0.358
PD-1$^+$LAG-3$^+$TIM-3$^-$	0.311	0.039
LAG-3$^+$TIM-3$^+$PD-1$^-$	0.747	0.935
PD-1$^+$TIM-3$^+$LAG-3$^-$	0.143	<0.0001
PD-1$^-$TIM-3$^-$LAG-3$^-$	0.288	0.971
Compared to CLL^{IR}		

[2] Statistical analysis (Mann-Whitney U test) was performed using SPICE 5.35. Statistically significant differences were highlighted in red.

4.3 Prognostic relevance of T-cells in CLL

4.3.1 Univariate analysis

To investigate the effects that T-cells may have on the progression of CLL, Cox proportional hazards regression analysis was conducted on 83 CLL patients with respect to progression-free survival (PFS). This tested whether the inversion in the CD4:CD8 ratio or the phenotypic markers studied (CD57, CD27, PD-1, TIM-3 and LAG-3) influenced PFS.

Analysis of the CD4:CD8 ratio indicated that it had a significant influence on patient prognosis. In keeping with a previous study (Nunes et al. 2012), patients with a CD4:CD8 ratio <1 showed significantly more progressive disease (P = 0.0417; HR = 2.2) (Fig 4.31).

Within the $CD4^+$ T-cell compartment CD57 (Fig 4.32a) and PD-1 (Fig 4.32c) both significantly influenced PFS, (P = 0.026 and P = 0.008, respectively). Patients that were above the median frequency for $CD4^+CD57^+$ and $CD4^+PD\text{-}1^+$ T-cells exhibited more progressive disease, HR = 2.6 and HR = 2.2, respectively.

Within the $CD8^+$ T-cell compartment, CD57 (Fig 4.33a) and CD27 (Fig 4.33b) both appeared to significantly influence PFS (P = 0.020 and P = 0.004, respectively). Patients that were above the median frequency for $CD8^+CD57^+$ and $CD8^+CD27^-$ T-cells exhibited more progressive disease (HR = 2.3 and HR = 2.9, respectively).

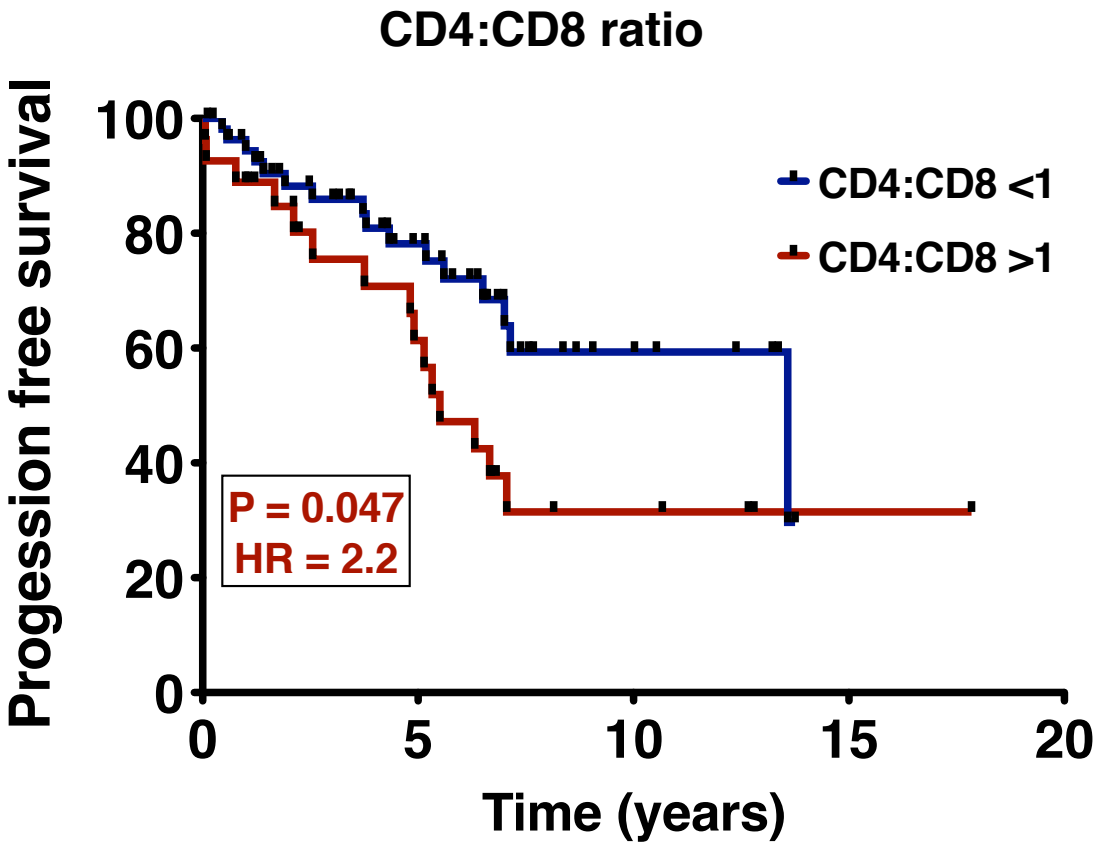

Figure 4.31 Kaplan–Meier curves for progression-free survival for CLL^{NR} and CLL^{IR} patients. Kaplan-Meier analysis was used to assess the effect of the CD4:CD8 ratio upon PFS. The patients were divided based upon a ratio of CD4:CD8 <1 (CLL^{IR}) or a ratio of CD4:CD8 >1 (CLL^{NR}). A log-rank test was used to test the difference between the two curves. (HR = Hazard ratio).

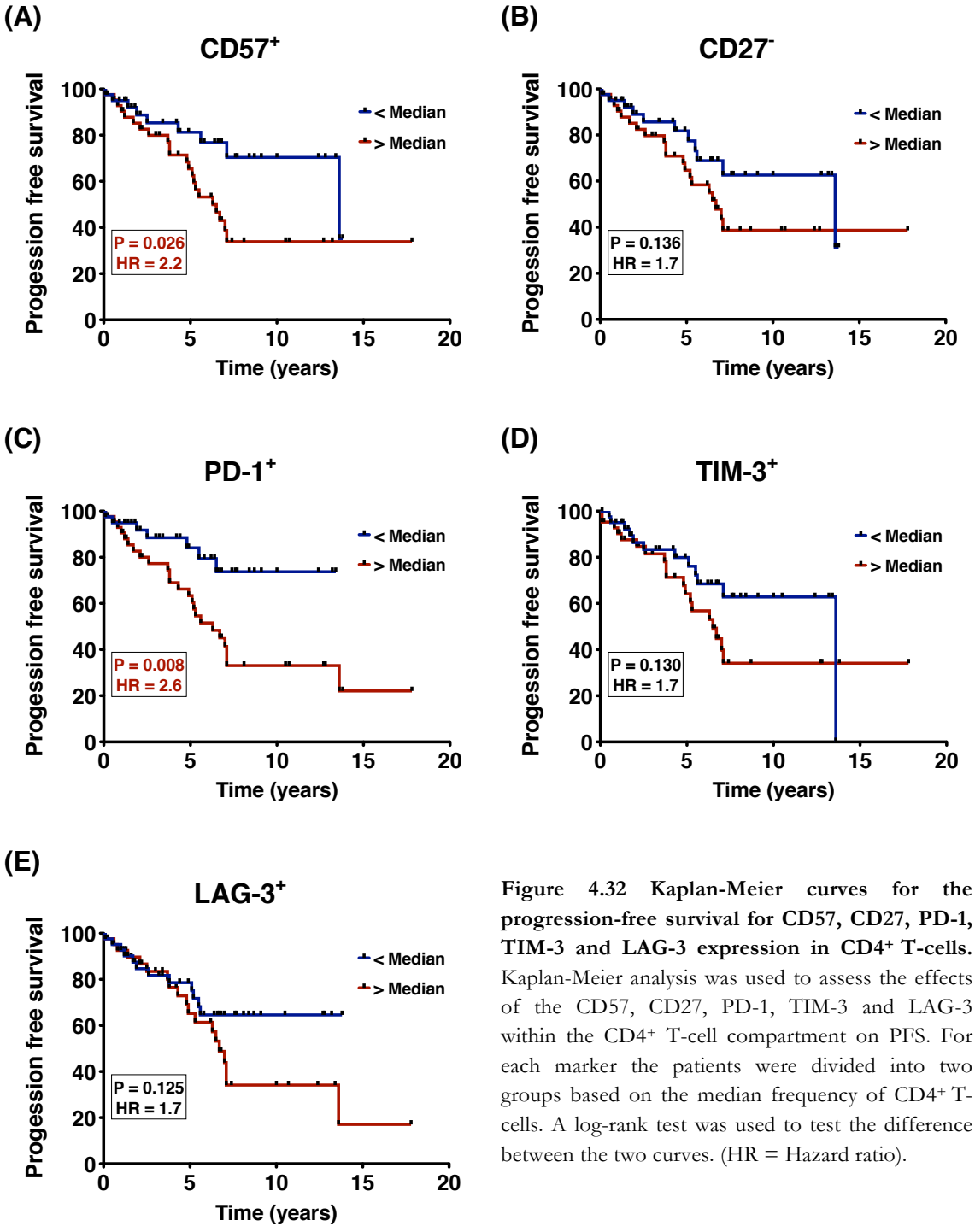

Figure 4.32 Kaplan-Meier curves for the progression-free survival for CD57, CD27, PD-1, TIM-3 and LAG-3 expression in CD4+ T-cells. Kaplan-Meier analysis was used to assess the effects of the CD57, CD27, PD-1, TIM-3 and LAG-3 within the CD4+ T-cell compartment on PFS. For each marker the patients were divided into two groups based on the median frequency of CD4+ T-cells. A log-rank test was used to test the difference between the two curves. (HR = Hazard ratio).

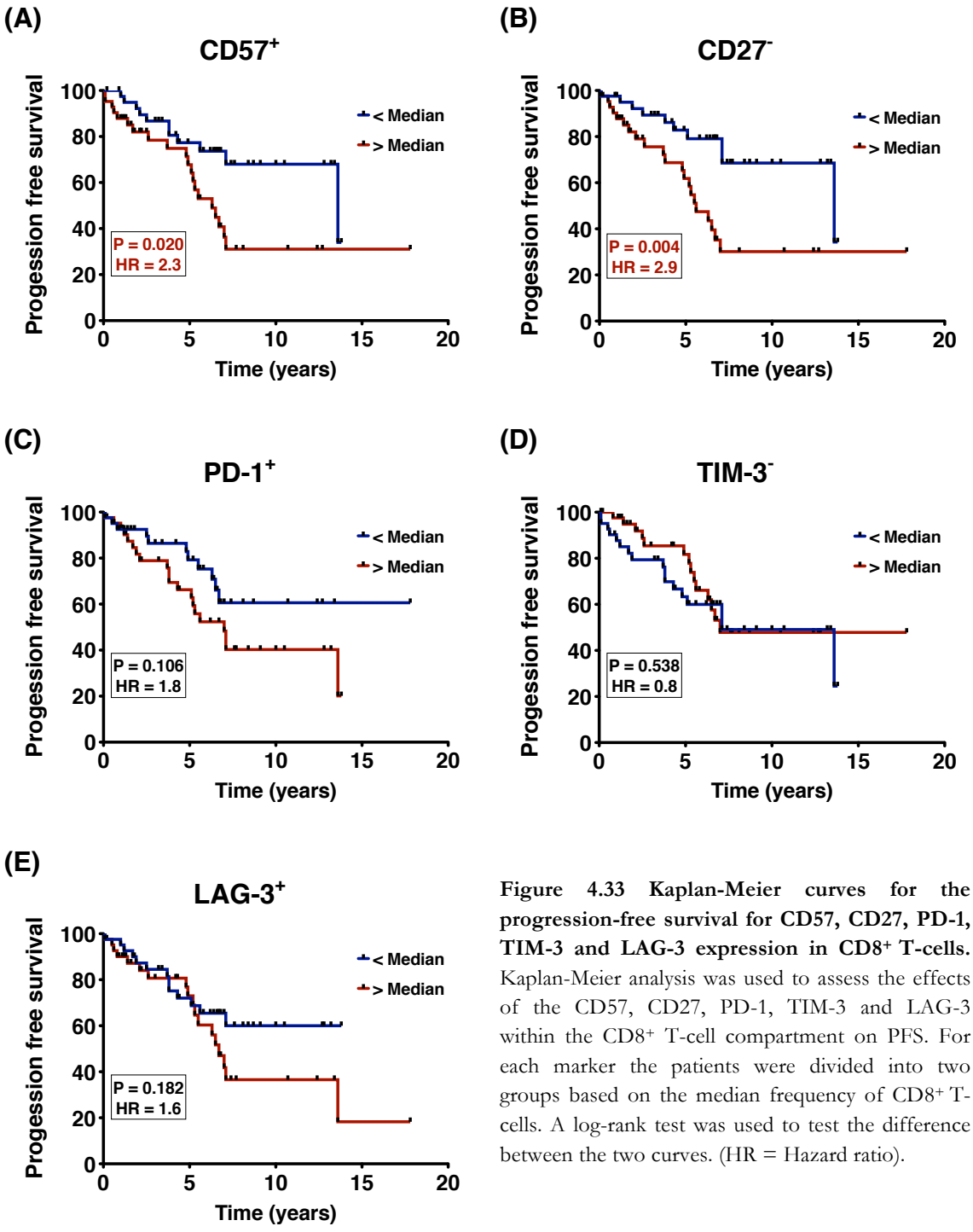

Figure 4.33 Kaplan-Meier curves for the progression-free survival for CD57, CD27, PD-1, TIM-3 and LAG-3 expression in CD8⁺ T-cells. Kaplan-Meier analysis was used to assess the effects of the CD57, CD27, PD-1, TIM-3 and LAG-3 within the CD8⁺ T-cell compartment on PFS. For each marker the patients were divided into two groups based on the median frequency of CD8⁺ T-cells. A log-rank test was used to test the difference between the two curves. (HR = Hazard ratio).

4.3.2 Multivariate analysis

Multivariate analysis was performed using Cox proportional hazards regression with forward selection by Dr Robert Hills (Dept. Haematology, Cardiff University, School of Medicine). A total of 459 T-cell subset variables were considered in the model. Two clusters of variables were shown to have the greatest influence on PFS: $CD4^+CD27^-PD\text{-}1^+LAG\text{-}3^+$ and $CD8^+CD27^-CD57^+PD\text{-}1^+$, respectively (Table 4.8).

Each of these clusters was then subjected to univariate analysis and Kaplan-Meier curves drawn. The patients were divided into two cohorts, again based on the median frequency of T-cells expressing the relevant markers. This analysis indicated that patients that were above the median for $CD4^+CD27^-PD\text{-}1^+LAG\text{-}3^+$ T-cells had significantly more progressive disease (P =0.0003; HR = 3.8) (Fig 4.34). The phenotype $CD8^+CD27^-CD57^+PD\text{-}1^+$ also appeared to significantly influence patient progression, but to a lesser degree (P =0.041, HR = 2.1) (Fig 4.35).

Overall this analysis showed that by using multivariate and univariate analysis, phenotypically distinct T-cell populations were potentially contributing to the clinical progression of CLL patients. Furthermore, it suggested that the T-cell populations that expressed multiple markers associated with T-cell dysfunction were having the most profound effect upon patient prognosis.

Table 4.9 Multivariate analysis was performed using Cox proportional hazards regression with forward selection

Summary of forward selection				
Phenotype	DF	Number in	Chi-Square	P-value
$CD4^+CD27^-PD\text{-}1^+LAG^+$	1	1	24.59	< 0.0001
$CD8^+CD27^-CD57^+PD\text{-}1^+$	1	2	12.66	0.0004

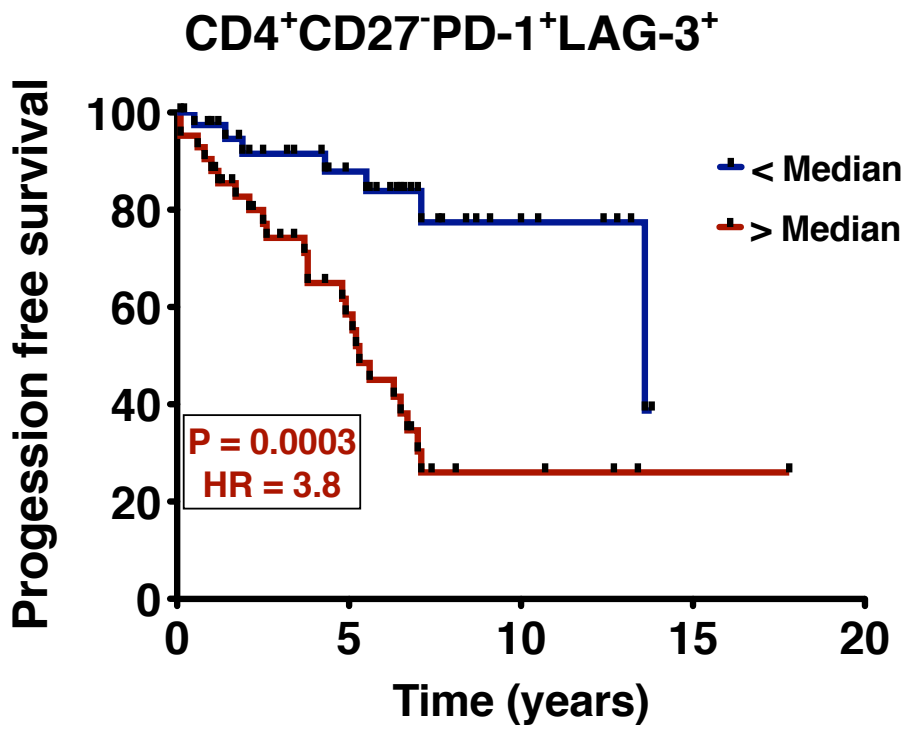

Figure 4.34 Kaplan-Meier curves for progression-free survival for the T-cell phenotype $CD4^+CD27^-PD\text{-}1^+LAG\text{-}3^+$. Kaplan-Meier analysis was used to assess the effect of the expression of the T-cell phenotypes $CD4^+CD27^-PD\text{-}1^+LAG\text{-}3^+$ on PFS. The patients were divided into two groups based on the median frequency of $CD4^+$ T-cells. A log-rank test was used to test the difference between the two curves. (HR = Hazard ratio).

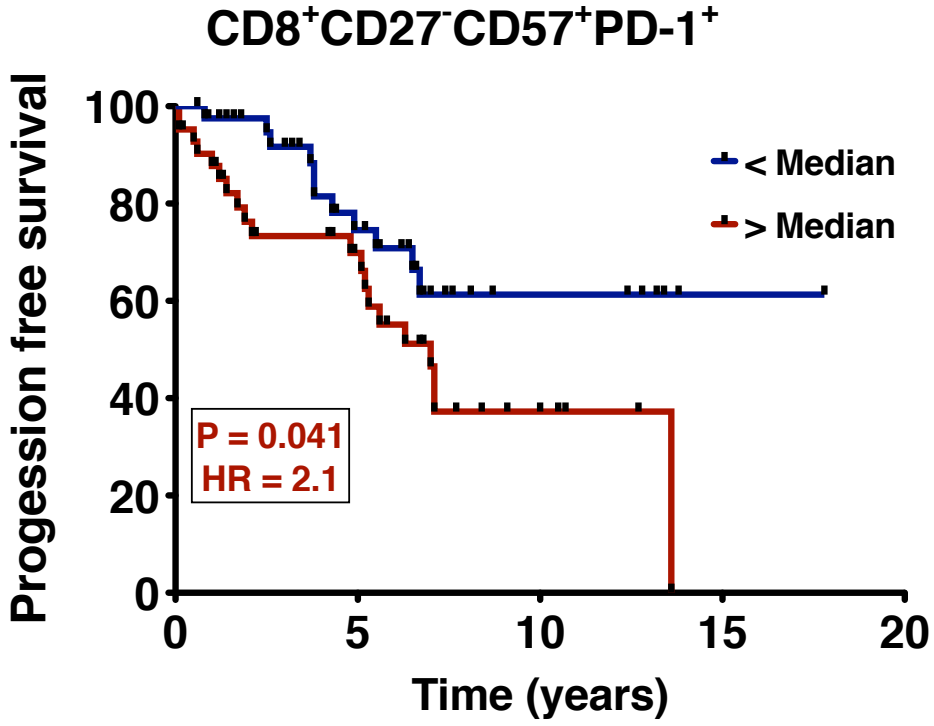

Figure 4.35 Kaplan-Meier curves for progression-free survival for the T-cell phenotype $CD8^+CD27^-CD57^+PD\text{-}1^+$. Kaplan-Meier analysis was used to assess the effect of the expression of the T-cell phenotype $CD8^+CD27^-CD57^+PD\text{-}1^+$ on PFS. The patients were divided into two groups based on the median frequency of $CD8^+$ T-cells. A log-rank test was used to test the difference between the two curves. (HR = Hazard ratio).

4.4 Expression of complementary ligands by CLL cells

The immunosuppressive effects associated with receptors such as PD-1, TIM-3 and LAG-3 are mediated through their interactions with complementary ligands (Keir et al. 2008; Zhu et al. 2005; Workman et al. 2002). In light of this the expression of the ligands PDL-1 (PD-1), GAL-9 (TIM-3) and MHC-II (LAG-3) were investigated on the malignant $CD19^+CD5^+$ CLL cells. The expression of the ligands was also investigated on normal $CD19^+$ B-cells from age-matched controls. This was due to the extremely low frequency/absence of $CD19^+CD5^+$ B-cells in non-CLL individuals.

No statistical differences between CLL patients and HD controls were observed regarding the percentage of PDL-1^+ and GAL-9^+ B-cells (Fig 4.37a and b). This was also the case when CLL patients were stratified into the CLL^{IR} and CLL^{NR} patient groups (Fig 4.38a and b). However, CLL^{IR} patients exhibited a trend towards increased frequency of PDL-1^+ and GAL-9^+ compared the HD controls.

Due to the constitutive expression of MHC-II molecules on professional APC, such as B-cells (Rodríguez-Pinto 2005; Vyas et al. 2008) it was unsurprising that greater than 97% of B-cell from both CLL patients and HD controls were positive for HLA-DR. However, comparisons between CLL patients and HD controls indicated that there was a small but significant ($P \leq 0.01$) increase in the percentage of HLA-DR expressing cells within CLL patients (Fig 4.37c). This finding was also observed when the patients were stratified; significant differences were observed in comparison to HD for both CLL^{IR} ($P \leq 0.05$) and CLL^{NR} ($P \leq 0.05$) (Fig 4.38c). These results show that while the complementary ligands investigated were commonly expressed on CLL cells, there were no striking differences in ligand expression between prognostic subsets.

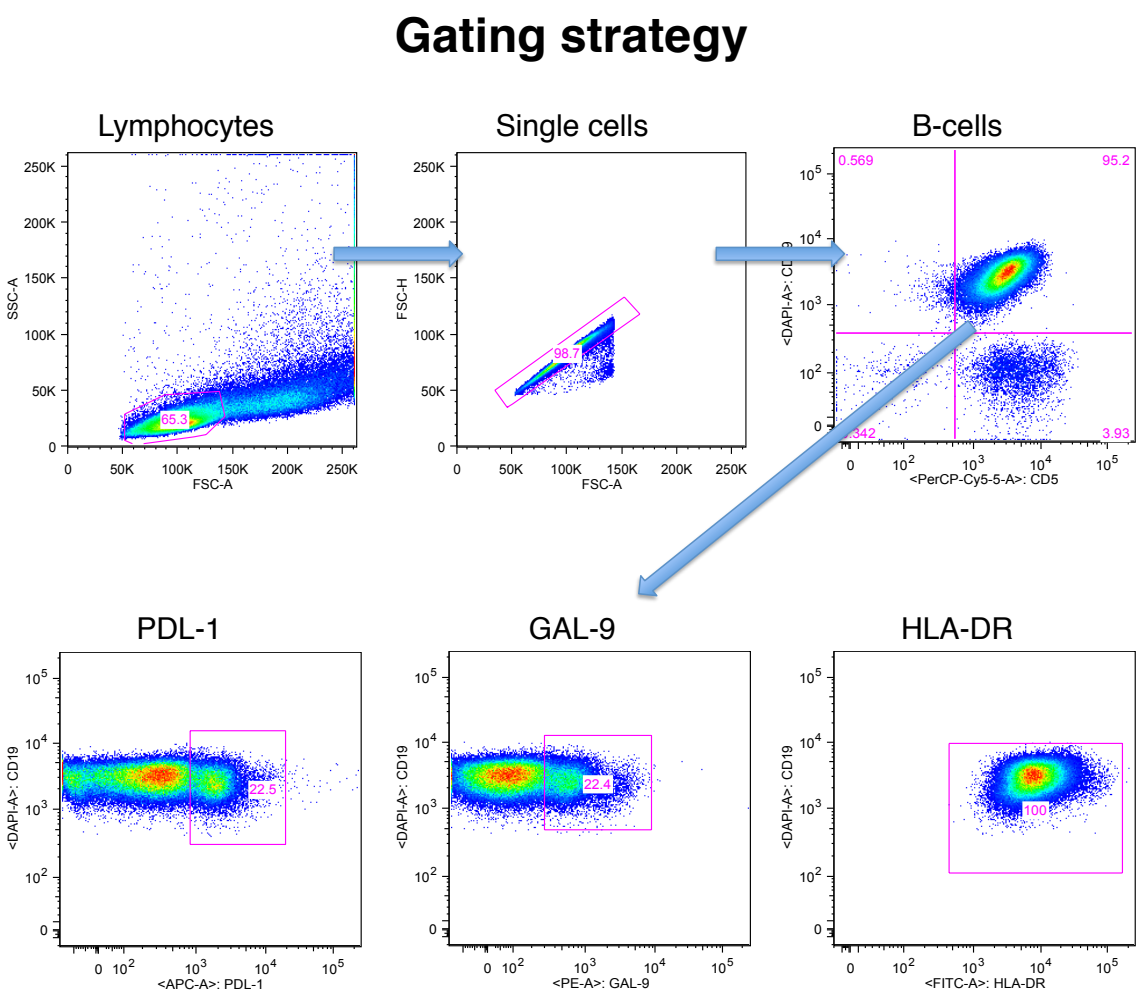

Figure 4.36 Representative results of B-cell immunosuppressive ligand expression analysis. The percentage of positive cells was determined by flow cytometry (FACSAria) and flow cytometric analysis was carried out using FlowJo software. Gating strategy was used to characterise the expression of PDL-1, GAL-9 and HLA-DR within the $CD19^{+}CD5^{+}$ B-cell compartment. To assist with the gating of positive cell populations FMO controls were applied where necessary.

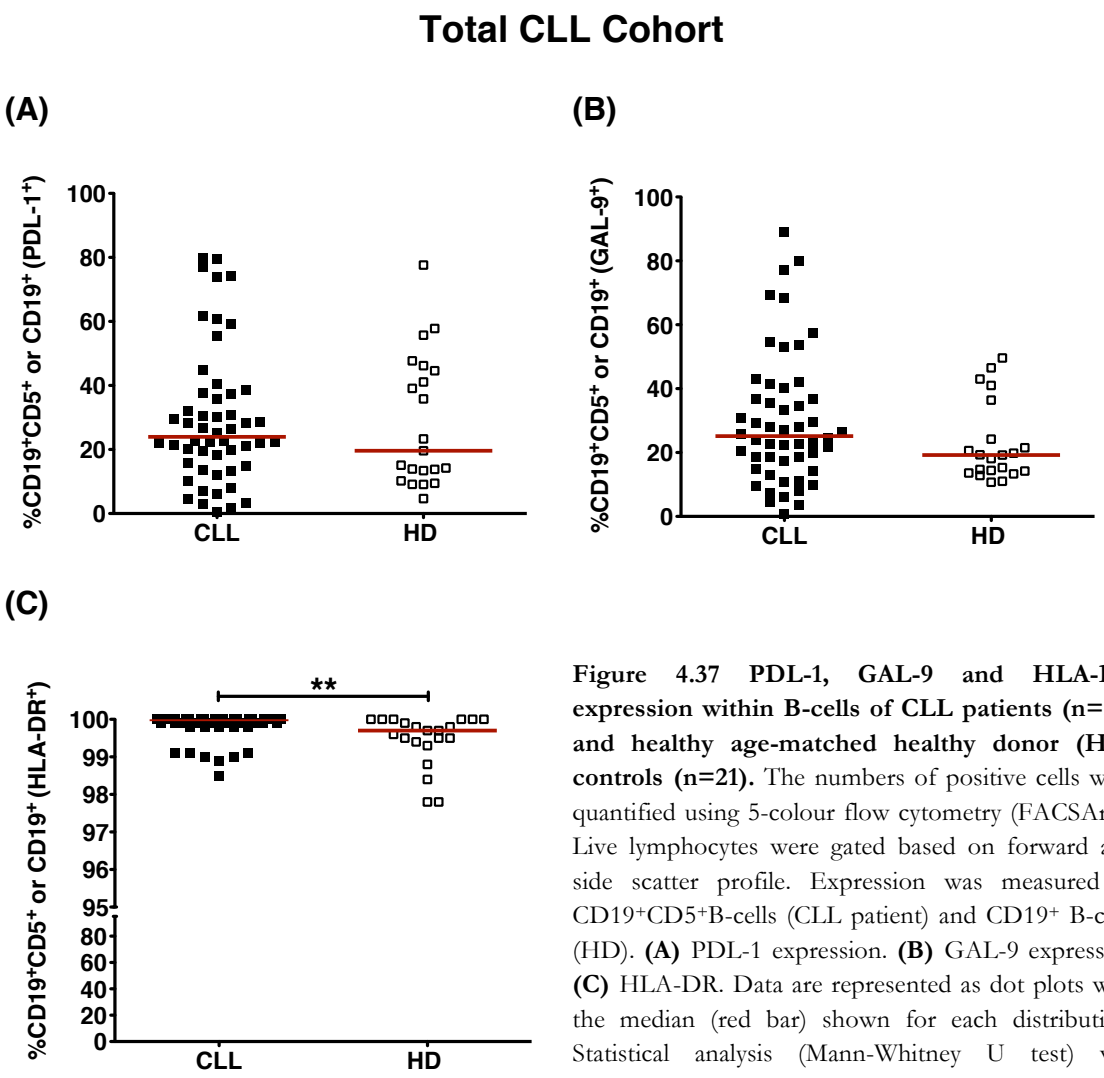

Figure 4.37 PDL-1, GAL-9 and HLA-DR expression within B-cells of CLL patients (n=52) and healthy age-matched healthy donor (HD) controls (n=21). The numbers of positive cells were quantified using 5-colour flow cytometry (FACSAria). Live lymphocytes were gated based on forward and side scatter profile. Expression was measured in $CD19^+CD5^+$B-cells (CLL patient) and $CD19^+$ B-cells (HD). **(A)** PDL-1 expression. **(B)** GAL-9 expression **(C)** HLA-DR. Data are represented as dot plots with the median (red bar) shown for each distribution. Statistical analysis (Mann-Whitney U test) was performed using GraphPad Prism 5.0. Statistical significance is denoted by asterisks (** $P \leq 0.01$).

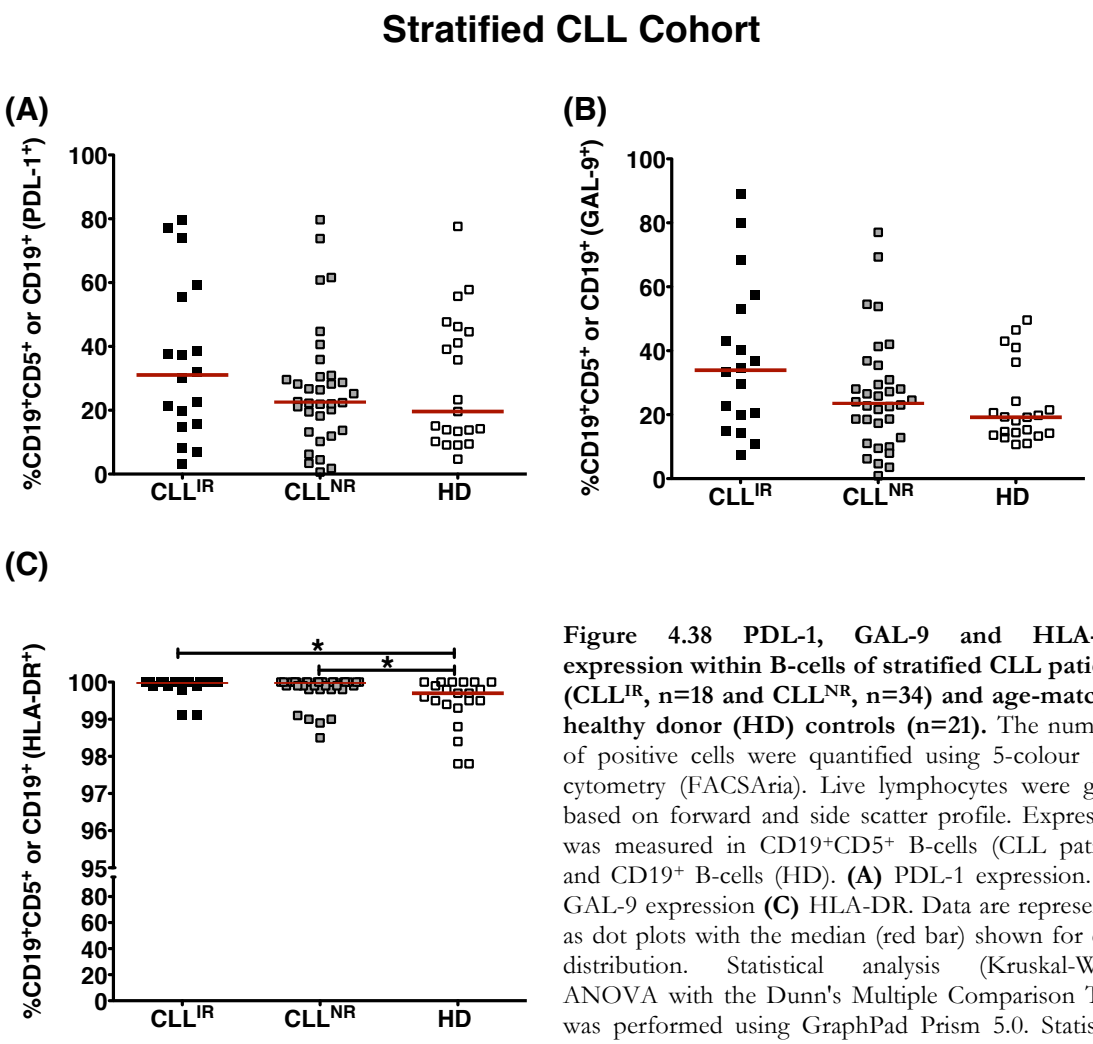

Figure 4.38 PDL-1, GAL-9 and HLA-DR expression within B-cells of stratified CLL patients (CLL^{IR}, n=18 and CLL^{NR}, n=34) and age-matched healthy donor (HD) controls (n=21). The numbers of positive cells were quantified using 5-colour flow cytometry (FACSAria). Live lymphocytes were gated based on forward and side scatter profile. Expression was measured in $CD19^+CD5^+$ B-cells (CLL patient) and $CD19^+$ B-cells (HD). **(A)** PDL-1 expression. **(B)** GAL-9 expression **(C)** HLA-DR. Data are represented as dot plots with the median (red bar) shown for each distribution. Statistical analysis (Kruskal-Wallis ANOVA with the Dunn's Multiple Comparison Test) was performed using GraphPad Prism 5.0. Statistical significance is denoted by asterisks (* $P \leq 0.05$)

4.5 Summary of phenotypic analysis

Table 4.10 Summary of phenotypic analysis of CD4$^+$ T-cells

CD4$^+$ T-cells	
Memory subset	
CLL vs HD	No statistically significant differences
CLL^{IR} vs CLL^{NR}	↓ % naïve T-cells, ↑ % EM T-cells
CLL^{IR} vs HD	↓ % naïve T-cells, ↑ % EM T-cells
CLL^{NR} vs HD	No statistically significant differences
Late differentiation marker	
CLL vs HD	No statistically significant differences
CLL^{IR} vs CLL^{NR}	↑ % CD57$^+$ T-cells, ↑ % CD27$^-$ T-cells
CLL^{IR} vs HD	↑ % CD57$^+$ T-cells
CLL^{NR} vs HD	No statistically significant differences
Immunosuppressive receptors	
CLL vs HD	↑ % TIM-3$^+$ T-cells
CLL^{IR} vs CLL^{NR}	↑ % TIM-3$^+$ T-cells, ↑ % PD-1$^+$ T-cells
CLL^{IR} vs HD	↑ % TIM-3$^+$ T-cells, ↑ % PD-1$^+$ T-cells
CLL^{NR} vs HD	No statistically significant differences

Table 4.11 Summary of phenotypic analysis of CD8$^+$ T-cells

CD8$^+$ T-cells	
Memory subset	
CLL vs HD	↓ % naïve T-cells, ↓ % CM T-cells
CLL^{IR} vs CLL^{NR}	↓ % naïve T-cells, ↓ % CM T-cells, ↑ % EMRA T-cells
CLL^{IR} vs HD	↓ % naïve T-cells, ↓ % CM T-cells
CLL^{NR} vs HD	No statistically significant differences
Late differentiation marker	
CLL vs HD	No statistically significant differences
CLL^{IR} vs CLL^{NR}	↑ % CD57$^+$ T-cells, ↑ % CD27$^-$ T-cells
CLL^{IR} vs HD	↑ % CD57$^+$ T-cells
CLL^{NR} vs HD	No statistically significant differences
Immunosuppressive receptors	
CLL vs HD	↓ % LAG-3$^+$ T-cells
CLL^{IR} vs CLL^{NR}	No statistically significant differences
CLL^{IR} vs HD	↓ % LAG-3$^+$ T-cells
CLL^{NR} vs HD	↓ % LAG-3$^+$ T-cells

Table 4.12 Summary of phenotypic analysis of CD19$^+$ / CD19$^+$CD5$^+$ B-cells

B-cells	
Immunosuppressive ligands	
CLL vs HD	↑ % HLA-DR$^+$ B-cells
CLL^{IR} vs CLL^{NR}	No statistically significant differences
CLL^{IR} vs HD	↑ % HLA-DR$^+$ B-cells
CLL^{NR} vs HD	↑ % HLA-DR$^+$ B-cells

4.6 Discussion

This study set out to perform phenotypic analysis of T-cells and B-cells from CLL patients with the aim of acquiring a deeper understanding of the immunological environment of CLL. The analysis was performed on both the $CD4^+$ and $CD8^+$ T-cells within a cohort of 97 CLL patients and 21 age-matched controls. Furthermore, within the CLL cohort the analysis was either performed on the entire cohort or on patient subsets stratified based their CD4:CD8 ratio.

Previous studies have shown that within CLL the absolute numbers of both $CD4^+$ T-cells and $CD8^+$ T-cells are elevated, however this elevation has been shown to be more pronounced within the $CD8^+$ T-cells compartment (Porakishvili et al. 2001; Serrano et al. 1997). The preferential expansion within the $CD8^+$ T-cell compartment results in an inversion in the CD4:CD8 ratio in some patients, which has been associated with phenotypic abnormalities and poor patient prognosis (Nunes et al. 2012).

Analysis of the T-cell memory subsets indicated no discernible difference between CLL patients as a whole and the HD controls. However, when the patients were stratified into two groups (CLL^{IR} and CLL^{NR}) it was revealed that there was substantial skewing within the distribution of memory T-cell subsets. A significant decrease in the proportion of naïve $CD4^+$ and $CD8^+$ T-cells within the CLL^{IR} patient group when compared to the CLL^{NR} and the HD controls was observed. Additionally, there was a significant increase in the proportion of EM $CD4^+$ T-cells and EMRA $CD8^+$ T-cells within the CLL^{IR} patient group compared to the CLL^{NR}. These findings indicate a skewing towards a more differentiated T-cell memory phenotype in the both the $CD4^+$ and $CD8^+$ T-cell compartments of the CLL^{IR} patient group, particularly in the $CD8^+$ compartment.

The process of memory differentiation induces functionally as well as phenotypic changes in T-cells. While EM and EMRA populations exhibit rapid effector functions, when compared to "less differentiated" T-cell populations such as naïve or CM, they also exhibit reductions in replicative potential, shorter telomeres and increased sensitivity to

apoptosis (Sallusto et al. 2004; Klebanoff et al. 2006; Geginat et al. 2003). Additionally, adoptive transfer of "less differentiation" T-cell populations has been shown to demonstrate superior *in vivo* expansion, persistence and anti-tumour activity in murine systems (Klebanoff et al. 2012). Furthermore, in human studies naïve T-cells have been shown to exhibit superior *in vitro* expansion and resistance to apoptosis (Hinrichs et al. 2011). Therefore it could be suggested that CLL patients who exhibit a shift in T-cell subset distribution from naïve to EM or EMRA may experience immune dysfunction and a reduced ability to respond to new antigens.

To further investigate the differentiation status of $CD4^+$ and $CD8^+$ T-cells from CLL patients the expression of CD57 and CD27 on T-cells was measured. Overall comparison between CLL patients and the HD controls revealed no significant differences regarding the frequency of $CD57^+$ or $CD27^-$ T-cells in either the $CD4^+$ or $CD8^+$ compartments. However, when the patients were stratified it was observed that increases in the frequency of $CD57^+$ or $CD27^-$ T-cells appeared to be associated with the CLL^{IR} group. These results, in combination with the observed skewing in the memory subsets suggest that T-cells from CLL^{IR} patients may have been driven further along the T-cell differentiation pathway.

The development of the $CD57^+CD27^-$ phenotype has been observed in chronic viral infections (Palmer et al. 2005) as well as haematological malignancies (Serrano et al. 1997; Nunes et al. 2012; Frassanito et al. 1998) and has historically been associated with T-cell differentiation, replicative senescence and a greater susceptibility to apoptosis (Dolfi et al. 2008; Brenchley et al. 2003). However, the specific fate conferred upon T-cells in response to the expression of CD57 is still controversial as it has been shown that $CD57^+$ T-cells can maintain functional competence (Chong et al. 2008).

Additionally, the down-regulation of other T-cell co-receptors such CD28, as well as the development of an EMRA phenotype, has been suggested to represent a T-cell population with reduced proliferative potential. However, given the appropriate co-

stimulatory signals, $CD28^{-}CD45RA^{hi}$ T-cells have been shown to maintain proliferative drive (Waller et al. 2007). This suggests that T-cell populations, which exhibit phenotypic hallmarks associated with replicative senescence, can still maintain functional competency under the appropriate conditions.

The development of $CD57^{+}$ and $CD27^{-}$ phenotypes within the T-cell compartment of CLL patients has been previously observed (Serrano et al. 1997) and has been shown to be more pronounced in CLL^{IR} patients (Nunes et al. 2012). Interestingly, the relationship between an inversion in the CD4:CD8 ratio and expression of CD57 does not appear to be a phenomenon specific to CLL as it has been observed in multiple myeloma (Frassanito et al. 1998) and also within aged healthy individuals (Olsson et al. 2000).

The process of T-cell differentiation is closely associated with the expansion of antigen-specific T-cell populations (Klebanoff et al. 2006) and aging (Olsson et al. 2000). Comparison between the two patient groups indicated that patients, which exhibited an inversion in their CD4:CD8, appeared to be significantly older, CLL^{IR} (median 79, range 53 – 92) and CLL^{NR} (median 70, range 43 – 94). Suggesting that age may be a factor in the inversion of the ratio and the phenotypic observations. However the age ranges overlap considerably suggesting that age may not be sole driving force behind the observations.

Additionally, it could be suggested that the "highly" differentiated T-cell phenotype observed within CLL, specifically in CLL^{IR} patients, may be due to an oligoclonal expansion of antigen-specific T-cells. The presence of clonal T-cell populations have been reported in CLL (Wen et al. 1990), within both the $CD8^{+}$ (Wikby et al. 2002) and $CD4^{+}$ T-cell compartments and has been suggested to be more pronounced within the $CD4^{+}CD57^{+}$ population (Serrano et al. 1997). Although the specific cause of T-cell expansions within CLL has yet to be universally agreed upon, several studies have suggested chronic antigen stimulation in response to CMV may play a role (Pourgheysari et al. 2010; Mackus 2003). Within this study, analysis of the effects of CMV serostatus suggested it did not have a significance influence on the CD4:CD8 ratio of CLL patients (Appendix 3), which is in line

with our previously published data (Nunes et al. 2012). CMV serostatus did appear to significantly influence the percentage of $CD57^+$ and $CD27^-$ cells within the $CD4^+$ and $CD8^+$ T-cell compartment, with these differences more pronounced within the $CD4^+$ compartment (Appendix 4).

This observation supports the concept that CMV infection can cause immunological changes within CLL patients, but suggests it may not be the sole driving force behind these observations. In support of this, T-cell expansions as well as functional and phenotypic changes have been observed within the T-cell compartment of CLL patients regardless of CMV serostatus (Pourgheysari et al. 2010; Riches et al. 2013). This suggests that other non-CMV antigen sources could potentially influence T-cell expansion and differentiation in CLL patients.

Numerous potential TAAs have been suggested for CLL such as Bax (Nunes et al. 2011), survivin (Schmidt et al. 2003), fibromodulin (Mayr et al. 2005) and MDM2 (Mayr et al. 2006). Furthermore, it has been shown that multiple mutations within CLL cells can result in the generation of immunogenic CLL-specific neoantigens (Rajasagi et al. 2014). Additionally, vaccinations with autologous CLL cells or CLL cell lysates have been shown to generate CLL-specific and personalised T-cell responses in some patients (Biagi et al. 2005; Burkhardt et al. 2013). All of these studies support the concept that CLL cells can express immunogenic tumour antigens, which could result in the activation and expansion of T-cells within some CLL patients. However, to date no dominant tumour-specific T-cell response has been correlated with $CD8^+$ or $CD4^+$ T-cell expansion in CLL. It also cannot be ruled out that chronic viral infections, other than CMV, may play a role in driving T-cell expansion and differentiation. However, it was not possible to investigate this concept in this study.

As the specificity of the T-cells investigated within this study were not determined, the extent of the role of CMV (or other antigen sources) on the development of a "highly" differentiated T-cell phenotype could not be directly assessed. This could be investigated

by the addition of specific tetramers (CMV, tumour antigens etc) to the previously utilised phenotyping strategy in order to determine if there is antigen specificity associated with the skewed T-cell phenotypes observed in this study.

Additionally, T-cell proliferation and differentiation in response to homeostatic cytokines, such as IL-7 and IL-15 has been previously reported (Geginat et al. 2003; Alves et al. 2003). Interestingly, the expression of IL-7 gene transcript (Frishman et al. 1993) and protein (Long et al. 1995) has been reported within CLL cells but not in normal B-cells. Therefore if CLL cells are capable of producing IL-7 and/or other homeostatic cytokines this could represent an alternative mechanism for the T-cell differentiation in CLL, which certainly warrants further investigation. For example, it would be interesting to determine the affects of exogenous homeostatic cytokines upon T-cells from CLL patients *in vitro*. It would also be useful to measure endogenous serum levels of homeostatic cytokines within CLL patients to determine if they correlate with phenotypic changes.

In addition to disrupting the normal formation of the immunological memory, chronic antigen stimulation can also result in the development of "exhausted" T-cell phenotypes, which can be characterised by the expression of immunosuppressive receptors. Signalling invoked by immunosuppressive ligand/receptor interactions have been shown to impair T-cell function through a variety of mechanisms (Wherry 2011).

PD-1 is an immunosuppressive receptor, which upon ligation with its ligand PDL-1 has been shown to negativity regulate T-cell function (Keir et al. 2008). The expression of PD-1 has previously been associated with the development of an T-cell "exhaustion" in chronic viral infection such as HIV and has been associated with increased viral load and disease progression (Day et al. 2006). Additionally, PD-1 expression has been observed within the T-cell populations of patients with solid tumours (Fourcade et al. 2009).

In this study it was observed that there was significant increase in the expression of PD-1 within the $CD4^+$ T-cell compartment of the CLL^{IR} patient group. This, in combination with other phenotypic observations, may suggest the development of a

potential immunosuppressed or "exhausted" T-cell phenotype. The increased expression of PD-1 within the $CD4^+$ T-cell compartment of CLL patients has been previously reported (Brusa et al. 2013), however they did not examine whether the high expression of PD-1 was a feature specifically associated with the CLL^{IR} patients within that cohort.

In contradiction to some previously published reports (Riches et al. 2013; Brusa et al. 2013; Nunes et al. 2012), this study showed no difference in PD-1 expression within the $CD8^+$ T-cell compartment when compared to HD controls or between the CLL^{IR} and CLL^{NR} patient groups. It should be noted that the cohort of patients in which the inversion of the CD4:CD8 ratio and PD-1 expression in the $CD8^+$ T-cell compartment was first reported (Nunes et al. 2012), and the cohort in this study showed no discernible differences in age or disease staging. The discrepancies between this study and previously published findings could be due to technical differences e.g. the use of different antibody panels, different flow cytometer set up and tracking and variations in gating strategies. Alternatively, it could be due to patient-to-patient variations between the cohorts in these studies or differences in the control groups. The majority of patients in the current study were stage A, untreated patients, and these were compared to age-matched healthy donor controls. The discrepancies between this study and others published findings highlight a requirement for multi-centre studies utilising standardised methodologies and respectively similar patient cohorts, when evaluating disease-specific phenomenon. Additionally combining results from multiple studies could provide a greater insight into the overall effect of the inversion of CD4:CD8 ratio. However this was not possible within the timeframe of this thesis but collation and analysis of data across multiple studies is currently underway. TIM-3 is an immunosuppressive receptor, which upon ligation with its ligand GAL-9 has been shown to negatively regulate T-cell function (Rangachari et al. 2012). Similar to PD-1, the expression of TIM-3 on T-cells has previously been associated with T-cell dysfunction in chronic viral infections (Wu et al. 2012) and patients with solid tumours (Fourcade et al. 2010).

In this study a significant increase in the expression of TIM-3 was observed within the $CD4^+$ T-cell compartment of the CLL patients when compared to HD controls, which appeared to be a feature specifically associated with the CLL^{IR} patient group. Potentially highlighting a population of T-cell that might be more susceptible to immunosuppression. However, analysis of the $CD8^+$ T-cell compartment showed that no differences were observed, either when the patients were considered as a whole or when stratified. It has been suggested that CLL patients exhibit no difference in the expression of TIM-3 when compared to age-matched controls (Riches et al. 2013; Zenz 2013). However, these authors did not present any data regarding the expression of TIM-3 nor did they state which T-cell population ($CD4^+$ or $CD8^+$) was studied.

LAG-3 is an immunosuppressive receptor, which upon ligation with its ligand MHC-II has been shown to negatively impact upon T-cell function (Hannier et al. 1998; Freeman and Sharpe 2012). When the expression of LAG-3 was investigated on $CD4^+$ T-cells in CLL, there were no differences in comparison to the age-matched controls. Biagi *et al* showed that there was an increase in the percentage of $CD4^+LAG\text{-}3^+$ cells within the $CD25^+$ population when compared to the $CD25^-$ population. Thus suggesting that CLL patients exhibit increased expression of LAG-3 within their T-reg population (Biagi et al. 2005). However, as Foxp3 staining was not included in this experiment it cannot be definitively stated that T-regs from CLL patients express more LAG-3, as CD25 is also a marker of activated T-cells (Caruso et al. 1997) and LAG-3 expression is linked to T-cell activation. Unexpectedly, when LAG-3 was investigated within the $CD8^+$ T-cell compartment, it appeared to be significantly higher in the age-matched controls, but the cause of this observation remains unresolved.

Analysis of the combined expression of PD-1, TIM-3 and LAG-3 was performed as T-cells multiple immunosuppressive receptors have been suggested represent populations that exhibit the most profound impairments in T-cell function (Sakuishi et al. 2010; McMahan et al. 2010; Fourcade et al. 2010).

Analysis of the combined expression of PD-1, TIM-3 and LAG-3 within the $CD4^+$ T-cell compartment indicated that CLL patients exhibited an increased frequency of T-cells expressing multiple immunosuppressive receptors. Additionally, this observation appeared to be a hallmark of the CLL^{IR} patient group, which is in keeping with previous observations that this group has an abnormal distribution of T-cell subsets. Analysis of the $CD8^+$ compartment revealed that there was a significant decrease in PD-1^+TIM-3^-LAG-3^+ $CD8^+$ T-cells within the CLL patient group when compared to the controls. However, an increase in the frequency of PD-1^+TIM-3^+LAG-3^- T-cells was observed within the CLL patients.

While differences in the frequency of T-cell populations expressing multiple immunosuppressive receptors has been observed, it is unknown if they represent populations that would exhibit the greater defects within CLL or if they represent activated T-cell phenotypes. Therefore functional analysis of the individual populations is essential to determine any potential differences between the groups.

The increased expression of immunosuppressive receptors (individually or in combination), particularly within the $CD4^+$ T-cell compartment of CLL^{IR} patients, indicates the presence of cell populations that exhibit phenotypic profiles previously associated with immune dysfunction. Blockade of the PD-1/PDL-1 pathway *in vitro* has been shown to alleviate defects in immunological synapse formation, (Ramsay et al. 2012) enhance the production of IFN-γ (Brusa et al. 2013). Furthermore, *in vivo* blockade in the TCL murine model of CLL (Johnson 2006) indicated that inhibition of PD-1/PDL-1 limited tumour progression, enhance T-cell function and prevent the inversion of the CD4:CD8 ratio (Hanna et al. 2014). This indicates that early intervention could enhance T-cell mediated tumour control and suggests a role for PD-1 in the inversion of CD4:CD8 ratio observed in CLL. However, populations expressing immunosuppressive receptors have been shown to maintain component T-cell function and been termed "pseudo-exhausted" in CLL (Riches et al. 2013) and other haematological malignancies (Lichtenegger et al. 2013).

Therefore to determine if any of these phenotypic observations translate into functional effects, further analysis is clearly essential.

The manifestation of these observations may be underpinned by responses to chronic antigen stimulation, due to the close association between elevated expression of immunosuppressive receptors and chronic viral infection (Day et al. 2006; Sakhdari et al. 2012). Within the $CD4^+$ T-cell compartment, CMV infection appeared to significantly influence the expression of TIM-3, it also appeared to increase the expression of PD-1 and LAG-3 however these observations did not reach significance (Appendix 5). Within the $CD8^+$ T-cell compartment, less distinct differences were observed and none reached significance (Appendix 5). These observations support the concept that CMV infection is playing a role in the manifestation of "exhausted" T-cell phenotypes within CLL, but are not consistent with CMV being the sole or dominant driver for expansion of these T-cells (Riches et al. 2013). Additionally, it has been suggested that CMV^+ T-cells from CLL patients may exhibit reduced expression of immunosuppressive markers in comparison to CMV^+ T-cells from healthy individuals (Raa et al. 2014). This further suggests a role of other antigens in driving the expression of immunosuppressive markers in CLL.

Prognostication has historically been a key feature of the clinical management of CLL, with numerous markers predicting good or bad patient outcome. However, the majority of these markers (CD38, ZAP70, *IGHV* mutational status etc) apply specifically to the malignant CLL cells (Gribben 2010), rather than other immune cells. In this chapter, I attempted to link the wide array of abnormalities observed in the neighbouring T-cell compartment of CLL patients with patient outcome. Several significant phenotypic differences were observed between the T-cells of CLL^{IR} and CLL^{NR} patient groups. The clinical importance of these observations was supported by the demonstration that patients displaying a CD4:CD8 <1, exhibited more progressive disease. This confirms previously reported data (Nunes et al. 2012), but the specific mechanism behind this relationship is unknown. Previous analysis indicated a significant relationship between the inversion in the

CD4:CD8 ratio and lymphocyte doubling time less than 12 months (Nunes et al. 2012). Therefore it could be suggested that the T-cell populations from CLL^{IR} patients mediate enhanced CLL cell proliferation. However, it is unknown whether this is due to defects in tumour control or due to T-cell populations supporting CLL cell proliferation.

Some clues to potential mechanisms were provided by further analysis of the relationship between individual markers and clinical prognosis. Univariate analysis demonstrated an increase frequency of $CD4^+PD\text{-}1^+$ T-cells was associated with shorter PFS and disease progression. This observation could be related to immune exhaustion and loss of immunological control, as $PD\text{-}1^+$ T-cells have been shown to represent a functionally impaired T-cell population (Keir et al. 2008). Additionally, increases in $CD4^+PD\text{-}1^+$ T-cells have been associated with the recurrence of melanoma in murine systems, suggesting a possible association between $CD4^+PD\text{-}1^+$ T-cells and tumour control (Goding et al. 2013).

However, the expression of PD-1 is tightly regulated by T-cell activation and thus there is a great deal of debate regarding the classification of PD-1 as a marker of T-cell exhaustion or activation (Keir et al. 2008). Interestingly, activated T-cells have been shown to be essential for the successful engraftment, survival, and proliferation of CLL cells *in vivo* in murine systems (Bagnara et al. 2011). Additionally, proliferating CLL have been shown to co-localise with activated $CD4^+$ T-cells within the lymph nodes of CLL patents (Patten et al. 2008), specifically $CD4^+PD\text{-}1^+$ T-cells (Brusa et al. 2013). Therefore, the association between $CD4^+PD\text{-}1^+$ T-cells and disease progression observed in this study could be due to enhanced CLL cell survival mediated via support from $CD4^+PD\text{-}1^+$ "activated" T-cells. This hypothesis could be explored by investigating the *in vitro* proliferative potential and survival of the autologous CLL cells in the presence and absence of $CD4^+PD\text{-}1^+$ T-cells.

Increased frequencies of $CD57^+$ T-cell within the $CD4^+$ and $CD8^+$ compartments were associated with shorter PFS and disease progression within this cohort. The association between $CD57^+$ T-cells and poor prognosis has been reported in patents with

solid malignancies (Akagi and Baba 2008) and increases in the frequency of $CD4^+CD57^+$ T-cells have been shown to be associated with advanced disease stage within CLL (Serrano et al. 1997). However, the mechanisms behind these observations remain unclear. The expression of CD57 within the $CD4^+$ and $CD8^+$ T-cell compartment has been associated with an increased sensitivity to apoptosis and reductions in proliferative potential (Brenchley et al. 2003; Focosi et al. 2010), both of which are characteristically associated with immune dysfunction. The classification of CD57 as true marker of replicative senescence is still contentious as Chong *et al* have shown, by several methods, that $CD8^+CD57^+$ T-cells are capable of maintaining proliferative competence (Chong et al. 2008).

Although the function of $CD57^+$ T-cells was not studied in this chapter, future work could test the proliferative potential of T-cells from CLL patients in several ways. For example, measuring the expression of Ki-67 within the $CD57^+$ and $CD57^-$ T-cell compartment of CLL patients in response to *in vitro* stimulation. Other assays for T-cell proliferations such as CFSE dilution and 7-amino-actinomycin D (7AAD) uptake experiments could also be performed.

Alternatively the poor prognosis associated with expression of CD57 could be due to this T-cell population supporting survival of the CLL cells. $CD8^+CD57^+$ T-cells have been shown to produce high levels of IFN-γ upon activation, which has been shown to support CLL cell survival *in vitro* (Van den Hove et al. 1998; Chong et al. 2008; Buschle et al. 1993). Stimulated $CD57^+$ and $CD57^-$ T-cells from CLL patients could be investigated *in vitro* through various assay systems (ICS, ELISA and cytometic bead array) to determine if these two cell subsets exhibit differential cytokine profiles, which could influence CLL cell survival. Additionally, the assessment of the viability (via annexin/PI staining) of autologous CLL cells cultured with the supernatant isolated from activated $CD57^+$ and $CD57^-$ T-cells, could provide indications as to whether factors produced by the different subtypes could augment CLL cell survival *in vitro*.

CD27 is a marker that is down-regulated during T-cell differentiation (Klebanoff et al. 2006). The $CD27^-$ phenotype within the $CD8^+$ T-cell compartment appeared to be associated with shorter PFS and disease progression. The expression and signalling through CD27 has been shown to play an essential role in supporting the T-cell survival, development and preventing apoptosis (Song et al. 2012; Dolfi et al. 2008; Ochsenbein et al. 2004). Therefore patients that exhibit reduced expression of CD27 may possess a population of $CD8^+$ T-cells with reduced proliferative potential and increased sensitivity to apoptosis. This could thereby limit their general immunological capacity and restrict their ability to mediate tumour control.

To further investigate the effects of specific T-cell populations on patient prognosis and the pathology of the disease, unbiased multivalent analysis was performed (Dr Robert Hills). This analysis indicated that two specific T-cell phenotypes $CD4^+CD27^-PD\text{-}1^+LAG\text{-}3^+$ and $CD8^+CD27^-CD57^+PD\text{-}1^+$ had the greatest influence upon PFS. The mechanism behind this observation could be due to reduced T-cell function associated with the combined expression of these phenotypes markers, which in turn could impair immune function and limit immunological control of the tumour. Conversely it could be due to the relationship between cellular activation state and the described markers and thus the T-cell populations could be supporting the survival and proliferation of CLL cells.

These hypotheses could be examined by investigating the functionality of these specific T-cell populations through cell sorting, then testing function through the various methods described above. The ability for the specific T-cell populations to support CLL cell survival and proliferation, either in a contact-dependent or independent manner, could be investigated, again utilising the experimental methodologies describe above.

The findings from this chapter highlight the existence of several abnormalities within the T-cell compartment of CLL patients, many of which seem to be specific features of patients that exhibit an inversion in the CD4:CD8 ratio. The involvement of an array of molecules and multiple T-cell subsets, suggest that it would require a combination of

approaches to circumvent T-cell dysfunction and allow for successful T-cell based therapies in CLL.

Additionally this analysis supports the concept that the frequency of specific T-cell populations can be used as markers of clinical progression. However, the precise role of T-cells in the pathology of CLL remains unknown; it is not clear whether they play an active or passive role. It remains to be determined whether defects in various T-cell functions, could result in loss of tumour control. Alternatively, the augmented T-cells populations could be supporting CLL cell survival. This highlights the necessity for further characterisation and understanding of the role of T-cells within CLL.

Chapter 5

Gene expression analysis of T-cells in CLL

Numerous studies have described transcriptional differences between T-cells derived from CLL patients and those isolated from healthy individuals (Göthert et al. 2013; Kiaii et al. 2013; Görgün et al. 2005; Görgün et al. 2009). However, differences between prognostic subsets of patients have not been evaluated to date. The inversion of the CD4:CD8 ratio has been shown to highlight a patient group with greater prognostic risk, which also exhibits numerous phenotypic differences within the $CD4^+$ and $CD8^+$ T-cell compartments (as described in Chapter 4). Therefore the aim of this study was to compare the expression of a subset of genes related to T-cell function and biological processes between CLL^{IR} and CLL^{NR} patients.

Commercial kits, purchased from SABiosciences, were utilised to investigate pathway-specific genes across two separate arrays: T-cell and B-cell activation RT^2 Profiler PCR array (PAMM-053Z) and T-cell anergy and tolerance RT^2 Profiler PCR array (PAMM-074Z). The analysis was performed on total mRNA isolated from purified $CD4^+$ and $CD8^+$ T-cells derived from CLL^{IR} and CLL^{NR} patients. The aim was to explore potential differences between the two patient groups in terms of T-cell related gene transcription and to highlight candidate genes and/or processes for further evaluation. A schematic diagram showing the experimental workflow for these assays is given in Figure 5.1.

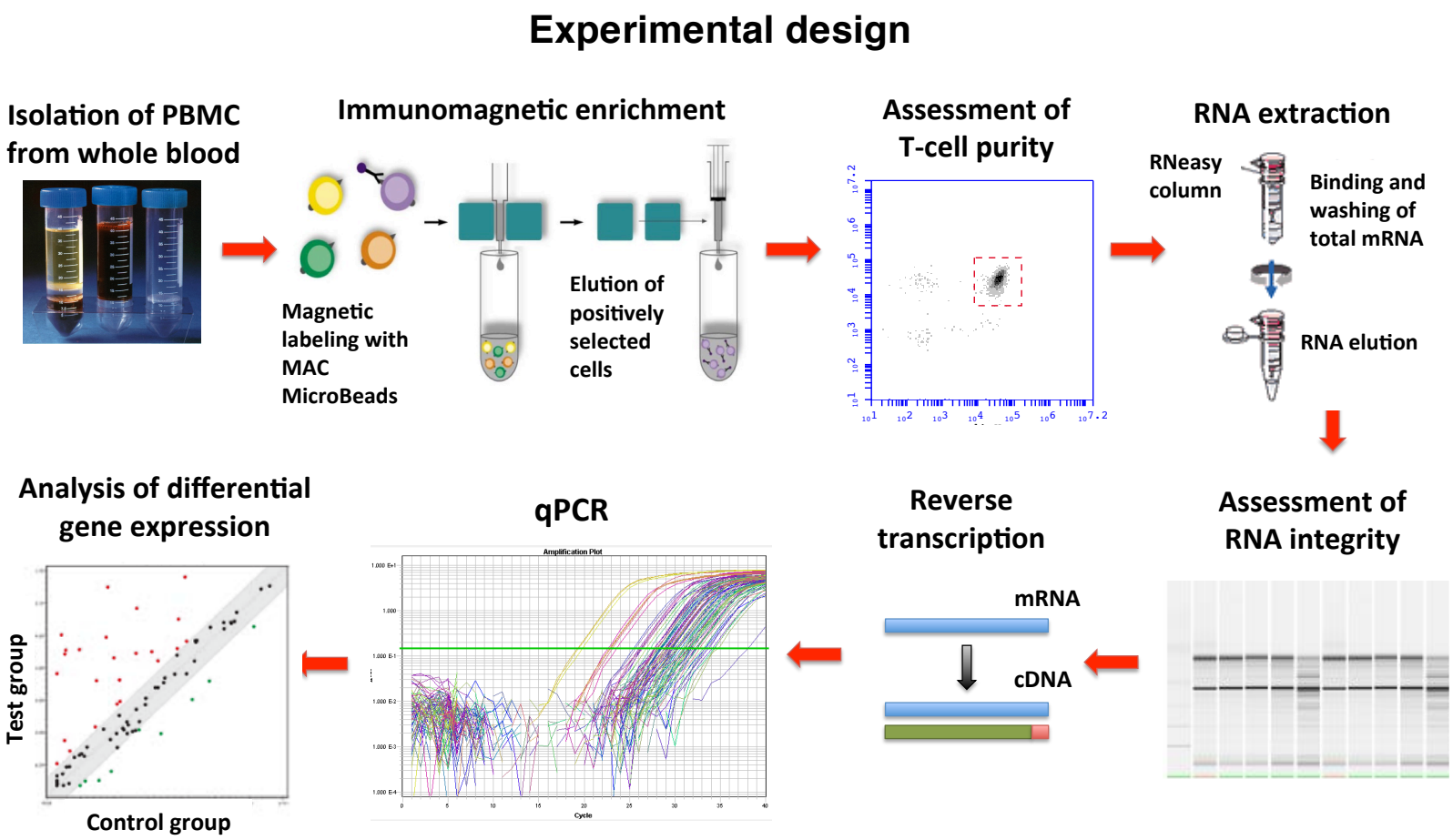

Figure 5.1 Schematic of experimental design. CD4$^+$ and CD8$^+$ T-cells (>90% purity) were isolated by immunomagnetic separation from CLL^{NR} patents (CD4:CD8 range 1.17 – 2.21, mean 2.13), CLL^{IR} patents (CD4:CD8 range 0.18 – 0.67, median 0.52). RNA extraction was performed using RNeasy Mini Kit (Qiagen) and was quantified using the Nanodrop (Thermo science). Investigation of the RNA integrity was performed using the RNA 6000 Nano Kit (Agilent). 60ng of RNA from each sample was then reverse transcribed using the RT^2 First Strand Kit (Qiagen) and qPCR performed using the 7500 Real-time PCR Systems (Life technologies) with the resulting cDNA.

5.1 $CD4^+$ T-cell analysis

Analysis of the differential expression of genes between the CLL^{IR} and CLL^{NR} patients was performed utilising two independent qPCR arrays. Due to the heterogeneity observed in the expression of the five housekeeping genes included on each array, ribosomal protein large P0 (RPLP0) was selected for data normalisation. This selection process was based upon relative abundance of the gene and as well the relatively low variation in expression across the samples (Appendix 4 and 5).

The transcriptional analysis indicated that a substantial number of genes were lower within CLL^{NR} patients when compared to the CLL^{IR}. Specifically, there was reduced transcription (>2 fold) in 61/84 genes in the T-cell activation array (Fig 5.2 and Appendix 8). Similarly, analysis of the T-cell anergy array revealed lower transcription (>2 fold) in 43/84 genes. In contrast, 7/84 genes showed increased transcription (>2 fold) within CLL^{NR} patients relative to the CLL^{IR} (Fig 5.3 and Appendix 9). Due to the limited number of samples analysed in these experiments, statistical analysis of the differentially expressed genes between the patient groups was not performed. However, to attempt to identify specific T-cell pathways/processes and to highlight genes of interest for validation, enrichment analysis was performed using the MetaCore Analytical Suite (https://portal.genego.com) with the assistance of Dr Robert Andrews (Bioinformatics support, Cardiff University).

The differentially expressed genes identified from the T-cell activation array (Fig 5.2 and Appendix 8) and T-cell anergy array (Fig 5.3 and Appendix 9) were utilised as the input gene list for analysis. The output from the analysis emphasised enrichment for processes involved in cellular activation, differentiation, cytokine production and survival.

To highlight specific genes for potential further investigation and validation, the focus of the analysis was on selected genes within the pre-defined Metacore pathways "Naive $CD4^+$ T cell differentiation" (IL-2, IL-1β, IL-5, CD28, IL-6, IL-12, CD40L, IL-13, IL-18, CD86, CD80, IRF4, IL-10, TGF-β1, CD40, CD4) and "Generation of memory

CD4" (IL-2, IL-2R α chain, CD28, IL4R α chain, Bcl-2, CD86, CD80, IL-7, CD4, STAT3, AP-1, IL-17, IRF4, IL-10). It is worthy of note that the transcription of all genes in these MetaCore pathways were reduced within the CLL^{NR} patient samples relative to the CLL^{IR} patient samples. Focus was placed upon these two pathways due to the importance of T-cell differentiation and appropriate development of immunological memory in sustaining a competent immune system.

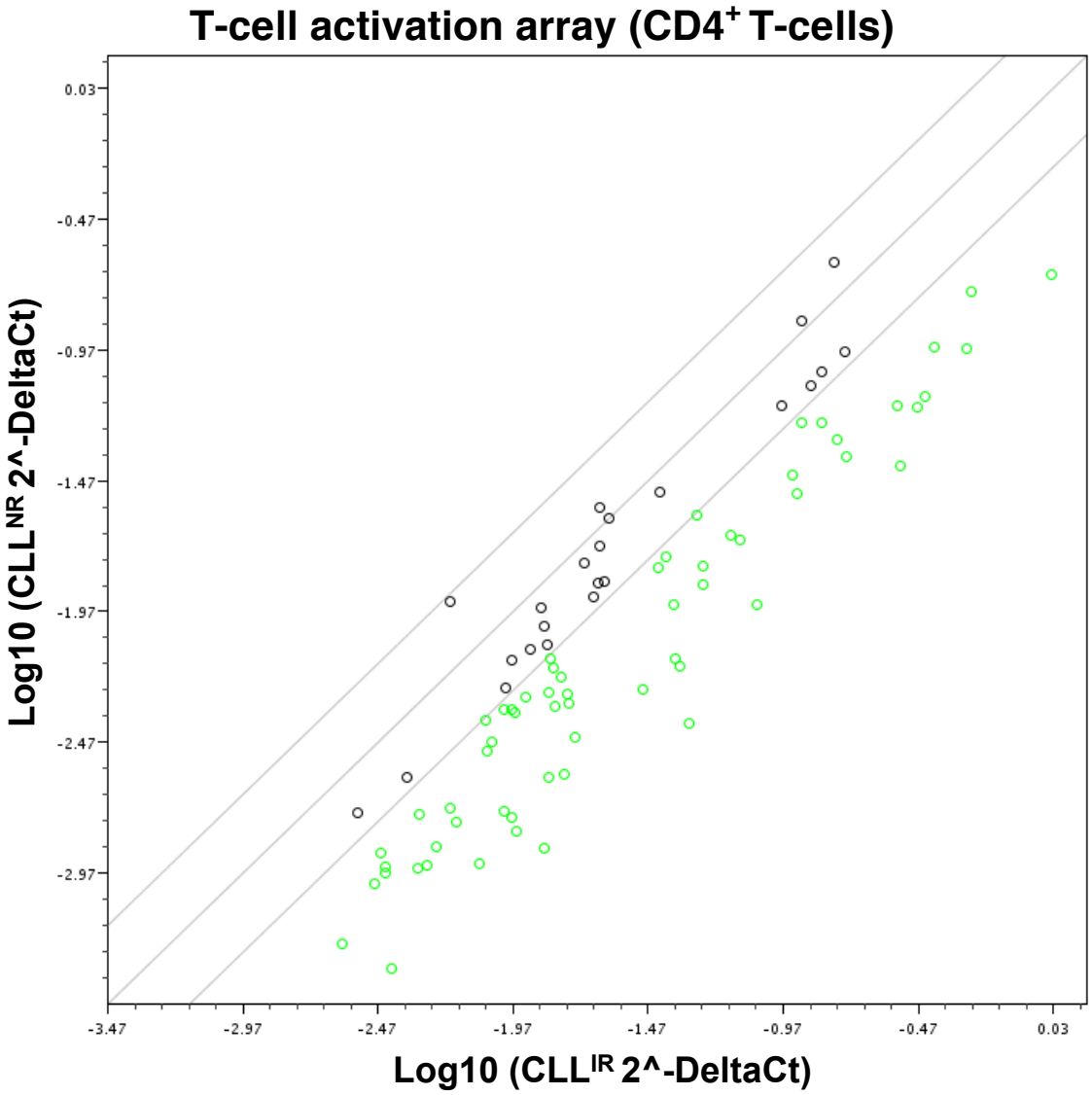

Figure 5.2 Differentially expressed genes (T-cell activation array) in CD4+ T-cells between CLL^{NR} patients and CLL^{IR} patients. qPCR was performed on the ABI Prism 7500HT Sequence Detector (Applied Biosystems) using primer sets embedded within T-cell and B-cell activation RT^2 Profiler PCR array. For data analysis the ΔΔCt method was used and the fold change for each gene were calculated as the difference in gene expression between CLL^{IR} patents (n = 4) and CLL^{NR} (n =2). Data are represented as a scatter plot with a fold change of >2 selected as the cut off. Data analysis and representation was performed with the RT^2 Profiler PCR Array Data Analysis 3.5 (Qiagen).

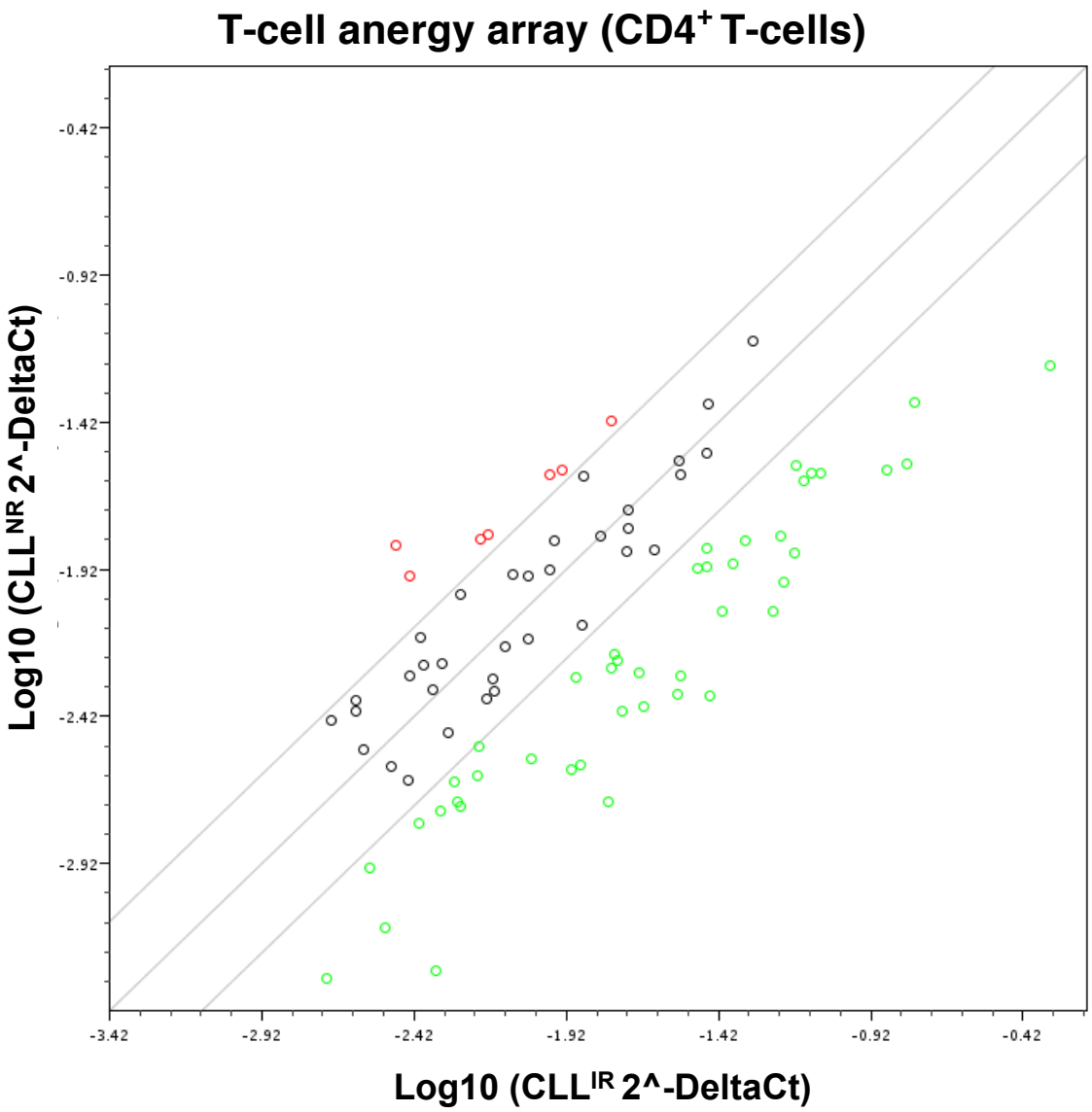

Figure 5.3 Differentially expressed genes (T-cell anergy array) in CD4⁺ T-cells between CLL^{NR} patients and CLL^{IR} patients. qPCR was performed on the ABI Prism 7500HT Sequence Detector (Applied Biosystems) using primer sets embedded within T-cell anergy and tolerance RT² Profiler PCR array. For data analysis the ΔΔCt method was used and the fold change for each gene were calculated as the difference in gene expression between CLL^{IR} patents (n = 4) and CLL^{NR} (n =2). Data are represented as a scatter plot with a fold change of >2 selected as the cut off. Data analysis and representation was performed with the RT² Profiler PCR Array Data Analysis 3.5 (Qiagen).

5.2 $CD8^+$ T-cell analysis

Similar to the $CD4^+$ analysis, two independent qPCR arrays were used and data normalisation was performed using RPLP0 as a housekeeping gene (Appendix 6 and 7).

The analysis indicated that the transcription of a substantial number of genes were lower within CLL^{NR} patients when compared to the CLL^{IR}. Specifically the T-cell activation array showed lower transcription (>2 fold) in 49/84 genes (Fig 5.4 and Appendix 10) and the T-cell anergy array showed lower transcription (>2 fold) in 68/84 genes (Fig 5.5 and Appendix 11).

The differentially expressed genes identified from the T-cell activation array (Fig 5.4 and Appendix 10) and T-cell anergy array (Fig 5.5 and Appendix 11) were utilised as the input gene list for enrichment analysis. Prior to input, the gene list was filtered for abnormally high and potentially anomalous fold changes, which resulted in the removal of TLR4 (-349.22) and TLR6 (-78.14) (Appendix 10).

To highlight specific genes for potential further investigation and validation, the focus of the analysis was placed upon selected genes within the pre-defined MetaCore pathways "Differentiation and clonal expansion of $CD8^+$ T-cells" (CD137, CD28, IFN-γ, NF-kB, NF-AT2, STAT3, CD40L, NF-AT1, CD27, GzmB, ICAM1, CD70, CD40, FasL, T-bet, perforin, OX40). The transcription of all genes was reduced within CLL^{NR} patients relative to CLL^{IR}. This process was selected due to the importance of appropriate $CD8^+$ T-cell differentiation and the acquisition of effector functions.

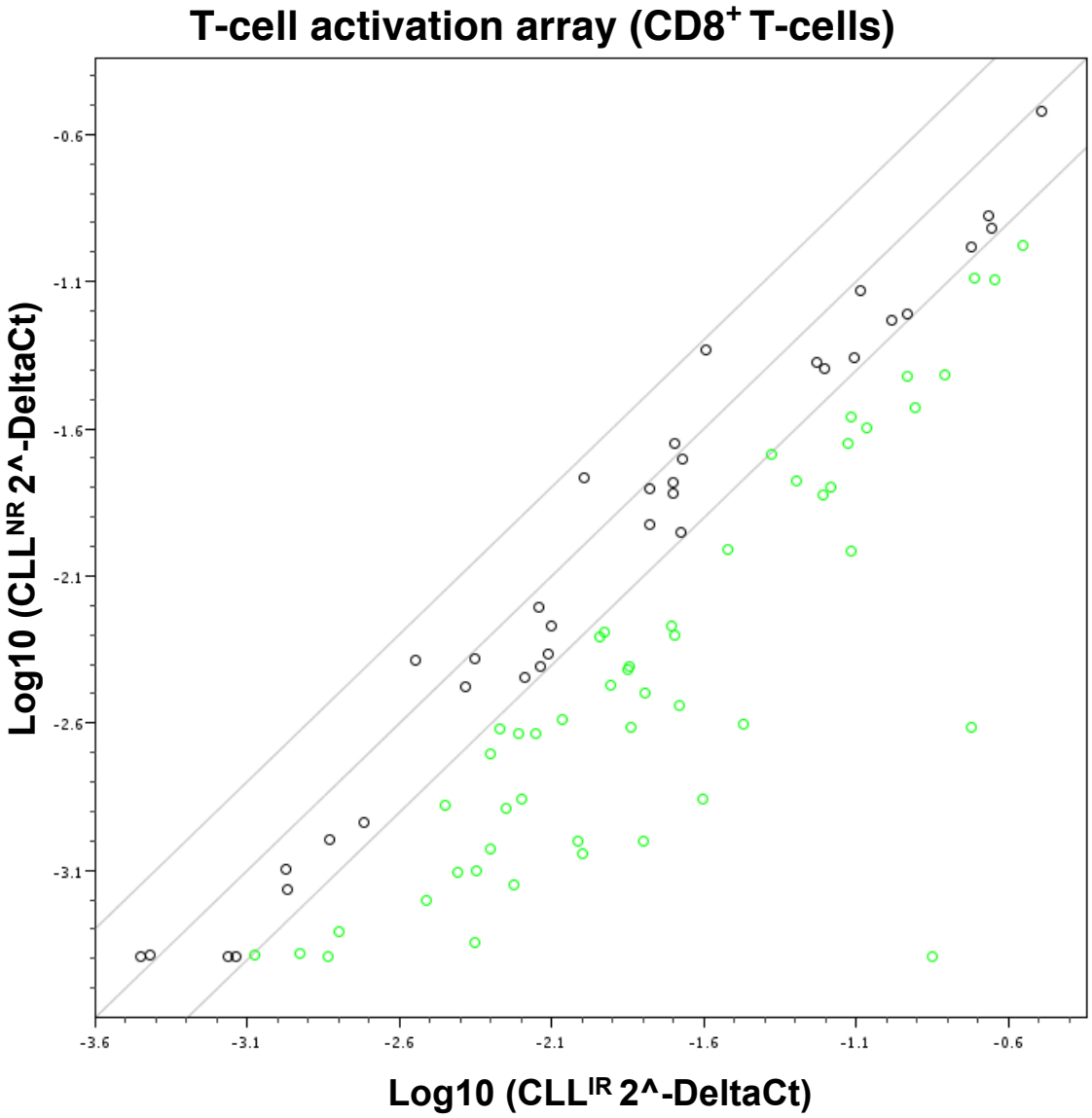

Figure 5.4 Differentially expressed genes (T-cell activation array) in CD8⁺ T-cells between CLL^{IR} patients and CLL^{IR} patients. qPCR was performed on the ABI Prism 7500HT Sequence Detector (Applied Biosystems) using primer sets embedded within T-cell and B-cell activation RT^2 Profiler PCR array. For data analysis the ΔΔCt method was used and the fold change for each gene were calculated as the difference in gene expression between CLL^{IR} patents (n = 5) and CLL^{NR} (n =2). Data are represented as a scatter plot with a fold change of >2 selected as the cut off. Data analysis and representation was performed with the RT^2 Profiler PCR Array Data Analysis 3.5 (Qiagen).

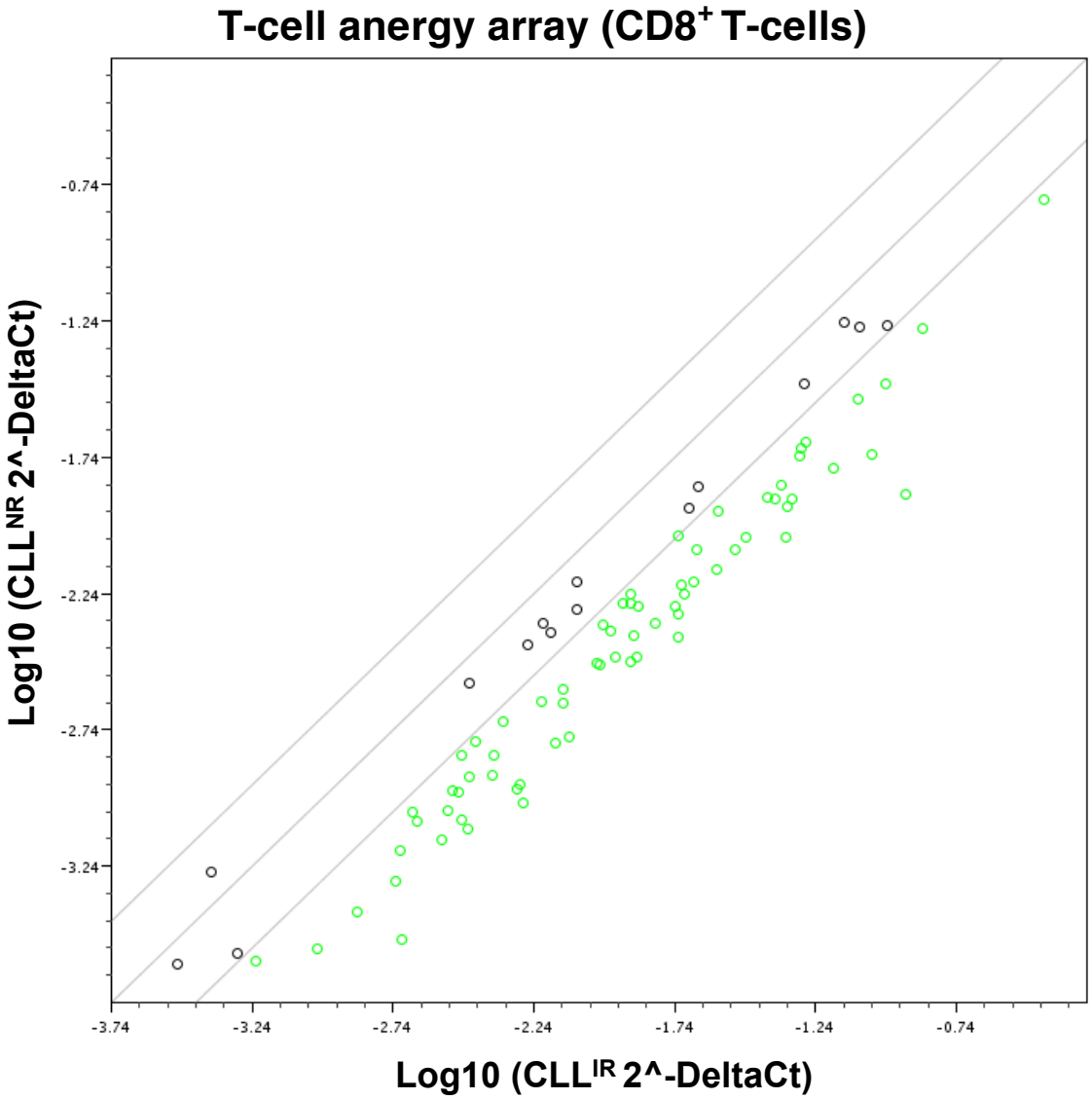

Figure 5.5 Differentially expressed genes (T-cell anergy array) in CD8$^+$ T-cells between CLL^{NR} patients and CLL^{IR} patients. qPCR was performed on the ABI Prism 7500HT Sequence Detector (Applied Biosystems) using primer sets embedded within T-cell anergy and tolerance RT^2 Profiler PCR array. For data analysis the ΔΔCt method was used and the fold change for each gene were calculated as the difference in gene expression between CLL^{IR} patents (n = 5) and CLL^{NR} (n =2). Data are represented as a scatter plot with a fold change of >2 selected as the cut off. Data analysis and representation was performed with the RT^2 Profiler PCR Array Data Analysis 3.5 (Qiagen).

5.3 Discussion

The underlying mechanisms that contribute to changes in T-cell number (Porakishvili et al. 2001; Frassanito et al. 1998), subset frequency (Nunes et al. 2012) and function (Sakuishi et al. 2010; Fourcade et al. 2010) in cancer patients have not yet been fully resolved within any specific malignancy. However, it seems likely that these perturbances could be due, in part, to factors secreted by tumour cells, cell-to-cell contact, repeated T-cell stimulation in response to tumour-specific antigen(s) or other antigen sources. Transcriptional analysis of the non-malignant T-cell compartment of cancer patients has been employed in an attempt to provide a further understanding of these observations, for example analysis of the $CD8^+$ T-cell compartment in melanoma patients highlighted an increase in the expression of genes associated with apoptosis when compared to healthy donors (Xu et al. 2004). This suggested that melanoma patients might exhibit immune dysfunction due to enhanced death of $CD8^+$ CTL.

The aim of this study was to generate preliminary data to determine whether there were differences in gene expression between CLL^{IR} and CLL^{NR} patients. Each T-cell subset ($CD4^+$ and $CD8^+$) was analysed independently in order to identify candidate genes of interest for further evaluation and investigation.

Previous transcriptional analysis of CLL patients using purified $CD3^+$ T-cells revealed an increase in the expression of numerous genes encoding for stimulatory and inhibitory co-receptors from the killer cell lectin-like receptor and NK-cell receptor families, relative to healthy donors. Additionally, the transcription of genes involved with cytotoxic effector functions such as CRTAM and perforin were also increased (Göthert et al. 2013). Gene set enrichment analysis (GSEA) of the data suggested that CLL patients exhibited enrichment in genes associated with $CD8^+$ effector T-cell function (Göthert et al. 2013). The authors, like many others (Nunes et al. 2012; Riches et al. 2013), showed that CLL patents exhibit an increased frequency of $CD8^+$ effector T-cells when compared to

controls (Göthert et al. 2013). However, they failed to perform transcriptional analysis on purified $CD8^+$ T-cells.

Other studies have also investigated the differential gene expression within the total T-cell population ($CD3^+$) from CLL patients by microarray and subsequently confirmed observations of interest by qPCR within the separate $CD4^+$ and $CD8^+$ T-cell compartments (Kiaii et al. 2013). An increased expression in chemokines such as CCL4 and CCL5 were observed Kiaii et al. 2013), which are both powerful chemoattractants for T-cells (Bystry et al. 2001; Schall et al. 1990). It has been suggested that the elevated expression of these chemokines could result in the recruitment of T-cells, which could in turn support CLL cell survival (Hacken and Burger 2014).

In a study by Gorgun *et al*, microarray analysis of the transcriptional differences within the separate $CD4^+$ and $CD8^+$ T-cell compartments, suggested that CLL patients' T-cells exhibited altered expression of genes involved in differentiation, proliferation and survival. Specifically, numerous genes involved in signalling pathways such as the Ras-dependent JNK and p38 MAPK pathways, together with PIK_3CB, which plays a key role in the transduction of stimulatory signals from the TCR/CD28, were down-regulated. Interestingly NF-κB, which plays a fundamental role in cellular activation, was also down-regulated at the level of transcription and protein expression. Overall these results suggested that the $CD4^+$ T-cells from CLL patients have defects in cellular activation (Görgün et al. 2005). Additionally, transcriptional defects in cytoskeletal formation were observed (Görgün et al. 2005), which have subsequently been shown to affect immunological synapse formation (Ramsay et al. 2008; Ramsay et al. 2012).

Analysis of the $CD8^+$ T-cell compartment indicated altered transcription of genes involved in the formation and trafficking of secretory vesicles and cytotoxicity. For example, decreased expression of VAMP2, which is involved in trafficking vesicles to the cell surface, was observed at the level of both mRNA and protein. This suggested that $CD8^+$ T-cells from CLL patents might show defects in secretory pathways involved in the

release of cytotoxic factors such as GzmB (Görgün et al. 2005). Reports of transcriptional differences remain conflicted as Gorgun *et al* initially observed no difference in GzmB expression (Görgün et al. 2005). This contrasted with subsequent studies that observed an increase in both primary human samples and the Eμ-TCL1 CLL mouse model (Gorgun et al. 2009). However, in both reports a decrease in protein expression was evident when compared to controls. This suggests that reduced CTL function may be due to defects in packaging and trafficking processes within secretory pathways rather than altered transcription *per se* (Görgün et al. 2005; Gorgun et al. 2009). However, T-cells from CLL patients have been shown to be effective at inducing the lysis of target cells in a GzmB-dependent manner, albeit in the context of forced immunological synapse following treatment with blinatumomab (Wong et al. 2013).

To determine if the differential gene and protein expression observed in T-cell from CLL patients was induced in a contact dependent manner, Gorgun *et al* went on to culture T-cells from health donors with sera from CLL patients or CLL cells. Changes in the expression of genes decreased in $CD4^+$ or $CD8^+$ T-cells derived from CLL patients, were not observed in normal T-cells in response to sera from CLL patients. However, co-culture with CLL cells induced similar changes to those observed in T-cells isolated from CLL patients. Furthermore, these changes were prevented by the blockade of adhesion molecules using anti-CD54 and anti-CD11a mAbs (Görgün et al. 2005). This indicates that cell-to-cell contact may be essential for the induction of CLL cell mediated changes within the T-cell compartment, a concept supported by others (Ramsay et al. 2008; Ramsay et al. 2012).

These examples highlight differences and potential defects within the T-cell compartment of CLL patients. However, CLL is a highly heterogeneous disease, wherein patients can be sub-divided based upon laboratory and prognostic markers (Gribben 2010). In all of the described studies to date CLL patients were analysed as a whole and compared

to healthy donors. In this study, patients were divided based upon their CD4:CD8 ratio and comparisons were made between these two patients groups.

Transcriptional analysis of the $CD4^+$ T-cells within this study highlighted the differential expression of numerous genes (T-cell activation array 61/84 genes, T-cell anergy array 50/84 genes), which were subsequently grouped and integrated utilising MetaCore Analysis Suite.

Transcriptional analysis indicated that CLL^{NR} patients exhibited a relative decrease in the expression of the transcripts of the stimulatory co-receptors CD28 and CD4. These co-receptors contribute to the amplification of TCR signalling, through the recruitment of components essential for the T-cell activation signalling cascade (Barber et al. 1989) and provide essential secondary T-cell activation, specifically through the P13K/AKT pathway (Rudd et al. 2009). Additionally, a relative decrease in the expression of the transcription factors such as AP-1 and IRF4, which facilitate T-cell activation, differentiation and inhibit apoptosis (Rincón and Flavell 1994; Brüstle et al. 2007; Honma et al. 2008; Lohoff et al. 2004), were observed within CLL^{NR} patients compared to CLL^{IR}.

Taken together, these data suggest that CLL^{NR} patients may exhibit comparative defects in processes relating to T-cell activation when compared to CLL^{IR} patients. Conversely this analysis could suggest that $CD4^+$ T-cell from CLL^{IR} patients represent a more activated T-cell populations. Thus evaluation of the expression and function of genes involved in T-cell activation and survival warrant further investigation.

CLL^{NR} patients further exhibited a relative decrease in the expression of cytokines and their associated receptors, which support T-cells, such as IL-2, IL-6 IL-2Rα and IL-7Rα chains, in comparison to CLL^{IR} patients. IL-2 plays an essential role in the proliferation and differentiation of activated T-cells, through interactions with the IL-2 receptor, composed of the constitutively expressed β and γ chains. However, addition of the inducible IL-2Rα chain results in the formation of the high affinity IL-2 receptor, making T-cells more sensitive to IL-2 signalling (Gaffen and Liu 2004). Additionally,

responses to IL-7 and IL-6 have been shown to mediate T-cell proliferation and enhance survival (Schluns et al. 2000; Lotz et al. 1988). However, others have suggested that IL-6 may inhibit T-cell proliferation and play a role in mediating the immune dysfunction associated within CLL (Buggins et al. 2007). It should be noted that in this study CLL cells were observed as the predominate source of IL-6.

Furthermore, CLL^{NR} patients further exhibited a relative decrease in the expression of cytokines such as IL-13 (Cocks et al. 1993; Chaouchi et al. 1996), IL-5 (Kouro and Takatsu 2009) and IL-6 (Tanner and Tosato 1992) as well as surface molecules such as CD40L (Schultze et al. 1997) which support B-cell proliferation, survival and differentiation. While these cytokines have been shown to support normal B-cells, published reports suggest that they have an opposing effect upon CLL cells (Aderka et al. 1993; Mainou-Fowler et al. 1994). Moreover, clinical evaluations have shown that elevated levels of serum IL-6 are associated with poor patient prognosis (Fayad et al. 2001). Overall the specific roles of IL-5, IL-6 and similar cytokines within CLL remains unclear and thus the differential expression and effects of these cytokines warrants further investigation.

Based on this gene expression data, $CD4^+$ T-cells from CLL^{NR} patients might exhibit defects in responsiveness and cytokine production, which could affect processes involved in supporting T-cell and B-cell proliferation and survival. However, due to the comparative nature of this analysis it could not be definitively determined if CLL^{NR} patients exhibit defects within these processes and thus may represent a "defective" T-cell population or whether CLL^{IR} patients exhibit relatively increased expression of these genes, suggesting that they represent a "more functional" or activated T-cell population.

$CD8^+$ T-cells represent a functionally distinct branch of the adaptive immune system and thus were analysed separately. Transcriptional analysis indicated a relative reduction in the transcription of genes encoding for the stimulatory co-receptors CD27, CD28, OX40 and CD137, which orchestrates divergent pathways that promote T-cells survival and proliferation (Rudd et al. 2009; Lee et al. 2002; Cannons et al. 2001; Croft et al.

2009; Denoeud and Moser 2011; Barber et al. 1989), within the CLL^{NR} patients relative to CLL^{IR}.

However, phenotypic analysis in this thesis, and confirmed by previously published findings (Nunes et al. 2012), showed a decrease in the surface expression of stimulatory co-receptors, such as CD27 and CD28, within CLL^{IR} patients compared to CLL^{NR} patients, in the total $CD8^+$ population and specific memory subsets (Nunes et al. 2012). These differences could be due altered translation of the CD27 and CD28 transcripts within $CD8^+$ T-cell from CLL^{IR} and CLL^{NR} patients, such as the differential expression of microRNA, which silences mRNA translation (Djuranovic et al. 2012). Therefore, further investigation into the relationship between mRNA expression, mRNA processing, protein production and protein expression could be informative.

Consistent with the down-regulation of genes encoding co-stimulatory molecules, there was also decreased expression of the genes encoding for transcription factors related to T-cell activation such as NF-κB, NFAT, T-bet and STAT-3, within the CLL^{NR} patients relative to CLL^{IR}. These transcription factors have been shown to mediate processes involved in T-cell differentiation and function (Arch and Thompson 1998; Gerondakis et al. 2014; Feau et al. 2013; Rincón and Flavell 1994; Sullivan et al. 2011; Olson and Jameson 2011).

CLL^{NR} patients further exhibited a relative decrease in the expression of GzmB, perforin and FasL, all of which are involved to cytotoxic T-cell processes, (Lieberman 2010; Ju et al. 1995; Dhein et al. 1995) as well as effector cytokines such as IFN-γ (Teixeira et al. 2005), relative to CLL^{IR}. The down-regulation of these genes suggests that $CD8^+$ T-cells from CLL^{NR} patients may exhibit defects in cytotoxic function. The expression factors associated with $CD8^+$ T-cell effector function, IFN-γ (Sica et al. 1997), GzmB (Huang et al. 2006) and FasL (Hsu et al. 1999) have been shown to be mediated by transcription factors such as NF-κB and NFAT. Therefore it could be hypothesised that decreased expression of cytotoxic and effector factors could be a related to a reduction in transcription factor

expression, due to defects in T-cell signalling. Therefore further investigation of T-cell co-receptor expression and signalling, transcription factor dynamics and the expression factors associated with $CD8^+$ cytotoxicity between these two patient groups would be beneficial to further elaborate upon these preliminary observations. In this regard, it is worth noting that a high proportion of the genes observed in this study (Appendix 10 and 11) are regulated by NF-κB (Glimore et al. 2015).

It should be noted that one of the limitations of this study, was the number of available samples that could be studied. Obtaining patient samples that exhibit a CD4:CD8 ratio of 0.5 or 2.0 proved to be challenging and initially limited the number of patient samples suitable for this study. The ratios 0.5 or 2.0 were selected to provide consistency within the patient groups and afford a large separation between the groups. Additionally, due to the overwhelming dominance of CLL cells in patient-derived peripheral blood samples, purification of $CD4^+$ and $CD8^+$ T-cells to >90% by immunomagnetic separation proved to be challenging and further limited the number of suitable of samples. Even in those samples where this was achieved, the absolute numbers of purified T-cells obtained was relatively small resulting in low RNA yields. A total of 60ng of RNA was used for the downstream qPCR analysis. This amount was selected as it was within the suitable range of RNA quantities recommended by the manufacturer (http://www.sabiosciences.com/pcrarrayperformance.php). However, it should be noted that the use of low concentrations of RNA might disproportionately affect the detection of low abundance transcripts.

To obtain a greater number of T-cells with higher purity, alternative methods of T-cell isolation could be employed in future, such as direct flow sorting. However, one of caveats associated with this process is the potential for FACS-induced activation of the T-cells due physical shear force, which could potentially influence the subsequent transcriptional profile.

Within this study transcriptional analysis was only performed on the total $CD4^+$ and $CD8^+$ T-cell populations. This approach was taken for pragmatic reasons associated

with the number of available T-cells and thus the subsequent amount of RNA. However, it is well established that both the $CD4^+$ and $CD8^+$ T-cell compartments are made up of a diverse range of subsets (Liu et al. 2013; Klebanoff et al. 2006), which exhibit differential gene expression profiles (Willinger et al. 2005). This appears to be particularly pronounced in CLL patients where there is a marked skewing towards memory subsets (Nunes et al. 2012; Riches et al. 2013). Therefore, it would be interesting to investigate if any of the changes in gene expression observed in this study occurred within specific T-cell populations. For this concept to be explored, highly sensitive analysis platforms would be required, which would be more suitable for very low concentrations of RNA, such as RNAseq (Saliba et al. 2014).

Additionally, while the target gene PCR array approach used in this study was an attractive option, to allow for the investigation of pathway-specific transcriptional differences, the approach could be seen as reductionist. By definition, the arrays pre-define the genes of interest and so prevented the evaluation of potentially novel and unexpected differences between the groups.

Because of the limitation and caveats of this study many of the initial observations presented will require further investigation and validation. Initially it would be logical to validate the differential expression of the gene list as defined in this preliminary study. This should be done using the original cDNA, using optimally designed primer sets. These primer sets could be further utilised to investigate the expression of genes in a much larger patient cohort to determine if the findings observed here are representative of the different patient groups. Investigation of changes at the protein level would also be a desirable and valuable way of continuing this work in order to determine if changes at the transcriptional level impact upon protein expression (Western blot / ICS / flow cytometry). As the genes highlighted in this discussion focused on the process of T-cell activation and effector function, the evaluation of functionally differences between the two patient groups would be a valuable progression of this study. Finally, to provide a more comprehensive

evaluation of the transcriptional differences between the two patient groups, an unbiased global gene analysis approach, such as microarray or RNAseq, could also be beneficial.

In conclusion, while several practical limitations have been highlighted in this study it still provides some preliminary data as a basis for further work (technical and biological) to evaluating transcriptional differences between CLL^{NR} and CLL^{IR} patients. Due to the large number of differentially expressed genes identified, a complete and comprehensive evaluation of all the genes and their related functions was not achievable within the timeframe of this thesis. However, pathway enrichment analysis, as well as hypothesis driven approaches (processes related to T-cell activation and function), were employed during data analysis in an effort to shortlist specific genes of interest for further investigation.

Based on the phenotypic observations from Chapter 4, it was hypothesised that T-cells from CLL^{IR} patients were representative of exhausted/highly differentiated or activated T-cell populations. These contrasting hypotheses were based upon the mechanisms and processes involved with the expression of the phenotypic markers in Chapter 4, such as T-cell activation and the historical knowledge associated with the presence and signalling through the markers, such as immune dysfunction. Therefore the observations from this transcriptional analysis potentially support the concept that T-cells from CLL^{IR} patients may be more representative of an activated T-cell population when compared to CLL^{NR}, which exhibited a greater capacity to support B-cells survival and proliferation. However, the role of the described genes in modulating T-cell behaviour in CLL requires further investigation.

5.4 Suggested further work

- Selection of candidate gene of interest from preliminary analysis for further investigation.

- Confirm transcriptional observation in initial cDNA samples using single gene qPCR.
- Validate transcriptional observation within a larger cohort of patients; CLL^{IR} (n=10) and CLL^{NR} (n=10), in addition to age-matched healthy controls.
- Determine differential protein expression of selected genes.
- Evaluate functional differences in processes involved in T-cell activation and effector functions between CLL^{IR} and CLL^{NR} patients.

Chapter 6

Final Discussion

The initial aim of Chapter 3 was to investigate the potential of peptides derived from the pro-apoptotic Bax protein to generate Bax-specific T-cells from CLL patients. Abnormally low levels of expression of the Bax protein have been observed within CLL cells, due to enhanced proteasomal degradation (Agrawal et al. 2008). Therefore, it was hypothesised that MHC-I molecules might preferentially present Bax-derived peptides to $CD8^+$ T-cells as a byproduct of the degradation process, providing a CLL-specific TAA.

The concept of a protein expressed at low levels serving as a TAA may seem counter-intuitive as many TAAs are derived from self proteins that exhibit over expression (Jäger et al. 2001). However, several studies have shown that endogenous proteins that are unstable and have increased susceptibility to protein degradation, can be recognised by $CD8^+$ T-cells (Castilleja et al. 2001; Sirianni et al. 2004). Encouragingly, this phenomenon has previously been observed with a peptide derived from Bax, but in a study in which the T-cell clones were isolated from healthy individuals not CLL patients (Nunes et al. 2011). Therefore it was not known, whether Bax-specific T-cells could be detected within CLL patients.

The use of T-cells in the treatment of CLL has gathered more attention with the recent development of CAR T-cell therapy. Polyclonal T-cell populations are genetically manipulated to redirect T-cell activity towards specific molecules expressed upon the malignant cells in a MHC-independent manner (Maus et al. 2014). Due to the lack of obvious TAAs, current experimental therapeutics have used the CART-19 construct to redirect T-cell activity towards the pan B-cell antigen CD19 (Kalos et al. 2011; Porter et al. 2011). However, this process targets healthy as well as malignant B-cells and so the identification of novel tumour-specific antigens would have considerable therapeutic

advantages. Additionally, while this has proven to be an efficacious treatment option, it has been reported that 5-10% of acute lymphoblastic leukaemia (ALL) patients treated with CART-19 (or with the CD3-CD19 Bi-specific antibody, Blinatumomab) relapse with a $CD19^-$ clone (Ruella et al 2014). If this observation holds true for the treatment of other $CD19^+$ malignancies, such as CLL, then this would further highlight the need for the discovery of novel CLL-specific TAAs.

Initial results suggested that $CD8^+$ T-cells from an HLA-$A2^+$ CLL patient recognised the Bax-derived peptides (P603 and P605). Furthermore, peptide-specific T-cells were capable of being isolated, cloned and expanded rapidly *in vitro* resulting in the maintenance of long-term peptide specificity. However, the subsequent T-cell clone identified in this study (6C5), failed to respond to HLA-$A2^+$ CLL cells *in vitro*, suggesting that either the Bax-derived peptide P603 was not expressed on the surface of CLL cells or that the peptide was expressed but T-cell recognition was of low affinity.

Further analysis of 6C5 demonstrated that it actually recognised a modified version of P603, P603 *t*Bu (LLSY(3-*t*Bu)FGTPT) rather than the Bax-derived wild type sequence (LLSYFGTPT). Since this modified peptide does not occur in nature, it was not surprising that T-cells recognising this peptide were unable to identify CLL cells. Thus the potential for the wild type P603 peptide to act as a TAA for CLL cannot be ruled out. However, without a T-cell specific for the wild type P603, the presentation of this peptide on CLL cells cannot be determined. An alternative approach to investigate the potential presence of P603 (or other Bax peptides) on the surface of CLL could be to elute the naturally occurring peptide complexes with MHC-I molecules from the CLL and interrogate their peptide sequences using mass spectrometry (Hunt et al. 1992; Cox et al. 1994).

Because P603 *t*bu is not a natural peptide it is likely that the observed specificity is due to TCR cross reactivity. A nonamer combinatorial peptide library screen was utilised to probe the entire repertoire of possible 9aa peptides to identify potential naturally occurring antigens. These results revealed that the index peptide (P603 *t*Bu) was suboptimal at 8/9

positions and suggested the potential for the TCR to cross-react with multiple naturally occurring peptide sequences.

While this method has proven to be effective at investigating the cross reactivity of other T-cell clones (Wooldridge et al. 2012), one of the limitations of this approach is that poorly binding peptides may be underrepresented, due to competition for available MHC molecules. Therefore it is unknown if the entire 9mer repertoire is truly being sampled and presented to T-cells. Furthermore, it has been shown the peptide affinity for MHC does not always correlate with immunogenicity (Khanna 2004), thus potentially highly immunogenic peptides could be out-competed and therefore not effectively sampled. Reconfiguring the assay into a high throughput screen to test each peptide individually could address this concern.

While this study failed to demonstrate the existence of Bax-specific T-cells within CLL patients, it did show that it was technically feasible to generate and expand large numbers of peptide-specific $CD8^+$ T-cell clones from limited amounts of patient material (2-3ml of whole blood). However, the approach utilised in this study would not be feasible in a clinical setting due to the protracted (3-4 month) timescale associated with the procedure. Several improvements to this protocol might be envisaged in order to identify novel CLL-specific T-cell from patients. While *in vitro* stimulation with pools of candidate peptides is advantageous, in order to investigate the potential of multiple epitopes simultaneously, subsequent T-cell cultures would require extensive processing and characterisation (limiting dilution cloning, antigen independent expansion and epitope mapping). The direct sorting and expansion of tetramer-specific T-cells could reduce the timescale of this process. Additionally, the tetramer staining protocol could be combined with the staining for other markers to identify desirable T-cell subsets, such as naïve T-cells, which have been suggested to resist terminal differentiation and maintain a high proliferative potential (Hinrichs et al. 2011).

Both approaches described above, are dependent on the existence of peptide-specific T-cells within an individual patient's T-cell repertoire. This could be overcome through the isolation and genetic modification (TCR transfer or CAR) of polyclonal populations of T-cells to express receptors for specific peptide or protein sequences. The efficacy of T-cell based therapies for the treatment of CLL (Porter et al. 2011; Kalos et al. 2011), other hematological malignancies (Grupp et al. 2013; Maude et al. 2014) and solid cancers (Rosenberg et al. 2011) has been shown in small scale clinical trials and patient case reports. However, this was cemented in 2014, with the FDA approval of the first T-cell therapy (CART-19 modified T-cells) for the treatment of relapsed or refractory ALL.

Despite this breakthrough, several obstacles could limit the efficacy of T-cell based immunotherapies for the treatment of CLL (and other malignancies), such as immune dysfunction and immunosuppression induced by tumour burden and/or tumour cell-mediated microenvironmental changes. Therefore a greater understanding of the processes and mechanisms, which could affect T-cell function to influence T-cell activation and suppression within CLL, is essential. This knowledge may identify immunological hallmarks of the disease and potential differences between patients, which would be beneficial in the development of novel immunotherapies and the stratification of the most suitable patients to receive them.

In Chapter 4 an immunophenotyping approach was employed to characterise the T-cells from CLL patients in an attempt to identify common immunological abnormalities. Within this study, CLL^{IR} patients exhibited a skewing in their T-cells towards "highly" differentiated effector memory phenotypes (EM and EMRA) and displayed an increased frequency of $CD57^{+}/CD27^{-}$ T-cells, which has been associated with limited proliferative potential and increased sensitivity to apoptosis (Dolfi et al. 2008; Brenchley et al. 2003; Focosi et al. 2010; Plunkett et al. 2007; Hendriks et al. 2000). In addition, there was a significant increase in T-cells expressing the immunosuppressive receptors $PD\text{-}1^{+}$ (Keir et al. 2008) and $TIM\text{-}3^{+}$ (Rangachari et al. 2012) within the $CD4^{+}$ T-cell compartment.

Therefore the altered phenotypes observed within the CLL^{IR} patient group could denote a T-cell pool, which exhibits defects in proliferative potential, function and survival.

Analysis of the prognostic impact of the increased frequencies of $CD8^+CD57^+$, $CD8^+CD27^-$, $CD4^+PD\text{-}1^+$ and $CD4^+CD57^+$ T-cells revealed that they were associated with shorter PFS. Thus suggesting a potential role for specific T-cell populations in the prognosis of CLL and implying that T-cell dysfunction may be a driver of disease progression or progressive disease could drive the accumulation of dysfunctional T-cells.

Accounts of T-cell dysfunction in CLL have been well documented within the field. CLL cells have been shown to negatively impact T-cell activation (Görgün et al. 2009) and proliferation (Hock et al. 2014), transcriptional profile (Görgün et al. 2005; Görgün et al. 2009), immunological synapse formation (Ramsay et al. 2008) and T-cell migration (Ramsay et al. 2013).

Defects in immunological synapse formation, induced by CLL cells, have been shown to be mediated by the interactions between immunosuppressive ligands and their corresponding receptors on T-cells (Ramsay et al. 2012). This demonstrated a mechanism by which CLL cells can actively reduce immune recognition and immune surveillance. The *in vitro* treatment of CLL cells with the immunomodulatory drug lenalidomide (Cortelezzi et al. 2012) was shown to down-regulate immunosuppressive ligand expression, alleviate tumour-induced synapse dysfunction and enhance CTL killing (Ramsay et al. 2008; Ramsay et al. 2012). *Ex vivo* analysis of CLL samples from patients treated with lenalidomide showed similar results, highlighting the clinical efficacy of the drug (Ramsay et al. 2012).

In addition to affecting the formation of the immunological synapse, the PD-1/PDL-1 pathway has been shown to impair the production of IFN-γ, IL-2 and TNF-α by T-cells in CLL xenograft murine models (McClanhan et al. 2014) (McClanhan et al. 2013). Treatment with lenalidomide (McClanhan et al. 2014) and ibrutinib (McClanhan et al. 2014) appeared to reduce PD-1 expression and enhance IFN-γ production. *In vitro* blockade of the PD-1/PDL-1 in primary CLL samples has also been shown to enhance the production

of IFN-γ (Brusa et al. 2013). Furthermore, *in vivo* blockade in the CLL TCL1 murine model (Johnson 2006), induced a significant reduction in the frequency of CLL cells, increased T-cell effector function and proliferative potential and prevented the loss of naïve $CD8^+$ T-cell and the inversion of the CD4:CD8 ratio (Hanna et al. 2014). Taken together, these data suggest that early blockade of the PD-1/PDL-1 could prevent the development of CLL associated immune dysfunction and facilitate tumour control.

However, others have shown that whilst T-cells from CLL patients may exhibit increased expression of markers associated with immunosuppression and exhaustion, they can maintain their ability to produce effector cytokines and so may actually represent pseudo-exhausted populations (Riches et al. 2013). This pseudo-exhaustion phenomenon has been observed in other haematological malignancies (Lichtenegger et al. 2013). Therefore the specific role of the PD-1/PDL-1 pathway (and other immunosuppressive pathways) in CLL requires further investigation. In addition to immunosuppressive receptors, the expression of markers associated with replicative senescence ($CD57^+$ / $KLRG1^+$ / $CD27^-$ / $CD28^-$) has been well documented within CLL (Serrano et al. 1997; (Göthert et al. 2013; Nunes et al. 2012; Porakishvili et al. 2001). Interestingly, high frequencies of $CD4^+CD57^+$ T-cells have been associated with advanced disease staging (Serrano et al. 1997). Therefore patients that exhibit high frequencies of T-cells expressing these markers could exhibit defects in immunosurveillance and ultimately more progressive disease.

Malignant cells can also induce T-cell dysfunction through cultivating a microenvironment that favours the development of immunosuppressive T-cell populations. Increased frequency and absolute numbers of T-regs, compared to healthy controls, has been reported in CLL (D'Arena et al. 2011; Giannopoulos et al. 2008; D'Arena et al. 2012). Elevated numbers of T-regs have been associated with a more advanced Rai and Binet stage classification (D'Arena et al. 2011; Giannopoulos et al. 2008), unfavorable prognostic patient groups, (Weiss et al. 2011) increased tumour burden

(D'Arena et al. 2011) and shorter TTFT (Weiss et al. 2011; D'Arena et al. 2012). Furthermore, patients that exhibited high frequencies of T-regs (≥10.5% of $CD4^+$ T-cells) also exhibited reduced responses against viral and tumour antigens (Giannopoulos et al. 2008). Therefore it could be hypothesised that the association between T-regs and the progression of CLL could be due to defects in immune surveillance. While numerous TAAs have been described in CLL (Nunes et al. 2011; Schmidt et al. 2003; Mayr et al. 2005; Mayr et al. 2006; Rajasagi et al. 2014), immunodominant epitopes have yet to be defined. Therefore the identification of a *bono fide* CLL-specific tumour antigen is essential to fully evaluate the effects of immunosuppressive pathways and cell types upon tumour-specific T-cell populations.

An alternative, and not mutually exclusive, role for the T-cell populations described in this study is that they directly support the growth of CLL cells. *In vitro* co-culture with autologous T-cells has been shown to have an anti-apoptotic effect upon CLL cells, even in the absence of cell-to-cell contact (Kiaii et al. 2013). Furthermore, the *in vitro* activation of T-cells from CLL patients has been associated with CLL cell activation and proliferation (Borge et al. 2012), which was enhanced by CXCL12. This is a chemokine that has been shown to mediate the migration of CLL cells and T-cells within CLL patients to secondary lymphoid organs (Burger et al. 1999) (Walsby et al. 2014). Therefore this chemokine may play multiple roles in the supportive relationship between T-cell and CLL cells.

The *in vivo* significance of T-cells in CLL was shown by Bagnara *et al*, who reported that autologous T-cells, specifically $CD4^+$ T-cells, play an essential role in supporting the proliferation and survival of CLL cells in murine model systems (Bagnara et al. 2011); a finding subsequently confirmed by others (Oldreive et al 2014). Moreover, proliferating CLL cells have been shown to co-localise with $CD4^+PD\text{-}1^+$ T-cells within the lymph nodes of CLL patients (Brusa et al. 2013). This suggests that CLL cell survival and proliferation may be preferentially enhanced by interaction with specific T-cell subsets.

Further evaluation of the capacity of specific T-cell subsets to influence CLL survival and potentially the development of the disease is needed. This could include investigating the differential expression and/or production of factors that could support CLL cell survival and proliferation, between the different T-cell populations. In addition, it would also be interesting to directly investigate the proliferative potential and survival of autologous CLL cells in the presence or absence of specific T-cell populations, such as those highlighted within this study.

While this study has provided a greater insight into the T-cell populations of CLL patients and highlighted multiple possibilities for further work, one of the main limitations of the work, was that only T-cells from the peripheral blood were sampled. Within the body, CLL cells have been shown to exist within three main anatomical locations (peripheral blood, lymph nodes and bone marrow), which provide different microenvironments (Zenz et al. 2010b). Comparative transcriptional analysis of CLL cells isolated from each anatomical site indicated that CLL cells from lymph nodes exhibited distinct hallmarks of BCR activation, canonical NF-κB signalling and cellular proliferation. These observations were confirmed at the protein level. Lymph node-derived CLL exhibited increased expression of phospho-SYK (BCR activation), increased phosphorylation and subsequent degradation of IκBα (canonical NF-κB signalling) and increased expression of the proliferation marker Ki67 (Herishanu et al. 2011). Similar observations have been made in xenograft murine models (Herman et al. 2013). Indicating the importance of the lymph node microenvironment for CLL cell activation and proliferation

Since activated T-cells play a pivotal role in CLL cell proliferation (Bagnara et al. 2011; Borge et al. 2012), it could be hypothesised that the lymph node may exhibit an enrichment of activated T-cells or habour distinct populations such as $CD4^{+}PD\text{-}1^{+}$ T-cells (Brusa et al. 2013), which could preferentially support CLL activation and proliferation. Conceivably this could be caused by increased homing of specific "supportive" T-cell

populations to the lymph node or microenvironment-mediated differentiation of resident T-cells in this niche. Indeed, T-cells from CLL patients have been shown to undergo more rapid proliferation within lymph nodes, when compared to the peripheral blood, in xenograft murine models (Herman et al. 2013). Therefore it would be valuable to investigate the distribution and characteristics of specific T-cell populations, such as those highlighted within this study, in different anatomical locations.

Additionally, many pharmacological therapies used in the treatment of CLL have also been shown to mediate effects on T-cell phenotype (Gassner et al. 2014) (Gassner et al. 2010) (Simone et al 2013), function (McClanhan et al. 2014) (McClanhan et al. 2013) (Gassner et al. 2010), migratory potential (Ramsay et al. 2013) and telomere dynamics (Jones et al. 2013), in multiple experimental models. The effects of these agents could have implications on T-cell associated tumour control or tumour support, and may impact upon the future use and efficacy of T-cell based immunotherapies. Therefore greater evaluation of T-cell phenotypes and function in response to treatment would be valuable.

While chapter 4 has highlighted differences in the relative frequencies of different cell populations, it cannot be definitively determined if these observations are due to population expansions, contractions or a combination of the two effects. This could be resolved by determining the absolute number of cells within the population of interest, through the use of reference beads such as Trucount™ (BD). Additionally while investigating the frequencies of cell populations expressing markers of interest is a common method utilised to interpret flow cytometry data, other approaches such as determining the level of expression through the analyses of the MFI could be employed in the analysis process.

Overall the findings from Chapter 4 suggest numerous immunological defects within the $CD4^+$ and $CD8^+$ T-cell compartments of CLL patents, which appear to be a specific feature of the CLL^{IR} patient group. Individually, increased expression of the markers, CD57, CD27 and PD-1 were associated with poorer patient prognosis. Since

these markers are enriched in the CLL^{IR}, this could explain the initial observation of a relationship between CD4:CD8 ratio and patient clinical outcome (Nunes et al. 2012). In addition, multivariate analysis highlighted the role of CD4 ($CD4^+CD27^-PD\text{-}1^+LAG3^+$) and and CD8 ($CD8^+CD27^-CD57^+PD\text{-}1^+$) T-cell subset phenotypes in influencing patient progression.

It is not yet clear whether these specific T-cell populations contribute to "immune dysfunction/poor immune surveillance" and/or supporting CLL cell growth. These observations could also have implications for selecting the appropriate patients for immunotherapy. For example CLL^{IR} patients might exhibit increased hallmarks of T-cell dysfunction, which could limit the efficacy of adoptive T-cell therapies. Additionally, this could affect the capacity of vaccines to activate T-cell effectors against CLL. Alternatively, vaccines might be very effective at expanding the "undesirable" T-cell populations and thereby drive CLL growth and disease progression.

In an attempt to further evaluate the differences between these two patient groups (CLL^{IR} and CLL^{NR}) the expression of a subset of genes involved with T-cell activation and anergy was investigated in Chapter 5. Previous transcriptional analysis of T-cells from CLL patients indicated dysregulation of genes involved in processes associated with T-cells survival, proliferative potential, intracellular signalling and effector function (Göthert et al. 2013; Kiaii et al. 2013; Görgün et al. 2005; Görgün et al. 2009). However, in each of these studies CLL patients were compared to healthy controls and differences between specific subsets of patients were not evaluated.

This analysis indicated that CLL^{NR} patients exhibited relatively lower expression of genes associated with T-cell activation and effector functions, when compared to CLL^{IR} patients in both the $CD4^+$ and $CD8^+$ T-cell compartments. This initial evaluation might suggest that T-cells from CLL^{NR} exhibit relative defects in processes involved with activation and functionality when compared to CLL^{IR}. However, because of the comparative nature of the analysis, it is conceivable that certain differences could be due to

increased gene transcription within the CLL^{IR} patient group. Comparison with healthy aged-matched controls could assist in resolving this matter.

Transcriptional analysis of the T-cell memory subsets of healthy individuals have shown that the EM and EMRA populations exhibit higher expression of genes associated with T-cell cytotoxicity such as Granzyme B, perforin and Fas ligand as well as transcription factors such as NFAT, when compared to naïve T-cells (Willinger et al. 2005). Therefore the enrichment of EMRA T-cells within the $CD8^+$ compartment of CLL^{IR} patients could explain the differential expression of genes related to cytotoxicity. Additionally, comparison between PD-1^{hi} and PD-1^{lo} T-cells from healthy individuals showed an up-regulation in co-stimulatory ligands such as CD27 and CD28, as well as molecules involved in effector functions, cell signalling and proliferation, with PD-1^{hi} T-cells (Duraiswamy et al. 2011). Therefore it could be inferred that the differential expression of genes within the $CD4^+$ T-cell compartment of CLL^{IR} and CLL^{NR} patients could, in part, be explained by differences in the distribution of PD-1^+ T-cells.

While both of these studies may suggest some mechanisms behind the transcriptional differences between CLL^{IR} and CLL^{NR} patients, they were both performed using T-cells from healthy individuals, which were not derived from individuals suffering with the high tumour burden and altered microenvironment often observed within CLL.

This analysis, while being preliminary and in need of validation, has highlighted potential differences at the transcriptional level between the CLL^{IR} and CLL^{NR} patients. The implication of these differences remains uncertain but indicate the potential for the further evaluation of the transcriptional profiles of T-cell populations with different CLL subsets.

In conclusion, three different approaches have been utilised to investigate the positive and negative roles of T-cells in CLL. Methodologies developed in Chapter 3 demonstrated the feasibility of isolating and expanding T-cell clones from CLL patients. Flow cytometry investigations in Chapter 4 highlighted numerous phenotypic differences

between CLL^{IR} and CLL^{NR} patients and the clinical relevance of specific T-cell populations. Furthermore, the preliminary transcriptional analysis in Chapter 5 emphasised further differences between CLL^{IR} and CLL^{NR} patients at the level of gene expression. Therefore, it is clear that further analysis of T-cell subset composition and function is warranted in this disease, specifically between different patient subsets.

Appendix

Appendix 1. Characteristics of the CLL patients

Factor	Subset	Number	%
Median age		72	
Range		43 - 94	
Stage	A	75	77
	B	6	6
	C	3	3
	Unknown	13	14
CD38	< 20%	35	36
	> 20%	20	21
	Unknown	42	43
LDT	< 12 months	7	7
	> 12 months	52	54
	Unknown	38	39

Appendix 2. Characteristics of the age-matched controls

Factor	Subset	Number	%
Median age		68	
Range		58 - 83	

Appendix 3. Investigating to the relationship between the CD4:CD8 ratio and CMV serostatus.

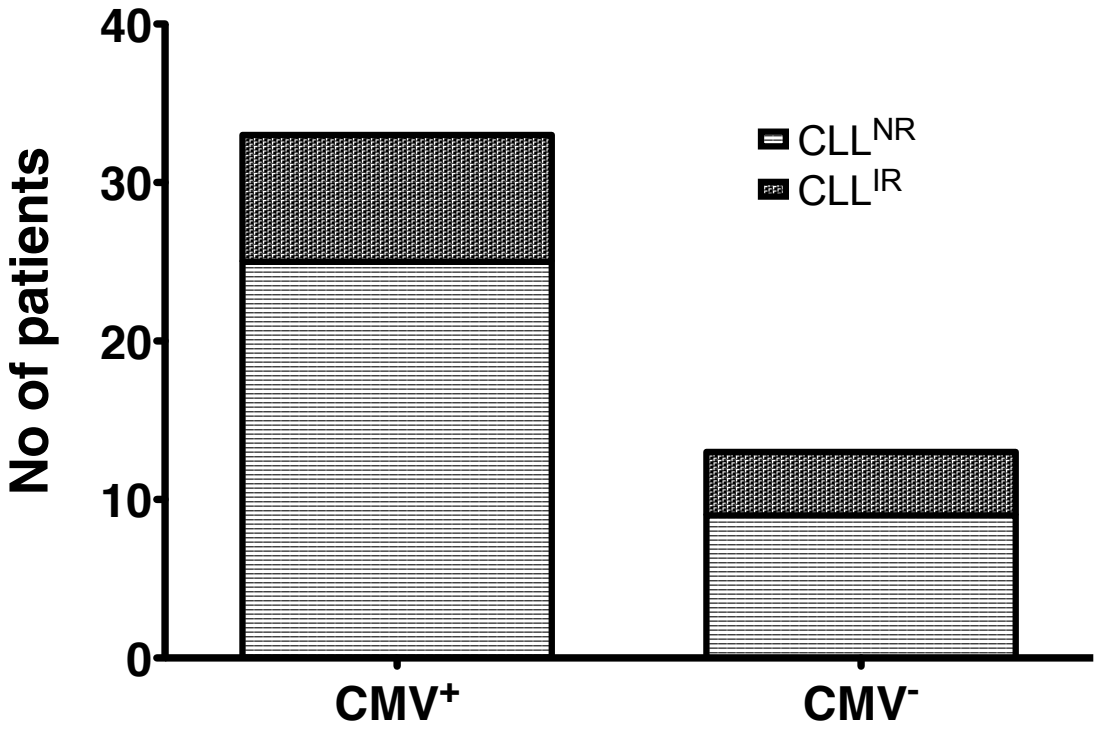

Serostatus was determined by the Public Health Wales Microbiology Lab, UHW, Cardiff.

Appendix 4. The effect of CMV serostatus on the expression of (A)CD27 and (B)CD57 within the $CD4^+$ and $CD8^+$ T-cell compartments.

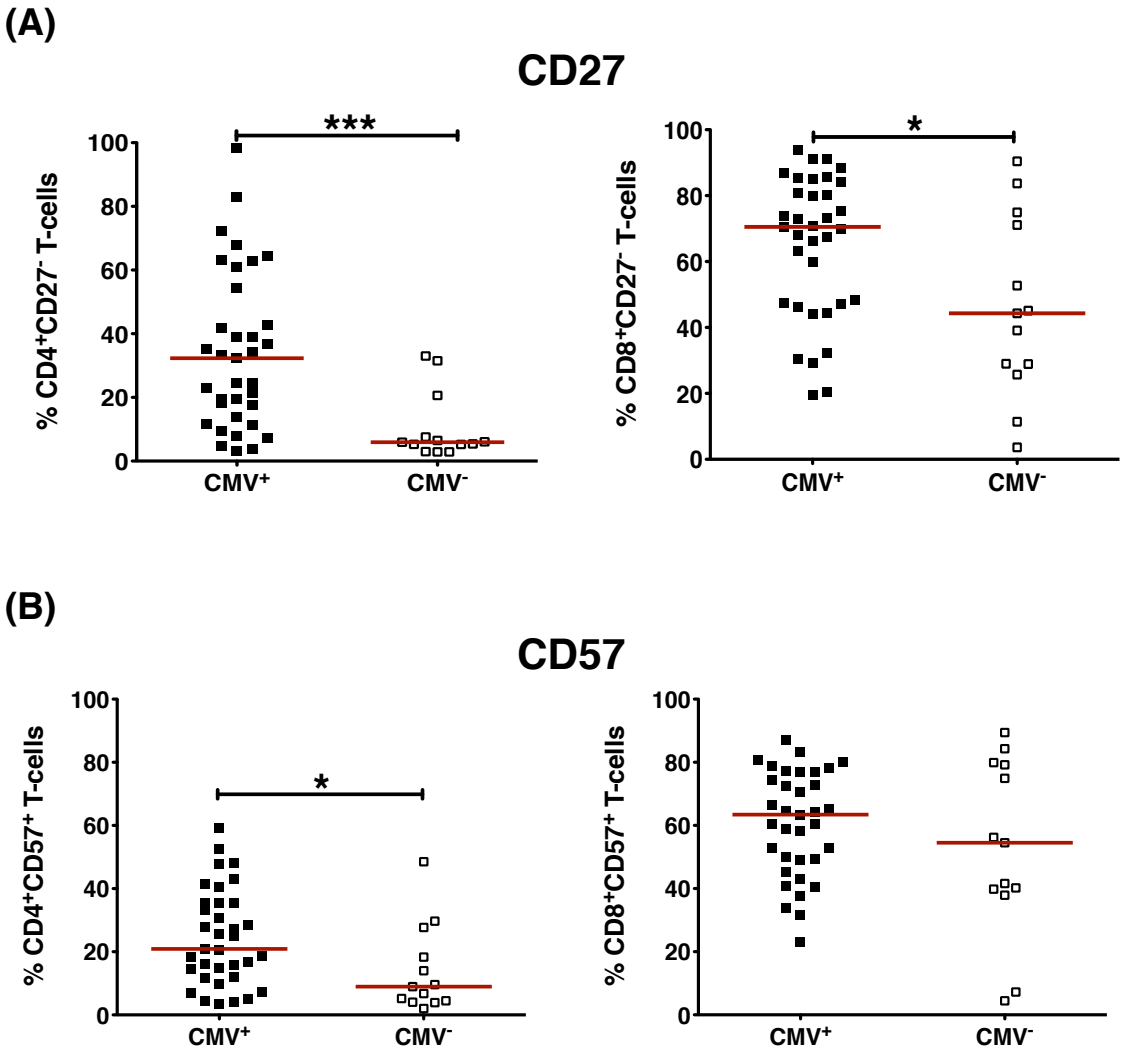

Appendix 5. The effect of CMV serostatus on the expression of (A)PD-1, (B)TIM-3 and (C)LAG-3 within the CD4⁺ and CD8⁺ T-cell compartments.

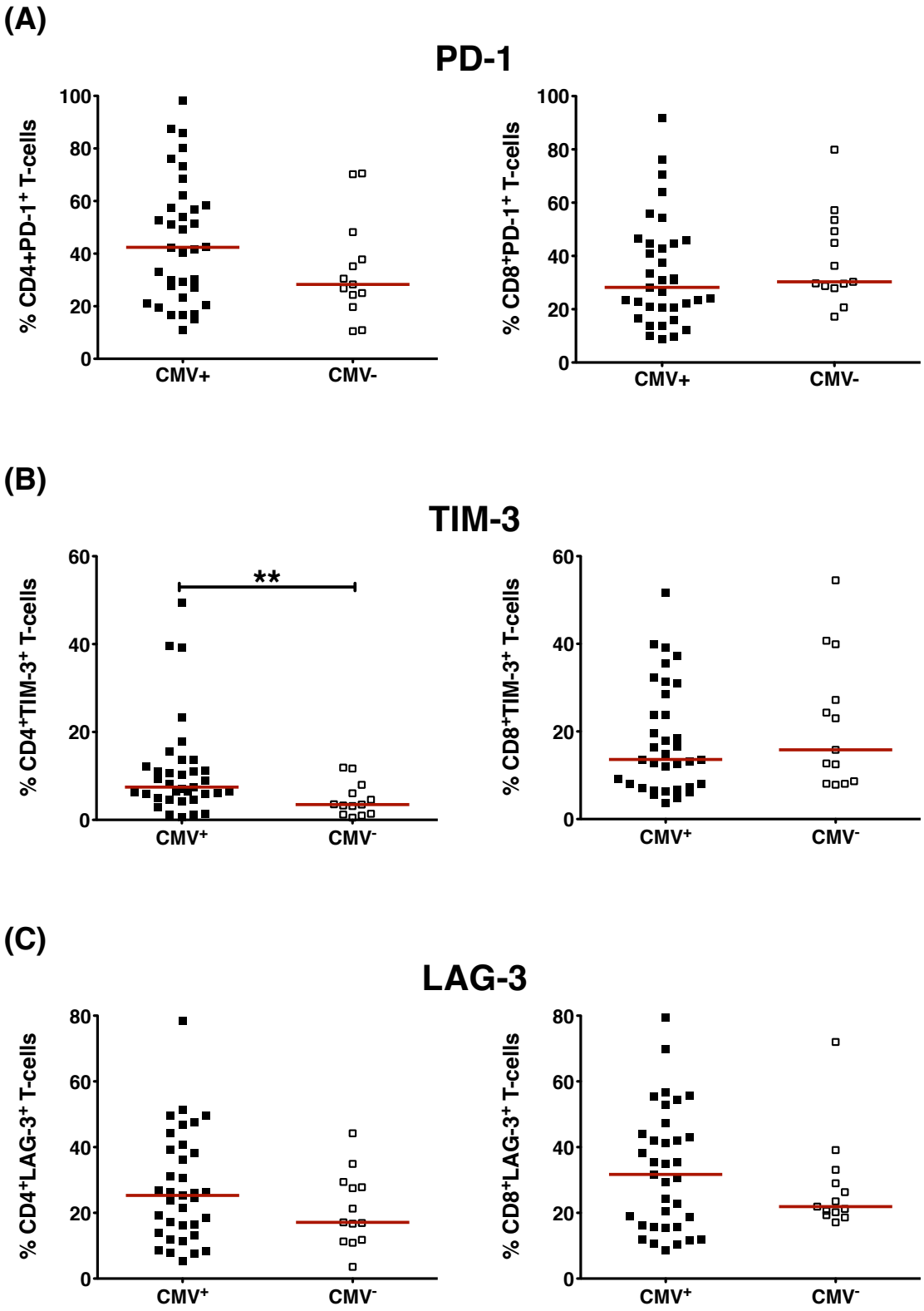

Appendix 6. CD4+ T-cell activation array housekeeping gene expression

CD4+ T-cell activation array								
Symbol	**Patient groups**						**Mean**	**STDEV**
	CLL^{NR}	CLL^{NR}	CLL^{IR}	CLL^{IR}	CLL^{IR}	CLL^{IR}		
ACTB	23.60	27.43	28.05	24.64	23.88	29.69	26.21	2.52
B2M	22.68	28.09	27.56	24.35	24.91	28.71	26.05	2.41
GAPDH	29.60	33.57	33.01	30.69	28.62	33.31	31.47	2.12
HPRT1	29.71	31.88	31.57	30.25	32.34	35.39	31.86	2.00
RPLP0	23.20	24.63	27.15	24.62	24.53	28.94	25.51	2.11

Appendix 7. CD4+ T-cell anergy array housekeeping gene expression

CD4+ T-cell anergy array								
Symbol	**Patient groups**						**Mean**	**STDEV**
	CLL^{NR}	CLL^{NR}	CLL^{IR}	CLL^{IR}	CLL^{IR}	CLL^{IR}		
ACTB	24.18	27.74	27.58	24.77	28.31	31.29	27.31	2.58
B2M	23.51	25.80	27.92	24.05	27.64	28.80	26.29	2.18
GAPDH	32.33	31.37	31.27	29.21	30.72	32.81	31.28	1.27
HPRT1	22.87	31.74	30.20	29.65	31.47	33.75	29.95	3.75
RPLP0	22.39	25.35	26.50	23.53	25.51	28.27	25.26	2.09

Appendix 8. CD8+ T-cell Activation array housekeeping gene expression

CD8+ T-cell activation array									
Symbol	**Patient groups**							**Mean**	**STDEV**
	CLL^{NR}	CLL^{NR}	CLL^{IR}	CLL^{IR}	CLL^{IR}	CLL^{IR}	CLL^{IR}		
ACTB	23.52	25.83	25.84	20.94	21.95	23.57	24.41	23.72	1.84
B2M	20.95	25.39	24.02	20.16	20.82	23.14	23.01	22.50	1.92
GAPDH	26.48	30.18	30.12	25.96	25.87	28.84	30.39	28.26	2.09
HPRT1	31.69	32.72	30.22	29.71	29.63	29.43	31.79	30.74	1.30
RPLP0	22.86	24.60	24.17	21.92	22.36	24.33	24.29	23.50	1.09

Appendix 9. CD8+ T-cell anergy array housekeeping gene expression

CD8+ T-cell anergy array									
Symbol	**Patient groups**							**Mean**	**STDEV**
	CLL^{NR}	CLL^{NR}	CLL^{IR}	CLL^{IR}	CLL^{IR}	CLL^{IR}	CLL^{IR}		
ACTB	22.74	26.17	22.73	21.79	21.63	23.94	24.65	23.38	1.64
B2M	21.18	23.78	23.67	20.81	20.58	22.58	22.24	22.12	1.31
GAPDH	27.23	29.11	26.29	25.75	24.99	28.19	27.84	27.06	1.45
HPRT1	29.58	31.23	29.60	29.20	28.01	28.08	28.50	29.17	1.12
RPLP0	21.77	24.28	23.24	22.12	22.33	23.96	24.57	23.18	1.12

Appendix 10. Genes from the T-cell activation array that exhibited a fold change of >2 within the $CD4^+$ T-cells of CLL^{NR} patients relative to CLL^{IR} patients.

Up-Down Regulation (CLL^{NR} compared to CLL^{IR})	
Symbol	Fold Regulation
IL3	-12.03
CD40	-10.41
AICDA	-8.19
CXCR3	-7.54
CCR1	-7.53
IL15	-7.07
IL5	-6.90
FASLG	-6.67
IL12B	-6.49
EGR1	-6.06
IL6	-6.01
IL18	-5.98
CCR2	-5.79
IL12A	-5.36
IL12RB1	-5.21
ICOSLG	-5.13
CX3CL1	-5.08
TLR6	-5.08
CD40LG	-4.68
CD1D	-4.44
SOCS1	-4.37
BLNK	-4.34
TLR4	-4.33
CD86	-4.28
APC	-4.13
BCL2	-4.00
CCR3	-3.96
IL1B	-3.93
MICB	-3.70
CD8A	-3.68
IRF4	-3.59
IL13	-3.53
LCK	-3.49
CD4	-3.41
IL7	-3.38
TLR1	-3.34
IL4R	-3.31
CD80	-3.30
LAG3	-3.30
VAV1	-3.28
CD7	-3.25

IL2RA	-3.21
FOXP3	-2.98
CD274	-2.74
NOS2	-2.73
DPP4	-2.70
MS4A1	-2.70
IL18R1	-2.68
BLM	-2.63
TLR9	-2.62
TNFSF14	-2.47
CD28	*-2.37*
IL10	-2.36
RIPK2	-2.35
PTPRC	-2.31
CD81	-2.28
TGFB1	-2.25
CD27	-2.20
CCL3	-2.09
CSF2	-2.06
IL2	-2.05

Appendix 11. Genes from the T-cell anergy array that exhibited a fold change of >2 within the $CD4^+$ T-cells of CLL^{NR} patients relative to CLL^{IR} patients.

Up-Down Regulation (CLL^{NR} compared to CLL^{IR})	
Symbol	**Fold Regulation**
CD70	-8.6566
CD28	-8.5031
PRKCG	-7.9809
GZMB	-7.8891
SELL	-6.6714
FOXP2	-6.1278
FOS	-5.7917
TNFRSF18	-5.7536
IL2RB	-5.4541
LEP	-5.233
TNFSF8	-5.2107
ING4	-5.1693
TNFRSF8	-4.9921
STAT3	-4.9491
PDCD1	-4.6006
IL1A	-4.5105
BTLA	-4.1722
IL17A	-4.0163
IL13	-3.924
CCR4	-3.8869
FOXP3	-3.7853
MEF2A	-3.3945

IL7R	-3.3445
HDAC9	-3.1982
EGR3	-3.1057
CD40LG	-3.0293
TNFRSF14	-3.0291
LGALS3	-3.026
CSF2	-3.0024
IRF4	-2.8674
TNFSF10	-2.845
DGKZ	-2.7963
IL6	-2.7139
DGKA	-2.6822
IL10	-2.5786
IL31	-2.5392
LTA	-2.5258
JUN	-2.5224
LAT	-2.4571
IL5	-2.4005
IL2	-2.333
CD40	-2.2783
CDK2	-2.0705
IFNG	+2.2466
FASLG	+2.2556
EOMES	+2.3681
PTGER2	+2.3687
ICOS	+2.412
ITGA1	+3.1281
IL15	+4.37

Appendix 12. Genes from the T-cell activation array that exhibited a fold change of >2 within the $CD8^+$ T-cells of CLL^{NR} patients relative to CLL^{IR} patients.

Up-Down Regulation (CLL^{NR} compared to CLL^{IR})	
Symbol	**Fold Regulation**
TLR4	-349.22
TLR6	-78.14
EGR1	-17.88
IL4	-15.93
CSF2	-13.59
IL11	-11.04
TLR9	-9.81
IL12B	-9.68
TNFSF14	-8.34
IL8	-7.96
FASLG	-7.28
RAG1	-5.93
IL6	-5.66
NOS2	-5.35

CCR5	-5.05
IL10	-5.00
IL18R1	-4.60
CD27	-4.36
IL13	-4.23
SOCS1	-4.13
MAP3K7	-4.11
CD2	-4.05
IL3	-4.01
PTPRC	-3.70
IL18	-3.68
LAG3	-3.66
CD4	-3.63
TLR1	-3.62
BLM	-3.41
IRF4	-3.33
CXCR3	-3.32
IL2	-3.23
LCK	-3.10
MICB	-3.07
VAV1	-3.03
CD40	-3.03
IL7	-2.86
CD8A	-2.82
CD81	-2.76
IL5	-2.68
CD3E	-2.67
CD274	-2.66
IL15	-2.53
TGFB1	-2.39
CCR3	-2.32
CCR4	-2.30
ICOSLG	-2.23
CD5	-2.05
TLR2	-2.04

Appendix 13. Genes from the T-cell anergy array that exhibited a fold change of >2 within the $CD8^+$ T-cells of CLL^{NR} patients relative to CLL^{IR} patients.

Up-Down Regulation (CLL^{NR} compared to CLL^{IR})	
Symbol	**Fold Regulation**
IL13	-9.04
ITGA1	-6.27
CD27	-5.41
LEP	-4.93
PRF1	-4.84

STAT6	-4.70
CD40	-4.56
CD28	-4.52
IL4	-4.48
CD70	-4.27
NFATC2	-4.24
TBX21	-4.03
ITCH	-3.95
NFKB1	-3.93
IL2RB	-3.86
IL7R	-3.80
TNFRSF10A	-3.78
NHLH2	-3.78
SELL	-3.68
BTLA	-3.65
TNFSF10	-3.65
EOMES	-3.56
DGKZ	-3.51
IL1A	-3.50
CDK4	-3.49
TNFRSF8	-3.48
IL2	-3.46
IL17A	-3.43
PDCD1	-3.34
ICAM1	-3.33
CDK2	-3.28
JAK3	-3.24
FASLG	-3.23
TNFRSF4	-3.21
FOXP2	-3.13
TNFSF8	-3.12
NOTCH1	-3.09
JAK1	-3.04
TNFRSF18	-3.04
PTGER2	-3.02
HDAC9	-3.01
IL31	-2.93
TNFRSF9	-2.89
ING4	-2.88
IRF4	-2.83
IL10	-2.75
IL10RA	-2.74
TNFRSF14	-2.72
IL15	-2.70
NFATC1	-2.65

IL6	-2.64
EGR2	-2.62
CSF2	-2.61
NFATC3	-2.60
LAT	-2.58
CD40LG	-2.57
TGFB1	-2.56
PRKCG	-2.40
IL5	-2.34
GZMB	-2.33
RNF128	-2.30
FOXP1	-2.28
TNFSF14	-2.28
DGKA	-2.25
LTA	-2.24
EGR3	-2.21
CSF1	-2.17
CTLA4	-2.17
STAT3	-2.02

Immunology
The Journal of cells, molecules, systems and technologies

British Society for immunology

IMMUNOLOGY ORIGINAL ARTICLE

CD8$^+$ T-cell recognition of a synthetic epitope formed by *t*-butyl modification

Reiss A. Reid,[1] James E. Redman,[2] Pierre Rizkallah,[3] Chris Fegan,[1] Chris Pepper[1] and Stephen Man[1]

[1]*School of Medicine, Institute of Cancer and Genetics, Cardiff University, Cardiff,* [2]*School of Chemistry, Cardiff University, Cardiff, and* [3]*School of Medicine, Institute of Infection & Immunity, Wales Heart Research Institute, Cardiff University, Cardiff, UK*

doi:10.1111/imm.12398
Received 08 September 2014; revised 30 September 2014; accepted 30 September 2014.
Correspondence: Stephen Man, School of Medicine, Institute of Cancer and Genetics, Cardiff University, Cancer and Genetics Building, Heath Park, Cardiff CF14 4XN, UK.
Email: mans@cf.ac.uk
Senior author: Stephen Man

Summary

We set out to clone Bax-specific CD8$^+$ T cells from peripheral blood samples of patients with primary chronic lymphocytic leukaemia. A number of clones were generated using a Bax peptide pool and their T-cell epitope was mapped to two peptides sharing a common 9-amino-acid sequence (LLSYFGTPT), restricted by HLA-A*0201. However, when these T-cell clones were tested against highly purified syntheses (> 95%) of the same peptide sequence, there was no functional response. Subsequent mass spectrometric analysis and HPLC fractionation suggested that the active component in the original crude peptide preparations (77% pure) was a peptide with a *tert*-butyl (*t*Bu) modification of the tyrosine residue. This was confirmed by modification of the inactive wild-type sequence to generate functionally active peptides. Computer modelling of peptide:HLA-A*0201 structures predicted that the *t*Bu modification would not affect interactions between peptide residues and the HLA binding site. However, these models did predict that the *t*Bu modification of tyrosine would result in an extension of the side chain out of the peptide-binding groove up towards the T-cell receptor. This modified product formed < 1% of the original P603 crude peptide preparation and < 0·05% of the original 23-peptide mixture used for T-cell stimulation. The data presented here, illustrate the potential for chemical modifications to change the immunogenicity of synthetic peptides, and highlight the exquisite capacity of T-cell receptors to discriminate between structurally similar peptide sequences. Furthermore, this study highlights potential pitfalls associated with the use of synthetic peptides for the monitoring and modulating of human immune responses.

Keywords: CD8$^+$ T cells; mass spectrometry; peptides.

Introduction

Synthetic peptides containing immunogenic T-cell epitopes have been widely used in various aspects of immunotherapy from adoptive cell transfer[1] to peptide vaccination.[2] This approach provides a cost effective and reliable source of antigens that can be synthesized to suitable quantities and purity grades. This process eliminates the introduction of potential virulence factors, which may occur with the use of recombinant viral vaccines. Furthermore, the nature of the chemical synthesis process allows for peptides to be modified to exacting specifications that can enhance their MHC binding capacity, their *in vivo* stability[3] and ultimately their immunogenicity.[2,4]

Historically mixtures of synthetic peptides containing multiple epitopes originating from specific proteins have been used to measure human memory T-cell responses against viruses such as human cytomegalovirus,[5] Epstein–Barr virus[6] and human papillomavirus.[7] Through the use of smaller and more refined peptide mixtures it is possible to map the precise epitope specificity of individual T-cell clones.[8] Such epitopes can then be incorporated into tetramer reagents to allow direct *ex vivo* measurement of memory T cells in response to natural infection or vaccination.[9]

In a previous study, we used pooled synthetic peptide mixtures as immunogens to generate human T cells (from healthy donors) against candidate tumour antigens

in vitro. This approach allowed us to test the concept that Bax, a pro-apoptotic protein that is abnormally degraded in human cancers, can generate T cells with activity against primary human cancer cells.[8]

In the current study, we used the same approach, but using blood from patients with chronic lymphocytic leukaemia (CLL) in an attempt to generate Bax-specific T-cell clones. We used a combined immunological (for the assessment of T-cell function and response) and physicochemical (for the identification and characterization of peptides) approach to map a human $CD8^+$ T-cell clone specificity to a novel synthetic epitope. This finding highlights the immunogenicity of chemically modified peptides and has implications for the use of synthetic peptides to generate tumour-specific T cells.

Materials and methods

Blood samples

Healthy volunteer blood samples were collected locally and CLL samples were derived from clinics at the University Hospital of Wales and Llandough Hospital. All samples were collected with informed consent with ethical approval [South East Wales Research Ethics Committee (02/4806)]. Peripheral blood mononuclear cells were isolated by Histopaque-1077 (Sigma-Aldrich, Poole, UK) centrifugation, as previously described.[10]

Induction of Bax-specific T cells

$CD8^+$ T cells were immunomagnetically enriched from peripheral blood mononuclear cells using anti-human CD8 microbeads according to the manufacturer's instructions (Miltenyi Biotec, Woking, UK). After enrichment, the T cells were cultured at 37°/5% CO_2 for 48 hr in AB-RPMI medium supplemented with interleukin-7 (IL-7; 10 ng/ml; Peprotech, London, UK) to allow for the activation of autologous CLL cells to be used as a source of antigen-presenting cells. AB-RPMI consisted of RPMI-1640 (Sigma-Aldrich) supplemented with 5% human AB serum, glutamine (2 mmol/l), streptomycin (100 μg/ml), penicillin (100 U/ml), HEPES (25 mmol/l) (all sourced from Life Technologies, Paisley, UK). After 48 hr the T cells were harvested, washed and cultured in the presence of irradiated activated autologous CLL cells at a 4 : 1 ratio in AB-RPMI supplemented with Bax peptide pool (10 μg/ml; Mimotopes, Clayton, Victoria, Australia)[8] and IL-2 (40 U/ml; Proleukin, Novartis, Frimley, UK). After 3 days, 500 μl of AB-RPMI supplemented with IL-2 (120 U/ml) and IL-7 (30 ng/ml) was added. The cultures were re-stimulated weekly with the peptide pool and autologous activated CLL cells. On day 35 the T cells were harvested and Bax peptide immunogenicity was tested by ELISpot assay.

Isolation and cloning of peptide-specific T cells

Peptide specific interferon-γ (IFN-γ) production was induced after culturing the polyclonal T cells with the Bax peptide pool (10 μg/ml) presented on autologous activated CLL cells for 5 hr at 37°/5% CO_2. Interferon-γ secreting T cells were immunomagnetically enriched using anti-human IFN-γ beads according to the manufacturer's protocol (Miltenyi Biotec). The isolated T cells were 'rested' overnight in AB-RPMI supplemented in IL-2 (40 U/ml) and IL-7 (10 ng/ml) before cloning by limiting dilution as previously described.[8]

Measurement of IFN-γ release

For IFN-γ ELISA, T cells (1×10^5) were cultured in 200 μl of AB-RPMI at a 1 : 1 ratio with peptide-pulsed T2 cells for 18 hr in U-bottomed tissue culture plates. T cells were also cultured with unpulsed T2 cells (negative control) or mitogen (positive control – phytohaemagglutinin, 10 μg/ml, P1585 – Sigma Aldrich). Cell-free supernatants were harvested and analysed by ELISA for human IFN-γ (Human IFN-γ ELISA^{PRO} kit; Mabtech, Nacka Strand, Sweden).

Interferon-γ ELISpots were performed as previously described.[7] Briefly, T cells were plated in triplicate at 1×10^5 (initial screen) or 1×10^4 to 3×10^4 cells (clones/lines) per well in MultiScreen HTS IP Filter Plates (Millipore, Watford, UK). T cells were cultured at 1 : 1 ratio with T2 cells ± Bax peptides (10 μg/ml). T cells were also incubated in the absence of T2 cells (negative control) or with mitogen (positive control). The plates were developed using the AP Conjugate substrate kit (BioRad, Hemel Hempstead, UK). The numbers of spots/well were counted with an ELISpot reader (AID, Oxford Biosystems Cadama, Wheatley, Oxfordshire, UK). Specific peptide responses were calculated by subtracting the background response (T cells + T2) from the T cells + T2 + peptide wells.

For IFN-γ ELISA intracellular cytokine staining, T cells (1×10^5) were cultured in AB-RPMI at 1 : 1 ratio with T2 cells ± peptide in the presence of GolgiStop™ and GolgiPlug™ (BD, Oxford, UK). T cells were also cultured in the presence of mitogen (positive control). After 5 hr the cells were washed and co-stained with anti-human CD3-FITC (Biolegend, London, UK – clone UCHT1) and CD8-peridinin chlorophyll protein (Biolegend – clone HIT8a). The cells were then fixed and permeabilized with Leucoperm™ (AbD Serotec, Kidlington, UK) and intracellular IFN-γ was identified using anti-human IFN-γ-phycoerythrin (eBioscience, Hatfield, UK – clone 4S.B3). The cells were analysed using an Accuri C6 (BD) and data analysis was performed using CFLOW software (BD).

CD107α surface staining

T cells (1×10^5) were cultured in AB-RPMI at 1 : 1 ratio with T2 cells ± peptide in the presence of GolgiStop™ and GolgiPlug™ (BD). T cells were also cultured in the presence of mitogen (positive control). Changes in the surface expression of CD107α were determined through the addition of anti-human CD107α-phycoerthrin (Biolegend – clone H4A3) to each culture. After 5 hr the cells were washed and co-stained with anti-human CD3-FITC (Biolegend – clone UCHT1) and CD8-peridinin chlorophyll protein (Biolegend – clone HIT8a). The cells were analysed using an Accuri C6 (BD) and data analysis was performed using CFLOW software (BD).

Peptides

Twenty-three candidate peptides were identified from the amino acid sequence of Bax using predictive computer algorithms for HLA binding, as previously described.[8] Aliquots from these stock peptides were pooled (Bax pool 601–23) and stored at −80°. Smaller pools of five or six peptides were made for epitope mapping. Highly purified (> 95%) Bax P603 peptides were synthesized (ProImmune, Oxford, UK and Peptide Synthetics, Bishops Waltham, UK). Highly purified (> 98%) Bax P603 *t*Bu peptide was synthesized using *t*-butyl-modified tyrosine (PolyPeptide Group, Strasbourg, France).

Peptide analysis

Liquid chromatography mass spectrometry (LCMS) was performed on an Ultimate 3000 (Dionex, Sunnyvale, CA) HPLC system interfaced to an amaZon SL ion trap spectrometer (Bruker, Billerica, MA). Chromatographic separation was performed with a 100 × 2·1 mm Ace Excel 2 column at a flow rate of 0·5 ml/min, eluting with a binary gradient of acetonitrile/water (0·1% formic acid). The column was equilibrated for 5 min with 5% acetonitrile, followed by a linear gradient to 95% acetonitrile over 20 min. MS^2 spectra were collected using collision-induced dissociation with automatic or manual precursor selection. Specific single amino acid deletion peptides were identified using multiple reaction monitoring of each of the corresponding $[M + H]^+$ precursor ions.

Peptide library synthesis

Peptides were synthesized manually on Rink Amide methylbenzhydryl amine resin (Novabiochem, Watford, UK) using standard fluorenylmethyloxycarbonyl (Fmoc) protocols, as previously described.[11] To prepare the libraries, the resin was split into three 50 mg portions (1–3) and single amino acid deletions were introduced into the C-terminal residues (GTPT, portion 2) and the N-terminal residues (LSYF, portion 3). After coupling of the sequence LLSYFGTPT (portion 1), a 20 mg peptide-resin sample was withdrawn and subjected to a further deprotection-coupling cycle with FmocLeu-OH to obtain LLLSYFGTPT (portion 4).

Fractionation of peptide

Fractionation of LLSYFGTPT-NH_2 (portion 1) was performed by HPLC (Waters 2525 pump and 2996 detector; Waters Corporation, Milford, MA) with a Vydac 218TP 250 × 22 mm column. Peptides were eluted with a binary gradient of 0 min 95% A/5% B, 1 min 95% A/5% B, 16 min 50% A/50% B where solvent A = H_2O, 0·05% trifluoroacetic acid (TFA) and solvent B = acetonitrile, 0·05% TFA at a flow rate of 22·9 ml/min. The principal peak eluted at 11·5 min, with further peaks collected at 9·1, 9·4, 10·0, 10·4, 13·9, 14·4 and 15·3 min.

Modification of wild-type P603 peptide

An aliquot of P603 (Peptide Synthetics, 95% Pure) in DMSO was added to diethyl ether and shaken vigorously to precipitate the peptide. Subsequently the precipitated peptide was recovered by centrifugation, washed with diethyl ether and dried *in vacuo*. The peptide was treated under different conditions to introduce *t*Bu groups into the wild-type (wt) peptide sequence.

Briefly, P603 peptide was added to a solution of di-*tert*-butyl dicarbonate (12 mg) in $CHCl_3$. The $CHCl_3$ was evaporated by a stream of N_2, then TFA (1 ml), triisopropylsilane (25 μl) and water (25 μl) were added. After 1 hr, the solution was concentrated by N_2 blowing to approximately 50% of its original volume, then pipetted into diethyl ether (14 ml). Precipitate was collected by centrifugation, washed twice with diethyl ether and allowed to dry in air.

P603 was also dissolved in TFA (1 ml) and methylpropene (Sigma-Aldrich) was bubbled through the solution for 15 min. The solution was blown with a stream of N_2 to evaporate volatile material and extracted with water (14 ml). The aqueous extract was concentrated by rotary evaporation then lyophilized.

MHC:peptide model preparation

The starting model was based on entry 4I4W[12] from the Protein Data Bank (http://www.rcsb.org). COOT[13] was used to modify the sequence of the peptide to be LLSYFGTPT. The conformation of the peptide was restricted to be as close as possible to that in 4I4W. For the purpose of the present work, this model was referred to as 'wild type', or wt. Y4 of the peptide was modified by adding a *t*Bu group at the meta position of the aromatic ring of the tyrosine side-chain. As this ring can rotate between two positions around the χ^2 dihedral, two

possible conformations need to be considered (Fig. 6). The geometry of the Tyr(3-*t*Bu) was regularized by applying the geometry restraints generated with JLIGAND.[14] PYMOL was used to generate the graphical representations in Fig. 7.

Results

Detection and isolation of Bax peptide-specific T cells

Our original aim was to isolate from patients with CLL $CD8^+$ T-cell clones specific for peptides derived from the pro-apoptotic protein, Bax. Subsequently a Bax peptide pool (P601–623) was used to stimulate $CD8^+$ T cells isolated from HLA-A*0201^+ patients and Bax immunogenicity was assessed by IFN-γ ELISpot. After 5 weeks of peptide stimulation a highly significant ($P = 0{\cdot}0008$) Bax-specific response was observed from patient R6A8R89 (Fig. 1a).

Bax-specific $CD8^+$ T cells were immunomagnetically enriched on the basis of IFN-γ secretion and cloned by limiting dilution. Six lines (6C2, 6E2, 6C5, 8C9, 7F7 and 9D7) exhibited positive Bax responses (> 20 spots/3×10^4) and were selected for further characterization (Fig. 1b). The putative T-cell clones were first tested against the full peptide pool to reaffirm Bax specificity; then against four smaller sub pools (Bax P601–606, Bax P607–612, Bax P613–618 and Bax P619–623) to narrow down the response, followed by individual peptides for

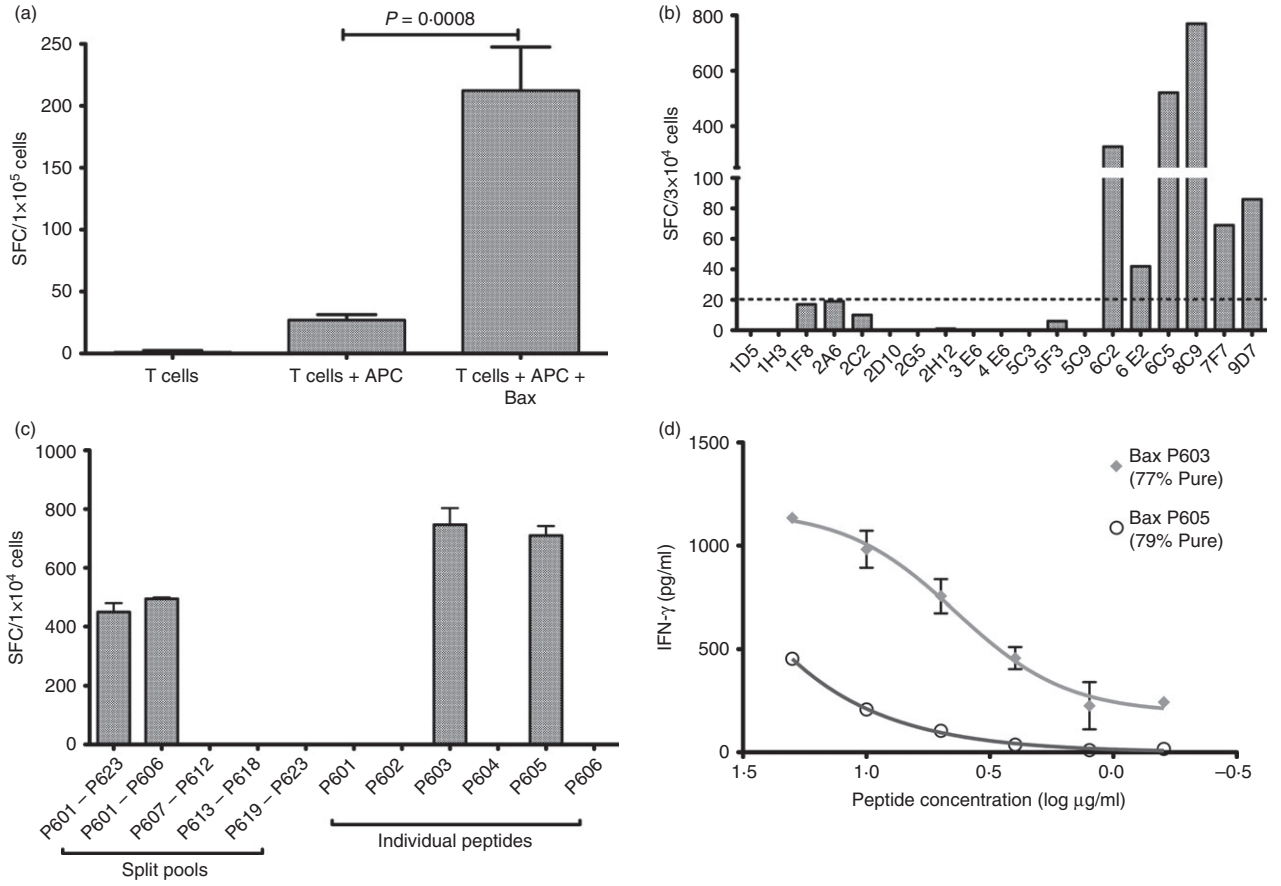

Figure 1. T-cell responses against Bax peptides and mapping the specificity of the $CD8^+$ T-cell clone 6C5. (a) Purified $CD8^+$ T cells were cultured with irradiated autologous activated B-CLL cells and Bax peptides 601–23 for 5 weeks before testing by interferon-γ (IFN-γ) ELISpot. Antigen-presenting cells (APC) were autologous activation B-CLL cells. Numbers shown are spots/10^5 T cells (mean of triplicates ± SD, $n = 1$) Statistical analysis (unpaired two-tailed *t*-test) was carried out using GraphPad Prism (GraphPad Software, Inc., La Jolla, CA). (b) T-cell cultures generated by limited dilution were tested for the recognition of Bax peptides 601–23 by IFN-γ ELISpot. T cells were plated (~2×10^4 to 3×10^4/well) with APC or with APC + peptides at a 1 : 1 ratio. APC were T2 cells. Background responses (T cells + T2) were subtracted from the data ($n = 1$). (c) 6C5 was tested by IFN-γ ELISpot against the Bax peptide pool 601–23, split pools, and individual peptides. T cells were plated (1×10^4/well) in triplicate with T2 or T2 + peptides at a 1 : 1 ratio. Background response (T cells + T2) was subtracted from the data (5 SFC/10^4 cells) (mean ± SD of triplicates, $n = 2$). (d) 6C5 was assayed against T2 cells pulsed with varying concentrations (20–6·25 μg/ml) of Bax P603 and Bax P605 at 1 : 1 ratio for 18 hr. Cell-free supernatants were harvested and tested for the presence of IFN-γ by ELISA. The EC_{50} value was calculated using the fitted curve, P603 – 4·92 μM and P605 > 100 μM (mean ± SD of duplicates, $n = 3$).

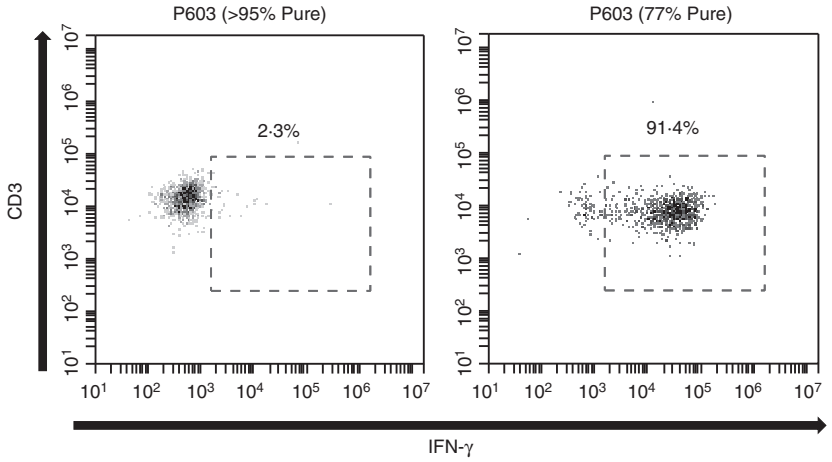

Figure 2. 6C5 recognition of crude P603 but not highly purified P603. Representative sample of flow cytometry analysis (three independent experiments) of intracellular staining of interferon-γ (IFN-γ). T cells (1×10^5/tube) were cultured in the presence of T2 or T2 + Bax peptide P603 (> 95% Pure, 10 μg/ml) or P603 (77% Pure, 10 μg/ml) at a 1 : 1 ratio for 5 hr. Lymphocytes were gated based on their forward and side scatter profile and then doublet exclusion was performed based on forward scatter height versus forward scatter width. T cells were then gated on $CD3^+$ $CD8^+$ cells and IFN-γ production was assessed through intracellular staining with anti-IFN-γ (mean ± SD of duplicates, $n = 3$). Statistical analysis (unpaired two-tailed *t*-test) was carried out using GraphPad Prism.

epitope identification (Fig. 1c). T-cell clones 6C5 and 8C9 both exhibited positive responses against the full Bax peptide pool and the sub-pool Bax P601–606. Of the peptides within the Bax P601–606 pool, only P603 and P605 induced an ELISpot response (Fig. 1c). Interestingly, these two peptides shared an overlapping nine amino acid sequence: Bax P603 is a 9mer ($Bax_{161–169}$; LLSYFGTPT) and Bax P605 is a 10mer ($Bax_{160–169}$; GLLSYFGTPT). T-cell receptor (TCR) Vβ chain staining was performed and indicated the presence of a single Vβ chain (Vβ 13.1) in both lines, indicating clonality (data not shown). Of the two clones identified, 6C5 was selected for further characterization because of its superior growth kinetics.

Peptide dose–response experiments confirmed that 6C5 recognized both peptides (P603 and P605) but had a greater avidity for P603 as determined by comparison of the EC_{50} values, P603 = 4·92 μM and P605 > 100 μM (Fig. 1d).

6C5 recognized crude but not highly purified P603 peptide

The initial results suggested that the T-cell clone 6C5 recognized the nine amino acid sequence (LLSYFGTPT) common to P603 and P605 (Fig. 1c,d). As neither peptide preparation was 100% pure it was possible that the activation of 6C5 was associated with other peptide

Table 1. Comparison of purified and crude P603 peptide samples by liquid chromatography mass spectrometry

Peptide	r.t. (min)	Transition	Crude P603	Purified P603
LLSYGTPT	5·5	851·5 → 617·3 (b_6-H_2O)	✓	✓
LSYFGTPT	6·3	885·4 → 651·3 (b_6-H_2O)	✓	✓
LLSFGTPT	6·8	835·5 → 601·3 (b_6-H_2O)	✓	✓
LLSYFGTT	7·0	901·5 → 764·4 (b_7-H_2O)	✓	✓
LLSYFGTPT	7·1	998·5 → 764·4 (b_7-H_2O)	✓	✓
LLSYFTPT	7·1	941·5 → 707·4 (b_6-H_2O)	✗	✓
LLSYFGTP	7·2	897·5 → 764·4 (b_7-H_2O)	✓	✗
LLYFGTPT	7·4	911·5 → 677·4 (b_6-H_2O)	✓	✓
LLLSYFGTPT	8·0	1111·6 → 877·5 (b_8-H_2O)	✓	✗
LLSY(3-*t*Bu)FGTPT	9·3	1054·6 → 820·5 (b_7-H_2O)	✓	✗

Chromatography was performed on an Ace Excel 2 100 × 2·1 mm column (C18), eluting with a linear gradient of 5–95% acetonitrile (0·1% formic acid) at 0·5 ml/min over 20 min. MS/MS spectra were measured on a Bruker amaZon SL ion trap spectrometer. The sequence and retention times of each of the peptides identified are indicated. The presence (✓) or absence (✗) of the peptides in each sample was assessed using extracted ion chromatograms for the indicated transition.

species (8mers, 10mers and modified 9mers). Therefore 6C5 was tested against highly purified P603 peptides (> 95% pure) obtained from two independent commercial sources (Proimmune and Peptide Synthetics). 6C5 failed to respond to the purified forms of P603 (95% pure), however the original P603 preparation (77% pure) induced a robust and highly significant ($P < 0{\cdot}0001$) IFN-γ response (Fig. 2). These results suggested that the immunogenicity associated with the original P603 (77% pure) was not a result of the peptide sequence (LLSYFGTPT).

Comparison of crude and highly purified P603

Samples of crude and purified P603 peptide were analysed by ion trap LCMS (see Supporting information, Fig. S1). The samples were investigated for the presence of 8mers, 10mers and modified 9mers (Table 1). Peaks corresponding to ΔF, ΔL, ΔY, ΔP, ΔT, ΔS 8mer peptides were observed in both the crude and purified samples. Fragmentation spectra of an ion of *m/z* 1111·6 and the corresponding doubly charged ion were consistent with a peptide carrying an additional N-terminal leucine residue,

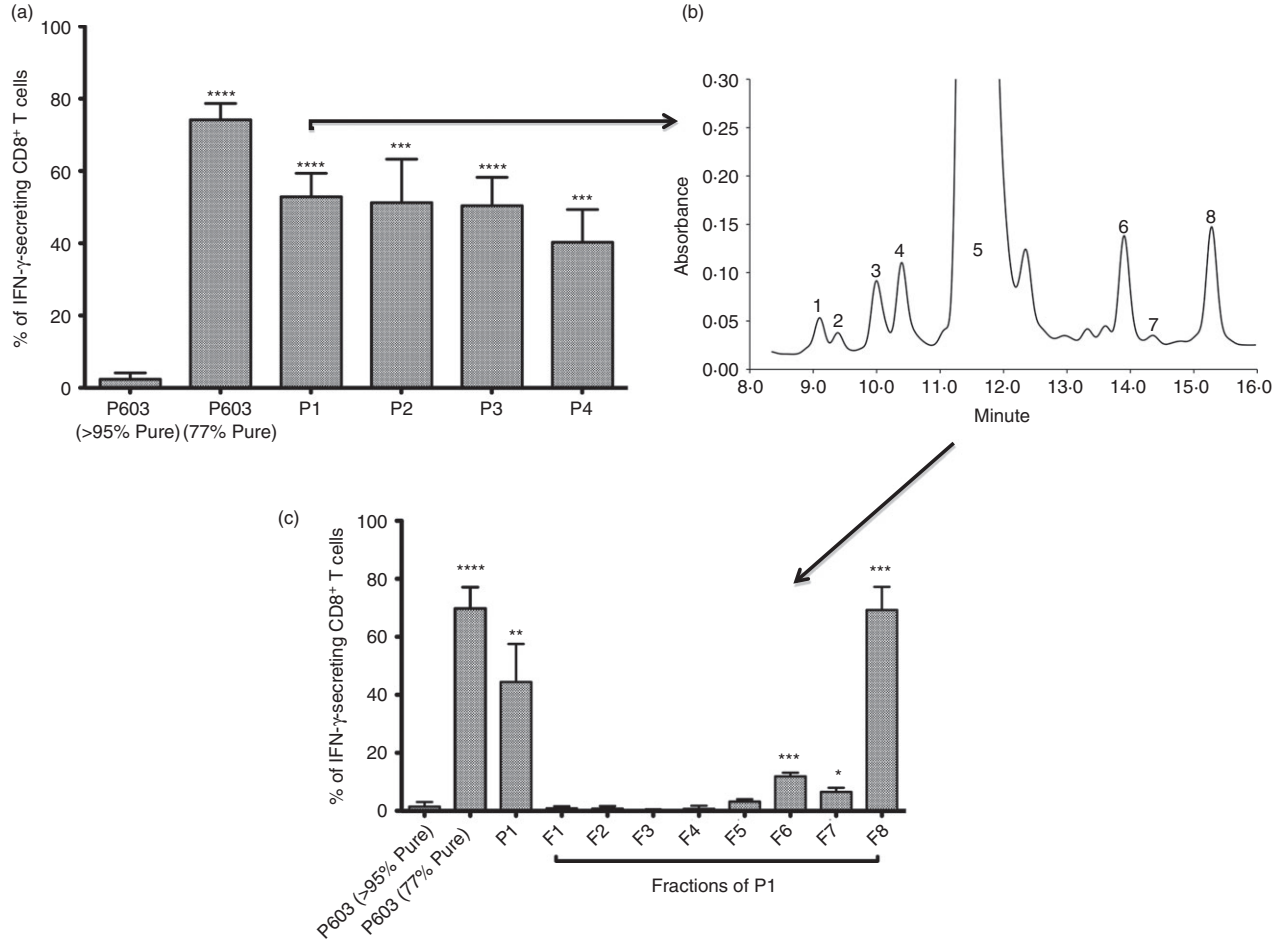

Figure 3. 6C5 recognizes a peptide present in fraction 8. (a) $CD8^+$ T-cell clone 6C5 was cultured in the presences of various peptide preparations representative of potential C-terminal (GTPT) and N-terminal (LSYF) deletions, as well as C-terminal additions. T cells (1×10^5/tube) were cultured in the presence of T2 or T2 + peptides at a 1 : 1 ratio for 5 hr. Interferon-γ (IFN-γ) production was assessed through intracellular staining with anti-IFN-γ. To facilitate gating, the cultures were also co-stained with anti-CD3 and anti-CD8. Background (T-cells + T2) were subtracted from the data (mean ± SD, $n = 3$). (b) Fractionation was performed by HPLC (Waters 2525 pump and 2996 detector) with a Vydac 218TP 250 × 22 mm column. Peptides were eluted with a binary gradient of 0 min 95% A, 1 min 95% A, 16 min 50% A where solvent A = H_2O, 0·05% trifluoroacetic acid (TFA) and solvent B = acetonitrile, 0·05% TFA at a flow rate of 22·9 ml/min. The chromatogram shows the absorbance at 220 nm. (c) $CD8^+$ T-cell clone 6C5 was cultured in the presence of fractions (F1–F8) generated from the fractionation of the P1 peptide preparation (crude full length 9mer, LLYSFGTPT). T cells (1×10^5/tube) were cultured in the presence of T2 or T2 + peptides at a 1 : 1 ratio for 5 hr. Lymphocytes were gated based on their forward and side scatter profile and then doublet exclusion was performed based on forward scatter height versus forward scatter width. T cells were then gated on $CD3^+$ $CD8^+$ cells and IFN-γ production was assessed through intracellular staining with anti-IFN-γ. Background (T-cells + T2) was subtracted from the data (mean ± SD, $n = 3$). Statistical analysis (unpaired two-tailed *t*-test, in comparison to P603 > 95% Pure) was carried out using GraphPad Prism. Significance is indicated by ****< 0·0001, ***0·0001–0·001, **0·001–0·01 and *0·01–0·05.

LLLSYFGTPT. An ion of *m/z* 1054·6 was assigned as a reaction product of the tyrosine side chain with tertiary butyl cations liberated during the final deprotection and cleavage of the peptide.

Identification of the immunogenic component of crude P603

Based on the earlier observations, the activity of 8mer and 10mer peptides was investigated by deliberate synthesis of a small library of crude peptides. The library consisted of four peptide preparations: (i) full length 9mer (LLYSFGTPT); (ii) enhanced deletions of the *C*-terminal residues (G/T/P/T); (iii) enhanced deletions of the *N*-terminal residues (L/S/Y/F); (iv) 10mer (LLLSYFGTPT, additional *N*-terminal leucine). All four peptide preparations induced similar levels of IFN-γ secretion, suggesting that neither a deletion peptide nor the 10mer in isolation were responsible for 6C5 activation (Fig. 3a). These results suggested a peptide entity common to all four preparations and the original crude P603 synthesis.

The portion 1 preparation (crude full-length 9mer, LLYSFGTPT) was fractionated by reverse phase HPLC, with fraction collection guided by UV absorbance (Fig. 3b). Individual fractions were collected, lyophilized and assayed to determine their capacity to induce T-cell activation. Activity was shown to be associated with a fraction eluting at longer retention time than the principal component (LLSYFGTPT) of the crude peptide preparation (Fig. 3c). LCMS analysis of the active fraction revealed a peptide with *m/z* 1053·6 that exhibited an essentially identical fragmentation pattern to the species pro-

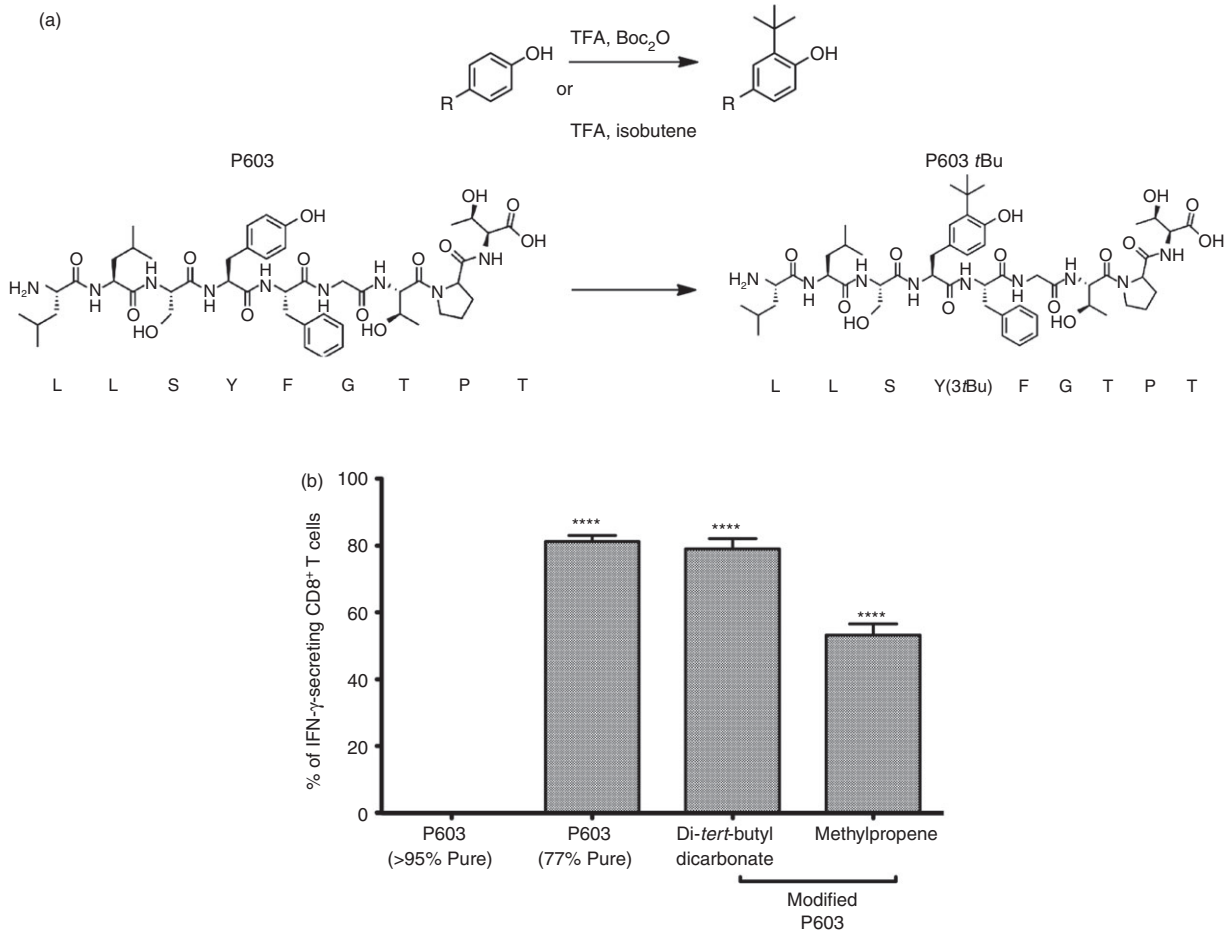

Figure 4. Butylation of the tyrosine residue of p603 confers peptide reactivity. (a) Structure of modified peptide containing the alkylated residue Tyr(3-*t*Bu). Unmodified P603 (> 95% Pure) was reacted with methylpropene and trifluoroacetic acid (TFA), or Boc_2O and TFA to induce *t*Bu groups on the tyrosine residue. (b) T cells (1×10^5/tube) were cultured in the presence of T2 or T2 + P603 (> 95% Pure, 10 μg/ml), P603 (77% Pure, 10 μg/ml) or the two P603 modified peptides (di-*tert*-butyl dicarbonate and methylpropene) at a 1 : 1 ratio for 5 hr. Lymphocytes were gated based on their forward and side scatter profile and then doublet exclusion was performed based on forward scatter height versus forward scatter width. T cells were then gated on $CD3^+$ $CD8^+$ cells and IFN-γ production was assessed through intracellular staining with anti-IFN-γ. Background (T-cells + T2) were subtracted from the data (mean ± SD, $n = 3$). Statistical analysis (unpaired two-tailed *t*-test, in comparison to P603 > 95% Pure) was carried out using GRAPHPAD PRISM. Significance was indicated by ****< 0·0001.

posed to contain Tyr(3-*t*Bu), that was identified in the crude P603 (see Supporting information, Fig. S1). The difference in *m/z* between the two species can be accounted for by the differences in C-termini of the peptides, amide versus acid, which arises due to the chemistry of the Rink resin used for preparation of the peptide library.

Modification of P603

To investigate whether a peptide species containing Tyr (3-*t*Bu) was responsible for the observed T-cell activation, the inactive wt P603 (95% pure) preparation was subjected to conditions intended to generate *t*Bu cations. It was predicted that this treatment would re-introduce the alkylated side products and confer activity to a previously inactive wt sequence. Two peptide samples were treated under different conditions, methylpropene with TFA and di-*tert*-butyl dicarbonate with TFA, to mimic the final step of peptide synthesis (Fig. 4a). Analysis of the reaction products by HPLC and LCMS demonstrated the introduction of peptides carrying the Tyr(3-*t*Bu). This was visible in both samples, and displayed the same retention time and MS^2 spectrum as the species observed in the crude P603 (see Supporting information, Fig. S2).

Both of the Tyr(3-*t*Bu) modified preparations were able to induce IFN-γ secretion; strongly suggesting that a Tyr (3-*t*Bu) modified peptide was responsible for the activity (Fig. 4b).

P603 Tyr(3-*t*Bu) stimulates the activation of 6C5

To confirm P603 Tyr(3-*t*Bu) was responsible for the activation of 6C5, a highly purified (> 98%) peptide preparation was obtained from a commercial supplier

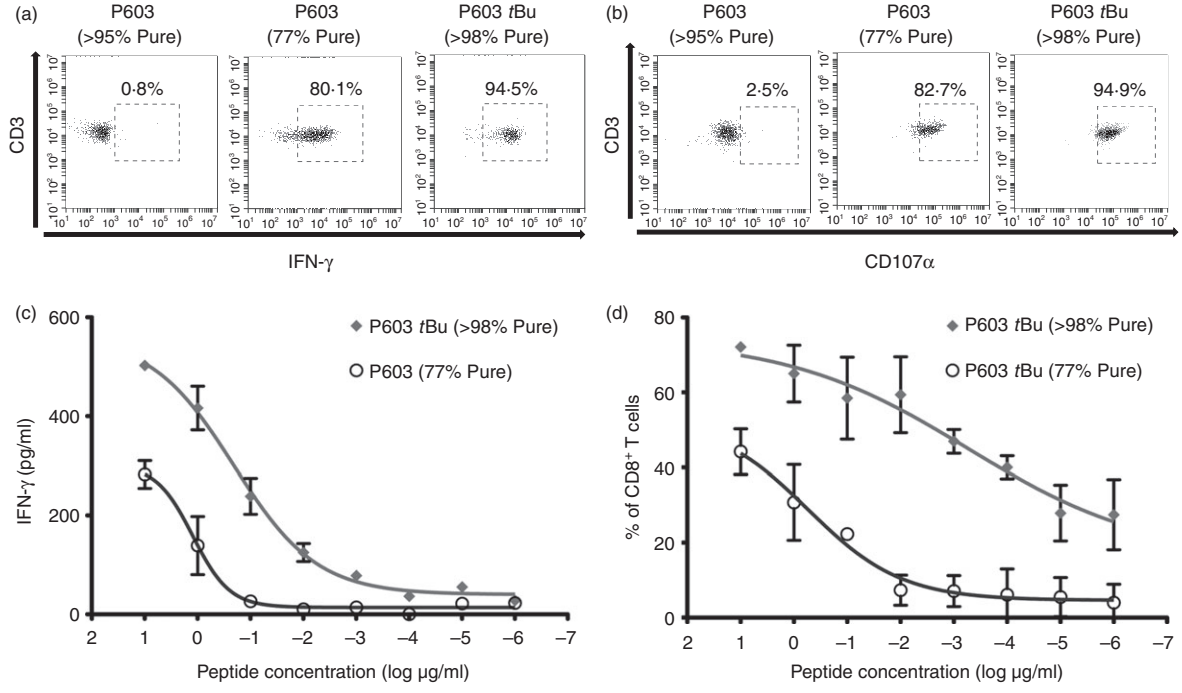

Figure 5. Activation of 6C5 is induced by *t*Bu P603. (a) and (b) Representative sample of flow cytometry analysis (three independent experiments) of intracellular staining of interferon-γ (IFN-γ) and surface staining of CD107α, respectively. T cells (1×10^5/tube) were cultured in the presence of T2 or T2 + P603 (> 95% Pure, 10 μg/ml), P603 (77% Pure, 10 μg/ml) or P603 *t*Bu (> 98% Pure, 10 μg/ml) at a 1 : 1 ratio for 5 hr. IFN-γ production was assessed through intracellular staining with anti-IFN-γ and CD107α expression through surface staining with anti-CD107α. To facilitate gating, the cultures were also co-stained with anti-CD3 and anti-CD8 (mean ± SD of duplicates, $n = 3$). Statistical analysis (unpaired two-tailed *t*-test) was carried out using GraphPad Prism. (c) 5×10^5 T2 cells were pulsed with varying concentrations of P603 (77% Pure, 10 μg/ml to 1×10^{-6} μg/ml) and P603 *t*Bu (> 98% Pure, 10 μg/ml to 1×10^{-6} μg/ml). After 1 hr, unbound peptide was washed off and the pulsed T2 cells were cultured with 1×10^5 6C5 $CD8^+$ T cells at a 1 : 1 ratio. Cell-free supernatant was harvested and tested for the presence of IFN-γ by ELISA (mean ± SD, $n = 3$). (d) 1×10^5 6C5 $CD8^+$ T-cells were cultured at 1 : 1 ratio with T2 cells in the presence of varying concentrations of P603 (77% Pure, 10 μg/ml to 1×10^{-6} μg/ml) and P603 *t*Bu (> 98% Pure, 10 μg/ml to 1×10^{-6} μg/ml) for 5 hr. Lymphocytes were gated based on their forward and side scatter profile and then doublet exclusion was performed based on forward scatter height versus forward scatter width. T cells were then gated on $CD3^+$ $CD8^+$ cells and changes in the surface expression of CD107α were determined through culturing the cells in the presences of anti-CD107α (mean ± SD, $n = 3$). The EC_{50} value was calculated using the fitted curve using GraphPad Prism.

(PolyPeptide Group). This peptide was able to stimulate robust and highly significant ($P < 0{\cdot}0001$) IFN-γ and CD107α responses in 6C5. However, the unmodified wt P603 (95% pure) failed to induce T-cell activation in the same assays (Fig. 5a,b).

Peptide dose–response experiments were performed to validate the activity of P603 Tyr(3-*t*Bu) and to compare the activity of this peptide against the original crude (77% pure) P603 preparation. P603 Tyr(3-*t*Bu) (> 98% pure) was more potent than P603 (77% pure) as determined by comparison of the calculated EC_{50} values (Fig. 5c,d). Using IFN-γ production as a functional read-out, the EC_{50} values were 0·2 μM for P603 Tyr(3-*t*Bu) (> 98% pure) and 1·4 μM for P603 (77% pure). By contrast using CD107α expression as a read-out, the EC_{50} values were 0·52 nM for P603 Tyr(3-*t*Bu) (> 98% pure) and 610 nM for P603 (77% pure). For both assays the highly purified P603 Tyr (3-*t*Bu) was recognized with greater activity (1–3 logs) than the crude P603 (77% pure). These results would be predicted, as the Tyr(3-*t*Bu) modified form of the peptide was found by HPLC to comprise < 1% of the crude P603 (77% pure) preparation.

Collectively these findings confirm that the activation of 6C5 is due to the modified P603 [LLSY(3-*t*Bu)FGTPT] rather than the wt P603 peptide (LLSYFGTPT). Molecular modelling of these two peptides indicates that the presence of the Tyr(3-*t*Bu) results in an extension of the tyrosine side chain out of the MHC towards the TCR (Fig. 7a,b). Using the model we have predicted that the presence of the Tyr(3-*t*Bu) could result in a peptide with the capacity to adopt two different conformations, due to the rotation of the aryl ring (Fig. 6b–d). As the presence of the Tyr(3-*t*Bu) does not appear to affect the peptide conformation or the position of the MHC anchor residue, we predict that the discrimination between the modified and unmodified peptides occurs largely at the level of the TCR. Peptide binding was assessed by the up-regulation of HLA-A*0201 expression on T2 cells. Neither the modified or unmodified peptide were able to significantly up-regulate HLA-A*0201 in comparison to the positive control MART1 peptide, suggesting poor or weak binding under the conditions used (see Supporting information, Fig. S3). Nevertheless, the results suggest that the modified peptide does not have better binding to HLA-A*0201 than the unmodified peptide. This supports our hypothesis that the primary effect of the Tyr(3-*t*Bu) modification is to alter interactions with the TCR.

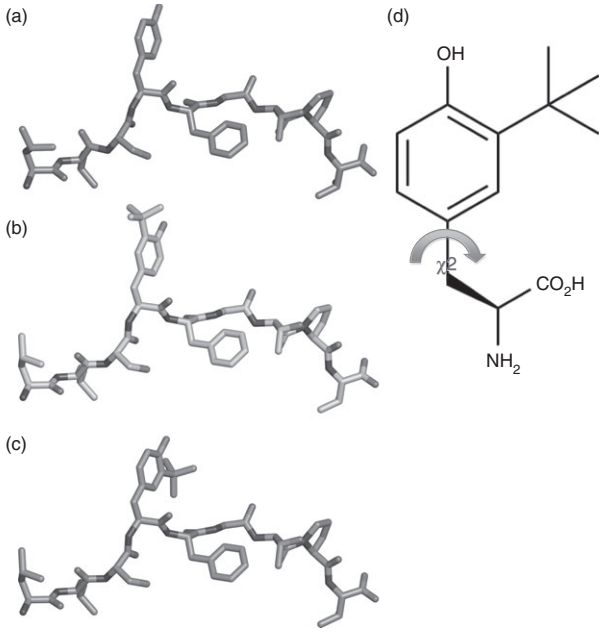

Figure 6. Peptide:MHC modelling of unmodified and Tyr(3-*t*Bu) modified peptides. Computer models illustrating the conformation of peptides bound to HLA-A*0201 were generated based on entry 4I4W from the PDB. The HLA-A*0201 structure has been removed for clarity. COOT was used to modify the sequence of the peptide to be LLSYFGTPT. (a) The resulting modified peptide is capable of adopting two possible conformations (b) and (c) due to the rotation of the aromatic ring about its axis (d).

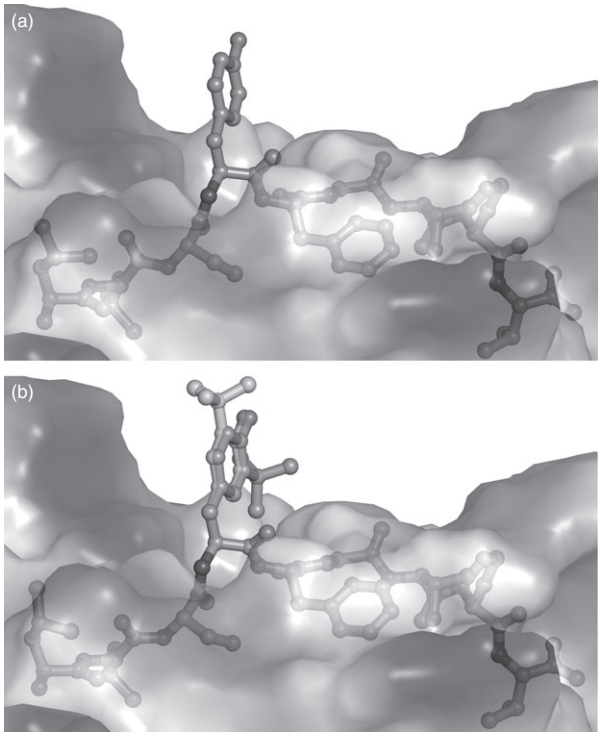

Figure 7. Peptide:MHC modelling of unmodified and Tyr(3-*t*Bu) modified peptide bound to HLA-A*0201. Computer models of Peptide:HLA*0201 complexes were generated using entry 4I4W from the PDB. COOT was used to modify the sequence of the peptide to be LLSYFGTPT. (a) and (b) show that for both peptides the anchor residues at either end of the peptide are well buried in the groove. However, the presence of the *t*Bu-modified tyrosine results in the extension of the side chain out of the MHC and towards the T-cell receptor, which is not observed with the wild-type peptide.

Discussion

Minor modifications of antigenic peptides have been shown to have profound positive and negative effects on peptide recognition. These modifications can vary from naturally occurring post-translation modifications[15] to specific synthetic alterations of the peptide sequence and/or individual amino acids.[4,16] These changes can alter MHC binding; the three-dimensional tertiary peptide structure and the TCR contact residues of the peptides, and so alter peptide immunogenicity.

We describe the novel discovery of a human $CD8^+$ T-cell clone that recognizes a *t*Bu-modified peptide LLSY(3-*t*Bu)FGTPT while showing no recognition of the wt peptide LLSYFGTPT. This modification appears to have no effect on the potential structure of the MHC:peptide complex (Fig. 7a,b). But it does have a profound effect on T-cell recognition. Similarly it has been observed that a minor change in tyrosine, the conversion of tyrosine to nitrotyrosine, can abrogate peptide recognition in both $CD4^+$ T cells[17] and $CD8^+$ T cells.[18]

Peptides containing Tyr(3-*t*Bu) are synthetic entities and do not occur in nature, so it is unclear how $CD8^+$ T cells with specificity for Tyr(3-*t*Bu) peptides could arise. There are two possibilities for the origin of T-cell clone 6C5. First, it could be a memory T-cell generated *in vivo* against a naturally occurring epitope that is able to cross-react on Tyr(3-*t*Bu) peptides. Theoretically, a different, naturally occurring residue that possesses an extended side chain could have the correct dimensions to allow for TCR contact. This could be tested by using large peptide libraries to establish the amino acid preference of 6C5 for each position in the peptide.[19] Second, the clone could have been generated from naive T cells primed against P603 *t*Bu *in vitro*. It is possible that such naive T cells could have been activated and expanded to functionally detectable levels during the 5-week culturing period.[20]

The identification of P603 Tyr(3-*t*Bu) resulted from the detection of a minor peptide contaminant (< 0·05%) present within a crude pool of synthetic peptides. Historically, synthetic peptide pools have been successfully used to generate peptide-specific T-cell responses and clones.[8] However, one of the major drawbacks associated with this process is the inability to produce completely pure peptide preparations. Commercially produced peptides are commonly subject to stringent purification and quality checking processes, such as reverse-phase HPLC and mass spectrometry. Despite these efforts, contaminants can still be present within the final peptide preparations, potentially causing misleading results.[21–24] This highlights the potential risk that the presence of traces of highly immunogenic contaminating peptides could result in misleading assessment of clinical responses to peptide vaccines. Typically clinical grade peptides used during *in vivo* human vaccine trials range in purity from 95 to ≥ 98%.[25–31] As the contaminant report here constituted < 1% of the original P603 crude peptide preparation and < 0·05% of the original 23-peptide mixture it is conceivable that minute, but highly immunogenic peptide species may be present within clinical grade peptide vaccines. This could lead to the induction of inappropriate responses in T cells with the wrong specificity or even cause adverse reactions.

We believe that the *t*Bu-modified peptide identified in this report was generated during the peptide synthesis process; most likely due to the alkylation of tyrosine by *t*Bu cations under peptide de-protection conditions. This reaction has been reported during model de-protection conditions[32] and for preparative scale synthesis[33] of Tyr(3-*t*Bu), therefore the observation of a peptide containing Tyr(3-*t*Bu) as a minor constituent of the crude P603 preparation is not surprising.

In conclusion, the data presented here highlight some issues with interpreting data obtained when using synthetic peptide mixtures. Additionally we have reported that the chemical modification of a single amino acid, Tyr→Tyr(3-*t*Bu), can completely dictate activation of the $CD8^+$ T-cell clone 6C5. This peptide modification appears to exert its primary effect via interaction with the TCR rather than influencing the conformation of the peptide within the HLA binding site. These findings emphasize the specificity and sensitivity of TCR and their ability to discriminate between peptides that have an identical primary amino sequence but differ by a single chemical modification.

Acknowledgements

This work was supported by a Cardiff University/Medical Research Council studentship (to RR), Leukaemia Lymphoma Research Programme Grant (to CP and CF) and a Cancer Research Wales Project Grant (to SM). We thank all the patients and healthy donors who provided blood samples for this study, and Peptide Synthetics (UK) for initial analysis of crude peptides.

Authors' contributions

RAR and JER designed and performed the experiments, analysed all data and co-wrote the manuscript. PR performed the peptide:MHC computer modelling. CF provided clinical samples. SM and CP contributed to experimental design and co-wrote the manuscript.

Disclosures

The authors declare that they have no conflict of interests.

References

1 Kawakami Y, Eliyahu S, Jennings C *et al.* Recognition of multiple epitopes in the human melanoma antigen gp100 by tumor-infiltrating T lymphocytes associated with *in vivo* tumor regression. *J Immunol* 1995; **154**:3961–8.

2 Rosenberg SA, Yang JC, Schwartzentruber DJ *et al.* Immunologic and therapeutic evaluation of a synthetic peptide vaccine for the treatment of patients with metastatic melanoma. *Nat Med* 1998; **4**:321–7.

3 Brinckerhoff LH, Kalashnikov VV, Thompson LW, Yamshchikov GV, Pierce RA, Galavotti HS, Engelhard VH, Slingluff CL Terminal modifications inhibit proteolytic degradation of an immunogenic mart-127-35 peptide: Implications for peptide vaccines. *Int J Cancer* 1999; **83**:326–34.

4 Valmori D, Fonteneau JF, Lizana CM *et al.* Enhanced generation of specific tumor-reactive CTL *in vitro* by selected Melan-A/MART-1 immunodominant peptide analogues. *J Immunol* 1998; **160**:1750–8.

5 Kern F, Faulhaber N, Frömmel C *et al.* Analysis of CD8 T cell reactivity to cytomegalovirus using protein-spanning pools of overlapping pentadecapeptides. *Eur J Immunol* 2000; **30**:1676–82.

6 Gavioli R, Kurilla MG, de Campos-Lima PO, Wallace LE, Dolcetti R, Murray RJ, Rickinson AB, Masucci MG. Multiple HLA A11-restricted cytotoxic T-lymphocyte epitopes of different immunogenicities in the Epstein–Barr virus-encoded nuclear antigen 4. *J Virol* 1993; **67**:1572–8.

7 Smith KL, Tristram A, Gallagher KM, Fiander AN, Man S. Epitope specificity and longevity of a vaccine-induced human T cell response against HPV18. *Int Immunol* 2005; **17**:167–76.

8 Nunes CT, Miners KL, Dolton G, Pepper C, Fegan C, Mason MD, Man S. A novel tumor antigen derived from enhanced degradation of bax protein in human cancers. *Cancer Res* 2011; **71**:5435–44.

9 Klenerman P, Cerundolo V, Dunbar PR. Tracking T cells with tetramers: new tales from new tools. *Nat Rev Immunol* 2002; **2**:263–72.

10 Wong R, Pepper C, Brennan P, Nagorsen D, Man S, Fegan C. Blinatumomab induces autologous T-cell killing of chronic lymphocytic leukemia cells. *Haematologica* 2013; **98**:1930–8.

11 Wellings DA, Atherton E. Standard FMOC protocols. *Methods Enzymol* 1996; **289**:44–67.

12 Ekeruche-Makinde J, Miles JJ, van den Berg HA *et al.* Peptide length determines the outcome of TCR/peptide-MHCI engagement. *Blood* 2013; **121**:1112–23.

13 Emsley P, Cowtan K. Coot: model-building tools for molecular graphics. *Acta Crystallogr D Biol Crystallogr* 2004; **60**:2126–32.

14 Lebedev AA, Young P, Isupov MN, Moroz OV, Vagin AA, Murshudov GN. JLigand: a graphical tool for the CCP4 template-restraint library. *Acta Crystallogr D Biol Crystallogr* 2012; **68**:431–40.

15 Engelhard VH, Altrich-Vanlith M, Ostankovitch M, Zarling AL. Post-translational modifications of naturally processed MHC-binding epitopes. *Curr Opin Immunol* 2006; **18**:92–7.

16 Parkhurst MR, Salgaller ML, Southwood S, Robbins PF, Sette A, Rosenberg SA, Kawakami Y. Improved induction of melanoma-reactive CTL with peptides from the melanoma antigen gp100 modified at HLA-A* 0201-binding residues. *J Immunol* 1996; **157**:
2539–48.

17 Birnboim HC, Lemay A-M, Lam DKY, Goldstein R, Webb JR. Cutting edge: MHC class II-restricted peptides containing the inflammation-associated marker 3-nitrotyrosine evade central tolerance and elicit a robust cell-mediated immune response. *J Immunol* 2003; **171**:528–32.

18 Hardy LL, Wick DA, Webb JR. Conversion of tyrosine to the inflammation-associated analog 3′-nitrotyrosine at either TCR-or MHC-contact positions can profoundly affect recognition of the MHC class I-restricted epitope of lymphocytic choriomeningitis virus glycoprotein 33 by CD8 T cells. *J Immunol* 2008; **180**:5956–62.

19 Wooldridge L, Ekeruche-Makinde J, van den Berg HA *et al.* A single autoimmune T cell receptor recognizes more than a million different peptides. *J Biol Chem* 2012; **287**:1168–77.

20 Cerny A, Fowler P, Brothers MA, Houghton M, Schlicht HJ, Chisari FV. Induction *in vitro* of a primary human antiviral cytotoxic T cell response. *Eur J Immunol* 1995; **25**:627–30.

21 Brezar V, Culina S, Østerbye T *et al.* T cells recognizing a peptide contaminant undetectable by mass spectrometry. *PLoS ONE* 2011; **12**:e28866.

22 Mannering SI, Purcell AW, Honeyman MC, McCluskey J, Harrison LC. Human T-cells recognise N-terminally Fmoc-modified peptide. *Vaccine* 2003; **21**:3638–46.

23 Currier JR, Galley LM, Wenschuh H *et al.* Peptide impurities in commercial synthetic peptides and their implications for vaccine trial assessment. *Clin Vaccine Immunol* 2008; **15**:267–76.

24 De Spiegeleer B, Vergote V, Pezeshki A, Peremans K, Burvenich C. Impurity profiling quality control testing of synthetic peptides using liquid chromatography-photodiode array-fluorescence and liquid chromatography-electrospray ionization-mass spectrometry: the obestatin case. *Anal Biochem* 2008; **376**:229–34.

25 Iinuma H, Fukushima R, Inaba T *et al.* Phase I clinical study of multiple epitope peptide vaccine combined with chemoradiation therapy in esophageal cancer patients. *J Transl Med* 2014; **12**:84.

26 Betancourt AA, Delgado CAG, Estévez ZC *et al.* Phase I clinical trial in healthy adults of a nasal vaccine candidate containing recombinant hepatitis B surface and core antigens. *Int J Infect Dis* 2007; **11**:394–401.

27 Hueman MT, Dehqanzada ZA, Novak TE *et al.* Phase I Clinical trial of a HER-2/neu peptide (E75) vaccine for the prevention of prostate-specific antigen recurrence in high-risk prostate cancer patients. *Clin Cancer Res* 2005; **11**:7470–9.

28 Okuno K, Sugiura F, Hida J, Tokoro T, Ishimaru E, Sukegawa Y, Ueda K. Phase I clinical trial of a novel peptide vaccine in combination with UFT/LV for metastatic colorectal cancer. *Exp Ther Med* 2010; **1**:73–9.

29 Aruga A, Takeshita N, Kotera Y, Okuyama R, Matsushita N, Ohta T, Kazuyoshi T, Yamamoto M Phase I clinical trial of multiple-peptide vaccination for patients with advanced biliary tract cancer. *J Transl Med* 2014; **12**:61.

30 Carreno BM, Becker-Hapak M, Huang A *et al.* IL-12p70-producing patient DC vaccine elicits Tc1-polarized immunity. *J Clin Invest* 2013; **123**:3383–94.

31 Muderspach L, Wilczynski S, Roman L *et al.* A phase I trial of a human papillomavirus (HPV) peptide vaccine for women with high-grade cervical and vulvar intraepithelial neoplasia who are HPV 16 positive. *Clin Cancer Res* 2000; **6**:3406–16.

32 Lundt BF, Johansen NL, Markussen J. Formation and synthesis of 3′-t-butyltyrosine. *Int J Pept Protein Res* 1979; **14**:344–6.

33 Taka N, Matsuoka H, Sato T *et al.* Discovery of novel motilin antagonists: conversion of tetrapeptide leads to orally available peptidomimetics. *Bioorg Med Chem Lett* 2009; **13**:3426–9.

Supporting Information

Additional Supporting Information may be found in the online version of this article:

Figure S1. Liquid chromatography mass spectrometry analysis of purified and crude P603 peptide samples.

Figure S2. MS^2 spectra of Tyr(3-*t*Bu) containing peptides.

Figure S3. Peptide binding to HLA-A2.

Bibliography

Adams, S., O'Neill, D.W. and Bhardwaj, N. 2005. Recent Advances in Dendritic Cell Biology. *Journal of Clinical Immunology* 25(2), pp. 87–98.

Aderka, D., Maor, Y., Novick, D., Engelmann, H., Kahn, Y., Levo, Y., Wallach, D., et al. 1993. Interleukin-6 inhibits the proliferation of B-chronic lymphocytic leukemia cells that is induced by tumor necrosis factor-alpha or -beta. *Blood* 81(8), pp. 2076–2084.

Adrain, C., Murphy, B.M. and Martin, S.J. 2005. Molecular ordering of the caspase activation cascade initiated by the cytotoxic T lymphocyte/natural killer (CTL/NK) protease granzyme B. *The Journal of biological chemistry* 280(6), pp. 4663–4673.

Agrawal, S.G., Liu, F.T., Wiseman, C., Shirali, S., Liu, H., Lillington, D., Du, M.Q., et al. 2008. Increased proteasomal degradation of Bax is a common feature of poor prognosis chronic lymphocytic leukemia. *Blood* 111(5), pp. 2790–2796.

Ahmadzadeh, M., Johnson, L.A., Heemskerk, B., Wunderlich, J.R., Dudley, M.E., White, D.E. and Rosenberg, S.A. 2009. Tumor antigen-specific CD8 T cells infiltrating the tumor express high levels of PD-1 and are functionally impaired. *Blood* 114(8), pp. 1537–1544.

Akagi, J. and Baba, H. 2008. Prognostic value of CD57+ T lymphocytes in the peripheral blood of patients with advanced gastric cancer. *International journal of clinical oncology* 13(6), pp. 528–535.

Alarcón, B., Mestre, D. and Martínez-Martín, N. 2011. The immunological synapse: a cause or consequence of T-cell receptor triggering? *Immunology* 133(4), pp. 420–425.

Alderton, G.K. and Bordon, Y. 2012. Tumour immunotherapy — leukocytes take up the fight. *Nature Reviews Immunology* 12(4), pp. 237–237.

Allam, A., Conze, D.B., Giardino Torchia, M.L., Munitic, I., Yagita, H., Sowell, R.T., Marzo, A.L., et al. 2009. The CD8+ memory T-cell state of readiness is actively maintained and reversible. *Blood* 114(10), pp. 2121–2130.

Alves, N.L., Hooibrink, B., Arosa, F.A. and van Lier, R.A.W. 2003. IL-15 induces antigen-independent expansion and differentiation of human naive CD8+ T cells in vitro. *Blood* 102(7), pp. 2541–2546.

Andersen, M.H., Fensterle, J., Ugurel, S., Reker, S., Houben, R., Guldberg, P., Berger, T.G., et al. 2004. Immunogenicity of constitutively active V599EBRaf. *Cancer Research* 64(15), pp. 5456–5460.

Androlewicz, M.J., Anderson, K.S. and Cresswell, P. 1993. Evidence that transporters associated with antigen processing translocate a major histocompatibility complex class I-binding peptide into the endoplasmic reticulum in an ATP-dependent manner. *Proceedings of the National Academy of Sciences* 90(19), pp. 9130–9134.

Arch, R.H. and Thompson, C.B. 1998. 4-1BB and Ox40 are members of a tumor necrosis factor (TNF)-nerve growth factor receptor subfamily that bind TNF receptor-associated factors and activate nuclear factor kappaB. *Molecular and Cellular Biology* 18(1), pp. 558–565.

Artyomov, M.N., Lis, M., Devadas, S., Davis, M.M. and Chakraborty, A.K. 2010. CD4 and CD8 binding to MHC molecules primarily acts to enhance Lck delivery. *Proceedings of the National Academy of Sciences* 107(39), pp. 16916–16921.

Badoux, X.C., Keating, M.J., Wang, X., O'Brien, S.M., Ferrajoli, A., Faderl, S., Burger, J., et al. 2011. Fludarabine, cyclophosphamide, and rituximab chemoimmunotherapy is highly effective treatment for relapsed patients with CLL. *Blood* 117(11), pp. 3016–3024.

Bagnara, D., Kaufman, M.S., Calissano, C., Marsilio, S., Patten, P.E.M., Simone, R., Chum, P., et al. 2011. A novel adoptive transfer model of chronic lymphocytic leukemia suggests a key role for T lymphocytes in the disease. *Blood* 117(20), pp. 5463–5472.

Bakker, A.B., Schreurs, M.W., de Boer, A.J., Kawakami, Y., Rosenberg, S.A., Adema, G.J. and Figdor, C.G. 1994. Melanocyte lineage-specific antigen gp100 is recognized by melanoma-derived tumor-infiltrating lymphocytes. *The Journal of Experimental Medicine* 179(3), pp. 1005–1009.

Banchereau, J. and Steinman, R.M. 1998. Dendritic cells and the control of immunity. *Nature* 392(6673), pp. 245–252.

Barber, E.K., Dasgupta, J.D., Schlossman, S.F., Trevillyan, J.M. and Rudd, C.E. 1989. The CD4 and CD8 antigens are coupled to a protein-tyrosine kinase (p56lck) that phosphorylates the CD3 complex. *Proceedings of the National Academy of Sciences* 86(9), pp. 3277–3281.

Bargou, R., Leo, E., Zugmaier, G., Klinger, M., Goebeler, M., Knop, S., Noppeney, R., et al. 2008. Tumor Regression in Cancer Patients by Very Low Doses of a T Cell-Engaging Antibody. *Science* 321(5891), pp. 974–977.

Basler, M., Lauer, C., Moebius, J., Weber, R., Przybylski, M., Kisselev, A.F., Tsu, C., et al. 2012. Why the structure but not the activity of the immunoproteasome subunit low molecular mass polypeptide 2 rescues antigen presentation. *The Journal of Immunology* 189(4), pp. 1868–1877.

Baumeister, W., Walz, J., Zühl, F. and Seemüller, E. 1998. The Proteasome: Paradigm of a Self-Compartmentalizing Protease. *Cell* 92(3), pp. 367–380.

Begleiter, A., Mowat, M., Israels, L.G. and Johnston, J.B. 1996. Chlorambucil in chronic lymphocytic leukemia: mechanism of action. *Leukemia & lymphoma* 23(3-4), pp. 187–201.

Behr, S.I., Korinth, D. and Schriever, F. 1998. Differential adhesion pattern of B cell chronic lymphocytic leukemia cells. *Leukemia* 12(1), pp. 71–77.

Biagi, E., Rousseau, R., Yvon, E., Schwartz, M., Dotti, G., Foster, A., Havlik-Cooper, D., et al. 2005. Responses to human CD40 ligand/human interleukin-2 autologous cell vaccine in patients with B-cell chronic lymphocytic leukemia. *Clinical Cancer Research* 11(19 Pt 1), pp. 6916–6923.

Binet, J.L., Auquier, A., Dighiero, G., Chastang, C., Piguet, H., Goasguen, J., Vaugier, G., et al. 1981. A new prognostic classification of chronic lymphocytic leukemia derived from a multivariate survival analysis. *Cancer* 48(1), pp. 198–206.

Birkholz, K., Schwenkert, M., Kellner, C., Gross, S., Fey, G., Schuler-Thurner, B., Schuler, G., et al. 2010. Targeting of DEC-205 on human dendritic cells results in efficient MHC class II-restricted antigen presentation. *Blood* 116(13), pp. 2277–2285.

Birnboim, H.C., Lemay, A.-M., Lam, D.K.Y., Goldstein, R. and Webb, J.R. 2003. Cutting edge: MHC class II-restricted peptides containing the inflammation-associated marker 3-nitrotyrosine evade central tolerance and elicit a robust cell-mediated immune response. *The Journal of Immunology* 171(2), pp. 528–532.

Blackburn, S.D., Shin, H., Haining, W.N., Zou, T., Workman, C.J., Polley, A., Betts, M.R., et al. 2008. Coregulation of CD8+ T cell exhaustion by multiple inhibitory receptors during chronic viral infection. *Nature immunology* 10(1), pp. 29–37.

Boatright, K.M., Renatus, M., Scott, F.L., Sperandio, S., Shin, H., Pedersen, I.M., Ricci, J.-E., et al. 2003. A Unified Model for Apical Caspase Activation. *Molecular Cell* 11(2), pp. 529–541.

Boehm, T. 2011. Design principles of adaptive immune systems. *Nature Reviews Immunology* 11(5), pp. 307–317.

Boniface, K., Guignouard, E., Pedretti, N., Garcia, M., Delwail, A., Bernard, F.X., Nau, F., et al. 2007. A role for T cell-derived interleukin 22 in psoriatic skin inflammation. *Clinical and experimental immunology* 150(3), pp. 407–415.

Bonifaz, L.C., Bonnyay, D.P., Charalambous, A., Darguste, D.I., Fujii, S.-I., Soares, H., Brimnes, M.K., et al. 2004. In vivo targeting of antigens to maturing dendritic cells via the DEC-205 receptor improves T cell vaccination. *The Journal of Experimental Medicine* 199(6), pp. 815–824.

Borysiewicz, L.K., Fiander, A., Nimako, M., Man, S., Wilkinson, G.W., Westmoreland, D., Evans, A.S., et al. 1996. A recombinant vaccinia virus encoding human papillomavirus types 16 and 18, E6 and E7 proteins as immunotherapy for cervical cancer. *Lancet* 347(9014), pp. 1523–1527.

Bozzacco, L., Trumpfheller, C., Siegal, F.P., Mehandru, S., Markowitz, M., Carrington, M., Nussenzweig, M.C., et al. 2007. DEC-205 receptor on dendritic cells mediates presentation of HIV gag protein to CD8+ T cells in a spectrum of human MHC I haplotypes. *Proceedings of the National Academy of Sciences* 104(4), pp. 1289–1294.

Brahmer, J.R., Tykodi, S.S., Chow, L.Q.M., Hwu, W.-J., Topalian, S.L., Hwu, P., Drake, C.G., et al. 2012. Safety and activity of anti-PD-L1 antibody in patients with advanced cancer. *New England Journal of Medicine* 366(26), pp. 2455–2465.

Brenchley, J.M. 2002. Expression of CD57 defines replicative senescence and antigen-induced apoptotic death of CD8+ T cells. *Blood* 101(7), pp. 2711–2720.

Brentjens, R., Yeh, R., Bernal, Y., Riviere, I. and Sadelain, M. 2009. Treatment of Chronic Lymphocytic Leukemia With Genetically Targeted Autologous T Cells: Case Report of an Unforeseen Adverse Event in a Phase I Clinical Trial. *Molecular Therapy* 18(4), pp. 666–668.

Brezar, V., Culina, S., Østerbye, T., Guillonneau, F., Chiappetta, G., Verdier, Y., Vinh, J., et al. 2011. T Cells Recognizing a Peptide Contaminant Undetectable by Mass Spectrometry. *PLoS ONE* 6(12), p. e28866.

Brossart, P., Stuhler, G., Flad, T., Stevanovic, S., Rammensee, H.-G., Kanz, L. and Brugger, W. 1998. Her-2/neu-derived peptides are tumor-associated antigens expressed by human renal cell and colon carcinoma lines and are recognized by in vitro induced specific cytotoxic T lymphocytes. *Cancer Research* 58(4), pp. 732–736.

Brossart, P., Wirths, S., Stuhler, G., Reichardt, V.L., Kanz, L. and Brugger, W. 2000. Induction of cytotoxic T-lymphocyte responses in vivo after vaccinations with peptide-pulsed dendritic cells. *Blood* 96(9), pp. 3102–3108.

Brown, J.R., Byrd, J.C., Coutre, S.E., Benson, D.M., Flinn, I.W., Wagner-Johnston, N.D., Spurgeon, S.E., et al. 2014. Idelalisib, an inhibitor of phosphatidylinositol 3-kinase p110 , for relapsed/refractory chronic lymphocytic leukemia. *Blood* 123(22), pp. 3390–3397.

Brownlie, R.J. and Zamoyska, R. 2013. T cell receptor signalling networks: branched, diversified and bounded. *Nature Reviews Immunology* 13(4), pp. 257–269.

Brusa, D., Serra, S., Coscia, M., Rossi, D., D'Arena, G., Laurenti, L., Jaksic, O., et al. 2013. The PD-1/PD-L1 axis contributes to T-cell dysfunction in chronic lymphocytic leukemia. *Haematologica* 98(6), pp. 953–963.

Brüstle, A., Heink, S., Huber, M., Rosenplänter, C., Stadelmann, C., Yu, P., Arpaia, E., et al. 2007. The development of inflammatory TH-17 cells requires interferon-regulatory factor 4. *Nature immunology* 8(9), pp. 958–966.

Buggins, A.G.S., Patten, P.E.M., Richards, J., Thomas, N.S.B., Mufti, G.J. and Devereux, S. 2007. Tumor-derived IL-6 may contribute to the immunological defect in CLL. *Leukemia* 22(5), pp. 1084–1087.

Bulian, P., Shanafelt, T.D., Fegan, C., Zucchetto, A., Cro, L., Nückel, H., Baldini, L., et al. 2014. CD49d is the strongest flow cytometry-based predictor of overall survival in chronic lymphocytic leukemia. *Journal of Clinical Oncology* 32(9), pp. 897–904.

Bund, D., Mayr, C., Kofler, D.M., Hallek, M. and Wendtner, C.-M. 2007. CD23 is recognized as tumor-associated antigen (TAA) in B-CLL by CD8+ autologous T lymphocytes. *Experimental Hematology* 35(6), pp. 920–930.

Bund, D., Mayr, C., Kofler, D.M., Hallek, M. and Wendtner, C.-M. 2006. Human Ly9 (CD229) as novel tumor-associated antigen (TAA) in chronic lymphocytic leukemia (B-CLL) recognized by autologous CD8+ T cells. *Experimental Hematology* 34(7), pp. 860–869.

Burgdorf, S., Schölz, C., Kautz, A., Tampé, R. and Kurts, C. 2008. Spatial and mechanistic separation of cross-presentation and endogenous antigen presentation. *Nature immunology* 9(5), pp. 558–566.

Burger, J.A. and Gribben, J.G. 2014. The microenvironment in chronic lymphocytic leukemia (CLL) and other B cell malignancies: insight into disease biology and new targeted therapies. *Seminars in Cancer Biology* 24, pp. 71–81.

Burger, J.A., Burger, M. and Kipps, T.J. 1999. Chronic lymphocytic leukemia B cells express functional CXCR4 chemokine receptors that mediate spontaneous migration beneath bone marrow stromal cells. *Blood* 94(11), pp. 3658–3667.

Burkhardt, U.E., Hainz, U., Stevenson, K., Goldstein, N.R., Pasek, M., Naito, M., Wu, D., et al. 2013. Autologous CLL cell vaccination early after transplant induces leukemia-specific T cells. *The Journal of Clinical Investigation* 123(9), pp. 3756–3765.

Burnet, M. 1957. Cancer—A Biological Approach: I. The Processes Of Control. II. The Significance of Somatic Mutation. *British Medical Journal* 1(5022), p. 779.

Burstein, H.J. 2005. The distinctive nature of HER2-positive breast cancers. *New England*

Journal of Medicine 353(16), pp. 1652–1654.

Buschle, M., Campana, D., Carding, S.R., Richard, C., Hoffbrand, A.V. and Brenner, M.K. 1993. Interferon gamma inhibits apoptotic cell death in B cell chronic lymphocytic leukemia. *The Journal of Experimental Medicine* 177(1), pp. 213–218.

Byrd, J.C., Brown, J.R., O'Brien, S., Barrientos, J.C., Kay, N.E., Reddy, N.M., Coutre, S., et al. 2014. Ibrutinib versus Ofatumumab in Previously Treated Chronic Lymphoid Leukemia. *New England Journal of Medicine* 371(3), pp. 213–223.

Bystry, R.S., Aluvihare, V., Welch, K.A., Kallikourdis, M. and Betz, A.G. 2001. B cells and professional APCs recruit regulatory T cells via CCL4. *Nature immunology* 2(12), pp. 1126–1132.

Calpe, E., Codony, C., Baptista, M.J., Abrisqueta, P., Carpio, C., Purroy, N., Bosch, F., et al. 2011. ZAP-70 enhances migration of malignant B lymphocytes toward CCL21 by inducing CCR7 expression via IgM-ERK1/2 activation. *Blood* 118(16), pp. 4401–4410.

Cambier, J.C., Gauld, S.B., Merrell, K.T. and Vilen, B.J. 2007. B-cell anergy: from transgenic models to naturally occurring anergic B cells? *Nature Reviews Immunology* 7(8), pp. 633–643.

Cannons, J.L., Lau, P., Ghumman, B., DeBenedette, M.A., Yagita, H., Okumura, K. and Watts, T.H. 2001. 4-1BB ligand induces cell division, sustains survival, and enhances effector function of CD4 and CD8 T cells with similar efficacy. *Journal of Immunology* 167(3), pp. 1313–1324.

Cao, E., Zang, X., Ramagopal, U.A., Mukhopadhaya, A., Fedorov, A., Fedorov, E., Zencheck, W.D., et al. 2007. T Cell Immunoglobulin Mucin-3 Crystal Structure Reveals a Galectin-9-Independent Ligand-Binding Surface. *Immunity* 26(3), pp. 311–321.

Carton, J.M., Uhlinger, D.J., Batheja, A.D., Derian, C., Ho, G., Argenteri, D. and D'Andrea, M.R. 2003. Enhanced Serine Palmitoyltransferase Expression in Proliferating Fibroblasts, Transformed Cell Lines, and Human Tumors. *Journal of Histochemistry & Cytochemistry* 51(6), pp. 715–726.

Caruso, A., Licenziati, S., Corulli, M., Canaris, A.D., De Francesco, M.A., Fiorentini, S., Peroni, L., et al. 1997. Flow cytometric analysis of activation markers on stimulated T cells and their correlation with cell proliferation. *Cytometry Part A* 27(1), pp. 71–76.

Cebecauer, M., Guillaume, P., Hozák, P., Mark, S., Everett, H., Schneider, P. and Luescher, I.F. 2005. Soluble MHC-peptide complexes induce rapid death of CD8+ CTL. *The Journal of Immunology* 174(11), pp. 6809–6819.

Chames, P., Van Regenmortel, M., Weiss, E. and Baty, D. 2009. Therapeutic antibodies: successes, limitations and hopes for the future. *British Journal of Pharmacology* 157(2), pp. 220–233.

Champagne, P., Ogg, G.S., King, A.S., Knabenhans, C., Ellefsen, K., Nobile, M., Appay, V., et al. 2001. Skewed maturation of memory HIV-specific CD8 T lymphocytes. *Nature* 410(6824), pp. 106–111.

Chang, C.-S., Chang, J.H., Hsu, N.C., Lin, H.-Y. and Chung, C.-Y. 2007. Expression of CD80 and CD86 costimulatory molecules are potential markers for better survival in nasopharyngeal carcinoma. *BMC cancer* 7, p. 88.

Chang, H.-C., Sehra, S., Goswami, R., Yao, W., Yu, Q., Stritesky, G.L., Jabeen, R., et al. 2010. The transcription factor PU.1 is required for the development of IL-9-producing T cells and allergic inflammation. *Nature immunology* 11(6), pp. 527–534.

Chang, H.-C., Zhang, S., Thieu, V.T., Slee, R.B., Bruns, H.A., Laribee, R.N., Klemsz, M.J., et al. 2005. PU.1 expression delineates heterogeneity in primary Th2 cells. *Immunity* 22(6), pp. 693–703.

Chaouchi, N., Wallon, C., Goujard, C., Tertian, G., Rudent, A., Caput, D., Ferrera, P., et al. 1996. Interleukin-13 inhibits interleukin-2-induced proliferation and protects chronic lymphocytic leukemia B cells from in vitro apoptosis. *Blood* 87(3), pp. 1022–1029.

Chapman, H.A. 2006. Endosomal proteases in antigen presentation. *Current opinion in immunology* 18(1), pp. 78–84.

Chaturvedi, P., Hengeveld, R., Zechel, M.A., Lee-Chan, E. and Singh, B. 2000. The functional role of class II-associated invariant chain peptide (CLIP) in its ability to variably modulate immune responses. *International immunology* 12(6), pp. 757–765.

Chemnitz, J.M., Parry, R.V., Nichols, K.E., June, C.H. and Riley, J.L. 2004. SHP-1 and SHP-2 associate with immunoreceptor tyrosine-based switch motif of programmed death 1 upon primary human T cell stimulation, but only receptor ligation prevents T cell activation. *The Journal of Immunology* 173(2), pp. 945–954.

Chen, L., Apgar, J., Huynh, L., Dicker, F., Giago-McGahan, T., Rassenti, L., Weiss, A., et al. 2005. ZAP-70 directly enhances IgM signaling in chronic lymphocytic leukemia. *Blood* 105(5), pp. 2036–2041.

Chen, W., Jin, W., Hardegen, N., Lei, K.-J., Li, L., Marinos, N., McGrady, G., et al. 2003. Conversion of peripheral CD4+CD25- naive T cells to CD4+CD25+ regulatory T cells by TGF-beta induction of transcription factor Foxp3. *The Journal of Experimental Medicine* 198(12), pp. 1875–1886.

Cheng, S., Ma, J., Guo, A., Lu, P., Leonard, J.P., Coleman, M., Liu, M., et al. 2014. BTK inhibition targets in vivo CLL proliferation through its effects on B-cell receptor signaling activity. *Leukemia* 28(3), pp. 649–657.

Chinnaiyan, A.M., O'Rourke, K., Tewari, M. and Dixit, V.M. 1995. FADD, a novel death domain-containing protein, interacts with the death domain of Fas and initiates apoptosis. *Cell* 81(4), pp. 505–512.

Chiorazzi, N. 2012. Implications of new prognostic markers in chronic lymphocytic leukemia. *Hematology / the Education Program of the American Society of Hematology. American Society of Hematology. Education Program* 2012, pp. 76–87.

Chiorazzi, N. and Ferrarini, M. 2011. Cellular origin(s) of chronic lymphocytic leukemia: cautionary notes and additional considerations and possibilities. *Blood* 117(6), pp. 1781–1791.

Chong, L.K., Aicheler, R.J., Llewellyn-Lacey, S., Tomasec, P., Brennan, P. and Wang, E.C.Y. 2008. Proliferation and interleukin 5 production by CD8hiCD57+ T cells. *European Journal of Immunology* 38(4), pp. 995–1000.

Chow, A., Toomre, D., Garrett, W. and Mellman, I. 2002. Dendritic cell maturation triggers retrograde MHC class II transport from lysosomes to the plasma membrane.

Nature 418(6901), pp. 988–994.

Cieri, N., Camisa, B., Cocchiarella, F., Forcato, M., Oliveira, G., Provasi, E., Bondanza, A., et al. 2013. IL-7 and IL-15 instruct the generation of human memory stem T cells from naive precursors. *Blood* 121(4), pp. 573–584.

Ciernik, I.F., Berzofsky, J.A. and Carbone, D.P. 1996. Human lung cancer cells endogenously expressing mutant p53 process and present the mutant epitope and are lysed by mutant-specific cytotoxic T lymphocytes. *Clinical Cancer Research* 2(5), pp. 877–882.

Cocks, B.G., de Waal Malefyt, R., Galizzi, J.P., de Vries, J.E. and Aversa, G. 1993. IL-13 induces proliferation and differentiation of human B cells activated by the CD40 ligand. *International immunology* 5(6), pp. 657–663.

Coe, H. and Michalak, M. 2010. ERp57, a multifunctional endoplasmic reticulum resident oxidoreductase. *International Journal of Biochemistry and Cell Biology* 42(6), pp. 796–799.

Cole, D.K., Edwards, E.S.J., Wynn, K.K., Clement, M., Miles, J.J., Ladell, K., Ekeruche, J., et al. 2010. Modification of MHC Anchor Residues Generates Heteroclitic Peptides That Alter TCR Binding and T Cell Recognition. *The Journal of Immunology* 185(4), pp. 2600–2610.

Couzin-Frankel, J. 2013. Breakthrough of the year 2013. Cancer immunotherapy. *Science* 342(6165), pp. 1432–1433.

Croft, M., So, T., Duan, W. and Soroosh, P. 2009. The significance of OX40 and OX40L to T-cell biology and immune disease. *Immunological reviews* 229(1), pp. 173–191.

Damle, R.N., Wasil, T., Fais, F., Ghiotto, F., Valetto, A., Allen, S.L., Buchbinder, A., et al. 1999. Ig V gene mutation status and CD38 expression as novel prognostic indicators in chronic lymphocytic leukemia. *Blood* 94(6), pp. 1840–1847.

Day, C.L., Kaufmann, D.E., Kiepiela, P., Brown, J.A., Moodley, E.S., Reddy, S., Mackey, E.W., et al. 2006. PD-1 expression on HIV-specific T cells is associated with T-cell exhaustion and disease progression. *Nature* 443(7109), pp. 350–354.

de Castro, E., Sigrist, C.J.A., Gattiker, A., Bulliard, V., Langendijk-Genevaux, P.S., Gasteiger, E., Bairoch, A., et al. 2006. ScanProsite: detection of PROSITE signature matches and ProRule-associated functional and structural residues in proteins. *Nucleic Acids Research* 34(Web Server issue), pp. W362–5.

de Haan, E.C., Moret, E.E., Wagenaar-Hilbers, J.P.A., Liskamp, R.M.J. and Wauben, M.H.M. 2005a. Possibilities and limitations in the rational design of modified peptides for T cell mediated immunotherapy. *Molecular Immunology* 42(3), pp. 365–373.

de Haan, E.C., Wagenaar-Hilbers, J.P.A., Liskamp, R.M.J., Moret, E.E. and Wauben, M.H.M. 2005b. Limited plasticity in T cell recognition of modified T cell receptor contact residues in MHC class II bound peptides. *Molecular Immunology* 42(3), pp. 355–364.

De Smet, C., Lurquin, C., van der Bruggen, P., De Plaen, E., Brasseur, F. and Boon, T. 1994. Sequence and expression pattern of the human MAGE2 gene. *Immunogenetics* 39(2), pp. 121–129.

de Verteuil, D., Muratore-Schroeder, T.L., Granados, D.P., Fortier, M.-H., Hardy, M.-P., Bramoullé, A., Caron, É., et al. 2010. Deletion of immunoproteasome subunits imprints on the transcriptome and has a broad impact on peptides presented by major

histocompatibility complex I molecules. *Molecular & cellular proteomics : MCP* 9(9), pp. 2034–2047.

Deaglio, S., Aydin, S., Grand, M.M., Vaisitti, T., Bergui, L., D'Arena, G., Chiorino, G., et al. 2010. CD38/CD31 interactions activate genetic pathways leading to proliferation and migration in chronic lymphocytic leukemia cells. *Molecular Medicine* 16(3-4), p. 87.

Dedeoglu, F., Horwitz, B. and Chaudhuri, J. 2004. Induction of activation-induced cytidine deaminase gene expression by IL-4 and CD40 ligation is dependent on STAT6 and NFκB. *International Immunology* 16(3), pp 395–404.

Del Poeta, G., Maurillo, L., Venditti, A., Buccisano, F., Epiceno, A.M., Capelli, G., Tamburini, A., et al. 2001. Clinical significance of CD38 expression in chronic lymphocytic leukemia. *Blood* 98(9), pp. 2633–2639.

Del Principe, M.I., Del Poeta, G., Buccisano, F., Maurillo, L., Venditti, A., Zucchetto, A., Marini, R., et al. 2006. Clinical significance of ZAP-70 protein expression in B-cell chronic lymphocytic leukemia. *Blood* 108(3), pp. 853–861.

Denkberg, G., Klechevsky, E. and Reiter, Y. 2002. Modification of a tumor-derived peptide at an HLA-A2 anchor residue can alter the conformation of the MHC-peptide complex: probing with TCR-like recombinant antibodies. *The Journal of Immunology* 169(8), pp. 4399–4407.

Denoeud, J. and Moser, M. 2011. Role of CD27/CD70 pathway of activation in immunity and tolerance. *Journal of leukocyte biology* 89(2), pp. 195–203.

Denzin, L.K. and Cresswell, P. 1995. HLA-DM induces CLIP dissociation from MHC class II alpha beta dimers and facilitates peptide loading. *Cell* 82(1), pp. 155–165.

Dhein, J., Walczak, H., Bäumler, C., Debatin, K.-M. and Krammer, P.H. 1995. Autocrine T-cell suicide mediated by APO-1/(Fas/CD95). *Nature* 373(6513), pp. 438–441.

Dhodapkar, M.V., Sznol, M., Zhao, B., Wang, D., Carvajal, R.D., Keohan, M.L., Chuang, E., et al. 2014. Induction of antigen-specific immunity with a vaccine targeting NY-ESO-1 to the dendritic cell receptor DEC-205. *Science Translational Medicine* 6(232), p. 232ra51.

Di Bernardo, M.C., Crowther-Swanepoel, D., Broderick, P., Webb, E., Sellick, G., Wild, R., Sullivan, K., et al. 2008. A genome-wide association study identifies six susceptibility loci for chronic lymphocytic leukemia. *Nature Genetics* 40(10), pp. 1204–1210.

Di Pucchio, T., Chatterjee, B., Smed-Sörensen, A., Clayton, S., Palazzo, A., Montes, M., Xue, Y., et al. 2008. Direct proteasome-independent cross-presentation of viral antigen by plasmacytoid dendritic cells on major histocompatibility complex class I. *Nature immunology* 9(5), pp. 551–557.

Dighe, A.S., Richards, E., Old, L.J. and Schreiber, R.D. 1994. Enhanced in vivo growth and resistance to rejection of tumor cells expressing dominant negative IFNγ receptors. *Immunity* 1(6), pp. 447–456.

Dighiero, G., Maloum, K., Desablens, B., Cazin, B., Navarro, M., Leblay, R., Leporrier, M., et al. 1998. Chlorambucil in Indolent Chronic Lymphocytic Leukemia. *New England Journal of Medicine* 338(21), pp. 1506–1514.

DiLillo, D.J., Weinberg, J.B., Yoshizaki, A., Horikawa, M., Bryant, J.M., Iwata, Y.,

Matsushita, T., et al. 2012. Chronic lymphocytic leukemia and regulatory B cells share IL-10 competence and immunosuppressive function. *Leukemia* 27(1), pp. 170–182.

Djuranovic, S., Nahvi, A. and Green, R. 2012. miRNA-mediated gene silencing by translational repression followed by mRNA deadenylation and decay. *Science* 336(6078), pp. 237–240.

Dolfi, D.V., Boesteanu, A.C., Petrovas, C., Xia, D., Butz, E.A. and Katsikis, P.D. 2008. Late Signals from CD27 Prevent Fas-Dependent Apoptosis of Primary CD8+ T Cells. *The Journal of Immunology* 180(5), pp. 2912–2921.

Döhner, H., Stilgenbauer, S., Benner, A., Leupolt, E., Kröber, A., Bullinger, L., Döhner, K., et al. 2000. Genomic Aberrations and Survival in Chronic Lymphocytic Leukemia. *New England Journal of Medicine* 343(26), pp. 1910–1916.

Dreger, P. and Montserrat, E. 2002. Autologous and allogeneic stem cell transplantation for chronic lymphocytic leukemia. *Leukemia* 16(6), pp. 985–992.

Dreger, P., Dohner, H., Ritgen, M., Bottcher, S., Busch, R., Dietrich, S., Bunjes, D., et al. 2010. Allogeneic stem cell transplantation provides durable disease control in poor-risk chronic lymphocytic leukemia: long-term clinical and MRD results of the German CLL Study Group CLL3X trial. *Blood* 116(14), pp. 2438–2447.

Dunbar, P.R., Chen, J.L., Chao, D., Rust, N., Teisserenc, H., Ogg, G.S., Romero, P., et al. 1999. Cutting edge: rapid cloning of tumor-specific CTL suitable for adoptive immunotherapy of melanoma. *The Journal of Immunology* 162(12), pp. 6959–6962.

Dunn, G.P., Bruce, A.T., Ikeda, H., Old, L.J. and Schreiber, R.D. 2002. Cancer immunoediting: from immunosurveillance to tumor escape. *Nature immunology* 3(11), pp. 991–998.

Dunn, G.P., Old, L.J. and Schreiber, R.D. 2004. The three Es of cancer immunoediting. *Annual Review of Immunology* 22, pp. 329–360.

DuPage, M., Mazumdar, C., Schmidt, L.M., Cheung, A.F. and Jacks, T. 2012. Expression of tumour-specific antigens underlies cancer immunoediting. *Nature* 482(7385), pp. 405–409.

Dustin, M.L., Chakraborty, A.K. and Shaw, A.S. 2010. Understanding the structure and function of the immunological synapse. *Cold Spring Harbor Perspectives in Biology* 2(10), p. a002311.

Dürig, J., Nückel, H., Cremer, M., Führer, A., Halfmeyer, K., Fandrey, J., Möröy, T., et al. 2003. ZAP-70 expression is a prognostic factor in chronic lymphocytic leukemia. *Leukemia* 17(12), pp. 2426–2434.

Ekeruche-Makinde, J., Miles, J.J., van den Berg, H.A., Skowera, A., Cole, D.K., Dolton, G., Schauenburg, A.J.A., et al. 2013. Peptide length determines the outcome of TCR/peptide-MHCI engagement. *Blood* 121(7), pp. 1112–1123.

Evans, L.S., Witte, P.R., Feldhaus, A.L., Nelson, B.H., Riddell, S.R., Greenberg, P.D., Lupton, S.D., et al. 1999. Expression of chimeric granulocyte-macrophage colony-stimulating factor/interleukin 2 receptors in human cytotoxic T lymphocyte clones results in granulocyte-macrophage colony-stimulating factor-dependent growth. *Human Gene Therapy* 10(12), pp. 1941–1951.

Evans, M., Borysiewicz, L.K., Evans, A.S., Rowe, M., Jones, M., Gileadi, U., Cerundolo, V., et al. 2001. Antigen processing defects in cervical carcinomas limit the presentation of a CTL epitope from human papillomavirus 16 E6. *The Journal of Immunology* 167(9), pp. 5420–5428.

Ewen, C.L., Kane, K.P. and Bleackley, R.C. 2012. A quarter century of granzymes. *Cell death and differentiation* 19(1), pp. 28–35.

Fayad, L., Keating, M.J., Reuben, J.M., O'Brien, S., Lee, B.N., Lerner, S. and Kurzrock, R. 2001. Interleukin-6 and interleukin-10 levels in chronic lymphocytic leukemia: correlation with phenotypic characteristics and outcome. *Blood* 97(1), pp. 256–263.

Feau, S., Schoenberger, S.P., Altman, A. and Bécart, S. 2013. SLAT regulates CD8+ T cell clonal expansion in a Cdc42- and NFAT1-dependent manner. *The Journal of Immunology* 190(1), pp. 174–183.

Fecteau, J.-F. and Kipps, T.J. 2012. Structure and function of the hematopoietic cancer niche: focus on chronic lymphocytic leukemia. *Frontiers in bioscience (Scholar edition)* 4, pp. 61–73.

Feugier, P., Van Hoof, A., Sebban, C., Solal-Celigny, P., Bouabdallah, R., Fermé, C., Christian, B., et al. 2005. Long-term results of the R-CHOP study in the treatment of elderly patients with diffuse large B-cell lymphoma: a study by the Groupe d'Etude des Lymphomes de l'Adulte. *Journal of Clinical Oncology* 23(18), pp. 4117–4126.

Finley, D. 2009. Recognition and processing of ubiquitin-protein conjugates by the proteasome. *Annual review of biochemistry* 78, pp. 477–513.

Focosi, D., Bestagno, M., Burrone, O. and Petrini, M. 2010. CD57+ T lymphocytes and functional immune deficiency. *Journal of leukocyte biology* 87(1), pp. 107–116.

Foster, A.E., Okur, F.V., Biagi, E., Lu, A., Dotti, G., Yvon, E., Savoldo, B., et al. 2010. Selective elimination of a chemoresistant side population of B-CLL cells by cytotoxic T lymphocytes in subjects receiving an autologous hCD40L/IL-2 tumor vaccine. *Leukemia* 24(3), pp. 563–572.

Fourcade, J., Kudela, P., Sun, Z., Shen, H., Land, S.R., Lenzner, D., Guillaume, P., et al. 2009. PD-1 is a regulator of NY-ESO-1-specific CD8+ T cell expansion in melanoma patients. *The Journal of Immunology* 182(9), pp. 5240–5249.

Fourcade, J., Sun, Z., Benallaoua, M., Guillaume, P., Luescher, I.F., Sander, C., Kirkwood, J.M., et al. 2010. Upregulation of Tim-3 and PD-1 expression is associated with tumor antigen-specific CD8+ T cell dysfunction in melanoma patients. *The Journal of Experimental Medicine* 207(10), pp. 2175–2186.

Frankel, S.R. and Baeuerle, P.A. 2013. Targeting T cells to tumor cells using bispecific antibodies. *Current Opinion in Chemical Biology* 17(3), pp. 385–392.

Frassanito, Silvestris, Cafforio and Dammacco 1998. CD8 +/CD57 +cells and apoptosis suppress T-cell functions in multiple myeloma. *British Journal of Haematology* 100(3), pp. 469–477.

Freeman, G.J. and Sharpe, A.H. 2012. A new therapeutic strategy for malaria: targeting T cell exhaustion. *Nature immunology* 13(2), pp. 113–115.

Frishman, J., Long, B., Knospe, W., Gregory, S. and Plate, J. 1993. Genes for interleukin 7 are transcribed in leukemic cell subsets of individuals with chronic lymphocytic leukemia. *The Journal of Experimental Medicine* 177(4), pp. 955–964.

Fruman, D.A. and Rommel, C. 2014. PI3K and cancer: lessons, challenges and opportunities. *Nature Reviews Drug Discovery* 13(2), pp. 140–156.

Fu, D., Calvo, J.A. and Samson, L.D. 2012. Balancing repair and tolerance of DNA damage caused by alkylating agents. *Nature Reviews Cancer* 12(2), pp. 104–120.

Furman, R.R., Sharman, J.P., Coutre, S.E., Cheson, B.D., Pagel, J.M., Hillmen, P., Barrientos, J.C., et al. 2014. Idelalisib and Rituximab in Relapsed Chronic Lymphocytic Leukemia. *New England Journal of Medicine* 370(11), pp. 997–1007.

Gabrilovich, D.I. and Nagaraj, S. 2009. Myeloid-derived suppressor cells as regulators of the immune system. *Nature Reviews Immunology* 9(3), pp. 162–174.

Gaffen, S.L. and Liu, K.D. 2004. Overview of interleukin-2 function, production and clinical applications. *Cytokine* 28(3), pp. 109–123.

Gallagher, K.M.E. and Man, S. 2007. Identification of HLA-DR1- and HLA-DR15-restricted human papillomavirus type 16 (HPV16) and HPV18 E6 epitopes recognized by CD4+ T cells from healthy young women. *Journal of General Virology* 88(5), pp. 1470–1478.

Garbi, N., Tiwari, N., Momburg, F. and Hämmerling, G.J. 2003. A major role for tapasin as a stabilizer of the TAP peptide transporter and consequences for MHC class I expression. *European Journal of Immunology* 33(1), pp. 264–273.

Gattei, V., Bulian, P., Del Principe, M.I., Zucchetto, A., Maurillo, L., Buccisano, F., Bomben, R., et al. 2008. Relevance of CD49d protein expression as overall survival and progressive disease prognosticator in chronic lymphocytic leukemia. *Blood* 111(2), pp. 865–873.

Gattinoni, L., Lugli, E., Ji, Y., Pos, Z., Paulos, C.M., Quigley, M.F., Almeida, J.R., et al. 2011. A human memory T cell subset with stem cell–like properties. *Nature medicine* 17(10), pp. 1290–1297.

Gattinoni, L., Powell, D.J., Rosenberg, S.A. and Restifo, N.P. 2006. Adoptive immunotherapy for cancer: building on success. *Nature Reviews Immunology* 6(5), pp. 383–393.

Gaugler, B., Van den Eynde, B., van der Bruggen, P., Romero, P., Gaforio, J.J., De Plaen, E., Lethé, B., et al. 1994. Human gene MAGE-3 codes for an antigen recognized on a melanoma by autologous cytolytic T lymphocytes. *The Journal of Experimental Medicine* 179(3), pp. 921–930.

Geginat, J., Lanzavecchia, A. and Sallusto, F. 2003. Proliferation and differentiation potential of human CD8+ memory T-cell subsets in response to antigen or homeostatic cytokines. *Blood* 101(11), pp. 4260–4266.

Gerondakis, S., Fulford, T.S., Messina, N.L. and Grumont, R.J. 2014. NF-κB control of T cell development. *Nature immunology* 15(1), pp. 15–25.

Giannopoulos, K., Dmoszynska, A., Kowal, M., Rolinski, J., Gostick, E., Price, D.A., Greiner, J., et al. 2010. Peptide vaccination elicits leukemia-associated antigen-specific

cytotoxic CD8+ T-cell responses in patients with chronic lymphocytic leukemia. *Leukemia* 24(4), pp. 798–805.

Giannopoulos, K., Li, L., Bojarska-Junak, A., Rolinski, J., Dmoszynska, A., Hus, I., Greiner, J., et al. 2006. Expression of RHAMM/CD168 and other tumor-associated antigens in patients with B-cell chronic lymphocytic leukemia. *International journal of oncology* 29(1), pp. 95–103.

Gilmore, T. 2015. *NF-kB Target Genes* [Online]. Available at: http://www.bu.edu/nf-kb/gene-resources/target-genes/ [Accessed: 25 February 2015].

Glickman, M.H. and Ciechanover, A. 2002. The Ubiquitin-Proteasome Proteolytic Pathway: Destruction for the Sake of Construction. *Physiological Reviews* 82, pp. 373–428.

Goding, S.R., Wilson, K.A., Xie, Y., Harris, K.M., Baxi, A., Akpinarli, A., Fulton, A., et al. 2013. Restoring immune function of tumor-specific CD4+ T cells during recurrence of melanoma. *The Journal of Immunology* 190(9), pp. 4899–4909.

Goede, V., Fischer, K., Busch, R., Engelke, A., Eichhorst, B., Wendtner, C.M., Chagorova, T., et al. 2014. Obinutuzumab plus chlorambucil in patients with CLL and coexisting conditions. *New England Journal of Medicine* 370(12), pp. 1101–1110.

Golden-Mason, L., Palmer, B., Klarquist, J., Mengshol, J.A., Castelblanco, N. and Rosen, H.R. 2007. Upregulation of PD-1 Expression on Circulating and Intrahepatic Hepatitis C Virus-Specific CD8+ T Cells Associated with Reversible Immune Dysfunction. *Journal of Virology* 81(17), pp. 9249–9258.

Goldin, L.R., Bjorkholm, M., Kristinsson, S.Y., Turesson, I. and Landgren, O. 2009. Elevated risk of chronic lymphocytic leukemia and other indolent non-Hodgkin's lymphomas among relatives of patients with chronic lymphocytic leukemia. *Haematologica* 94(5), pp. 647–653.

Gorgun, G., Ramsay, A.G., Holderried, T.A.W., Zahrieh, D., Le Dieu, R., Liu, F., Quackenbush, J., et al. 2009. E -TCL1 mice represent a model for immunotherapeutic reversal of chronic lymphocytic leukemia-induced T-cell dysfunction. *Proceedings of the National Academy of Sciences* 106(15), pp. 6250–6255.

Gourley, T.S., Wherry, E.J., Masopust, D. and Ahmed, R. 2004. Generation and maintenance of immunological memory. *Seminars in Immunology* 16(5), pp. 323–333.

Görgün, G., Holderried, T.A.W., Zahrieh, D., Neuberg, D. and Gribben, J.G. 2005. Chronic lymphocytic leukemia cells induce changes in gene expression of CD4 and CD8 T cells. *The Journal of Clinical Investigation* 115(7), pp. 1797–1805.

Göthert, J.R., Eisele, L., Klein-Hitpass, L., Weber, S., Zesewitz, M.-L., Sellmann, L., Röth, A., et al. 2013. Expanded CD8+ T cells of murine and human CLL are driven into a senescent KLRG1+ effector memory phenotype. *Cancer Immunology, Immunotherapy* 62(11), pp. 1697–1709.

Gribben, J.G. 2010. How I treat CLL up front. *Blood* 115(2), pp. 187–197.

Gribben, J.G. 2009. Stem cell transplantation in chronic lymphocytic leukemia. *Biology of blood and marrow transplantation : journal of the American Society for Blood and Marrow Transplantation* 15(1 Suppl), pp. 53–58.

Grupp, S.A., Kalos, M., Barrett, D., Aplenc, R., Porter, D.L., Rheingold, S.R., Teachey, D.T., et al. 2013. Chimeric Antigen Receptor–Modified T Cells for Acute Lymphoid Leukemia. *New England Journal of Medicine* 368(16), pp. 1509–1518.

Hacken, ten, E. and Burger, J.A. 2014. Molecular pathways: targeting the microenvironment in chronic lymphocytic leukemia--focus on the B-cell receptor. *Clinical Cancer Research* 20(3), pp. 548–556.

Hainsworth, J.D., Litchy, S., Barton, J.H., Houston, G.A., Hermann, R.C., Bradof, J.E. and Greco, F.A. 2003. Single-agent rituximab as first-line and maintenance treatment for patients with chronic lymphocytic leukemia or small lymphocytic lymphoma: a phase II trial of the Minnie Pearl Cancer Research Network. *Journal of Clinical Oncology* 21(9), pp. 1746–1751.

Hallek, M. 2005. Chronic Lymphocytic Leukemia (CLL): First-Line Treatment. *Hematology / the Education Program of the American Society of Hematology. American Society of Hematology. Education Program* 2005(1), pp. 285–291.

Hallek, M., Fischer, K., Fingerle-Rowson, G., Fink, A.M., Busch, R., Mayer, J., Hensel, M., et al. 2010. Addition of rituximab to fludarabine and cyclophosphamide in patients with chronic lymphocytic leukaemia: a randomised, open-label, phase 3 trial. *Lancet* 376(9747), pp. 1164–1174.

Hamblin, T.J., Davis, Z., Gardiner, A., Oscier, D.G. and Stevenson, F.K. 1999. Unmutated Ig VH Genes Are Associated With a More Aggressive Form of Chronic Lymphocytic Leukemia. *Blood* 94(6), pp. 1848–1854.

Hamid, O., Robert, C., Daud, A., Hodi, F.S., Hwu, W.-J., Kefford, R., Wolchok, J.D., et al. 2013. Safety and tumor responses with lambrolizumab (anti-PD-1) in melanoma. *New England Journal of Medicine* 369(2), pp. 134–144.

Hanna, B., McClanahan, F., Clear, A., Miller, S., Lichter, P., Seiffert, M and Gribben, J. 2014. Immune Checkpoint Blockade with Anti-PD-L1 Prevents Immune Dysfuntion and CLL Development in the TCL1 Adoptive Transfer Mouse Model. *56th American Society of Hematology Annual Meeting & Exposition*. San Francisco, 6-9 December. Blood

Hannier, S. and Triebel, F. 1999. The MHC class II ligand lymphocyte activation gene-3 is co-distributed with CD8 and CD3–TCR molecules after their engagement by mAb or peptide–MHC class I complexes. *International immunology* 11(11), pp. 1745–1752.

Hannier, S., Tournier, M., Bismuth, G. and Triebel, F. 1998. CD3/TCR complex-associated lymphocyte activation gene-3 molecules inhibit CD3/TCR signaling. *The Journal of Immunology* 161(8), pp. 4058–4065.

Hanson, D.A., Kaspar, A.A., Poulain, F.R. and Krensky, A.M. 1999. Biosynthesis of granulysin, a novel cytolytic molecule. *Molecular Immunology* 36(7), pp. 413–422.

Hardy, L.L., Wick, D.A. and Webb, J.R. 2008. Conversion of tyrosine to the inflammation-associated analog 3′-nitrotyrosine at either TCR-or MHC-contact positions can profoundly affect recognition of the MHC class I-restricted epitope of lymphocytic choriomeningitis virus glycoprotein 33 by CD8 T cells. *The Journal of Immunology* 180(9), pp. 5956–5962.

Haribhai, D., Williams, J.B., Jia, S., Nickerson, D., Schmitt, E.G., Edwards, B., Ziegelbauer, J., et al. 2011. A Requisite Role for Induced Regulatory T Cells in Tolerance Based on Expanding Antigen Receptor Diversity. *Immunity* 35(1), pp. 109–122.

Harndahl, M., Justesen, S., Lamberth, K., Røder, G., Nielsen, M. and Buus, S. 2009. Peptide binding to HLA class I molecules: homogenous, high-throughput screening, and affinity assays. *Journal of biomolecular screening* 14(2), pp. 173–180.

Hayashida, K., Shimaoka, Y., Ochi, T. and Lipsky, P.E. 2000. Rheumatoid arthritis synovial stromal cells inhibit apoptosis and up-regulate Bcl-xL expression by B cells in a CD49/CD29-CD106-dependent mechanism. *The Journal of Immunology* 164(2), pp. 1110–1116.

He, L.-Z., Prostak, N., Thomas, L.J., Vitale, L., Weidlick, J., Crocker, A., Pilsmaker, C.D., et al. 2013. Agonist anti-human CD27 monoclonal antibody induces T cell activation and tumor immunity in human CD27-transgenic mice. *The Journal of Immunology* 191(8), pp. 4174–4183.

Hegazy, A.N., Peine, M., Helmstetter, C., Panse, I., Fröhlich, A., Bergthaler, A., Flatz, L., et al. 2010. Interferons direct Th2 cell reprogramming to generate a stable GATA-3(+)T-bet(+) cell subset with combined Th2 and Th1 cell functions. *Immunity* 32(1), pp. 116–128.

Heibein, J.A., Goping, I.S., Barry, M., Pinkoski, M.J., Shore, G.C., Green, D.R. and Bleackley, R.C. 2000. Granzyme B-Mediated Cytochrome C Release Is Regulated by the Bcl-2 Family Members Bid and Bax. *The Journal of Experimental Medicine* 192(10), pp. 1391–1402.

Herishanu, Y., Perez-Galan, P., Liu, D., Biancotto, A., Pittaluga, S., Vire, B., Gibellini, F., et al. 2011. The lymph node microenvironment promotes B-cell receptor signaling, NF- B activation, and tumor proliferation in chronic lymphocytic leukemia. *Blood* 117(2), pp. 563–574.

Herman, S.E.M., Sun, X., McAuley, E.M., Hsieh, M.M., Pittaluga, S., Raffeld, M., Liu, D., et al. 2013. Modeling tumor–host interactions of chronic lymphocytic leukemia in xenografted mice to study tumor biology and evaluate targeted therapy. *Leukemia* 27(12), pp. 2311–2321.

Hendriks, J., Gravestein, L.A., Tesselaar, K., van Lier, R.A., Schumacher, T.N. and Borst, J. 2000. CD27 is required for generation and long-term maintenance of T cell immunity. *Nature immunology* 1(5), pp. 433–440.

Hendriks, R.W., Yuvaraj, S. and Kil, L.P. 2014. Targeting Bruton's tyrosine kinase in B cell malignancies. *Nature Reviews Cancer* 14(4), pp. 219–232.

Henrickson, S.E., Mempel, T.R., Mazo, I.B., Liu, B., Artyomov, M.N., Zheng, H., Peixoto, A., et al. 2008. In Vivo Imaging of T Cell Priming. *Science Signaling* 1(12), pp. pt2–pt2.

Herman, S.E.M., Gordon, A.L., Hertlein, E., Ramanunni, A., Zhang, X., Jaglowski, S., Flynn, J., et al. 2011. Bruton tyrosine kinase represents a promising therapeutic target for treatment of chronic lymphocytic leukemia and is effectively targeted by PCI-32765. *Blood* 117(23), pp. 6287–6296.

Hershko, A., Ciechanover, A., Heller, H., Haas, A.L. and Rose, I.A. 1980. Proposed role of ATP in protein breakdown: conjugation of protein with multiple chains of the polypeptide of ATP-dependent proteolysis. *Proceedings of the National Academy of Sciences* 77(4), pp. 1783–1786.

Heslop, H.E. 2010. Safer CARS. *Molecular Therapy* 18(4), pp. 661–662.

Hewitt, E.W. 2003. The MHC class I antigen presentation pathway: strategies for viral immune evasion. *Immunology* 110(2), pp. 163–169.

Hicklin, D.J., Marincola, F.M. and Ferrone, S. 1999. HLA class I antigen downregulation in human cancers: T-cell immunotherapy revives an old story. *Molecular Medicine Today* 5(4), pp. 178–186.

Hinrichs, C.S., Borman, Z.A., Gattinoni, L., Yu, Z., Burns, W.R., Huang, J., Klebanoff, C.A., et al. 2011. Human effector CD8+ T cells derived from naive rather than memory subsets possess superior traits for adoptive immunotherapy. *Blood* 117(3), pp. 808–814.

Hodi, F.S., O'Day, S.J., McDermott, D.F., Weber, R.W., Sosman, J.A., Haanen, J.B., Gonzalez, R., et al. 2010. Improved Survival with Ipilimumab in Patients with Metastatic Melanoma. *New England Journal of Medicine* 363(8), pp. 711–723.

Hoellenriegel, J., Meadows, S.A., Sivina, M., Wierda, W.G., Kantarjian, H., Keating, M.J., Giese, N., et al. 2011. The phosphoinositide 3'-kinase delta inhibitor, CAL-101, inhibits B-cell receptor signaling and chemokine networks in chronic lymphocytic leukemia. *Blood* 118(13), pp. 3603–3612.

Hong, J.J., Rosenberg, S.A., Dudley, M.E., Yang, J.C., White, D.E., Butman, J.A. and Sherry, R.M. 2010. Successful Treatment of Melanoma Brain Metastases with Adoptive Cell Therapy. *Clinical Cancer Research* 16(19), pp. 4892–4898.

Honma, K., Kimura, D., Tominaga, N., Miyakoda, M., Matsuyama, T. and Yui, K. 2008. Interferon regulatory factor 4 differentially regulates the production of Th2 cytokines in naive vs. effector/memory CD4+ T cells. *Proceedings of the National Academy of Sciences* 105(41), pp. 15890–15895.

Hori, S., Nomura, T. and Sakaguchi, S. 2003. Control of regulatory T cell development by the transcription factor Foxp3. *Science* 299(5609), pp. 1057–1061.

Hsu, S.C., Gavrilin, M.A., Lee, H.H., Wu, C.C., Han, S.H. and Lai, M.Z. 1999. NF-kappa B-dependent Fas ligand expression. *European Journal of Immunology* 29(9), pp. 2948–2956.

Huang, C., Bi, E., Hu, Y., Deng, W., Tian, Z., Dong, C., Hu, Y., et al. 2006. A novel NF-kappaB binding site controls human granzyme B gene transcription. *The Journal of Immunology* 176(7), pp. 4173–4181.

Huard, B., Prigent, P., Tournier, M., Bruniquel, D. and Triebel, F. 1995. CD4/major histocompatibility complex class II interaction analyzed with CD4-and lymphocyte activation gene-3 (LAG-3)-Ig fusion proteins. *European Journal of Immunology* 25(9), pp. 2718–2721.

Hudecek, M., Lupo-Stanghellini, M.T., Kosasih, P.L., Sommermeyer, D., Jensen, M.C., Rader, C. and Riddell, S.R. 2013. Receptor Affinity and Extracellular Domain Modifications Affect Tumor Recognition by ROR1-Specific Chimeric Antigen Receptor T Cells. *Clinical Cancer Research* 19(12), pp. 3153–3164.

Hudecek, M., Schmitt, T.M., Baskar, S., Lupo-Stanghellini, M.T., Nishida, T., Yamamoto, T.N., Bleakley, M., et al. 2010. The B-cell tumor-associated antigen ROR1 can be targeted with T cells modified to express a ROR1-specific chimeric antigen receptor. *Blood* 116(22), pp. 4532–4541.

Hudis, C.A. 2007. Trastuzumab--mechanism of action and use in clinical practice. *New*

England Journal of Medicine 357(1), pp. 39–51.

Ibegbu, C.C., Xu, Y.-X., Harris, W., Maggio, D., Miller, J.D. and Kourtis, A.P. 2005. Expression of killer cell lectin-like receptor G1 on antigen-specific human CD8+ T lymphocytes during active, latent, and resolved infection and its relation with CD57. *The Journal of Immunology* 174(10), pp. 6088–6094.

Ito, D., Visus, C., Hoffmann, T.K., Balz, V., Bier, H., Appella, E., Whiteside, T.L., et al. 2007. Immunological characterization of missense mutations occurring within cytotoxic T cell-defined p53 epitopes in HLA-A*0201+ squamous cell carcinomas of the head and neck. *International Journal of Cancer* 120(12), pp. 2618–2624.

Ivanov, I.I., McKenzie, B.S., Zhou, L., Tadokoro, C.E., Lepelley, A., Lafaille, J.J., Cua, D.J., et al. 2006. The Orphan Nuclear Receptor RORγt Directs the Differentiation Program of Proinflammatory IL-17+ T Helper Cells. *Cell* 126(6), pp. 1121–1133.

Janeway, C.A. 2012. *Janeway's Immunobiology 8th Ed.* Garland Science.

Janeway, C.A. and Medzhitov, R. 2002. Innate immune recognition. *Annual Review of Immunology* 20, pp. 197–216.

Jäger, D., Jäger, E. and Knuth, A. 2001. Immune responses to tumour antigens: implications for antigen specific immunotherapy of cancer. *Journal of clinical pathology* 54(9), pp. 669–674.

Jiang, S. and Dong, C. 2013. A complex issue on CD4(+) T-cell subsets. *Immunological reviews* 252(1), pp. 5–11.

Johnson, A.J. 2006. Characterization of the TCL-1 transgenic mouse as a preclinical drug development tool for human chronic lymphocytic leukemia. *Blood* 108(4), pp. 1334–1338.

Jones, C., Lin, T., Pratt, G., Fegan, C., Baird, D., and Pepper, C. 2013. Longitudinal Analysis Reveals Telomere Length Maintenance In CLL B-Cells But Marked Erosion In CLL Patient T-Cells. *55th American Society of Hematology Annual Meeting & Exposition*. New Orleans, 7-10 December. Blood.

Jonker, D.J., O'Callaghan, C.J., Karapetis, C.S., Zalcberg, J.R., Tu, D., Au, H.-J., Berry, S.R., et al. 2007. Cetuximab for the Treatment of Colorectal Cancer. *New England Journal of Medicine* 357(20), pp. 2040–2048.

Ju, S.-T., Panka, D.J., Cui, H., Ettinger, R., EI-Khatib, M., Sherr, D.H., Stanger, B.Z., et al. 1995. Fas(CD95)/FasL interactions required for programmed cell death after T-cell activation. *Nature* 373(6513), pp. 444–448.

June, C.H. 2007. Adoptive T cell therapy for cancer in the clinic. *The Journal of Clinical Investigation* 117(6), pp. 1466–1476.

Kaech, S.M. and Cui, W. 2012. Transcriptional control of effector and memory CD8+ T cell differentiation. *Nature Reviews Immunology* 12(11), pp. 749–761.

Kalos, M., Levine, B.L., Porter, D.L., Katz, S., Grupp, S.A., Bagg, A. and June, C.H. 2011. T cells with chimeric antigen receptors have potent antitumor effects and can establish memory in patients with advanced leukemia. *Science Translational Medicine* 3(95), p. 95ra73.

Kantoff, P.W., Higano, C.S., Shore, N.D., Berger, E.R., Small, E.J., Penson, D.F., Redfern,

C.H., et al. 2010. Sipuleucel-T Immunotherapy for Castration-Resistant Prostate Cancer. *New England Journal of Medicine* 363(5), pp. 411–422.

Kaspar, A.A., Okada, S., Kumar, J., Poulain, F.R., Drouvalakis, K.A., Kelekar, A., Hanson, D.A., et al. 2001. A Distinct Pathway of Cell-Mediated Apoptosis Initiated by Granulysin. *The Journal of Immunology* 167(1), pp. 350–356.

Kawakami, Y., Eliyahu, S., Jennings, C., Sakaguchi, K., Kang, X., Southwood, S., Robbins, P.F., et al. 1995. Recognition of multiple epitopes in the human melanoma antigen gp100 by tumor-infiltrating T lymphocytes associated with in vivo tumor regression. *The Journal of Immunology* 154(8), pp. 3961–3968.

Keating, M.J., Flinn, I., Jain, V., Binet, J.-L., Hillmen, P., Byrd, J., Albitar, M., et al. 2002. Therapeutic role of alemtuzumab (Campath-1H) in patients who have failed fludarabine: results of a large international study. *Blood* 99(10), pp. 3554–3561.

Keir, M.E., Butte, M.J., Freeman, G.J. and Sharpe, A.H. 2008. PD-1 and its ligands in tolerance and immunity. *Annual Review of Immunology* 26, pp. 677–704.

Kerkar, S.P. and Restifo, N.P. 2012. Cellular constituents of immune escape within the tumor microenvironment. *Cancer Research* 72(13), pp. 3125–3130.

Kershaw, M.H., Westwood, J.A., Slaney, C.Y. and Darcy, P.K. 2014. Clinical application of genetically modified T cells in cancer therapy. *Clinical & translational immunology* 3(5), p. e16.

Khaled, Y.S., Ammori, B.J. and Elkord, E. 2013. Myeloid-derived suppressor cells in cancer: recent progress and prospects. *Immunology and cell biology* 91(8), pp. 493–502.

Khanna, R. 2004. Predictive algorithms and T cell epitope mapping. *The Journal of Immunology* 173(5), pp. 2895–author reply 2895–6.

Kiaii, S., Kokhaei, P., Mozaffari, F., Rossmann, E., Pak, F., Moshfegh, A., Palma, M., et al. 2013. T cells from indolent CLL patients prevent apoptosis of leukemic B cells in vitro and have altered gene expression profile. *Cancer Immunology, Immunotherapy* 62(1), pp. 51–63.

Kim, R., Emi, M. and Tanabe, K. 2007. Cancer immunoediting from immune surveillance to immune escape. *Immunology* 121(1), pp. 1–14.

Kim, R., Emi, M., Tanabe, K. and Arihiro, K. 2006. Tumor-driven evolution of immunosuppressive networks during malignant progression. *Cancer Research* 66(11), pp. 5527–5536.

King, J., Waxman, J. and Stauss, H. 2008. Advances in tumour immunotherapy. *QJM : monthly journal of the Association of Physicians* 101(9), pp. 675–683.

Klebanoff, C.A., Acquavella, N., Yu, Z. and Restifo, N.P. 2010. Therapeutic cancer vaccines: are we there yet? *Immunological reviews* 239(1), pp. 27–44.

Klebanoff, C.A., Gattinoni, L. and Restifo, N.P. 2006. CD8+ T-cell memory in tumor immunology and immunotherapy. *Immunological reviews* 211, pp. 214–224.

Klebanoff, C.A., Gattinoni, L. and Restifo, N.P. 2012. Sorting Through Subsets. *Journal of Immunotherapy* 35(9), pp. 651–660.

Knauf, W.U., Lissichkov, T., Aldaoud, A., Liberati, A., Loscertales, J., Herbrecht, R.,

Juliusson, G., et al. 2009. Phase III Randomized Study of Bendamustine Compared With Chlorambucil in Previously Untreated Patients With Chronic Lymphocytic Leukemia. *Journal of Clinical Oncology* 27(26), pp. 4378–4384.

Kobayashi, K.S. and van den Elsen, P.J. 2012. NLRC5: a key regulator of MHC class I-dependent immune responses. *Nature Reviews Immunology* 12(12), pp. 813–820.

Kochenderfer, J.N., Dudley, M.E., Feldman, S.A., Wilson, W.H., Spaner, D.E., Maric, I., Stetler-Stevenson, M., et al. 2012. B-cell depletion and remissions of malignancy along with cytokine-associated toxicity in a clinical trial of anti-CD19 chimeric-antigen-receptor-transduced T cells. *Blood* 119(12), pp. 2709–2720.

Koelle, D.M., Chen, H.B., Gavin, M.A., Wald, A., Kwok, W.W. and Corey, L. 2001. CD8 CTL from genital herpes simplex lesions: recognition of viral tegument and immediate early proteins and lysis of infected cutaneous cells. *The Journal of Immunology* 166(6), pp. 4049–4058.

Kono, K., Takahashi, A., Ichihara, F., Amemiya, H., Iizuka, H., Fujii, H., Sekikawa, T., et al. 2002. Prognostic significance of adoptive immunotherapy with tumor-associated lymphocytes in patients with advanced gastric cancer: a randomized trial. *Clinical Cancer Research* 8(6), pp. 1767–1771.

Koopman, G., Keehnen, R.M., Lindhout, E., Newman, W., Shimizu, Y., van Seventer, G.A., de Groot, C., et al. 1994. Adhesion through the LFA-1 (CD11a/CD18)-ICAM-1 (CD54) and the VLA-4 (CD49d)-VCAM-1 (CD106) pathways prevents apoptosis of germinal center B cells. *The Journal of Immunology* 152(8), pp. 3760–3767.

Kouro, T. and Takatsu, K. 2009. IL-5- and eosinophil-mediated inflammation: from discovery to therapy. *International immunology* 21(12), pp. 1303–1309.

Kurosaki, T., Kometani, K. and Ise, W. 2015. Memory B cells. *Nature Reviews Immunology* 15(3), pp. 149–159.

Landsverk, O.J.B., Bakke, O. and Gregers, T.F. 2009. MHC II and the Endocytic Pathway: Regulation by Invariant Chain. *Scandinavian Journal of Immunology* 70(3), pp. 184–193.

Larson, R.A., Sievers, E.L., Stadtmauer, E.A., Löwenberg, B., Estey, E.H., Dombret, H., Theobald, M., et al. 2005. Final report of the efficacy and safety of gemtuzumab ozogamicin (Mylotarg) in patients with CD33-positive acute myeloid leukemia in first recurrence. *Cancer* 104(7), pp. 1442–1452.

Lee, H.-W., Park, S.-J., Choi, B.K., Kim, H.H., Nam, K.-O. and Kwon, B.S. 2002. 4-1BB promotes the survival of CD8+ T lymphocytes by increasing expression of Bcl-xL and Bfl-1. *The Journal of Immunology* 169(9), pp. 4882–4888.

Lee, J., Su, E.W., Zhu, C., Hainline, S., Phuah, J., Moroco, J.A., Smithgall, T.E., et al. 2011. Phosphotyrosine-Dependent Coupling of Tim-3 to T-Cell Receptor Signaling Pathways. *Molecular and Cellular Biology* 31(19), pp. 3963–3974.

Li, F.-J., Zhang, Y., Jin, G.-X., Yao, L. and Wu, D.-Q. 2013. Expression of LAG-3 is coincident with the impaired effector function of HBV-specific CD8+ T cell in HCC patients. *Immunology Letters* 150(1-2), pp. 116–122.

Li, Z. 2004. The generation of antibody diversity through somatic hypermutation and class switch recombination. *Genes & Development* 18(1), pp. 1–11.

Lichtenegger, F.S., Schnorfeil, F.M., Emmerig, K., Neitz, J.S., Beck, B., Draenert, R., Hiddemann, W., et al. 2013. Pseudo-Exhaustion Of CD8+ T Cells in AML. *55th American Society of Hematology Annual Meeting & Exposition*. New Orleans, 7-10 December. Blood.

Lieberman, J. 2010. Anatomy of a murder: how cytotoxic T cells and NK cells are activated, develop, and eliminate their targets. *Immunological reviews* 235(1), pp. 5–9.

Lin, K., Doolan, K., Hung, C.-F. and Wu, T.-C. 2010. Perspectives for preventive and therapeutic HPV vaccines. *Journal of the Formosan Medical Association = Taiwan yi zhi* 109(1), pp. 4–24.

Linsley, P.S. and Ledbetter, J.A. 1993. The role of the CD28 receptor during T cell responses to antigen. *Annual Review of Immunology* 11, pp. 191–212.

Liu, D.-W., Yang, Y.-C., Lin, H.-F., Lin, M.-F., Cheng, Y.-W., Chu, C.-C., Tsao, Y.-P., et al. 2007. Cytotoxic T-lymphocyte responses to human papillomavirus type 16 E5 and E7 proteins and HLA-A*0201-restricted T-cell peptides in cervical cancer patients. *Journal of Virology* 81(6), pp. 2869–2879.

Liu, F.T., Agrawal, S.G., Gribben, J.G., Ye, H., Du, M.Q., Newland, A.C. and Jia, L. 2008. Bortezomib blocks Bax degradation in malignant B cells during treatment with TRAIL. *Blood* 111(5), pp. 2797–2805.

Liu, Z., Fan, H. and Jiang, S. 2013. CD4(+) T-cell subsets in transplantation. *Immunological reviews* 252(1), pp. 183–191.

Lohoff, M., Mittrücker, H.-W., Brüstle, A., Sommer, F., Casper, B., Huber, M., Ferrick, D.A., et al. 2004. Enhanced TCR-induced apoptosis in interferon regulatory factor 4-deficient CD4(+) Th cells. *The Journal of Experimental Medicine* 200(2), pp. 247–253.

Long, B.W., Witte, P.L., Abraham, G.N., Gregory, S.A. and Plate, J.M. 1995. Apoptosis and interleukin 7 gene expression in chronic B-lymphocytic leukemia cells. *Proceedings of the National Academy of Sciences* 92(5), pp. 1416–1420.

Long, E.O., Kim, H.S., Liu, D., Peterson, M.E. and Rajagopalan, S. 2013. Controlling Natural Killer Cell Responses: Integration of Signals for Activation and Inhibition. *Annual Review of Immunology* 31, pp. 227–258.

Lotz, M., Jirik, F., Kabouridis, P., Tsoukas, C., Hirano, T., Kishimoto, T. and Carson, D.A. 1988. B cell stimulating factor 2/interleukin 6 is a costimulant for human thymocytes and T lymphocytes. *The Journal of Experimental Medicine* 167(3), pp. 1253–1258.

Lugli, E., Dominguez, M.H., Gattinoni, L., Chattopadhyay, P.K., Bolton, D.L., Song, K., Klatt, N.R., et al. 2013. Superior T memory stem cell persistence supports long-lived T cell memory. *The Journal of Clinical Investigation* 123(2), pp. 594–599.

Luhder, F., Huang, Y., Dennehy, K.M., Guntermann, C., Muller, I., Winkler, E., Kerkau, T., et al. 2003. Topological Requirements and Signaling Properties of T Cell-activating, Anti-CD28 Antibody Superagonists. *The Journal of Experimental Medicine* 197(8), pp. 955–966.

Lukenbill, J. and Kalaycio, M. 2013. Fludarabine: A review of the clear benefits and potential harms. *Leukemia research* 37(9), pp. 986–994.

Lundin, J., Kimby, E., Björkholm, M., Broliden, P.-A., Celsing, F., Hjalmar, V., Möllgård, L., et al. 2002. Phase II trial of subcutaneous anti-CD52 monoclonal antibody alemtuzumab (Campath-1H) as first-line treatment for patients with B-cell chronic lymphocytic leukemia (B-CLL). *Blood* 100(3), pp. 768–773.

Lundt, B.F., Johansen, N.L. and Markussen, J. 1979. FORMATION AND SYNTHESIS OF 3 '-t-BUTYLTYROSINE. *International journal of peptide and protein research* 14(4), pp. 344–346.

Mackus, W.J.M. 2003. Expansion of CMV-specific CD8+CD45RA+CD27- T cells in B-cell chronic lymphocytic leukemia. *Blood* 102(3), pp. 1057–1063.

Maeurer, M.J., Necker, A., Salter, R.D., Castelli, C., Höhn, H., Karbach, J., Freitag, K., et al. 2002. Improved detection of melanoma antigen-specific T cells expressing low or high levels of CD8 by HLA-A2 tetramers presenting a Melan-A/Mart-1 peptide analogue. *International Journal of Cancer* 97(1), pp. 64–71.

Mainou-Fowler, T., Craig, V.A., Copplestone, J.A., Hamon, M.D. and Prentice, A.G. 1994. Interleukin-5 (IL-5) increases spontaneous apoptosis of B-cell chronic lymphocytic leukemia cells in vitro independently of bcl-2 expression and is inhibited by IL-4. *Blood* 84(7), pp. 2297–2304.

Majid, A., Lin, T.T., Best, G., Fishlock, K., Hewamana, S., Pratt, G., Yallop, D., et al. 2011. CD49d is an independent prognostic marker that is associated with CXCR4 expression in CLL. *Leukemia research* 35(6), pp. 750–756.

Malavasi, F., Deaglio, S., Damle, R., Cutrona, G., Ferrarini, M. and Chiorazzi, N. 2011. CD38 and chronic lymphocytic leukemia: a decade later. *Blood* 118(13), pp. 3470–3478.

Maloney, D.G., Grillo-López, A.J., White, C.A., Bodkin, D., Schilder, R.J., Neidhart, J.A., Janakiraman, N., et al. 1997. IDEC-C2B8 (Rituximab) anti-CD20 monoclonal antibody therapy in patients with relapsed low-grade non-Hodgkin's lymphoma. *Blood* 90(6), pp. 2188–2195.

Mannering, S.I., Purcell, A.W., Honeyman, M.C., McCluskey, J. and Harrison, L.C. 2003. Human T-cells recognise N-terminally Fmoc-modified peptide. *Vaccine* 21(25-26), pp. 3638–3646.

Mantovani, A., Cassatella, M.A., Costantini, C. and Jaillon, S. 2011. Neutrophils in the activation and regulation of innate and adaptive immunity. *Nature Reviews Immunology* 11(8), pp. 519–531.

Mariotti, S. and Nisini, R. 2009. Generation of human T cell clones. *Methods in molecular biology (Clifton, N.J.)* 514, pp. 65–93.

Marks, M.S., Roche, P.A., van Donselaar, E., Woodruff, L., Peters, P.J. and Bonifacino, J.S. 1995. A lysosomal targeting signal in the cytoplasmic tail of the beta chain directs HLA-DM to MHC class II compartments. *The Journal of Cell Biology* 131(2), pp. 351–369.

Matsuzaki, J., Gnjatic, S., Mhawech-Fauceglia, P., Beck, A., Miller, A., Tsuji, T., Eppolito, C., et al. 2010. Tumor-infiltrating NY-ESO-1-specific CD8+ T cells are negatively regulated by LAG-3 and PD-1 in human ovarian cancer. *Proceedings of the National Academy of Sciences* 107(17), pp. 7875–7880.

Maupin-Furlow, J. 2011. Proteasomes and protein conjugation across domains of life.

Nature Reviews Microbiology 10(2), pp. 100–111.

Maus, M.V., Grupp, S.A., Porter, D.L. and June, C.H. 2014. Antibody-modified T cells: CARs take the front seat for hematologic malignancies. *Blood* 123(17), pp. 2625–2635.

Mayr, C., Bund, D., Schlee, M., Bamberger, M., Kofler, D.M., Hallek, M. and Wendtner, C.-M. 2006. MDM2 is recognized as a tumor-associated antigen in chronic lymphocytic leukemia by CD8+ autologous T lymphocytes. *Experimental Hematology* 34(1), pp. 44–53.

Mayr, C., Bund, D., Schlee, M., Moosmann, A., Kofler, D.M., Hallek, M. and Wendtner, C.-M. 2005. Fibromodulin as a novel tumor-associated antigen (TAA) in chronic lymphocytic leukemia (CLL), which allows expansion of specific CD8+ autologous T lymphocytes. *Blood* 105(4), pp. 1566–1573.

McClanahan, F., Miller, S., Riches, J., Ghazaly, E., Day, W., Capasso, M., and Gribben, J. 2013. T-Cell Dysfunction In CLL Is Mediated Not Only By PD-1/PD-L1 But Also By PD-1/PD-L2 Interactions - Partial Functionality Is Maintained In PD-1 Defined CD8 Subsets and This Can Be Further Promoted By Ibrutinib Treatment. *55th American Society of Hematology Annual Meeting & Exposition*. New Orleans, 7-10 December. Blood.

McClanahan, F., Riches, J., Ghazaly, E., Hanna, B., Day, W., Capasso, M., and Gribben, J. 2014. PD-1/PD-L1 mediated T-cell dysfunction in CLL is not absolute and can be at least partially reversed *in vivo* by the immune-modulatory drug lenalidomide. *NCRI Cancer Conference*. London, 2 - 5 November.

McMahan, R.H., Golden-Mason, L., Nishimura, M.I., McMahon, B.J., Kemper, M., Allen, T.M., Gretch, D.R., et al. 2010. Tim-3 expression on PD-1+ HCV-specific human CTLs is associated with viral persistence, and its blockade restores hepatocyte-directed in vitro cytotoxicity. *The Journal of Clinical Investigation* 120(12), p. 4546.

Medzhitov, R. and Janeway, C.A. 2002. Decoding the patterns of self and nonself by the innate immune system. *Science* 296(5566), pp. 298–300.

Mempel, T.R., Henrickson, S.E. and Andrian, von, U.H. 2004. T-cell priming by dendriticcells in lymph nodes occurs in three distinct phases. *Nature* 427(6970), pp. 154–159.

Menendez, D., Inga, A. and Resnick, M.A. 2009. The expanding universe of p53 targets. *Nature Reviews Cancer* 9(10), pp. 724–737.

Messmer, B.T., Messmer, D., Allen, S.L., Kolitz, J.E., Kudalkar, P., Cesar, D., Murphy, E.J., et al. 2005. In vivo measurements document the dynamic cellular kinetics of chronic lymphocytic leukemia B cells. *The Journal of Clinical Investigation* 115(3), pp. 755–764.

Meydan, C., Otu, H.H. and Sezerman, O. 2013. Prediction of peptides binding to MHC class I and II alleles by temporal motif mining. *BMC Bioinformatics* 14(Suppl 2), p. S13.

Mittendorf, E.A., Clifton, G.T., Holmes, J.P., Clive, K.S., Patil, R., Benavides, L.C., Gates, J.D., et al. 2011. Clinical trial results of the HER-2/neu (E75) vaccine to prevent breast cancer recurrence in high-risk patients. *Cancer* 118(10), pp. 2594–2602.

Montillo, M., Ricci, F., Miqueleiz, S., Tedeschi, A. and Morra, E. 2008. Alemtuzumab in the treatment of fludarabine refractory B-cell chronic lymphocytic leukemia (CLL). *Biologics : targets & therapy* 2(1), pp. 41–52.

Morgan, R.A., Yang, J.C., Kitano, M., Dudley, M.E., Laurencot, C.M. and Rosenberg, S.A. 2010. Case Report of a Serious Adverse Event Following the Administration of T Cells Transduced With a Chimeric Antigen Receptor Recognizing ERBB2. *Molecular Therapy* 18(4), pp. 843–851.

Morrison, V.A. 2010. Infectious complications of chronic lymphocytic leukaemia: pathogenesis, spectrum of infection, preventive approaches. *Best practice & research. Clinical haematology* 23(1), pp. 145–153.

Muniz, V.S., Weller, P.F. and Neves, J.S. 2012. Eosinophil crystalloid granules: structure, function, and beyond. *Journal of leukocyte biology* 92(2), pp. 281–288.

Murray, P.J. and Wynn, T.A. 2011. Protective and pathogenic functions of macrophage subsets. *Nature Reviews Immunology* 11(11), pp. 723–737.

Nakayamada, S., Takahashi, H., Kanno, Y. and O'Shea, J.J. 2012. Helper T cell diversity and plasticity. *Current opinion in immunology* 24(3), pp. 297–302.

Nandi, D., Jiang, H. and Monaco, J.J. 1996. Identification of MECL-1 (LMP-10) as the third IFN-gamma-inducible proteasome subunit. *The Journal of Immunology* 156(7), pp. 2361–2364.

Neefjes, J., Jongsma, M.L.M., Paul, P. and Bakke, O. 2011. Towards a systems understanding of MHC class I and MHC class II antigen presentation. *Nature Reviews Immunology* 11(12), pp. 823–836.

Neefjes, J.J., Momburg, F. and Hämmerling, G.J. 1993. Selective and ATP-dependent translocation of peptides by the MHC-encoded transporter. *Science* 261(5122), pp. 769–771.

Ngiow, S.F., Scheidt, von, B., Akiba, H., Yagita, H., Teng, M.W.L. and Smyth, M.J. 2011. Anti-TIM3 Antibody Promotes T Cell IFN- -Mediated Antitumor Immunity and Suppresses Established Tumors. *Cancer Research* 71(10), pp. 3540–3551.

Noelle, R.J., Roy, M., Shepherd, D.M., Stamenkovic, I., Ledbetter, J.A. and Aruffo, A. 1992. A 39-kDa protein on activated helper T cells binds CD40 and transduces the signal for cognate activation of B cells. *Proceedings of the National Academy of Sciences of the United States of America* 89(14), pp. 6550–6554.

Nunes, C., Wong, R., Mason, M., Fegan, C., Man, S. and Pepper, C. 2012. Expansion of a CD8+PD-1+ Replicative Senescence Phenotype in Early Stage CLL Patients Is Associated with Inverted CD4:CD8 Ratios and Disease Progression. *Clinical Cancer Research* 18(3), pp. 678–687.

Nunes, C.T., Miners, K.L., Dolton, G., Pepper, C., Fegan, C., Mason, M.D. and Man, S. 2011. A novel tumor antigen derived from enhanced degradation of bax protein in human cancers. *Cancer Research* 71(16), pp. 5435–5444.

Nurieva, R.I., Chung, Y., Martinez, G.J., Yang, X.O., Tanaka, S., Matskevitch, T.D., Wang, Y.H., et al. 2009. Bcl6 Mediates the Development of T Follicular Helper Cells. *Science* 325(5943), pp. 1001–1005.

Nückel, H., Switala, M., Collins, C.H., Sellmann, L., Grosse-Wilde, H., Dührsen, U. and Rebmann, V. 2009. High CD49d protein and mRNA expression predicts poor outcome in chronic lymphocytic leukemia. *Clinical Immunology* 131(3), pp. 472–480.

Ochsenbein, A.F. 2004. CD27 Expression Promotes Long-Term Survival of Functional Effector-Memory CD8+ Cytotoxic T Lymphocytes in HIV-infected Patients. *The Journal of Experimental Medicine* 200(11), pp. 1407–1417.

Oh, J.M., Kim, S.H., Cho, E.A., Song, Y.S., Kim, W.H. and Juhnn, Y.S. 2010. Human papillomavirus type 16 E5 protein inhibits hydrogen peroxide-induced apoptosis by stimulating ubiquitin-proteasome-mediated degradation of Bax in human cervical cancer cells. *Carcinogenesis* 31(3), pp. 402–410.

Okada, R., Kondo, T., Matsuki, F., Takata, H. and Takiguchi, M. 2008. Phenotypic classification of human CD4+ T cell subsets and their differentiation. *International immunology* 20(9), pp. 1189–1199.

Okazaki, T., Maeda, A., Nishimura, H., Kurosaki, T. and Honjo, T. 2001. PD-1 immunoreceptor inhibits B cell receptor-mediated signaling by recruiting src homology 2-domain-containing tyrosine phosphatase 2 to phosphotyrosine. *Proceedings of the National Academy of Sciences* 98(24), pp. 13866–13871.

Oldreive, C., Skowronska, A., Agathanggelou, A., Parry, H., Krysov, S., Packham, G., Zbgniew, R., et al. 2014. Primary CLL Xenograft: A Model System to Study the Role of T-Cells in CLL Biology and Therapeutic Response. *56th American Society of Hematology Annual Meeting & Exposition*. San Francisco, 6-9 December. Blood

Olivier, M., Hollstein, M. and Hainaut, P. 2010. TP53 Mutations in Human Cancers: Origins, Consequences, and Clinical Use. *Cold Spring Harbor Perspectives in Biology* 2(1), pp. a001008–a001008.

Olson, J.A. and Jameson, S.C. 2011. Keeping STATs on Memory CD8+ T Cells. *Immunity* 35(5), pp. 663–665.

Olsson, J., Wikby, A., Johansson, B., Löfgren, S., Nilsson, B.O. and Ferguson, F.G. 2000. Age-related change in peripheral blood T-lymphocyte subpopulations and cytomegalovirus infection in the very old: the Swedish longitudinal OCTO immune study. *Mechanisms of Ageing and Development* 121(1-3), pp. 187–201.

Onishi, Y., Fehervari, Z., Yamaguchi, T. and Sakaguchi, S. 2008. Foxp3+ natural regulatory T cells preferentially form aggregates on dendritic cells in vitro and actively inhibit their maturation. *Proceedings of the National Academy of Sciences* 105(29), pp. 10113–10118.

Os, A., Bürgler, S., Ribes, A.P., Funderud, A., Wang, D., Thompson, K.M., Tjønnfjord, G.E., et al. 2013. Chronic Lymphocytic Leukemia Cells Are Activated and Proliferate in Response to Specific T Helper Cells. *Cell Reports* 4(3), pp. 566–577.

Osorio, L.M., Aguilar-Santelises, M., De Santiago, A., Hachiya, T., Mellstedt, H. and Jondal, M. 2001. Increased serum levels of soluble Fas in progressive B-CLL. *European Journal of Haematology* 66(5), pp. 342–346.

Paavonen, J., Naud, P., Salmerón, J., Wheeler, C.M., Chow, S.-N., Apter, D., Kitchener, H., et al. 2009. Efficacy of human papillomavirus (HPV)-16/18 AS04-adjuvanted vaccine against cervical infection and precancer caused by oncogenic HPV types (PATRICIA): final analysis of a double-blind, randomised study in young women. *Lancet* 374(9686), pp. 301–314.

Palmer, B.E., Blyveis, N., Fontenot, A.P. and Wilson, C.C. 2005. Functional and phenotypic characterization of CD57+CD4+ T cells and their association with HIV-1-

induced T cell dysfunction. *The Journal of Immunology* 175(12), pp. 8415–8423.

Palucka, K. and Banchereau, J. 2012. Cancer immunotherapy via dendritic cells. *Nature Reviews Cancer* 12(4), pp. 265–277.

Palucka, K. and Banchereau, J. 2013. Dendritic-Cell-Based Therapeutic Cancer Vaccines. *Immunity* 39(1), pp. 38–48.

Parkhurst, M.R., Salgaller, M.L., Southwood, S., Robbins, P.F., Sette, A., Rosenberg, S.A. and Kawakami, Y. 1996. Improved induction of melanoma-reactive CTL with peptides from the melanoma antigen gp100 modified at HLA-A* 0201-binding residues. *The Journal of Immunology* 157(6), pp. 2539–2548.

Parry, R.V., Chemnitz, J.M., Frauwirth, K.A., Lanfranco, A.R., Braunstein, I., Kobayashi, S.V., Linsley, P.S., et al. 2005. CTLA-4 and PD-1 Receptors Inhibit T-Cell Activation by Distinct Mechanisms. *Molecular and Cellular Biology* 25(21), pp. 9543–9553.

Patten, P.E.M., Buggins, A.G.S., Richards, J., Wotherspoon, A., Salisbury, J., Mufti, G.J., Hamblin, T.J., et al. 2008. CD38 expression in chronic lymphocytic leukemia is regulated by the tumor microenvironment. *Blood* 111(10), pp. 5173–5181.

Pede, V., Rombout, A., Vermeire, J., Naessens, E., Vanderstraeten, H., Philippé, J. and Verhasselt, B. 2013. Expression of ZAP70 in chronic lymphocytic leukaemia activates NF-κB signalling. *British Journal of Haematology* 163(5), pp. 621–630.

Penel, N., Adenis, A. and Bocci, G. 2012. Cyclophosphamide-based metronomic chemotherapy: after 10 years of experience, where do we stand and where are we going? *Critical reviews in oncology/hematology* 82(1), pp. 40–50.

Pepper, C., Ward, R., Lin, T.T., Brennan, P., Starczynski, J., Musson, M., Rowntree, C., et al. 2007. Highly purified CD38+ and CD38- sub-clones derived from the same chronic lymphocytic leukemia patient have distinct gene expression signatures despite their monoclonal origin. *Leukemia* 21(4), pp. 687–696.

Pettitt, A.R. 2003. Mechanism of action of purine analogues in chronic lymphocytic leukaemia. *British Journal of Haematology* 121(5), pp. 692–702.

Pham, C.D., Woo, M.Y., Kim, Y.S., Park, S. and Kwon, M.H. 2012. An Anti-Nucleic Acid Antibody Delivers Antigen to the Cross-Presentation Pathway in Dendritic Cells and Potentiates Therapeutic Antitumor Effects. *The Journal of Immunology* 189(12), pp. 5755–5763.

Plunkett, F.J., Franzese, O., Finney, H.M., Fletcher, J.M., Belaramani, L.L., Salmon, M., Dokal, I., et al. 2007. The Loss of Telomerase Activity in Highly Differentiated CD8+CD28-CD27- T Cells Is Associated with Decreased Akt (Ser473) Phosphorylation. *The Journal of Immunology* 178(12), pp. 7710–7719.

Ponader, S., Chen, S.-S., Buggy, J.J., Balakrishnan, K., Gandhi, V., Wierda, W.G., Keating, M.J., et al. 2012. The Bruton tyrosine kinase inhibitor PCI-32765 thwarts chronic lymphocytic leukemia cell survival and tissue homing in vitro and in vivo. *Blood* 119(5), pp. 1182–1189.

Porakishvili, N., Roschupkina, T., Kalber, T., Jewell, A.P., Patterson, K., Yong, K. and Lydyard, P.M. 2001. Expansion of CD4+ T cells with a cytotoxic phenotype in patients with B-chronic lymphocytic leukaemia (B-CLL). *Clinical and experimental immunology* 126(1),

pp. 29–36.

Porter, D.L., Levine, B.L., Kalos, M., Bagg, A. and June, C.H. 2011. Chimeric Antigen Receptor–Modified T Cells in Chronic Lymphoid Leukemia. *New England Journal of Medicine* 365(8), pp. 725–733.

Pourgheysari, B., Bruton, R., Parry, H., Billingham, L., Fegan, C., Murray, J. and Moss, P. 2010. The number of cytomegalovirus-specific CD4+ T cells is markedly expanded in patients with B-cell chronic lymphocytic leukemia and determines the total CD4+ T-cell repertoire. *Blood* 116(16), pp. 2968–2974.

Prosser, M.E., Brown, C.E., Shami, A.F., Forman, S.J. and Jensen, M.C. 2012. Tumor PD-L1 co-stimulates primary human CD8+ cytotoxic T cells modified to express a PD1:CD28 chimeric receptor. *Molecular Immunology* 51(3-4), pp. 263–272.

Qiao, M., Thornton, A.M. and Shevach, E.M. 2007. CD4+ CD25+ regulatory T cells render naive CD4+ CD25- T cells anergic and suppressive. *Immunology* 120(4), pp. 447–455.

Qureshi, O.S., Zheng, Y., Nakamura, K., Attridge, K., Manzotti, C., Schmidt, E.M., Baker, J., et al. 2011. Trans-Endocytosis of CD80 and CD86: A Molecular Basis for the Cell-Extrinsic Function of CTLA-4. *Science* 332(6029), pp. 600–603.

Raa, te, G.D., Pascutti, M.F., García-Vallejo, J.J., Reinen, E., Remmerswaal, E.B., Berge, ten, I.J., van Lier, R.A., et al. 2014. CMV-specific CD8+ T-cell function is not impaired in chronic lymphocytic leukemia. *Blood* 123(5), pp. 717–724.

Raghavan, M., Del Cid, N., Rizvi, S.M. and Peters, L.R. 2008. MHC class I assembly: out and about. *Trends in Immunology* 29(9), pp. 436–443.

Rai, K.R., Sawitsky, A., Cronkite, E.P., Chanana, A.D., Levy, R.N. and Pasternack, B.S. 1975. Clinical staging of chronic lymphocytic leukemia. *Blood* 46(2), pp. 219–234.

Rajasagi, M., Shukla, S.A., Fritsch, E.F., Keskin, D.B., DeLuca, D., Carmona, E., Zhang, W., et al. 2014. Systematic identification of personal tumor-specific neoantigens in chronic lymphocytic leukemia. *Blood* 124(3), pp. 453–462.

Ramsay, A.G., Clear, A.J., Fatah, R. and Gribben, J.G. 2012. Multiple inhibitory ligands induce impaired T-cell immunologic synapse function in chronic lymphocytic leukemia that can be blocked with lenalidomide: establishing a reversible immune evasion mechanism in human cancer. *Blood* 120(7), pp. 1412–1421.

Ramsay, A.G., Johnson, A.J., Lee, A.M., Görgün, G., Le Dieu, R., Blum, W., Byrd, J.C., et al. 2008. Chronic lymphocytic leukemia T cells show impaired immunological synapse formation that can be reversed with an immunomodulating drug. *The Journal of Clinical Investigation*.

Rangachari, M., Zhu, C., Sakuishi, K., Xiao, S., Karman, J., Chen, A., Angin, M., et al. 2012. Bat3 promotes T cell responses and autoimmunity by repressing Tim-3–mediated cell death and exhaustion. *Nature medicine* 18(9), pp. 1394–1400.

Rassenti, L.Z., Jain, S., Keating, M.J., Wierda, W.G., Grever, M.R., Byrd, J.C., Kay, N.E., et al. 2008. Relative value of ZAP-70, CD38, and immunoglobulin mutation status in predicting aggressive disease in chronic lymphocytic leukemia. *Blood* 112(5), pp. 1923–1930.

Redaelli, A., Laskin, B.L., Stepehens, J.M., Bottenman, M.F. and Pashos, C.L. 2004. The

clinical and epidemiological burden of chronic lymphocytic leukaemia. *European journal of cancer care* 13(3), pp. 279–287.

Relland, L.M., Mishra, M.K., Haribhai, D., Edwards, B., Ziegelbauer, J. and Williams, C.B. 2009. Affinity-based selection of regulatory T cells occurs independent of agonist-mediated induction of Foxp3 expression. *The Journal of Immunology* 182(3), pp. 1341–1350.

Rezk, S.A. and Weiss, L.M. 2007. Epstein-Barr virus–associated lymphoproliferative disorders. *Human Pathology* 38(9), pp. 1293–1304.

Ricci, F., Tedeschi, A., Morra, E. and Montillo, M. 2009. Fludarabine in the treatment of chronic lymphocytic leukemia: a review. *Therapeutics and clinical risk management* 5(1), pp. 187–207.

Richardson, S.J., Matthews, C., Catherwood, M.A., Alexander, H.D., Carey, B.S., Farrugia, J., Gardiner, A., et al. 2006. ZAP-70 expression is associated with enhanced ability to respond to migratory and survival signals in B-cell chronic lymphocytic leukemia (B-CLL). *Blood* 107(9), pp. 3584–3592.

Riches, J.C., Davies, J.K., McClanahan, F., Fatah, R., Iqbal, S., Agrawal, S., Ramsay, A.G., et al. 2013. T cells from CLL patients exhibit features of T-cell exhaustion but retain capacity for cytokine production. *Blood* 121(9), pp. 1612–1621.

Riedl, S.J. and Salvesen, G.S. 2007. The apoptosome: signalling platform of cell death. *Nature Reviews Molecular Cell Biology* 8(5), pp. 405–413.

Riese, R.J., Wolf, P.R., Brömme, D., Natkin, L.R., Villadangos, J.A., Ploegh, H.L. and Chapman, H.A. 1996. Essential role for cathepsin S in MHC class II-associated invariant chain processing and peptide loading. *Immunity* 4(4), pp. 357–366.

Rincón, M. and Flavell, R.A. 1994. AP-1 transcriptional activity requires both T-cell receptor-mediated and co-stimulatory signals in primary T lymphocytes. *The EMBO Journal* 13(18), pp. 4370–4381.

Rivoltini, L., Carrabba, M., Huber, V., Castelli, C., Novellino, L., Dalerba, P., Mortarini, R., et al. 2002. Immunity to cancer: attack and escape in T lymphocyte-tumor cell interaction. *Immunological reviews* 188(1), pp. 97–113.

Robak, T., Dmoszynska, A., Solal-Celigny, P., Warzocha, K., Loscertales, J., Catalano, J., Afanasiev, B.V., et al. 2010. Rituximab Plus Fludarabine and Cyclophosphamide Prolongs Progression-Free Survival Compared With Fludarabine and Cyclophosphamide Alone in Previously Treated Chronic Lymphocytic Leukemia. *Journal of Clinical Oncology* 28(10), pp. 1756–1765.

Roche, P.A. and Cresswell, P. 1990. Invariant chain association with HLA-DR molecules inhibits immunogenic peptide binding. *Nature* 345(6276), pp. 615–618.

Roche, P.A., Marks, M.S. and Cresswell, P.J. 1991. Formation of a nine-subunit complex by HLA class II glycoproteins and the invariant chain. *Nature* 354(6352), pp. 392–394.

Rock, K.L. and Shen, L. 2005. Cross-presentation: underlying mechanisms and role in immune surveillance. *Immunological reviews* 207(1), pp. 166–183.

Rodig, S.J., Abramson, J.S., Pinkus, G.S., Treon, S.P., Dorfman, D.M., Dong, H.Y., Shipp, M.A., et al. 2006. Heterogeneous CD52 Expression among Hematologic Neoplasms:

Implications for the Use of Alemtuzumab (CAMPATH-1H). *Clinical Cancer Research* 12(23), pp. 7174–7179.

Rodríguez-Pinto, D. 2005. B cells as antigen presenting cells. *Cellular immunology* 238(2), pp. 67–75.

Romero, P., Zippelius, A., Kurth, I., Pittet, M.J., Touvrey, C., Iancu, E.M., Corthesy, P., et al. 2007. Four functionally distinct populations of human effector-memory CD8+ T lymphocytes. *The Journal of Immunology* 178(7), pp. 4112–4119.

Rose, D.M., Han, J. and Ginsberg, M.H. 2002. alpha4 integrins and the immune response. *Immunological reviews* 186(1), pp. 118–124.

Rosenberg, H.F., Dyer, K.D. and Foster, P.S. 2012. Eosinophils: changing perspectives in health and disease. *Nature Reviews Immunology* 13(1), pp. 9–22.

Rosenberg, S.A., Restifo, N.P., Yang, J.C., Morgan, R.A. and Dudley, M.E. 2008. Adoptive cell transfer: a clinical path to effective cancer immunotherapy. *Nature Reviews Cancer* 8(4), pp. 299–308.

Rosenberg, S.A., Yang, J.C., Schwartzentruber, D.J., Hwu, P., Marincola, F.M., Topalian, S.L., Restifo, N.P., et al. 1998. Immunologic and therapeutic evaluation of a synthetic peptide vaccine for the treatment of patients with metastatic melanoma. *Nature medicine* 4(3), pp. 321–327.

Rosenberg, S.A., Yang, J.C., Sherry, R.M., Kammula, U.S., Hughes, M.S., Phan, G.Q., Citrin, D.E., et al. 2011. Durable complete responses in heavily pretreated patients with metastatic melanoma using T-cell transfer immunotherapy. *Clinical Cancer Research* 17(13), pp. 4550–4557.

Rossi, D., Khiabanian, H., Spina, V., Ciardullo, C., Bruscaggin, A., Famà, R., Rasi, S., et al. 2014. Clinical impact of small TP53 mutated subclones in chronic lymphocytic leukemia. *Blood* 123(14), pp. 2139–2147.

Rudd, C.E., Taylor, A. and Schneider, H. 2009. CD28 and CTLA-4 coreceptor expression and signal transduction. *Immunological reviews* 229(1), pp. 12–26.

Ruella, M., Barrett, D., Kenderian, S., Shestova, O., Hofmann, T., Scholler, J., Lacey, S., et al. 2014. Novel Chimeric Antigen Receptor T Cells for the Treatment of CD19-Negative Relapses Occurring after CD19-Targeted Immunotherapies. *56th American Society of Hematology Annual Meeting & Exposition*. San Francisco, 6-9 December. Blood.

Rufer, N., Migliaccio, M., Antonchuk, J., Humphries, R.K., Roosnek, E. and Lansdorp, P.M. 2001. Transfer of the human telomerase reverse transcriptase (TERT) gene into T lymphocytes results in extension of replicative potential. *Blood* 98(3), pp. 597–603.

Sakaguchi, S., Yamaguchi, T., Nomura, T. and Ono, M. 2008. Regulatory T Cells and Immune Tolerance. *Cell* 133(5), pp. 775–787.

Sakhdari, A., Mujib, S., Vali, B., Yue, F.Y., MacParland, S., Clayton, K., Jones, R.B., et al. 2012. Tim-3 Negatively Regulates Cytotoxicity in Exhausted CD8+ T Cells in HIV Infection Lichterfeld, M. ed. *PLoS ONE* 7(7), p. e40146.

Sakuishi, K., Apetoh, L., Sullivan, J.M., Blazar, B.R., Kuchroo, V.K. and Anderson, A.C. 2010. Targeting Tim-3 and PD-1 pathways to reverse T cell exhaustion and restore anti-

tumor immunity. *The Journal of Experimental Medicine* 207(10), pp. 2187–2194.

Sakuishi, K., Jayaraman, P., Behar, S.M., Anderson, A.C. and Kuchroo, V.K. 2011. Emerging Tim-3 functions in antimicrobial and tumor immunity. *Trends in Immunology* 32(8), pp. 345–349.

Saliba, A.-E., Westermann, A.J., Gorski, S.A. and Vogel, J. 2014. Single-cell RNA-seq: advances and future challenges. *Nucleic Acids Research* 42(14), pp. 8845–8860.

Sallusto, F., Geginat, J. and Lanzavecchia, A. 2004. Central memory and effector memory T cell subsets: function, generation, and maintenance. *Annual Review of Immunology* 22, pp. 745–763.

Sallusto, F., Lenig, D., Förster, R., Lipp, M. and Lanzavecchia, A. 1999. Two subsets of memory T lymphocytes with distinct homing potentials and effector functions. *Nature* 401(6754), pp. 708–712.

Sandler, A., Gray, R., Perry, M.C., Brahmer, J., Schiller, J.H., Dowlati, A., Lilenbaum, R., et al. 2006. Paclitaxel–Carboplatin Alone or with Bevacizumab for Non–Small-Cell Lung Cancer. *New England Journal of Medicine* 355(24), pp. 2542–2550.

Saunders, A.E. and Johnson, P. 2010. Modulation of immune cell signalling by the leukocyte common tyrosine phosphatase, CD45. *Cellular signalling* 22(3), pp. 339–348.

Savina, A. and Amigorena, S. 2007. Phagocytosis and antigen presentation in dendritic cells. *Immunological reviews* 219, pp. 143–156.

Schall, T.J., Bacon, K., Toy, K.J. and Goeddel, D.V. 1990. Selective attraction of monocytes and T lymphocytes of the memory phenotype by cytokine RANTES. *Nature* 347(6294), pp. 669–671.

Scheuer, W., Friess, T., Burtscher, H., Bossenmaier, B., Endl, J. and Hasmann, M. 2009. Strongly enhanced antitumor activity of trastuzumab and pertuzumab combination treatment on HER2-positive human xenograft tumor models. *Cancer Research* 69(24), pp. 9330–9336.

Schluns, K.S., Kieper, W.C., Jameson, S.C. and Lefrançois, L. 2000. Interleukin-7 mediates the homeostasis of naïve and memory CD8 T cells in vivo. *Nature immunology* 1(5), pp. 426–432.

Schmidt, S.M., Schag, K., Müller, M.R., Weck, M.M., Appel, S., Kanz, L., Grünebach, F., et al. 2003. Survivin is a shared tumor-associated antigen expressed in a broad variety of malignancies and recognized by specific cytotoxic T cells. *Blood* 102(2), pp. 571–576.

Scholler, J., Brady, T.L., Binder-Scholl, G., Hwang, W.-T., Plesa, G., Hege, K.M., Vogel, A.N., et al. 2012. Decade-long safety and function of retroviral-modified chimeric antigen receptor T cells. *Science Translational Medicine* 4(132), p. 132ra53.

Schultze, J.L., Michalak, S., Seamon, M.J., Dranoff, G., Jung, K., Daley, J., Delgado, J.C., et al. 1997. CD40-activated human B cells: an alternative source of highly efficient antigen presenting cells to generate autologous antigen-specific T cells for adoptive immunotherapy. *The Journal of Clinical Investigation* 100(11), pp. 2757–2765.

Schroeder, H.W. and Cavacini, L. 2010. Structure and function of immunoglobulins. *The Journal of allergy and clinical immunology* 125(2 Suppl 2), pp. S41–52.

Schumacher, T.N.M. 2002. T-cell-receptor gene therapy. *Nature Reviews Immunology* 2(7), pp. 512–519.

Schwartzentruber, D.J., Lawson, D.H., Richards, J.M., Conry, R.M., Miller, D.M., Treisman, J., Gailani, F., et al. 2011. gp100 Peptide Vaccine and Interleukin-2 in Patients with Advanced Melanoma. *New England Journal of Medicine* 364(22), pp. 2119–2127.

Schwarz, K., van Den Broek, M., Kostka, S., Kraft, R., Soza, A., Schmidtke, G., Kloetzel, P.M., et al. 2000. Overexpression of the proteasome subunits LMP2, LMP7, and MECL-1, but not PA28 alpha/beta, enhances the presentation of an immunodominant lymphocytic choriomeningitis virus T cell epitope. *The Journal of Immunology* 165(2), pp. 768–778.

Scott, A.M., Wolchok, J.D. and Old, L.J. 2012. Antibody therapy of cancer. *Nature Reviews Cancer* 12(4), pp. 278–287.

Scott, F.L., Stec, B., Pop, C., Dobaczewska, M.K., Lee, J.J., Monosov, E., Robinson, H., et al. 2009. The Fas-FADD death domain complex structure unravels signalling by receptor clustering. *Nature* 457(7232), pp. 1019–1022.

Seifert, M., Sellmann, L., Bloehdorn, J., Wein, F., Stilgenbauer, S., Dürig, J. and Küppers, R. 2012. Cellular origin and pathophysiology of chronic lymphocytic leukemia. *The Journal of Experimental Medicine* 209(12), pp. 2183–2198.

Serrano, D., Monteiro, J., Allen, S.L., Kolitz, J., Schulman, P., Lichtman, S.M., Buchbinder, A., et al. 1997. Clonal expansion within the CD4+CD57+ and CD8+CD57+ T cell subsets in chronic lymphocytic leukemia. *The Journal of Immunology* 158(3), pp. 1482–1489.

Sharpe, A.H. and Freeman, G.J. 2002. THE B7–CD28 SUPERFAMILY. *Nature Reviews Immunology* 2(2), pp. 116–126.

Shen, L., Sigal, L.J., Boes, M. and Rock, K.L. 2004. Important role of cathepsin S in generating peptides for TAP-independent MHC class I crosspresentation in vivo. *Immunity* 21(2), pp. 155–165.

Shi, L., Sings, H.L., Bryan, J.T., Wang, B., Wang, Y., Mach, H., Kosinski, M., et al. 2007. GARDASIL: prophylactic human papillomavirus vaccine development--from bench top to bed-side. *Clinical pharmacology and therapeutics* 81(2), pp. 259–264.

Sica, A., Dorman, L., Viggiano, V., Cippitelli, M., Ghosh, P., Rice, N. and Young, H.A. 1997. Interaction of NF-κB and NFAT with the interferon-γ promoter. *The Journal of biological chemistry* 272(48), pp. 30412–30420.

Simone, R., Marsilio, S., Patten, P., Ferrer, G., Chen, S., Yan, X., Vergani, S., et al. 2013. Lenalidomide Promotes The Expansion Of CD8 T Cells With An Effector Memory Phenotype In a Murine Xenograft Model Of Chronic Lymphocytic Leukemia. *55th American Society of Hematology Annual Meeting & Exposition*. New Orleans, 7-10 December. Blood.

Slamon, D.J., Leyland-Jones, B., Shak, S., Fuchs, H., Paton, V., Bajamonde, A., Fleming, T., et al. 2001. Use of Chemotherapy plus a Monoclonal Antibody against HER2 for Metastatic Breast Cancer That Overexpresses HER2. *New England Journal of Medicine* 344(11), pp. 783–792.

Slingluff, C.L., Jr 2011. The Present and Future of Peptide Vaccines for Cancer. *The Cancer Journal* 17(5), pp. 343–350.

Sloan, V.S., Cameron, P., Porter, G., Gammon, M., Amaya, M., Mellins, E. and Zaller, D.M. 1995. Mediation by HLA-DM of dissociation of peptides from HLA-DR. *Nature* 375(6534), pp. 802–806.

Smith, D.M., Benaroudj, N. and Goldberg, A. 2006. Proteasomes and their associated ATPases: A destructive combination. *Journal of Structural Biology* 156(1), pp. 72–83.

Song, D.G., Ye, Q., Poussin, M., Harms, G.M., Figini, M. and Powell, D.J. 2012. CD27 costimulation augments the survival and antitumor activity of redirected human T cells in vivo. *Blood* 119(3), pp. 696–706.

Speedy, H.E., Di Bernardo, M.C., Sava, G.P., Dyer, M.J.S., Holroyd, A., Wang, Y., Sunter, N.J., et al. 2013. A genome-wide association study identifies multiple susceptibility loci for chronic lymphocytic leukemia. *Nature Genetics* 46(1), pp. 56–60.

Srinivasan, L., Sasaki, Y., Calado, D.P., Zhang, B., Paik, J.H., DePinho, R.A., Kutok, J.L., et al. 2009. PI3 Kinase Signals BCR-Dependent Mature B Cell Survival. *Cell* 139(3), pp. 573–586.

Stavnezer, J., Guikema, J.E.J. and Schrader, C.E. 2008. Mechanism and regulation of class switch recombination. *Annual Review of Immunology* 26, pp. 261–292.

Steimle, V., Siegrist, C.-A., Mottet, A., Lisowska-Grospierre, B. and Mach, B. 1994. Regulation of MHC Class II Expression by Interferon-γ Mediated by the Transactivatior Gene CIITA. *Science* 265, pp. 106–109.

Steinman, R.M. and Idoyaga, J. 2010. Features of the dendritic cell lineage. *Immunological reviews* 234(1), pp. 5–17.

Stern, L.J., Potolicchio, I. and Santambrogio, L. 2006. MHC class II compartment subtypes: structure and function. *Current opinion in immunology* 18(1), pp. 64–69.

Strindhall, J., Nilsson, B.-O., Löfgren, S., Ernerudh, J., Pawelec, G., Johansson, B. and Wikby, A. 2007. No Immune Risk Profile among individuals who reach 100 years of age: Findings from the Swedish NONA immune longitudinal study. *Experimental Gerontology* 42(8), pp. 753–761.

Sullivan, B.M., Juedes, A., Szabo, S.J., Herrath, von, M. and Glimcher, L.H. 2011. Antigen-driven effector CD8 T cell function regulated by T-bet. *Proceedings of the National Academy of Sciences* 100(26), pp. 15818–15823.

Suntharalingam, G., Perry, M.R., Ward, S., Brett, S.J., Castello-Cortes, A., Brunner, M.D. and Panoskaltsis, N. 2006. Cytokine storm in a phase 1 trial of the anti-CD28 monoclonal antibody TGN1412. *New England Journal of Medicine* 355(10), pp. 1018–1028.

Szabo, S.J., Kim, S.T., Costa, G.L., Zhang, X., Fathman, C.G. and Glimcher, L.H. 2000. A novel transcription factor, T-bet, directs Th1 lineage commitment. *Cell* 100(6), pp. 655–669.

Taka, N., Matsuoka, H., Sato, T., Yoshino, H., Imaoka, I., Sato, H., Kotake, K.-I., et al. 2009. Discovery of novel motilin antagonists: Conversion of tetrapeptide leads to orally available peptidomimetics. *Bioorganic & Medicinal Chemistry Letters* 19(13), pp. 3426–3429.

Takata, H. and Takiguchi, M. 2006. Three memory subsets of human CD8+ T cells differently expressing three cytolytic effector molecules. *The Journal of Immunology* 177(7), pp. 4330–4340.

Talmadge, J.E. and Gabrilovich, D.I. 2013. History of myeloid-derived suppressor cells. *Nature Reviews Cancer* 13(10), pp. 739–752.

Tam, C.S., O'Brien, S., Wierda, W., Kantarjian, H., Wen, S., Do, K.-A., Thomas, D.A., et al. 2008. Long-term results of the fludarabine, cyclophosphamide, and rituximab regimen as initial therapy of chronic lymphocytic leukemia. *Blood* 112(4), pp. 975–980.

Tanner, J.E. and Tosato, G. 1992. Regulation of B-cell growth and immunoglobulin gene transcription by interleukin-6. *Blood* 79(2), pp. 452–459.

Taylor, G.P. 2006. Molecular aspects of HTLV-I infection and adult T-cell leukaemia/lymphoma. *Journal of clinical pathology* 60(12), pp. 1392–1396.

Teixeira, L.K., Fonseca, B.P.F., Vieira-de-Abreu, A., Barboza, B.A., Robbs, B.K., Bozza, P.T. and Viola, J.P.B. 2005. IFN-gamma production by CD8+ T cells depends on NFAT1 transcription factor and regulates Th differentiation. *The Journal of Immunology* 175(9), pp. 5931–5939.

Thiery, J., Keefe, D., Boulant, S., Boucrot, E., Walch, M., Martinvalet, D., Goping, I.S., et al. 2011. Perforin pores in the endosomal membrane trigger the release of endocytosed granzyme B into the cytosol of target cells. *Nature immunology* 12(8), pp. 770–777.

Thomas, S., Stauss, H.J. and Morris, E.C. 2010. Molecular immunology lessons from therapeutic T-cell receptor gene transfer. *Immunology* 129(2), pp. 170–177.

Toda, A. and Piccirillo, C.A. 2006. Development and function of naturally occurring CD4+CD25+ regulatory T cells. *Journal of leukocyte biology* 80(3), pp. 458–470.

Topalian, S.L., Hodi, F.S., Brahmer, J.R., Gettinger, S.N., Smith, D.C., McDermott, D.F., Powderly, J.D., et al. 2012. Safety, Activity, and Immune Correlates of Anti–PD-1 Antibody in Cancer. *New England Journal of Medicine* 366(26), pp. 2443–2454.

Topp, M.S., Kufer, P., Gokbuget, N., Goebeler, M., Klinger, M., Neumann, S., Horst, H.A., et al. 2011. Targeted Therapy With the T-Cell-Engaging Antibody Blinatumomab of Chemotherapy-Refractory Minimal Residual Disease in B-Lineage Acute Lymphoblastic Leukemia Patients Results in High Response Rate and Prolonged Leukemia-Free Survival. *Journal of Clinical Oncology* 29(18), pp. 2493–2498.

Topp, M.S., Riddell, S.R., Akatsuka, Y., Jensen, M.C., Blattman, J.N. and Greenberg, P.D. 2003. Restoration of CD28 Expression in CD28- CD8+ Memory Effector T Cells Reconstitutes Antigen-induced IL-2 Production. *The Journal of Experimental Medicine* 198(6), pp. 947–955.

Trifari, S., Kaplan, C.D., Tran, E.H., Crellin, N.K. and Spits, H. 2009. Identification of a human helper T cell population that has abundant production of interleukin 22 and is distinct from T(H)-17, T(H)1 and T(H)2 cells. *Nature immunology* 10(8), pp. 864–871.

Turley, S.J., Inaba, K., Garrett, W.S., Ebersold, M., Unternaehrer, J., Steinman, R.M. and Mellman, I. 2000. Transport of peptide-MHC class II complexes in developing dendritic cells. *Science* 288(5465), pp. 522–527.

Vaisitti, T., Audrito, V., Serra, S., Buonincontri, R., Sociali, G., Mannino, E., Pagnani, A., et al. 2015. The enzymatic activities of CD38 enhance CLL growth and trafficking: implications for therapeutic targeting. *Leukemia* 29(2), pp. 356–368.

Vaisitti, T., Aydin, S., Rossi, D., Cottino, F., Bergui, L., D'Arena, G., Bonello, L., et al. 2010. CD38 increases CXCL12-mediated signals and homing of chronic lymphocytic leukemia cells. *Leukemia* 24(5), pp. 958–969.

Valmori, D., Scheibenbogen, C., Dutoit, V., Nagorsen, D., Asemissen, A., Rubio-Godoy, V., Rimoldi, D., et al. 2002. Circulating tumor-reactive CD8(+) T cells in melanoma patients contain a CD45RA(+)CCR7(-) effector subset exerting ex vivo tumor-specific cytolytic activity. *Cancer Research* 62(6), pp. 1743–1750.

van de Weyer, P.S., Muehlfeit, M., Klose, C., Bonventre, J.V., Walz, G. and Kuehn, E.W. 2006. A highly conserved tyrosine of Tim-3 is phosphorylated upon stimulation by its ligand galectin-9. *Biochemical and Biophysical Research Communications* 351(2), pp. 571–576.

van den Broek, M.E., Kägi, D., Ossendorp, F., Toes, R., Vamvakas, S., Lutz, W.K., Melief, C.J., et al. 1996. Decreased tumor surveillance in perforin-deficient mice. *The Journal of Experimental Medicine* 184(5), pp. 1781–1790.

Van den Hove, L.E., Van Gool, S.W., Vandenberghe, P., Bakkus, M., Thielemans, K., Boogaerts, M.A. and Ceuppens, J.L. 1997. CD40 triggering of chronic lymphocytic leukemia B cells results in efficient alloantigen presentation and cytotoxic T lymphocyte induction by up-regulation of CD80 and CD86 costimulatory molecules. *Leukemia* 11(4), pp. 572–580.

Van den Hove, L.E., Van Gool, S.W., Vandenberghe, P., Boogaerts, M.A. and Ceuppens, J.L. 1998. CD57+/CD28-T cells in untreated hemato-oncological patients are expanded and display a Th1-type cytokine secretion profile, ex vivo cytolytic activity and enhanced tendency to apoptosis. *Leukemia* 12(10), pp. 1573–1582.

van der Bruggen, P., Traversari, C., Chomez, P., Lurquin, C., De Plaen, E., Van den Eynde, B., Knuth, A., et al. 1991. A gene encoding an antigen recognized by cytolytic T lymphocytes on a human melanoma. *Science* 254(5038), pp. 1643–1647.

van der Burg, S.H., Ressing, M.E., Kwappenberg, K.M., de Jong, A., Straathof, K., de Jong, J., Geluk, A., et al. 2001. Natural T-helper immunity against human papillomavirus type 16 (HPV16) E7-derived peptide epitopes in patients with HPV16-positive cervical lesions: identification of 3 human leukocyte antigen class II-restricted epitopes. *International Journal of Cancer* 91(5), pp. 612–618.

van Oers, M.H.J., Klasa, R., Marcus, R.E., Wolf, M., Kimby, E., Gascoyne, R.D., Jack, A., et al. 2006. Rituximab maintenance improves clinical outcome of relapsed/resistant follicular non-Hodgkin lymphoma in patients both with and without rituximab during induction: results of a prospective randomized phase 3 intergroup trial. *Blood* 108(10), pp. 3295–3301.

Venturi, G.M., Tu, L., Kadono, T., Khan, A.I., Fujimoto, Y., Oshel, P., Bock, C.B., et al. 2003. Leukocyte migration is regulated by L-selectin endoproteolytic release. *Immunity* 19(5), pp. 713–724.

Voehringer, D. 2013. Protective and pathological roles of mast cells and basophils. *Nature Reviews Immunology* 13(5), pp. 362–375.

Voskoboinik, I., Dunstone, M.A., Baran, K., Whisstock, J.C. and Trapani, J.A. 2010. Perforin: structure, function, and role in human immunopathology. *Immunological reviews* 235(1), pp. 35–54.

Vu, T. and Claret, F.X. 2012. Trastuzumab: updated mechanisms of action and resistance in breast cancer. *Frontiers in oncology* 2, p. 62.

Vyas, J.M., Van der Veen, A.G. and Ploegh, H.L. 2008. The known unknowns of antigen processing and presentation. *Nature Reviews Immunology* 8(8), pp. 607–618.

Waller, E.C.P., McKinney, N., Hicks, R., Carmichael, A.J., Sissons, J.G.P. and Wills, M.R. 2007. Differential costimulation through CD137 (4 1BB) restores proliferation of human virus-specific 'effector memory' (CD28 CD45RAHI) CD8+ T cells. *Blood* 110(13), pp. 4360–4366.

Walsby, E., Buggins, A., Devereux, S., Jones, C., Pratt, G., Brennan, P., Fegan, C., et al. 2014. Development and characterization of a physiologically relevant model of lymphocyte migration in chronic lymphocytic leukemia. *Blood* 123(23), pp. 3607–3617.

Walsby, E., Brennan, P., Pratt, G., Hartmann, T., Yoshizawa, T., Fegan, C., et al. 2014. CXCL12 Enhances CLL Cell and T-Cell Migration in a Dynamic Circulating Model of CLL That Can be Abrogated By the CXCR4 Antagonist ONO-7161. *56th American Society of Hematology Annual Meeting & Exposition*. San Francisco, 6-9 December. Blood, pp. 3293-3293

Wang, H., Kadlecek, T.A., Au-Yeung, B.B., Goodfellow, H.E.S., Hsu, L.-Y., Freedman, T.S. and Weiss, A. 2010. ZAP-70: an essential kinase in T-cell signaling. *Cold Spring Harbor Perspectives in Biology* 2(5), p. a002279.

Wang, W., Epler, J., Salazar, L.G. and Riddell, S.R. 2006. Recognition of breast cancer cells by CD8+ cytotoxic T-cell clones specific for NY-BR-1. *Cancer Research* 66(13), pp. 6826–6833.

Warmerdam, P.A., Long, E.O. and Roche, P.A. 1996. Isoforms of the invariant chain regulate transport of MHC class II molecules to antigen processing compartments. *The Journal of Cell Biology* 133(2), pp. 281–291.

Watts, C. 2001. Antigen processing in the endocytic compartment. *Current opinion in immunology* 13, pp. 26–31.

Wearsch, P.A. and Cresswell, P. 2008. The quality control of MHC class I peptide loading. *Current Opinion in Cell Biology* 20(6), pp. 624–631.

Wei, F., Zhong, S., Ma, Z., Kong, H., Medvec, A., Ahmed, R., Freeman, G.J., et al. 2013. Strength of PD-1 signaling differentially affects T-cell effector functions. *Proceedings of the National Academy of Sciences* 110(27), pp. E2480–9.

Wen, T., Mellstedt, H. and Jondal, M. 1990. Presence of clonal T cell populations in chronic B lymphocytic leukemia and smoldering myeloma. *The Journal of Experimental Medicine* 171(3), pp. 659–666.

Wherry, E.J. 2011. T cell exhaustion. *Nature immunology* 12(6), pp. 492–499.

Wherry, E.J., Teichgräber, V., Becker, T.C., Masopust, D., Kaech, S.M., Antia, R., Andrian, von, U.H., et al. 2003. Lineage relationship and protective immunity of memory CD8 T cell

subsets. *Nature immunology* 4(3), pp. 225–234.

Wierda, W.G., Kipps, T.J., Mayer, J., Stilgenbauer, S., Williams, C.D., Hellmann, A., Robak, T., et al. 2010. Ofatumumab As Single-Agent CD20 Immunotherapy in Fludarabine-Refractory Chronic Lymphocytic Leukemia. *Journal of Clinical Oncology* 28(10), pp. 1749–1755.

Wierda, W.G., Padmanabhan, S., Chan, G.W., Gupta, I.V., Lisby, S., Osterborg, A.for the Hx-CD20-406 Study Investigators 2011. Ofatumumab is active in patients with fludarabine-refractory CLL irrespective of prior rituximab: results from the phase 2 international study. *Blood* 118(19), pp. 5126–5129.

Wikby, A., Johansson, B., Olsson, J., Löfgren, S., Nilsson, B.-O. and Ferguson, F. 2002. Expansions of peripheral blood CD8 T-lymphocyte subpopulations and an association with cytomegalovirus seropositivity in the elderly: the Swedish NONA immune study. *Experimental Gerontology* 37(2-3), pp. 445–453.

Willinger, T., Freeman, T., Hasegawa, H., McMichael, A.J. and Callan, M.F.C. 2005. Molecular signatures distinguish human central memory from effector memory CD8 T cell subsets. *The Journal of Immunology* 175(9), pp. 5895–5903.

Wills, M.R., Carmichael, A.J., Weekes, M.P., Mynard, K., Okecha, G., Hicks, R. and Sissons, J.G. 1999. Human virus-specific CD8+ CTL clones revert from CD45ROhigh to CD45RAhigh in vivo: CD45RAhighCD8+ T cells comprise both naive and memory cells. *The Journal of Immunology* 162(12), pp. 7080–7087.

Winkler, U., Jensen, M., Manzke, O., Schulz, H., Diehl, V. and Engert, A. 1999. Cytokine-release syndrome in patients with B-cell chronic lymphocytic leukemia and high lymphocyte counts after treatment with an anti-CD20 monoclonal antibody (rituximab, IDEC-C2B8). *Blood* 94(7), pp. 2217–2224.

Wolchok, J.D., Kluger, H., Callahan, M.K., Postow, M.A., Rizvi, N.A., Lesokhin, A.M., Segal, N.H., et al. 2013. Nivolumab plus Ipilimumab in Advanced Melanoma. *New England Journal of Medicine* 369(2), pp. 122–133.

Wong, R., Pepper, C., Brennan, P., Nagorsen, D., Man, S. and Fegan, C. 2013. Blinatumomab induces autologous T-cell killing of chronic lymphocytic leukemia cells. *Haematologica* 98(12), pp. 1930–1938.

Woo, S.R., Turnis, M.E., Goldberg, M.V., Bankoti, J., Selby, M., Nirschl, C.J., Bettini, M.L., et al. 2012. Immune Inhibitory Molecules LAG-3 and PD-1 Synergistically Regulate T-cell Function to Promote Tumoral Immune Escape. *Cancer Research* 72(4), pp. 917–927.

Wooldridge, L., Ekeruche-Makinde, J., van den Berg, H.A., Skowera, A., Miles, J.J., Tan, M.P., Dolton, G., et al. 2012. A Single Autoimmune T Cell Receptor Recognizes More Than a Million Different Peptides. *Journal of Biological Chemistry* 287(2), pp. 1168–1177.

Workman, C.J. and Vignali, D.A.A. 2003. The CD4-related molecule, LAG-3 (CD223), regulates the expansion of activated T cells. *European Journal of Immunology* 33(4), pp. 970–979.

Workman, C.J., Dugger, K.J. and Vignali, D.A.A. 2002. Cutting edge: molecular analysis of the negative regulatory function of lymphocyte activation gene-3. *The Journal of Immunology* 169(10), pp. 5392–5395.

Wu, W., Shi, Y., Li, S., Zhang, Y., Liu, Y., Wu, Y. and Chen, Z. 2012. Blockade of Tim-3 signaling restores the virus-specific CD8+T-cell response in patients with chronic hepatitis B. *European Journal of Immunology* 42(5), pp. 1180–1191.

Xu, T., Shu, C.-T., Purdom, E., Dang, D., Ilsley, D., Guo, Y., Weber, J., et al. 2004. Microarray analysis reveals differences in gene expression of circulating CD8(+) T cells in melanoma patients and healthy donors. *Cancer Research* 64(10), pp. 3661–3667.

Yang, X.O., Nurieva, R., Martinez, G.J., Kang, H.S., Chung, Y., Pappu, B.P., Shah, B., et al. 2008. Molecular Antagonism and Plasticity of Regulatory and Inflammatory T Cell Programs. *Immunity* 29(1), pp. 44–56.

Yee, C., Thompson, J.A., Byrd, D., Riddell, S.R., Roche, P., Celis, E. and Greenberg, P.D. 2002. Adoptive T cell therapy using antigen-specific CD8+ T cell clones for the treatment of patients with metastatic melanoma: In vivo persistence, migration, and antitumor effect of transferred T cells. *Proceedings of the National Academy of Sciences* 99(25), pp. 16168–16173.

Yokosuka, T., Takamatsu, M., Kobayashi-Imanishi, W., Hashimoto-Tane, A., Azuma, M. and Saito, T. 2012. Programmed cell death 1 forms negative costimulatory microclusters that directly inhibit T cell receptor signaling by recruiting phosphatase SHP2. *The Journal of Experimental Medicine* 209(6), pp. 1201–1217.

Younes, A., Gopal, A.K., Smith, S.E., Ansell, S.M., Rosenblatt, J.D., Savage, K.J., Ramchandren, R., et al. 2012. Results of a Pivotal Phase II Study of Brentuximab Vedotin for Patients With Relapsed or Refractory Hodgkin's Lymphoma. *Journal of Clinical Oncology* 30(18), pp. 2183–2189.

Zamorano, J., Kelly, A.E., Austrian, J., Wang, H.Y. and Keegan, A.D. 2001. Costimulation of resting B lymphocytes alters the IL-4-activated IRS2 signaling pathway in a STAT6 independent manner: implications for cell survival and proliferation. *Cell research* 11(1), pp. 44–54.

Zenz, T. 2013. Exhausting T cells in CLL. *Blood* 121(9), pp. 1485–1486.

Zenz, T., Eichhorst, B., Busch, R., Denzel, T., Häbe, S., Winkler, D., Bühler, A., et al. 2010a. TP53 mutation and survival in chronic lymphocytic leukemia. *Journal of Clinical Oncology* 28(29), pp. 4473–4479.

Zenz, T., Mertens, D., Küppers, R., Döhner, H. and Stilgenbauer, S. 2010b. From pathogenesis to treatment of chronic lymphocytic leukaemia. *Nature Reviews Cancer* 10(1), pp. 37–50.

Zhao, Y., Wang, Q.J., Yang, S., Kochenderfer, J.N., Zheng, Z., Zhong, X., Sadelain, M., et al. 2009. A herceptin-based chimeric antigen receptor with modified signaling domains leads to enhanced survival of transduced T lymphocytes and antitumor activity. *The Journal of Immunology* 183(9), pp. 5563–5574.

Zhou, Q., Munger, M.E., Veenstra, R.G., Weigel, B.J., Hirashima, M., Munn, D.H., Murphy, W.J., et al. 2011. Coexpression of Tim-3 and PD-1 identifies a CD8+ T-cell exhaustion phenotype in mice with disseminated acute myelogenous leukemia. *Blood* 117(17), pp. 4501–4510.

Zhu, C., Anderson, A.C., Schubart, A., Xiong, H., Imitola, J., Khoury, S.J., Zheng, X.X., et al. 2005. The Tim-3 ligand galectin-9 negatively regulates T helper type 1 immunity. *Nature immunology* 6(12), pp. 1245–1252.

Zhu, J. and Paul, W.E. 2008. CD4 T cells: fates, functions, and faults. *Blood* 112(5), pp. 1557–1569.

Ziegler, K. and Unanue, E.R. 1981. Identification of a macrophage antigen-processing event required for I-region-restricted antigen presentation to T lymphocytes. *The Journal of Immunology* 127(5), pp. 1869–1875.

Zucchetto, A., Vaisitti, T., Benedetti, D., Tissino, E., Bertagnolo, V., Rossi, D., Bomben, R., et al. 2012. The CD49d/CD29 complex is physically and functionally associated with CD38 in B-cell chronic lymphocytic leukemia cells. *Leukemia* 26(6), pp. 1301–1312.